

**Biosynthesis of Metal Nanoparticles of Selected
Medicinal Plants and their Biological Activities**



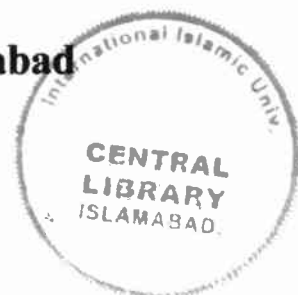
PhD Thesis

Submitted by

ASIA NOUREEN

**Sulaiman Bin Abdullah Aba Al-Khail - Center for
Interdisciplinary Research in Basic Sciences (SA-CIRBS),
Faculty of Sciences,
International Islamic University, Islamabad**

2023



Accession No. TH-27483 K.

PHD

615.32

ASB

Biosynthesis

Medicinal plants

Metal Nanoparticles

Biological Activities

Biosynthesis of Metal Nanoparticles of Selected Medicinal Plants and their Biological Activities



PhD Thesis

Submitted by

Asia Noureen

24-FBAS/PHDNS/F15

Supervisor

Prof. Dr. Masoom Yasinzai

**Sulaiman Bin Abdullah Aba Al-Khail - Center for
Interdisciplinary Research in Basic Sciences (SA-CIRBS),
Faculty of Sciences,
International Islamic University, Islamabad**

2023

Biosynthesis of Metal Nanoparticles of Selected Medicinal Plants and their Biological Activities



Researcher

Asia Noureen

Supervisor

Prof. Dr. Masoom Yasinzai

Reg. No. 24-FBAS/PHDNS/F15

Professor, SA-CIRBS

**Sulaiman Bin Abdullah Aba Al-Khail - Center for
Interdisciplinary Research in Basic Sciences (SA-CIRBS),
Faculty of Sciences,
International Islamic University, Islamabad**

2023

Sulaiman Bin Abdullah Aba Al-Khail-Centre for Interdisciplinary
Research in Basic Sciences (SA-CIRBS)
Faculty of Sciences
International Islamic University, Islamabad

Date: 12-7-2023

FINAL APPROVAL

It is certified that we have read the thesis submitted by *Ms. Asia Noureen* and it is our judgment that this project is of sufficient standard to warrant its acceptance by the International Islamic University, Islamabad, in partial fulfillment of the requirements for the degree of Doctor of Philosophy in Biosciences.

COMMITTEE



External Examiner 1
Prof. Dr. Aamer Ali Shah
Professor, Department of
Microbiology,
QAU, Islamabad



External Examiner 2
Dr. Farha Masood
Associate Professor
Department of Biosciences, COMSATS,
Islamabad



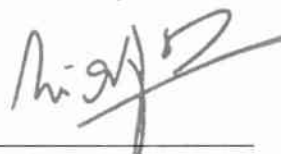
Internal Examiner
Dr. Ikram Ullah
Assistant Professor
SA-CIRBS, FoS,
IIU, Islamabad



Supervisor
Prof. Dr. Masoom Yasinzai
Ex- Professor
SA-CIRBS, FoS,
IIU, Islamabad



Chairperson
Dr. Ikram Ullah
Assistant Professor
SA-CIRBS, FoS
IIU, Islamabad



Dean
Dr. Muhammad Irfan Khan
Faculty of Sciences
IIU, Islamabad,
Pakistan

بِسْمِ اللَّهِ الرَّحْمَنِ الرَّحِيمِ

A thesis submitted to Sulaiman bin Abdullah Aba Al-Khail Center for Interdisciplinary Research for Basic Sciences (SA-CIRBS), International Islamic University Islamabad, as a partial fulfillment of the requirement for the award of the degree of Doctorate in Philosophy in Biosciences

DECLARATION

I hereby declare that this Ph.D. thesis entitled “**Biosynthesis of Metal Nanoparticles of Selected Medicinal Plants and their Biological Activities**” is an independent work based on the research and experimental work carried out by me at **Sulaiman bin Abdullah Aba Al-Khail Center for Interdisciplinary Research in Basic Sciences, International Islamic University Islamabad**, Under the supervision of Prof. Dr. Masoom Yasinzai and this has not been submitted anywhere else for any other degree.

Date: _____



Asia Noreen
24-FBAS/PHDNS/F-15

FORWARDING SHEET BY RESEARCH SUPERVISOR

The thesis entitled "Biosynthesis of Metal Nanoparticles of Selected Medicinal Plants and Their Biological Activities" submitted by **Asia Noureen**, registration no. **24/FBAS/PHDNS/F-15** in partial fulfillment of PhD degree in Biological Sciences at Sulaiman Bin Abdullah Aba Al-Khail - Center for Interdisciplinary Research in Basic Sciences (SA-CIRBS), has been completed under my guidance and supervision. I am satisfied with the quality of student's research work and allow her to submit this thesis for further process to graduate with Doctor of Philosophy degree from Sulaiman Bin Abdullah Aba Al-Khail-Center for Interdisciplinary Research in Basic Sciences (SA-CIRBS), as per IIUI rules and regulations.

Prof. Dr. Masoom Yasinzai,

Dated: 19-8-2022

Sulaiman Bin Abdullah Aba Al-Khail - Center for Interdisciplinary Research in
Basic Sciences (SA-CIRBS),

International Islamic University, Islamabad.

DEDICATION

***Dedicated to my Beloved
Parents***

TABLE OF CONTENT

| Chapter # | Title | Page # |
|-------------------|--|----------|
| | Acknowledgments | i |
| | List of Abbreviations | ii |
| | List of Figures | iv |
| | List of Tables | xv |
| | Abstract | xviii |
| CHAPTER 1: | Introduction..... | 1 |
| 1.1 | Nanotechnology..... | 1 |
| 1.2 | Metal and Metal Oxide Nanoparticles..... | 2 |
| 1.3 | Synthesis of Nanoparticles..... | 2 |
| 1.4 | Methods for the Synthesis of Nanoparticles..... | 3 |
| 1.5 | Silver Nanoparticles (AgNPs)..... | 4 |
| 1.6 | Zinc Nanoparticles (ZnNPs)..... | 6 |
| 1.7 | Biological synthesis of Nanoparticles (NPs)..... | 8 |
| 1.8 | Green Nanotechnology..... | 9 |
| 1.9 | Plant as Remedy..... | 11 |
| 1.10 | Plant used for Nanoparticles synthesis..... | 12 |
| 1.11 | <i>Berberis lyceum</i> | 13 |
| 1.11.1 | Medicinal uses of <i>Berberis lyceum</i> | 14 |
| 1.12 | <i>Cinnamomum Zeylanicum</i> | 15 |
| 1.12.1 | <i>Medicinal Importance of Cinnamomum Zeylanicum</i> | 16 |
| 1.13 | Biosynthesis of nanoparticles from <i>Cinnamon zeylanicum bark extract</i> | 17 |

| | | |
|-------------------|--|-----------|
| 1.14 | Biosynthesis of nanoparticles from <i>Berberis lycium</i> <i>Roots</i> | 20 |
| 1.15 | Antimicrobial Activities..... | 21 |
| 1.16 | Antioxidant Activities..... | 24 |
| 1.17 | Leishmaniasis..... | 25 |
| 1.17.1 | Classification of <i>Leishmania tropica</i> | 25 |
| 1.17.2 | Epidemiology of <i>Leishmania tropica</i> | 25 |
| 1.17.3 | Stages of leishmania..... | 26 |
| 1.17.4 | Life cycle of Leishmania..... | 27 |
| 1.17.5 | Life Cycle..... | 28 |
| 1.17.6 | Drugs Leishmaniasis..... | 28 |
| 1.17.7 | Limitations of drugs..... | 29 |
| 1.18 | Nanoparticles inducing toxicity..... | 29 |
| 1.19 | Aim and Objectives..... | 30 |
| CHAPTER 2: | Materials and Methods | 32 |
| 2.1 | Collection of Plant Materials..... | 32 |
| 2.2 | Green synthesis of Silver nanoparticles of <i>Berberis</i> <i>lycium</i> roots and Berberine..... | 32 |
| 2.3 | Green synthesis of silver nanoparticles of <i>Cinnamomum</i> <i>zeylanicum</i> bark and Cinnamaldehyde..... | 33 |
| 2.4 | Green synthesis of Zinc Oxide nanoparticles of <i>Berberis</i> <i>lycium</i> roots and Berberine..... | 34 |
| 2.5 | Green synthesis of Zinc oxide nanoparticles of <i>Cinnamomum zeylanicum</i> and cinnamaldehyde..... | 34 |
| 2.6 | Optimization of nanoparticles..... | 36 |
| 2.6.1 | Concentrations of plant extracts, silver nitrate solution. | 36 |
| 2.6.2 | pH-Optimization..... | 36 |

| | | |
|-------------------|---|-----------|
| 2.6.3 | Temperature optimization..... | 37 |
| 2.6.4 | Time optimization..... | 37 |
| 2.7 | Characterization of the synthesized nanoparticles..... | 37 |
| 2.8 | Antibacterial Activity..... | 37 |
| 2.8.1 | Source and Maintenance of Microorganisms..... | 38 |
| 2.8.1.1 | Test microorganism..... | 38 |
| 2.8.1.2 | Culture Media..... | 38 |
| 2.8.2 | Growth Media..... | 38 |
| 2.8.2.1 | Nutrient broth..... | 38 |
| 2.8.3 | Inoculation of fresh bacterial culture..... | 39 |
| 2.8.4 | Preparation of Mcfarland Standard (0.5%)..... | 39 |
| 2.8.5 | Agar well diffusion for antibacterial susceptibility testing..... | 40 |
| 2.8.6 | Spectrophotometric assay (Determination of MIC)..... | 40 |
| 2.9 | Antifungal Activity..... | 41 |
| 2.9.1 | Fungal strains used..... | 41 |
| 2.9.2 | Disc diffusion assay for antifungal activity..... | 41 |
| 2.9.3 | Spectrophotometric assay (Determination of MIC)..... | 42 |
| 2.10 | Antioxidant Assay..... | 42 |
| 2.11 | Antileishmanial activity of AgNps and ZnNps against <i>Leishmania tropica</i> | 43 |
| 2.11.1 | Anti-Promastigotes Assay..... | 43 |
| 2.11.2 | Anti-amastigote Assay..... | 44 |
| 2.12 | Cytotoxicity of Nanoparticles on human blood cells..... | 44 |
| 2.13 | Statistical analysis..... | 45 |
| CHAPTER 3: | Results..... | 46 |

| | | |
|---------|---|-----|
| 3.1 | Green synthesis of silver nanoparticles..... | 46 |
| 3.2 | Optimization of nanoparticles..... | 46 |
| 3.2.1 | Concentrations of plant extracts, silver nitrate solution.. | 46 |
| 3.2.2 | pH optimization..... | 46 |
| 3.2.3 | Temperature optimization..... | 46 |
| 3.2.4 | Time optimization..... | 47 |
| 3.3 | Characterization of Nanoparticles..... | 47 |
| 3.3.1 | UV-Vis Spectroscopy..... | 47 |
| 3.3.1.1 | Silver nanoparticles..... | 47 |
| 3.3.1.2 | Zinc Nanoparticles..... | 50 |
| 3.3.2 | Fourier -Transform Infra-Red Spectroscopy (FT-IR).... | 52 |
| 3.3.2.1 | Silver Nanoparticles..... | 52 |
| 3.3.2.2 | Zinc Nanoparticles..... | 56 |
| 3.3.3 | XRD Analysis..... | 59 |
| 3.3.3.1 | Silver Nanoparticles..... | 59 |
| 3.3.3.2 | Zinc nanoparticles..... | 63 |
| 3.3.4 | Scanning electron microscopy (SEM) | 67 |
| 3.3.4.1 | Silver nanoparticles..... | 67 |
| 3.3.4.2 | Zinc Nanoparticles..... | 70 |
| 3.4 | Antibacterial Activity..... | 73 |
| 3.4.1 | Antibacterial assay of biologically synthesized Silver and Zinc Nanoparticles a giant <i>E. coli</i> strain (ATCC: 8739)... | 73 |
| 3.4.2 | Antibacterial assay of biologically synthesized Silver and Zinc Nanoparticles a giant <i>S. aureus</i> strain (ATCC: 6538).. | 88 |
| 3.5 | Antifungal Activity..... | 106 |

| | | |
|-------------------|--|------------|
| 3.5.1 | Antifungal assay of biologically synthesized Silver Nanoparticles against <i>Trichoderma herzianum</i> | 106 |
| 3.6 | Antioxidant activity..... | 115 |
| 3.6.1 | DPPH free radical scavenging activity (Spectro photometric method) | 115 |
| 3.6.2 | Silver Nanoparticle..... | 115 |
| 3.6.3 | Zinc Nanoparticles..... | 120 |
| 3.7 | Antileishmanial Activity of AgNPs against <i>Leishmania tropica</i> | 124 |
| 3.7.1 | Anti-promastigote Assay of AgNPs..... | 124 |
| 3.7.2 | Anti-promastigote Assay of ZnNPs..... | 126 |
| 3.7.3 | Anti-amastigote Assay of AgNPs..... | 128 |
| 3.7.4 | Anti-amastigote Assay of ZnNPs..... | 130 |
| 3.8 | Cytotoxic Activity..... | 132 |
| 3.8.1 | Assessment of cytotoxic effect of AgNPs in normal cell (Hemolytic assay) | 132 |
| 3.8.2 | Assessment of cytotoxic effect of ZnNPs in normal cell (Hemolytic assay) | 135 |
| CHAPTER 4: | Discussion..... | 137 |
| CHAPTER 5: | Conclusion and Future Aspects..... | 143 |
| CHAPTER 6: | References..... | 145 |

ACKNOWLEDGEMENT

Foremost, I want to thank Almighty **ALLAH** for making my goal into reality and helping me in the most difficult time of this journey. I sincerely wish to express my greatest gratitude to my supervisor Prof. Dr. Masoom Yasinzai for his guidance and sincere support.

I would like to acknowledge Dr. Ikram Ullah, Dr. Farhan Younas, Prof. Dr. Muhammad Riaz, Dr. Syeda Aaliya Shahzadi, Dr. Muhammad Tariq Rafiq, Dr. Waqar Un Nisa, Dr. Basharat Ali for their guidance and support. I would not be where I am today without all their help, guidance and support as “Their guidance always put me on the right way”. I also wish to express my feeling of gratitude to many people at each of the university where I conducted my research. To them, I owe the deepest gratitude and thanks.

Finally, I would like to thank my family for their support and sacrifice during this journey.

Asia Noureen
August 19th, 2022

LIST OF ABBREVIATIONS

| Words | Abbreviations |
|----------------------|---|
| Ag | Silver |
| AgCl ₂ | Silver cholride |
| AgNO ₃ | Silver Nitrate |
| AgNPs | Silver Nanoparticles |
| ATCC | American Type Culture Collection |
| AuNPs | Gold Nanoparticles |
| <i>B. lycium</i> | <i>Berberis lycium</i> |
| <i>C. zeylanicum</i> | <i>Cinnamomum zeylanicum</i> |
| C° | Degree centigrade |
| CC | Crystalline Cubic Structure |
| CFU | Colony-Forming Unit |
| CuO | Copper Oxoide |
| DNA | Deoxyribonucleic acid |
| DPPH | 1,1- Diphenyl-2-Picrylhydrazyl |
| <i>E. coli</i> | <i>Escherichia coli</i> |
| FT-IR | Fourier Transform Infrared Spectroscopy |
| FWHM | Full Width and Half Maximum |
| g | Gram |

| | |
|-------------------|----------------------------------|
| MIC | Minimum Inhibitory Concentration |
| mL | Milli Liter |
| mM | Milli Molar |
| mg | milligram |
| NPs | Nanoparticles |
| OD | Optical Density |
| PBS | Phosphate Buffer solution |
| rpm | Revolution Per Minute |
| <i>S. aureus</i> | <i>Staphylococcus aureus</i> |
| SD | Standard Deviation |
| SEM | Scanning Electron Microscope |
| UV- spectroscopy | Ultraviolet-Visible Spectroscopy |
| WHO | World Health Organization |
| XRD | X-ray Diffraction |
| Zn | Zinc |
| ZnNPs | Zinc Nanoparticles |
| ZnO | Zinc Oxide |
| ZnSO ₄ | Zinc sulphate |

LIST OF FIGURES

| Figure No. | Caption | Page No |
|-------------------|--|---------|
| Figure 1.1 | Various methods for the synthesis of nanoparticles..... | 4 |
| Figure 1.2 | Nanoparticles Reaction Mechanisms on Bacterial Cell..... | 23 |
| Figure 1.3 | Morphological forms of <i>Leishmania tropica</i> | 27 |
| Figure 1.4 | The life cycle of <i>Leishmania tropica</i> | 28 |
| Figure 1.5 | Nanoparticles inducing toxicity..... | 30 |
| Figure 2.1 | <i>B. lycium</i> root extract..... | 33 |
| Figure 2.2 | <i>C. zeylanicum</i> bark extract..... | 34 |
| Figure 2.3 | <i>C. zeylanicum</i> bark extract..... | 35 |
| Figure 2.4 | Formation NPs at different Concentration of plant extract, salt solutions and water..... | 36 |
| Figure 2.5 | McFarland Standard preparation..... | 39 |
| Figure 3.1 | UV-vis Spectrum of AgNPs synthesized in the presence of <i>B. lycium</i> root extract | 48 |
| Figure 3.2 | UV-Vis spectrum of AgNPs synthesized in the presence of berberine | 48 |
| Figure 3.3 | UV-Vis spectrum of AgNPs synthesized in the presence of <i>C. zeylanicum</i> bark extract | 49 |
| Figure 3.4 | UV-Vis spectrum of AgNPs synthesized in the presence of Cinnamaldehyde | 49 |
| Figure 3.5 | UV-Vis spectrum of ZnNPs synthesized in the presence of <i>B. lycium</i> root extract | 50 |

| | | |
|--------------------|---|-----------|
| Figure 3.6 | UV-Vis spectrum of ZnNPs synthesized in the presence of berberine | 51 |
| Figure 3.7 | UV-Vis spectrum of ZnNPs synthesized in the presence of <i>C. zeylanicum</i> bark extract | 51 |
| Figure 3.8 | UV-Vis spectrum of ZnNPs synthesized in the presence of Cinnamaldehyde | 52 |
| Figure 3.9 | FTIR spectra of AgNPs synthesized in the presence of <i>B. lycium</i> root extract | 54 |
| Figure 3.10 | FTIR spectra of AgNPs synthesized in the presence of berberine | 54 |
| Figure 3.11 | FTIR spectra of AgNPs synthesized in the presence of <i>C. zeylanicum</i> bark extract | 55 |
| Figure 3.12 | FTIR spectra of AgNPs synthesized in the presence of cinnamaldehyde | 55 |
| Figure 3.13 | FTIR spectra of ZnNPs synthesized in the presence of <i>B. lycium</i> root extract | 57 |
| Figure 3.14 | FTIR spectra of ZnNPs synthesized in the presence of berberine..... | 58 |
| Figure 3.15 | FTIR spectra of ZnNPs synthesized in the presence of <i>C. zeylanicum</i> bark extract | 58 |
| Figure 3.16 | FTIR spectra of ZnNPs synthesized in the presence of cinnamaldehyde | 59 |
| Figure 3.17 | XRD spectra of AgNPs synthesized in the presence of <i>B. lycium</i> root extract | 61 |
| Figure 3.18 | XRD spectra of AgNPs synthesized in the presence of berberine | 62 |

| | | |
|--------------------|--|-----------|
| Figure 3.19 | XRD spectra of AgNPs synthesized in the presence of <i>C. zeylanicum</i> bark extract | 62 |
| Figure 3.20 | XRD spectra of AgNPs synthesized in the presence of cinnamaldehyde | 63 |
| Figure 3.21 | XRD spectra of ZnNPs synthesized in the presence of <i>B. lycium</i> root extract | 65 |
| Figure 3.22 | XRD spectra of ZnNPs synthesized in the presence of berberine | 65 |
| Figure 3.23 | XRD spectra of ZnNPs synthesized in the presence of <i>C. zeylanicum</i> bark extract | 66 |
| Figure 3.24 | XRD spectra of ZnNPs synthesized in the presence of cinnamaldehyde | 66 |
| Figure 3.25 | Field emission scanning electron micrographs of AgNPs synthesized in the presence of <i>B. lycium</i> root extract (a) 100nm (b) 100nm 500nm | 68 |
| Figure 3.26 | Field emission scanning electron micrographs of AgNPs synthesized in the presence of Berberine (a) 100nm (b) 100nm (c) 500nm | 68 |
| Figure 3.27 | Field emission scanning electron micrographs of AgNPs synthesized in the presence of <i>C. zeylanicum</i> bark extract (a) 100nm (b) 100nm (c) 100nm | 69 |
| Figure 3.28 | Field emission scanning electron micrographs of AgNPs synthesized in the presence of Cinnamaldehyde (a) 100nm (b) 1 μ m (c) 100nm | 69 |
| Figure 3.29 | Field emission scanning electron micrographs of ZnNPs synthesized in the presence of <i>B. lycium</i> root extract (a) 1 μ m (b) 500nm (c) 100nm | 71 |

| | | |
|--------------------|---|----|
| Figure 3.30 | Field emission scanning electron micrographs of ZnNPs synthesized in the presence of Berberine (a) 100 nm (b) 1µm (c) 100nm | 72 |
| Figure 3.31 | Field emission scanning electron micrographs of ZnNPs synthesized in the presence of <i>C. zeylanicum</i> (a) 100 nm (b) 1µm (c) 100nm | 72 |
| Figure 3.32 | Field emission scanning electron micrographs of ZnNPs synthesized in the presence of Cinnamaldehyde (a) 100 nm (b) 1µm (c) 100nm | 73 |
| Figure 3.33 | Evaluation of antibacterial activity of AgNPs synthesized in the presence of <i>B. lycium</i> root extract via agar well diffusion method against <i>E. coli</i> ATCC # 8739 (Gram negative bacterial strain) | 77 |
| Figure 3.34 | Photographs of Zone of inhibition of AgNPs synthesized in the presence of <i>B. lycium</i> root extract against <i>E. coli</i> ATCC # 8739 (Gram negative bacterial strain)..... | 77 |
| Figure 3.35 | Evaluation of antibacterial activity of AgNPs synthesized in the presence of berberine via agar well diffusion method against <i>E. coli</i> ATCC # 8739 (Gram negative bacterial strain) | 78 |
| Figure 3.36 | Photographs of Zone of inhibition of AgNPs synthesized in the presence of berberine against <i>E. coli</i> ATCC # 8739 (Gram negative bacterial strain) | 78 |
| Figure 3.37 | Evaluation of antibacterial activity of AgNPs synthesized in the presence of <i>C. zeylanicum</i> bark extract via agar well diffusion method against <i>E. coli</i> ATCC # 8739 (Gram negative bacterial strain) | 80 |

| | | |
|--------------------|---|-----------|
| Figure 3.38 | Photographs of Zone of inhibition of AgNPs synthesized in the presence of <i>C. zeylanicum</i> bark extract against <i>E. coli</i> ATCC # 8739 (Gram negative bacterial strain) | 80 |
| Figure 3.39 | Evaluation of antibacterial activity of AgNPs synthesized in the presence of cinnamaldehyde via agar well diffusion method against <i>E. coli</i> ATCC # 8739 (Gram negative bacterial strain) | 81 |
| Figure 3.40 | Photographs of Zone of inhibition of AgNPs synthesized in the presence of Cinnamaldehyde against <i>E. coli</i> ATCC # 8739 (Gram negative bacterial strain) | 81 |
| Figure 3.41 | Evaluation of antibacterial activity of ZnNPs synthesized in the presence of <i>B. lycium</i> root extract via agar well diffusion method against <i>E. coli</i> ATCC # 8739 (Gram negative bacterial strain) | 83 |
| Figure 3.42 | Photographs of Zone of inhibition of ZnNPs synthesized in the presence of <i>B. lycium</i> root extract against <i>E. coli</i> ATCC # 8739 (Gram negative bacterial strain) | 83 |
| Figure 3.43 | Evaluation of antibacterial activity of ZnNPs synthesized in the presence of berberine via agar well diffusion method against <i>E. coli</i> ATCC # 8739 (Gram negative bacterial strain) | 84 |
| Figure 3.44 | Photographs of Zone of inhibition of ZnNPs synthesized in the presence of berberine against <i>E. coli</i> ATCC # 8739 (Gram negative bacterial strain) | 84 |
| Figure 3.45 | Evaluation of antibacterial activity of ZnNPs synthesized in the presence of <i>C. zeylanicum</i> bark extract via agar well diffusion method against <i>E. coli</i> ATCC # 8739 (Gram negative bacterial strain) | 86 |

| | | |
|--------------------|--|-----------|
| Figure 3.46 | Photographs of Zone of inhibition of ZnNPs synthesized in the presence of <i>C. zeylanicum</i> against <i>E. coli</i> ATCC # 8739 (Gram negative bacterial strain) | 86 |
| Figure 3.47 | Evaluation of antibacterial activity of ZnNPs synthesized in the presence of cinnamaldehyde via agar well diffusion method against <i>E. coli</i> ATCC # 8739 (Gram negative bacterial strain) | 87 |
| Figure 3.48 | Photographs of Zone of inhibition of ZnNPs synthesized in the presence of cinnamaldehyde against <i>E. coli</i> ATCC # 8739 (Gram negative bacterial strain) | 87 |
| Figure 3.49 | Evaluation of antibacterial activity of AgNPs synthesized in the presence of <i>B. lycium</i> root extract via agar well diffusion method against <i>S. aureus</i> ATCC: 6538 (Gram positive bacterial strain) | 91 |
| Figure 3.50 | Photographs of Zone of inhibition of AgNPs synthesized in the presence of <i>B. lycium</i> root extract against <i>S. aureus</i> ATCC: 6538 (Gram positive bacterial strain) ... | 91 |
| Figure 3.51 | Evaluation of antibacterial activity of AgNPs synthesized in the presence of berberine via agar well diffusion method against <i>S. aureus</i> ATCC: 6538 (Gram positive bacterial strain) | 92 |
| Figure 3.52 | Photographs of Zone of inhibition of AgNPs synthesized in the presence of berberine against <i>S. aureus</i> ATCC: 6538 (Gram positive bacterial strain) | 92 |
| Figure 3.53 | Evaluation of antibacterial activity of AgNPs synthesized in the presence of <i>C. zeylanicum</i> bark extract via agar well diffusion method against <i>S. aureus</i> ATCC: 6538 (Gram positive bacterial strain) | 94 |

| | | |
|--------------------|--|------------|
| Figure 3.54 | Photographs of Zone of inhibition of AgNPs synthesized in the presence of <i>C. zeylanicum</i> bark extract against <i>S. aureus</i> ATCC: 6538 (Gram positive bacterial strain) | 94 |
| Figure 3.55 | Evaluation of antibacterial activity of AgNPs synthesized in the presence of cinnamaldehyde via agar well diffusion method against <i>S. aureus</i> ATCC: 6538 (Gram positive bacterial strain) | 95 |
| Figure 3.56 | Photographs of Zone of inhibition of AgNPs synthesized in the presence of cinnamaldehyde against <i>S. aureus</i> ATCC: 6538 (Gram positive bacterial strain) | 95 |
| Figure 3.57 | Evaluation of antibacterial activity of ZnNPs synthesized in the presence of <i>B. lycium</i> root extract via agar well diffusion method against <i>S. aureus</i> ATCC: 6538 (Gram positive bacterial strain) | 97 |
| Figure 3.58 | Photographs of Zone of inhibition of ZnNPs synthesized in the presence of <i>B. lycium</i> root extract against <i>S. aureus</i> ATCC: 6538 (Gram positive bacterial strain) | 97 |
| Figure 3.59 | Evaluation of antibacterial activity of ZnNPs synthesized in the presence of berberine via agar well diffusion method against <i>S. aureus</i> ATCC: 6538 (Gram positive bacterial strain) | 98 |
| Figure 3.60 | Photographs of Zone of inhibition of ZnNPs synthesized in the presence of berberine against <i>S. aureus</i> ATCC: 6538 (Gram positive bacterial strain) | 98 |
| Figure 3.61 | Evaluation of antibacterial activity of ZnNPs synthesized in the presence of <i>C. zeylanicum</i> bark extract via agar well diffusion method against <i>S. aureus</i> ATCC: 6538 (Gram positive bacterial strain) | 100 |

| | | |
|--------------------|---|------------|
| Figure 3.62 | Photographs of Zone of inhibition of ZnNPs synthesized in the presence of <i>C. zeylanicum</i> bark extract against <i>S. aureus</i> ATCC: 6538 (Gram positive bacterial strain) | 100 |
| Figure 3.63 | Evaluation of antibacterial activity of ZnNPs synthesized in the presence of cinnamaldehyde via agar well diffusion method against <i>S. aureus</i> ATCC: 6538 (Gram positive bacterial strain) | 101 |
| Figure 3.64 | Photographs of Zone of inhibition of ZnNPs synthesized in the presence of cinnamaldehyde against <i>S. aureus</i> ATCC: 6538 (Gram positive bacterial strain) | 101 |
| Figure 3.65 | Comparison of IC ₅₀ value of AgNPs synthesized in the presence of (a) <i>B. lycium</i> root extract (b) Berberine (c) Cinnamaldehyde (d) <i>C. zeylanicum</i> bark extract against <i>E. coli</i> (ATCC # 8739) | 103 |
| Figure 3.66 | Comparison of IC ₅₀ value of ZnNPs synthesized in the presence of (a) <i>B. lycium</i> root extract (b) Berberine (c) Cinnamaldehyde (d) <i>C. zeylanicum</i> bark extract against <i>E. coli</i> (ATCC # 8739) | 104 |
| Figure 3.67 | Comparison of IC ₅₀ value of AgNPs synthesized in the presence of (a) <i>B. lycium</i> root extract (b) Berberine (c) Cinnamaldehyde (d) <i>C. zeylanicum</i> bark extract against <i>S. aureus</i> (ATCC: 6538) | 105 |
| Figure 3.68 | Comparison of IC ₅₀ value of ZnNPs synthesized in the presence of (a) <i>B. lycium</i> root extract (b) Berberine (c) Cinnamaldehyde (d) <i>C. zeylanicum</i> bark extract against <i>S. aureus</i> (ATCC: 6538) | 106 |
| Figure 3.69 | Evaluation of antifungal activity of AgNPs synthesized in the presence of <i>B. lycium</i> root extract via agar well diffusion method against <i>Trichoderma herzianum</i> (Fungal strain) | 109 |

| | | |
|--------------------|--|------------|
| Figure 3.70 | Evaluation of antifungal activity of AgNPs synthesized in the presence of berberine via agar well diffusion method against <i>Trichoderma herzianum</i> (Fungal strain) | 109 |
| Figure 3.71 | Photographs of Zone of inhibition of AgNPs synthesized in the presence of <i>B. lycium</i> root extract against <i>Trichoderma herzianum</i> (Fungal strain) | 110 |
| Figure 3.72 | Photographs of Zone of inhibition of AgNPs synthesized in the presence of berberine against <i>Trichoderma herzianum</i> (Fungal strain) | 110 |
| Figure 3.73 | Evaluation of antifungal activity of AgNPs synthesized in the presence of <i>C. zeylanicum</i> bark extract via agar well diffusion method against <i>Trichoderma herzianum</i> (Fungal strain) | 112 |
| Figure 3.74 | Evaluation of antifungal activity of AgNPs synthesized in the presence of Cinnamaldehyde via agar well diffusion method against <i>Trichoderma herzianum</i> (Fungal strain) | 112 |
| Figure 3.75 | Photographs of Zone of inhibition of AgNPs synthesized in the presence of <i>C. zeylanicum</i> bark extract against <i>Trichoderma herzianum</i> (Fungal strain) | 113 |
| Figure 3.76 | Photographs of Zone of inhibition of AgNPs synthesized in the presence of cinnamaldehyde against <i>Trichoderma herzianum</i> (Fungal strain) | 113 |
| Figure 3.77 | Comparison of IC ₅₀ value of AgNPs synthesized in the presence of (a) <i>B. lycium</i> root extract (b) Berberine (c) Cinnamaldehyde (d) <i>C. zeylanicum</i> bark extract against <i>Trichoderma herzianum</i> | 114 |
| Figure 3.78 | DPPH scavenging activity of AgNPs synthesized in the presence of <i>B. lycium</i> root extract | 116 |
| Figure 3.79 | DPPH scavenging activity of AgNPs synthesized in the presence of berberine | 117 |

| | | |
|--------------------|---|------------|
| Figure 3.80 | DPPH scavenging activity of AgNPs synthesized in the presence of <i>C. zeylanicum</i> bark extract | 118 |
| Figure 3.81 | DPPH scavenging activity of AgNPs synthesized in the presence of cinnamaldehyde | 119 |
| Figure 3.82 | DPPH scavenging activity of ZnNPs synthesized in the presence of <i>B. lycium</i> root extract | 121 |
| Figure 3.83 | DPPH scavenging activity of ZnNPs synthesized in the presence of berberine | 122 |
| Figure 3.84 | DPPH scavenging activity of ZnNPs synthesized in the presence of <i>C. zeylanicum</i> | 123 |
| Figure 3.85 | DPPH scavenging activity of ZnNPs synthesized in the presence of cinnamaldehyde | 124 |
| Figure 3.86 | Inhibitory concentration (IC ₅₀) of promastigotes of <i>L. tropica</i> at different concentration of AgNPs synthesized in the presence of (a) <i>B. lycium</i> root extract (b) Berberine (c) <i>C. zeylanicum</i> bark extract (d) Cinnamaldehyde..... | 126 |
| Figure 3.87 | Inhibitory concentration (IC ₅₀) of promastigotes of <i>L. tropica</i> at different concentration of ZnNPs synthesized in the presence of (a) <i>B. lycium</i> root extract (b) Berberine (c) <i>C. zeylanicum</i> bark extract (c) Cinnamaldehyde | 128 |
| Figure 3.88 | Inhibitory concentration (IC ₅₀) of Anti-amastigoates of <i>L. tropica</i> at different concentration of AgNPs synthesized in the presence of (a) <i>B. lycium</i> root extract (b) Berberine (c) <i>C. zeylanicum</i> bark extract (d) Cinnamaldehyde | 130 |
| Figure 3.89 | Inhibitory concentration (IC ₅₀) of Anti-amastigoates of <i>L. tropica</i> at different concentration of ZnNPs synthesized in the presence of (a) <i>B. lycium</i> root extract (b) Berberine (c) <i>C. zeylanicum</i> bark extract (d) ZnNPs Cinnamaldehyde..... | 132 |

| | | |
|--------------------|---|------------|
| Figure 3.90 | Hemolysis of AgNPs synthesized in the presence of <i>B. lycium</i> root extract and berberine on normal human blood cell..... | 134 |
| Figure 3.91 | Hemolysis of AgNPs synthesized in the presence of of <i>B. lycium</i> root extract and berberine on normal human blood cell | 134 |
| Figure 3.92 | Hemolysis of AgNPs synthesized in the presence of <i>C. zeylanicum</i> root extract and Cinnamaldehyde on normal human blood cell | 136 |
| Figure 3.93 | Hemolysis of ZnNPs synthesized in the presence of <i>C. zeylanicum</i> root extract and Cinnamaldehyde on normal human blood cell | 136 |

LIST OF TABLES

| Table No. | Title | Page No. |
|------------------|---|----------|
| Table 1.1 | Chemical ingredients of different parts of <i>B. lycium</i> plant (Ali et al., 2015) | 14 |
| Table 1.2 | Chemical ingredients of various fragments of cinnamon (G. K. Jayaprakasha <i>et al.</i> , 2002) (Vangalapati <i>et al.</i> , 2012). | 19 |
| Table 3.1 | Evaluation of antibacterial activities of different concentration of AgNPs synthesized in the presence of <i>B. lycium</i> root extract and berberine (n=3, results are expressed mean \pm SE) | 76 |
| Table 3.2 | Evaluation of antibacterial activities of different concentration of AgNPs synthesized in the presence of <i>C. zeylanicum</i> bark Extract and Cinnamaldehyde (n=3, results are expressed mean \pm SE) | 79 |
| Table 3.3 | Evaluation of antibacterial activities of different concentration of ZnNPs synthesized in the presence of <i>B. lycium</i> root extract and berberine (n=3, results are expressed mean \pm SE) | 82 |
| Table 3.4 | Evaluation of antibacterial activities of different concentration of ZnNPs synthesized in the presence of <i>C. zeylanicum</i> bark Extract and Cinnamaldehyde (n=3, results are expressed mean \pm SE) | 85 |
| Table 3.5 | Evaluation of antibacterial activities of different concentration of AgNPs synthesized in the presence of <i>B. lycium</i> root extract and berberine (n=3, results are expressed mean \pm SE) | 90 |

| | | |
|-------------------|--|------------|
| Table 3.6 | Evaluation of antibacterial activities of different concentration of synthesized in the presence of AgNPs of <i>C. zeylanicum</i> bark Extract and Cinnamaldehyde (n=3, results are expressed mean \pm SE) | 93 |
| Table 3.7 | Evaluation of antibacterial activities of different concentration of ZnNPs synthesized in the presence of <i>B. lycium</i> root extract and berberine (n=3, results are expressed mean \pm SE) | 96 |
| Table 3.8 | Evaluation of antibacterial activities of different concentration of ZnNPs synthesized in the presence of <i>C. zeylanicum</i> bark Extract and Cinnamaldehyde (n=3, results are expressed mean \pm SE) | 99 |
| Table 3.9 | MIC and IC50 of AgNPs and ZnNPs against <i>E. coli</i> | 102 |
| Table 3.10 | MIC and IC50 of AgNPs and ZnNPs against <i>S. aureus</i> | 102 |
| Table 3.11 | Evaluation of antifungal activities of different concentration of AgNPs synthesized in the presence of <i>B. lycium</i> root extract and berberine (n=3, results are expressed mean \pm SE) | 108 |
| Table 3.12 | Evaluation of antifungal activity of different concentration of synthesized in the presence of AgNPs of <i>C. zeylanicum</i> bark Extract and Cinnamaldehyde (n=3, results are expressed mean \pm SE) | 111 |
| Table 3.13 | Comparison of MIC and IC50 value of AgNPs synthesized in the presence of extract and compounds against <i>Trichoderma herzianum</i> | 115 |
| Table 3.14 | Effect of different concentrations of AgNPs synthesized in the presence of of <i>B. lycium</i> root extract on %Inhibition of DPPH..... | 116 |

| | | |
|-------------------|--|------------|
| Table 3.15 | Effect of different concentration of AgNPs synthesized in the presence of of berberine on % Inhibition of DPPH | 117 |
| Table 3.16 | Effect of different concentration of AgNPs synthesized in the presence of <i>C. zeylanicum</i> bark extract on % Inhibition of DPPH..... | 118 |
| Table 3.17 | Effect of different concentration of AgNPs synthesized in the presence of cinnamaldehyde on %Inhibition of DPPH | 119 |
| Table 3.18 | Effect of different concentration of ZnNPs synthesized in the presence of <i>B. lycium</i> root extract on %Inhibition of DPPH | 121 |
| Table 3.19 | Effect of different concentration of ZnNPs synthesized in the presence of berberine on %Inhibition of DPPH | 122 |
| Table 3.20 | Effect of different concentration of ZnNPs synthesized in the presence of <i>C. zeylanicum</i> bark extract on %Inhibition of DPPH | 123 |
| Table 3.21 | Effect of different concentration of ZnNPs synthesized in the presence of Cinnamaldehyde on %Inhibition of DPPH | 124 |

Abstract

Researchers from all around the world are now interested in metallic nanoparticles because of their unique antibacterial and anti-inflammatory characteristics. Sustainable green synthesis of metallic nanoparticles that uses less hazardous chemicals is constantly needed. Green synthesis of silver and Zn nanoparticles has been an important and innovative technology especially in the medical field and in the control of pathogenic microorganisms. Silver and Zinc nanoparticles were synthesized from *Berberis lycium* roots extract and their pure compound Berberine. Silver and Zinc nanoparticles from *Cinnamomum zeylanicum* bark extract and their pure compound Cinnamaldehyde were synthesized through green method. Optimal conditions for silver and Zn nanoparticles synthesis were obtained by varying the temperature, pH, concentration of AgNO_3 salt, concentration of ZnSO_4 salt, concentration of plant extracts, reaction time and concentration of pure compounds berberine and cinnamaldehyde. These NPs were characterized by various techniques i-e *UV-Visible* spectroscopy, Fourier transform infrared (FT-IR), X-ray diffraction analysis (XRD) and Scanning electron microscopy (SEM). The biological potential of the characterized NPs was assessed. The antibacterial activity results revealed that the biologically synthesized silver nanoparticles and zinc nanoparticles were active against Gram-negative bacterial strain (*E. coli*) and Gram-positive bacterial strain (*S. aureus*) and showed good antifungal activity against *Trichoderma herzianum*. 2,2-diphenyl-1-picrylhydrazyl (DPPH) radical scavenging activity (% inhibition) of the tested Nps at different concentrations was also measured. Considerable variations in antioxidant profile were recorded at different concentrations. Antileishmanial efficacy of biologically synthesized AgNps and ZnNps was assessed against *Leishmania tropica* KWH23 Promastigotes and Amastigotes. It was concluded that these NPs at low concentrations expressively killed the leishmanial cells and considered as the suitable candidates for the leishmania treatment. AgNPs and ZnNPs have the potential to be use as an effective drug for the treatment of fatal diseases. According to the results of the current study, AgNPs and ZnNPs of *B. lycium* root extract and Berberine, AgNPs and ZnNPs of *C. zeylanicum* bark extract and Cinnamaldehyde can be used as an effective antimicrobial drug with minimum toxicity.

**CHAPTER I:
INTRODUCTION**

INTRODUCTION

1.1 Nanotechnology

Nanotechnology is an innovative technology which offers potential applications in multidisciplinary zones of science (Thomé et al., 2015). Nanoparticles are the smallest particles with largest applications (Prathna et al., 2011). The nanotechnology is a reliable and environment friendly process for the development of nano scale particles ranging from 1-100nm (Ramya & Subapriya, 2012). Biosynthesis provides advancement over chemical and physical strategies because high temperature and dangerous chemicals are not required (Forough & Farhadi, 2010). Huge development in nanotechnology has opened up the novel basic and applied achievements in materials science and designing, for example, nanobiotechnology (Klefenz, 2004), bio-nanotechnology (Goodsell, 2004), quantum dots (Chan & Nie, 1998), surface-improved Raman dispersing (SERS) (Tian & Ren, 2004), and applied microbiology. In the past decades, attempts have been made to improve the biological process at sub-cellular levels for example, the association of the cell, self-duplicating, self-repairing mechanisms (Miyata et al., 2001). Nanobiotechnology can additionally be categorized into two classes; wet and dry nanobiotechnology. Wet nanotechnology includes the investigation and control of living bio frameworks while dry nanobiotechnology accords in vitro synthesis and characterization of nanoparticles i.e. nanobubbles, and so on (Mubarak et al., 2011). Different nano-technology based medical approaches are already in use (Krumov et al., 2009). Metal nanoparticles are intensively investigated in diagnosis and treatment due to their unique and feasible electrical, synergistic as well as optical properties. To improve the physical, chemical and optical properties of nano-sized metal nanoparticles, significant research is being done to improve the properties of the metal nanoparticles (Alivisatos, 1996; Bruchez Jr et al., 1998; Coe et al., 2002). Nano silver particles have a defined structure which make them intriguing for antimicrobial applications. They have extremely high activity against a wide spectrum of microorganisms and parasites even at micrograms level (Le Ouay & Stellacci, 2015).

1.2 Metal and Metal Oxide Nanoparticles

With the emergence of metal oxide nanoparticles, material science has been revolutionized. These are being used for the fabrication of fuel cells, sensors, microelectronic circuits, coverings for the preservation of surface area to prevent corrosion. Oxides of metal have capacity to sorbent certain environmental pollutants. Due to their very small size and highly dense edge or corner surfaces, metal oxide nanoparticles can possess unique chemical properties. A range of physical and chemical methods of preparation of nano-sized oxide particles have been developed. Among various metal oxides characterized so far, nano sized ZnNPs displays huge exciton binding energy (60meV) and comparatively massive band gap (-3.4eV), owing to such characteristics ZnNPs is considered to be most suitable candidate for developing Nano sensors, Nano optoelectronics, UV-detection and transistors (Chen et al., 2006). Many intriguing optical, electrical, and chemical features of semiconductor and noble metal nano clusters in the nanometer size system are size-dependent. These nanoscale materials have efficient and effective applications in the field of fabricating optoelectronic as well as nano-sensors based nano devices. In the last few years, an efficient and potential research area is created that is based on the fabrication and functionalization of various nano-shaped nanoparticles. The optical properties of nano-size and shape-dependent metal nanoparticles have a significant application in the field of photobiology and photochemistry to investigate their role in accelerating light-induced chemical reaction processes (Kamat, 2002).

1.3 Synthesis of Nanoparticles

Metal nanoparticles are comprehensively studied due to their distinctive electrical, physical, optical, and catalytic properties. Various methodologies have been developed such as chemical, physical and biological to synthesize metal nanoparticles by following different synthesis procedures including electrochemical reduction, photochemical reduction, chemical reduction, heat evaporation, etc. Since nanoparticles usually aggregate after synthesis, surface passivator reagents are typically required to stop the aggregation. Various organic passivators which are used includes: mercapto acetate, thiophenol, and so on seemed to be highly toxic compounds, and if they produced on a large-scale pollute the environment and hazardous to human health concerned (Nayak et al., 2011). Although, chemical and

physical methods are famous for nanoparticle synthesis, but in biological synthesis, the use of toxic compounds is limited for the synthesis of less toxic, chemically safe, and environment friendly nanoparticle. These techniques are now catching extra interest due to their naturalness and versatility of the procedure (Li et al., 2011).

1.4 Methods for the Synthesis of Nanoparticles

Biosynthesis of nanoparticles has received considerable attention because of the growing need to develop environment friendly synthesis processes. Instantaneously, a pivotal consideration has been made for the biosynthesis of inorganic nanomaterial's such as metal nanoparticles by using various sources of microorganisms (Bar et al., 2009). The synthesis procedure of these metal nanoparticles has been chiefly documented. Furthermore, among all nanoparticles, silver nanoparticles have been playing a potential role in the field of life science particularly in biomedicine, agriculture, food chemistry, and biomedicine, and also act as a dopant in cosmetics and photo catalysis field. Moreover, they have also been utilized in optical, electrical as well as catalytic mechanisms. Various techniques have been potentially designed for the fabrication of silver nanoparticles including biochemical, physical, and chemical methods, respectively. Green chemistry in which natural molecules such as glucose, chitosan, soluble starch, and certain microorganisms, among others are used, have gained great study attention as safer alternatives, reducing and stabilizing agents to produce the silver nano-sphere. Nanoparticles synthesis follows the biological process by using various plant extracts which act as capping and reducing agents, concerned great consideration, due to sustaining an eco-friendly mechanisms during the overall process (Ashokkumar et al., 2014).

Extremely ionic metal oxide nanoparticles including zinc oxide nanoparticles ZnNPs possess exclusive features by which they could easily produce huge surface area with an exceptional crystalline morphology (Klabunde et al., 1996). Zinc oxide nanoparticles showed a larger extent of temperature tolerance and selectivity, and superior durability, respectively (Padmavathy & Vijayaraghavan, 2008).

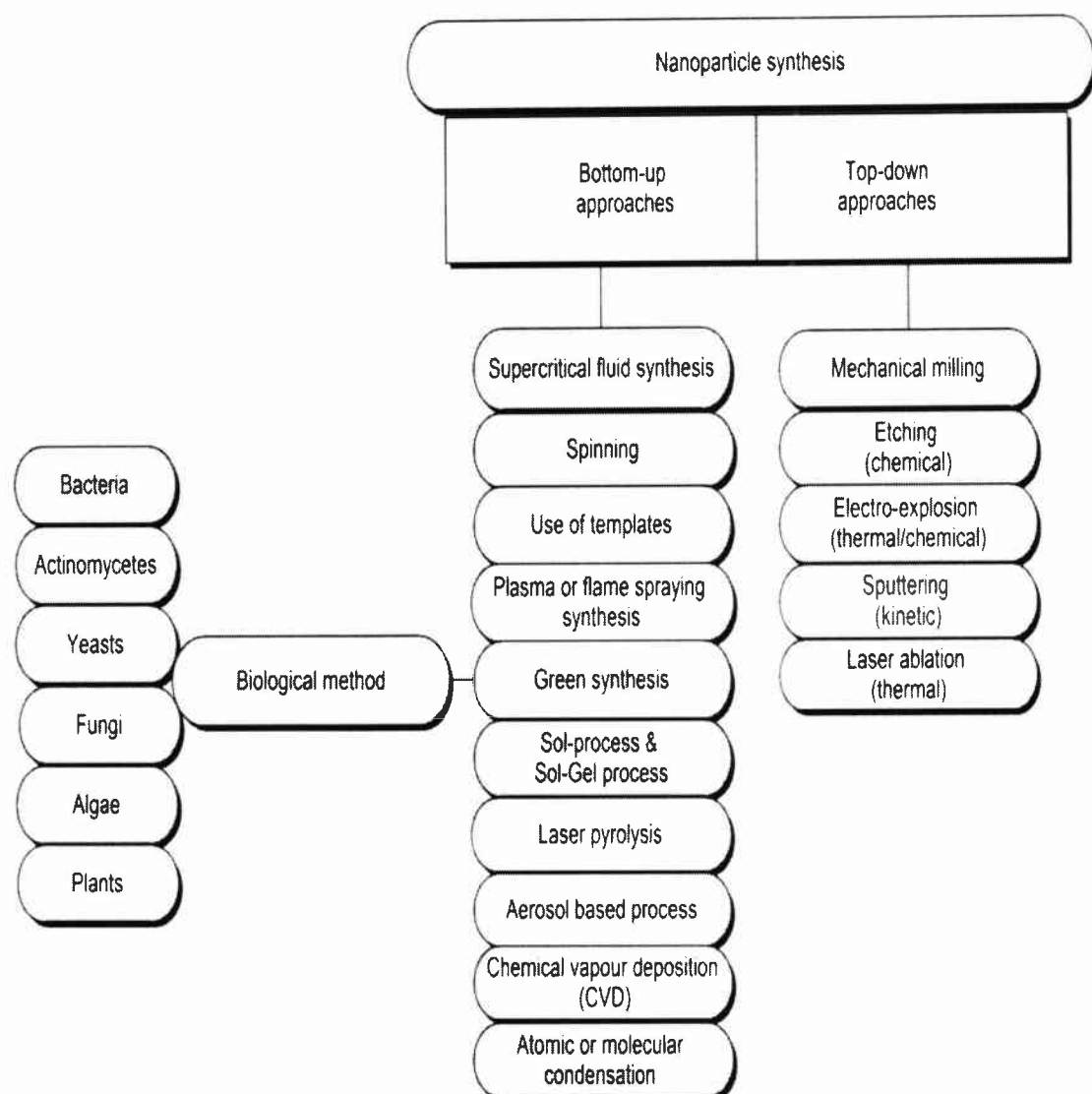


Figure 1.1: Various methods for the synthesis of nanoparticles

1.5 Silver Nanoparticles (AgNPs)

Silver is one of the most fundamental components of our world. Silver itself does not dissolve in water, yet metallic salts, for example, AgNO_3 and AgCl_2 are soluble in water (WHO, 2002). Among all the synthesis approaches for nanoparticles, silver is important due to their contribution in life sciences especially in the food chemistry (Li et al., 2010), cosmetics (Kokura et al., 2010), biomedicine (Chaloupka et al., 2010), agriculture (Park et al., 2006), and as a dopant in photoactinic activity's (Subash, Krishnakumar, Pandiyan, et al., 2013; Subash, Krishnakumar, Swaminathan, et al., 2013; Subash et al., 2012). Metallic Ag is used for operating prosthesis. Soluble silver mixtures, for instance, silver wires, have been used for treating epilepsy, nicotine

development, digestive problems and overwhelming diseases i.e., syphilis and gonorrhoea (Gulbranson et al., 2000).

Comprehensively, it is well documented that silver-based nanoparticles and silver ions are toxic to all microorganisms including 16 bacterial species (Slawson et al., 1992; Zhao & Stevens, 1998). The characteristic features of silver metal make it an excellent choice and have a significant role in the research and medical areas. Silver (Ag) is used in the form of nitrate to enhance the anti-microbial effect, but when the synthesized silver nanoparticles are being used, there is an increase in the outer part area of the microbial species to be exposed easily. Although, silver nanoparticles have a tremendous role in various antibacterial applications, however, interaction of the silver metal with microbes is not fully understood yet. Therefore, it has been hypothetically approved that silver nanoparticles caused cell inhibition, cell transduction, and cell lysis, respectively. Furthermore, many mechanisms have been reported that are involved in cell growth inhibition and cell lysis (Prabhu & Poulouse, 2012). The chemistry of silver showed that it is a soft acid, and an acid has the natural capability to interact with base, hence a soft acid reacts with a soft base (Morones et al., 2005). The majority of the cells are made up of phosphorus and sulfur which are soft bases in nature. The mechanism and action of these nanoparticles on the cell surface cause the reaction and the result leads to cell apoptosis. Interestingly, the DNA molecule is made up of phosphorus and sulfur. Hence, the silver nanoparticles can strongly act on these intercalating bases and destroy the DNA molecule and at the end, cell death may occur (Hatchett & White, 1996). Silver nanoparticles interact with phosphorus and sulfur backbone of the DNA and initiate many problems in the process of DNA replication in bacteria and microbes and thus terminate all the DNA replication process (Shrivastava et al., 2007).

AgNPs have enormous applications in all the fields of life sciences including food chemistry (Li et al., 2010), biomedicine (Chaloupka et al., 2010), agriculture (Park et al., 2006), as a dopant in photocatalysis field, and cosmetics (Kokura et al., 2010). AgNPs also have the respective electrical, optical, catalytic properties (Cao & Liu, 2008). Various procedure for the fabrication of AgNPs includes chemical, physical as well as biochemical methods being widely used (J. Huang et al., 2007). With an increasing focus on green chemistry, natural compounds such as glucose (Raveendran

et al., 2003), chitosan (Li et al., 2011), soluble starch (El-Rafie et al., 2011), and some microorganisms (Shahverdi et al., 2007; Vigneshwaran et al., 2006) have been of significant research interest as stabilizing and reducing agents, and safer alternatives to fabricate silver nanosphere. Silver nanoparticles are synthesized through biochemical reactions, using plant extracts which act as capping and reducing agents and have seemed much effective and efficient among others because it has the ability to stabilizing the aseptic environment during the whole process (Basavaraja et al., 2008; Gardea-Torresdey et al., 2002; Prathna et al., 2011). The fabrication of silver nanoparticles (AgNPs) by utilizing the phytochemicals transformation process in the test tube offers a crucial role due to the presence of functional groups on various phytochemicals that increases the reduction of silver ions and turned into the silver element. The synthesis of functionalized AgNPs depends on plant-derived methods by following Zingiber officinale root extract (Velmurugan et al., 2014), soybean (Sasikala et al., 2012), sacha inchi oil (Kumar et al., 2014), agricultural wastes (Kumar et al., 2014), and leaves (Kumar et al., 2014), respectively. Citrus sinensis peel extract (Kaviya et al., 2011), edible mushroom extract (Philip, 2009), clove extract (Vijayaraghavan et al., 2012) and extracts from Passiflora tripartite (Kumar, Smita, et al., 2015), are extensively gained popularity. Substantially, due to accelerating and forthright synthesis, interacting with functional groups, and ease of stability for targeting host, AgNPs have possesses enormous applications against antifungal species (Wiley et al., 2006), Antibacterial (Sondi & Salopek-Sondi, 2004), Anti-inflammatory (Nadworny et al., 2008), Antiviral (Elechiguerra et al., 2005), antiangiogenesis (Gurunathan et al., 2009) etc.

1.6 Zinc Nanoparticles (ZnNPs)

In contrast with natural materials, inorganic materials, for example, ZnO has unrivaled resilience, more prominent choosiness, and warmth resistance. The characteristics features of Zinc which is a mineral component are being utilized for everyday life, however, the ZnNPs have a biological compatible nature with human cell lines (He et al., 2011).

The zinc and its derivative compounds are chiefly being used as fungicides (Waxman & Bahcall, 1998). But it is very challenging to control the growth of fungal because fungal growth has itself resistance towards various conventional fungicides

includes: dicarboximides, and benzimidazoles, respectively (Elad et al., 1992). To prevent this resistance, new antifungal medications must be investigated, as they may be able to replace present control strategies. Nanoparticles (NPs) have got a lot of interest in recent years because of their unique physical and chemical features that set them apart from their traditional ones (Stoimenov et al., 2002). More recently many researchers and their colleagues reported in their findings that antimicrobial properties of various synthesized NPs such as copper (Cioffi et al., 2005), silver (Kim et al., 2007; Kumar et al., 2008), and zinc oxide (Liu et al., 2007), respectively. However, Zinc NPs also possesses tremendous applications and act as an antimicrobial agent. Additionally, it is also reported by the previous findings that smaller sized fabricated ZnNPs showed great potential towards antimicrobial activity (Matsunaga et al., 2001). According to Brayner et al. (2006) preliminary research suggests that the antibacterial activity of ZnNPs is linked to the generation of free radicals on the surface of the NPs, as well as free radical damage to the lipids in bacterial cell membranes, which leads to leakage and collapse of the bacterial cell membrane. Diabetes mellitus is a metabolic disease that is recognized by high blood glucose levels and is one of the most five causative agents of human death concerned. Therefore, Zinc has been testified to show a significant and efficient work in glucose homeostasis and also treated for the cure of diabetes therapy.

The compound Zinc is an essential micronutrient that is linked with more than 300 enzymes and performs an essential role in various biological mechanisms such as glucose metabolism. The action of Zinc increases hepatic glycogenesis through the insulin signaling pathway and therefore, enhances glucose utilization. Reduction in glucose absorption by intestinal cells and an increase in the glucose uptake level by adipose and skeletal muscle tissues also imparts the fluctuation and lowering of blood glucose levels. Interestingly, through various pieces of literature, it is reported that Zinc reduces glucagon secretion, and therefore, also reducing the process of glycogenolysis as well as gluconeogenesis, respectively.

Zinc nanoparticles reduces waste products that eventually most imperative to atomically defined molecular development with fewer waste products. It works as catalytic agent with better efficiency in existing manufacturing methods by eliminating or minimizing the usage of toxic constituents for pollution reduction. Like air and

water, fuel cells and solar are the alternative energy products. The objective of nanotechnology is to minimize the size gap among the minimum lithographically developed structures and chemically synthesized large fragments (Wilkinson et al., 2004).

ZnNPs can be easily synthesized through physical and chemical methods and it is also biocompatible, biodegradable, and nontoxic in nature, therefore can also be utilized in medical industry and environmental science (Stoimenov et al., 2002). Currently employed methods for the production of ZnNPs include; thermal decomposition (Lin et al., 2005), pulsed laser deposition (PLD) (Chen et al., 2006), thermal evaporation (Masaki & Kim, 2003), reactive electron beam evaporation (Wu et al., 2002), ion implantation (Wang et al., 2005), and sol-gel method (Vafae & Ghamsari, 2007). Synthesis of size-controlled ZnO nanoparticles and exploring their potentials is a major concern for the scientists working in respective field. In cancer therapy, drug delivery and in medicines, nanoparticles are widely used (Delavari & Hashemabadi, 2014). ZnNPs have been successfully tried for the treatment of cancer and diabetes. Now they are tried on leishmaniasis to check their efficacy on leishmanial cells. ZnNPs are newly emerging and promising therapeutic endeavor that can kill tumor cells with minimal effect on the normal cells (Hanley et al., 2008) unlike micron-sized particles with zilch effect on tumor cells. Consideration of zinc nanoparticles, as applicable novel strategy for treating common liver tumor owing to their promising preclinical anticancer efficacy in HCC is proposed by (Hassan et al., 2017).

Several chemical and physical methods were used for stabilizing and synthesizing zinc oxide nanoparticles. For the manufacture of zinc oxide nanoparticles, recognized chemical methods such as chemical reduction employing a wide range of inorganic and organic reducing agents, physicochemical reduction, electrochemical procedures, and radiolysis are commonly applied. Also, zinc nanoparticles strongly prevent or resist a microorganism (Waghmare et al., 2011).

1.7 Biological synthesis of Nanoparticles (NPs)

Nowadays, biological synthesis is preferred as the most efficient method because possesses following characteristics such as: cheap, eco-friendly, and safe and

do not involve any toxic reagents or by-product (Gade et al., 2010). In contrast to plants, the fabrication of microbial-mediated nanoparticles is not affected by seasonal or geographical fluctuations, by mitigating the following biological properties, and inconsistent morphologies, various studies from literature reported on the synthesis of AuNPs which investigating the pathogenic and non-pathogenic behavior of supplemented supernatant or bacterial cells such as *Enterobacter spp*, *Pseudomonas aeruginosa*, *Klebsiella pneumonia*, and *Bacillus spp*, respectively (Kumar et al., 2008; Kumar, Kumari, et al., 2015; Mokhtari et al., 2009; Shahverdi et al., 2007). Nanoparticles are synthesized by microorganisms by following extracellular or intracellular method. The synthesis of NPs followed by the extracellular method has more advantages compared to the intracellular method because in the extracellular method the recovery stages are easier and cheaper whereas the intracellular method requires additional recovery stages.

ZnNPs are used enormously due to their physical properties, small size, and orientation, apparently which are revealed to alter the performance of other tiny materials that are in contact with these particles. Several approaches can be used to prepare these particles; biological, chemical, and physical. The biological approach is considered as the most emerging approach because other methods are more complicated than this method, little time consuming and environment friendly (Fedlheim & Foss, 2001). Consequently, the synthesis of AgNPs through plant-based methods abundantly growing in popularity. Owing to the straight-arrow fabrication process, ease of intercalating functional group, stability, and targeting capabilities, AgNPs have possesses tremendous application due to its outstanding significance (Kumar, Kumari, et al., 2015). In contrast to all metal nanoparticles, the fabrication of synthesized nanoparticles (AgNPs) by following phytochemicals transformations in test tube perform an extraordinary role, because the presence of various functional groups on the phytochemicals increases the reduction of silver ions to elemental silver metal.

1.8 Green Nanotechnology

‘Green nanotechnology’ depicts as a state-of-the-art, outstanding, and eco-friendly technology in nature. It tunes and governs the nanotechnology’s principles by controlling the matter and shape of the world that varies from ‘atom to atom’ into a

green environment. Therefore, we come across a new green nano world in which the process of production is optimized, and based on the waste-free method is now becomes a useful possibility. Hazardous wastes that pave their ways by entering into the environment can be easily identified and erased without any trace (Schwarz, 2009).

Synthesis, involving bio-organisms, particularly plants that exude the reaction's functional chemicals, is in line with green chemistry principles (i) reducing agent, (ii) eco-friendly nature (iii) capping agent involved in the reaction, respectively (Gardea-Torresdey et al., 2003). This is a biologically and environmentally safe technology, since no toxic chemicals are used, and much easier than chemical and physical synthesis of metallic nanoparticles. In addition, High temperature and pressure is not required for this method. Plants are relatively more suitable for green synthesis than microorganisms because they don't require artificial culture media for their maintenance; secondly their production can be easily scale up to obtain required products (Jones et al., 2011).

The synthesis procedure of metal nanoparticles, more specifically AgNPs using plant extract has become a major concern for the scientists due to its potential stability and has an outstanding application in biological imaging, drug delivery, gene silencing, antimicrobial, and chemical sensing, respectively (Wei & Qian, 2008). Instantly, silver ions are reduced by electrochemical radiation, photochemical methods, chemical, biological methods, and Langmuir-Blodgett, respectively. Including the above-mentioned methods, biological synthesis is not only an effective way to synthesize nanostructure nanomaterial but also have a steady way to mitigate the use of newly originated toxic agents and compounds that are hazardous to the environment and also human health concerned. This method makes it simple and convenient to make a variety of inorganic nanoparticles (Li et al., 2007).

Green synthesis of ZnNPs offers huge benefits; these are also compatible for several biomedical applications and in pharmaceutical industry (Raveendran et al., 2003). In a short time interval huge number of nanoparticles can be synthesized by chemical method. In this technique, capping agent is required for size stabilization. Chemicals used for size stabilization and nanoparticles synthesis are lethal and lead to non-eco-friendly consequences. The need for environment friendly protocols for synthesis of nanoparticles is the reason of the interest in biological methods which are environment friendly (Fedlheim & Foss, 2001).

When the main reactions occurring during the biosynthesis of nanoparticles i.e., oxidation/reduction, the approach being employed is termed as a bottom-up approach. Phytochemicals produced from plant extracts or microbial enzymes having reducing and antioxidant capabilities that are usually concerned in the conversion of metallic compounds into the respective nanoparticles. In order to proceed with an effective synthesis procedure, three main steps must be considered: including the selection of naturally reducing agent, a suitable bio friendly solvent and a non-toxic stabilizing agent for nanoparticles. Organic solvents have heavily been used in most of the synthesis processes reported so far. Capping agents might be used due to their hydrophobic nature (Raveendran et al., 2003). Organisms are the most suitable and compatible choice for biosynthesis because they are eco-friendly, has good reducing capacity and can act as stabilizers or capping agents (Li et al., 2007).

Chemical method might lead to the absorption of certain chemo toxins to the surface of nanoparticles, that when delivered in the living body, might cause adverse side effects (Parashar et al., 2009). In contrast, biologically synthesized nanoparticles are quite safe and do not pose such issues as they are biocompatible and eco-friendly, thus very suitable for pharmaceutical applications.

1.9 Plant as Remedy

Mostly, plants are preferred by humans for remedies due to their strong belief that plants have been created to provide mankind with food, medical aid and other benefits. It is estimated by WHO that 80 % population of world out of 5.2 billion people who live in less developed countries used and strongly rely for their primary health needs on such traditional medicinal plants, their parts and extracts (WHO, 2016). Out of many, one of the requisites for the achievement of primary health attention is the accessibility and usage of appropriate drugs or medication. Commonly plants are always a source of easy and cost-effective medication, whether in the form of pure energetic principal agents or traditional preparations (Al-Snafi, 2013, 2015).

Plants play a leading role in the energy balances and environmental ecosystem by supplying food and oxygen for all living organisms. Due to the increasing complexities in our natural ecosystems by the interference of man and global environmental changes the pathogens are becoming more resistant and complex due to

frequent mutations, which have resulted in extreme consequences like treatment failure. Natural products were discovered as an alternate to synthetic antibacterial agents (Shinwari et al., 2015). As a consequence of global environmental changes and complexities aroused due to man's interference in natural ecosystem, the pathogens are adopting more resistance and getting complex due to frequent mutations due to horizontal gene transfer. The worst consequence of this problem is complete failure of treatment. Thus, exploring natural products as an alternate to synthetic antibiotics is the basic demand of the present time. Nanoparticles due to their high penetration ability and functional strategies are opening new promising ways not only for medical applications but for other industries as well (Jeambey et al., 2009).

1.10 Plant used for Nanoparticles synthesis

There are many advantages of using plant extracts for the green synthesis of nanoparticles because they are quite safe, easily available, and own a massive diversity of metabolites that might support reduction reactions. Several plants are currently examined for their ability to synthesize nanoparticles. The live alfa alfa plants have been employed in the synthesis of gold nanoparticles, and the range of nanoparticles is from 2-20nm (Gardea-Torresdey et al., 2003; Gardea-Torresdey et al., 2002). Recently, AuONPs were synthesized by using the leaf extract of and *Diopyros lcaki* in addition to *Magnolia Kobus*. Temperature directly effects on nanoparticle formation process, it was stated that, at lesser temperature poly-disperse particles were formed in the range of 5-300nm while at high temperature relatively small and mono dispersed spherical particles were formed (Song et al., 2009).

In addition, nanoparticles of zinc, silver, copper, cobalt, and nickel have also been manufactured inside the plants of *Medicago saliva* (Alfa alfa), *Brassica juncea* (Indian mustard), *Annus* (Sunflower), and *Helianthus*. Several plants are recognized as hyper accumulators due to their capacity to accumulate higher metal concentrations relative to others and such plants. Among the plants examined to date, *Brassica juncea* showed to possess much better metal accumulating capacity and assembles it into nanoparticles quite effectively (Bali et al., 2006). Recently researchers have been focused on exploring the role of plants in the reduction of metallic nanoparticles and respective phytochemicals (Jha et al., 2009).

It has been reported that bacteria and fungi need a relatively long time for incubation to reduce ions (metallic), whereas water solvable phytochemicals do the same in a short period. Thus, plants are suitable candidates for the synthesis of nanoparticles as compared to bacteria and fungi. On industrial scale, plant tissue culture techniques and other processing techniques can be employed to synthesize metallic nanoparticles as well as metal oxide nanoparticles.

1.11 *Berberis lycium*

| | |
|-----------------|-------------------------------------|
| ➤ Kingdom | Plantae – Plants |
| ➤ Subkingdom | Tracheobionta – Vascular plants |
| ➤ Superdivision | Spermatophyta – Seed plants |
| ➤ Division | Magnoliophyta – Flowering plants |
| ➤ Class | <u>Magnoliopsida</u> – Dicotyledons |
| ➤ Subclass | Magnoliidae |
| ➤ Order | Ranunculales |
| ➤ Family | Berberidaceae – Barberry family |
| ➤ Genus | <i>Berberis</i> L. – barberry |

B. lycium Royle belongs to the family *Berberidaceae* and is considered to be a threatened remedial plant species worldwide. This semi-deciduous plant can be seen in the hilly areas of Kashmir valley and North-western Himalayan region of Asia. In past, *Berberidaceae* family members were well-known for their therapeutic properties and were a component of British and sub-continent pharmacopeias (Imanshahidi & Hosseinzadeh, 2008; Sharma et al., 2009). *Berberis lycium* is a kind of erect shrub with a thick woody shoot and mainly grows to a height of about 3 meters, with thin brittle bark (Hooker, 1882).

Previously reported literature on this plant investigated that this plant upon isolation showed the presence of various types of secondary metabolites such as steroids and alkaloids. Most of the biologically significant, active, and isolated chemical compounds are berberine, palmatine (Balandrin et al., 1993), Berbamine (Khan et al., 1969), Aromoline, Oxyacanthine, Umbellatine (Hamidulla et al., 2003), β -sitosterol (Ali & Sharma, 1996), Punjabine, Balochistanamine, oxyberberine (Krane & Shamma, 1982), berberine chloroform and palmatine chloroform, respectively

(Miana, 1973). Berberine, an isoquinoline alkaloid extracted from the roots and bark, is the most important and major phytochemical among them. The antioxidant and proapoptotic effects of berberine and palmatin alkaloids isolated from *B. lycium* have been documented (Jamwal et al., 2016). The chemical Berberine and its correspondent derivatives showed an organic class of organic cations, that is derived from various generic plants of Berberis, Mohania, and Coptis, respectively. These chemicals have represented a broad application of anticarcinogenic, antimicrobial, and antimutagenic activity, respectively (Chiang & Hanssen, 1977; Chopra & Chopra, 1994). According to (Bhardwaj & Kaushik, 2012) Berberine has been identified as the predominant active ingredient in practically all Berberis species. Berberine is abundant in *B. lycium* root. Berberine was discovered to be 80 percent dry weight in the root extract of *B. lycium*, with only trace levels of other alkaloids present (Gulfraz et al., 2008).

Table: 1.1 Chemical ingredients of different parts of *B. lycium* plant (Ali et al., 2015)

| Parts of the plant | compounds |
|--------------------|-----------------|
| Root | Palmatine: 3.1% |
| | Berberine: 4.5% |
| | Vitamin C: 0.3% |
| Fruit | Berberine: 2.9% |
| | Vitamin C: 0.8% |

Andola et al. (2010) have found 4.0 percent berberine in *B. lycium* roots and 2.8 percent berberine in stem bark. In Pakistan, the *Berberis lycium* species also possesses outstanding significance and also utilized as a household remedy for the cure of many diseases.

1.11.1 Medicinal uses of *Berberis lycium*

Berberis lycium is the most famous plant being widely used due to its significant medicinal properties. The synthetic method for the use of this medicinal plant is as follows: boil the roots and bark in water. The boiled water containing root and bark extract is strained appropriately and again boiled till the semi-solid thick mass termed as "Rasaut" obtained. The obtained root and bark extract is being used to treat various diseases includes urinary tract infection, spleen, liver disorders, and gastric and duodenal ulcers, respectively. The obtained extract when mixed with alum and butter is used as an external remedy for the cure of eyelids for acute conjunctivitis.

Sustainably, camphor which is an ointment is used for skin infections, pimples, and acne, respectively (Chauhan, 1990; Chiang & Hanssen, 1977).

The foremost biological activities are ascribed by the use of its principal fundamental component, berberine (alkaloid) which is the extracted secondary metabolites. The properties of this compound are bitter and chiefly governs the Rasaut distasteful taste. To make it more tasteful and pleasant, sometimes Rasunt is mixed with maize and sugar like a meal. This mixture upon cooking termed as "Halva". The cooked Halva is routinely used as a remedy for a long period to treat rheumatic patients (Hasan et al., 2007).

The surrounding areas also consumed the dried and powdered mass of barks and roots when mixing with molten animal fat to treat bone fractures and for bandage purposes. Indochina's people consumed the fruit mass and used it as a natural medicine to treat and cure renal diseases. For teeth and gum illnesses fruit juice extract is most efficiently used. Additionally, for the treatment of cold, and typhoid the decoction of the fruit is also effectively used (Shah & Khan, 2006).

The stems and the extracted biomass are also consumed and have an adverse effect to treat for various disorders includes diarrhea, stomach pain, jaundice as well as in the reduction of melanohialdehyde (MDA) (Ahmad et al., 2010). Similarly, barks also have adequate and effective effects on wound healing (Asif et al., 2007). Subsequently, leaves are used as a tea representative agent. And fruits in the form of berries in fresh or dried form are also being used. The whole plant is used by the population is used for the cure of broken bones, internal injuries, swollen and sore eyes, ulcer, as well as rheumatism, respectively (Khan et al., 2010).

1.12 *Cinnamomum Zeylanicum*

Cinnamomum originates from the Greek kinnamomon, Malaysian, and Indonesian Kayu Manis, which implies "sweet wood". Common cinnamon is appropriately used to "real cinnamon" or its equivalent word *Ceylon cinnamon* (*Cinnamomum Verum*, *C. zeylanicum*). Cinnamon bark is broadly utilized as a zest and enhancing Specialist. Cinnamon is said in the Bible and Chinese writing composed 4000 years back (Leung & Foster, 1996).

Scientific classification

- Kingdom: Plantae
- unranked: Angiosperms
- unranked: Magnoliids
- Order: Laurales
- Family: Lauraceae
- Genus: *Cinnamomum*
- Species: *C. zeylanicum*

Common Names

- Arabic: دارسين Dâr sînî
- Bengali: দাড়চিনি Darchini.
- English: Bastard cinnamon, Cassia bark, Chinese cinnamon,
- Urdu: دارچینی, پات نیج

1.12.1 Medicinal Importance of *Cinnamomum Zeylanicum*

Cinnamon is a typical flavor utilized by various societies around the globe during different time periods. It is extracted from the innermost part of the bark from the *Cinnamomum* specie, which is an evergreen tree and has two independent varieties; *Cinnamon cassia* (CC), other names (*Cinnamomum aromaticum* Chinese cinnamon), and *Cinnamomum zeylanicum* respectively situated in the tropical regions. On the other hand, it's cooking uses, the local Ayurvedic drug Cinnamon has an effective remedy for the treatment of gynecological illness, respiratory, and stomach related disease, respectively. Every part of the tree can be used for medicinal or culinary purposes. The extracted and unstable oil obtained from leaf, root barks, and bark fundamentally accelerate in the formation of the concoction, which showed that the properties are different from the pharmacological point of view (Shen et al., 2006).

Furthermore, cinnamon actually utilized as a spice and additive mediators and also used in chewing exudates due to its mouth invigorating inspirations and ability to eliminate the unpleasant breath (Jakhetia et al., 2010). Cinnamon can likewise improve the fitness of the colon, thus the risk of colon cancer well reduced (Wondrak et al.,

2010). Cinnamon work as a coagulant to stop the bleeding (Nazari et al., 2013). Cinnamon plant involve in a key role as a flavor, but their important oils and related ingredients likewise plays a significant role in antimicrobial, antidiabetics and antifungal activities (Chang et al., 2001; Kim et al., 2006; Wang et al., 2005). In addition, the cinnamon has anti-inflammatory, anti-termitic, insecticidal, nematocidal, mosquito larvicidal, antimycotic and anticancer properties (Bandara et al., 2012; Chao et al., 2005; Cheng et al., 2009; Cheng et al., 2004; Park et al., 2006; Tang et al., 2010). Traditionally cinnamon also work as tooth powder to treat toothaches, dental complications, oral microbiota and awful breath (Aneja et al., 2009).

1.13 Biosynthesis of nanoparticles from *Cinnamon zeylanicum* bark extract

In current times, the plant extract used through biosynthetic method has got more consideration than physical and chemical techniques and also gain high importance than usage of microorganism and maintenance of clean environment is not required for the synthesis of nano scale metal. The idea of employing plant materials for the synthesis of nano-scale metals was first described by (Gardea-Torresdey et al., 2003; Gardea-Torresdey et al., 2002).

C. zeylanicum bark is extensively utilized as a fragrance. It is predominantly worked as a sauce and flavoring substantial and also greatly used in the preparation of some foods like, sweets, spicy candies, chocolate tea hot cocoa and liqueurs. It acts as a volatile oil in medicine preparation and also used for the treatment of colds. Furthermore, it is actively used for digestive problems and also used for diarrhea treatment. The bark of *C. zeylanicum* have highly anti-oxidant reaction (Shan et al., 2005). Cinnamon oil is highly essential and has an antimicrobial property, which can provide help in the preservation of various foods (Lopes et al., 2005). Previous study has been reported that pharmacological effects of *C. zeylanicum* bark is highly remarkable in type II diabetes treatment and insulin resistance (Verspohl et al., 2005). According to the efficiency and various application of *C. zeylanicum* bark have high commercial productivity and promisingly available for the synthesis of nano scale metal at commercial level.

In essence and aroma industries the cinnamon is commonly used for its good fragrance, which can be combined with different kinds of food products, perfumes, and therapeutic products (T.-C. Huang et al., 2007). The cinnamaldehyde and trans-cinnamaldehyde (Cin) is the most essential ingredients of the cinnamon which are found in essential oil. Therefore, these compounds play a vital role in various biological activities and fragrance normally detected in cinnamon (Yeh et al., 2013). Cinnamon contains different kind of Sticky compounds, like cinnamaldehyde, cinnamate, cinnamic acid and several oils which are essential for living organism (Senanayake et al., 1978). Previous study of Singh et al. (2007) revealed that the existence of cinnamaldehyde produced spicy test and cologne and occur because of oxygen absorption. The eternities of cinnamon, it looks darkens in color to improving the sticky compounds (Singh et al., 2007). The work of Sangal (2011) investigated different physiochemical aspects of cinnamon shown in Table 1.1. The previous study also has been reported that various compounds comprises a lot of important oils, including transcinnamaldehyde, cinnamyl acetate, eugenol, L-borneol, caryophyllene oxide, β -caryophyllene, L-bronyl acetate, E- nerolidol, cubebene, terpinol, terpinolene, and thujene (Tang et al., 2010).

Table 1.2: Chemical ingredients of various fragments of cinnamon (G. K. Jayaprakasha *et al.*, 2002) (Vangalapati *et al.*, 2012).

| Part of the plant | Compound |
|------------------------------|--|
| Leaves | Cinnamaldehyde: 1.00 to 5.00% |
| | Eugenol: 70.00 to 95.00% |
| Bark | Cinnamaldehyde: 65.00 to 80.00% |
| | Eugenol: 5.00 to 10.00% |
| Fruit | <i>trans</i> -Cinnamyl acetate (42.00 to 54.00%) |
| | and caryophyllene (9.00 to 14.00%) |
| <i>C. zeylanicum</i> buds | <i>alpha</i> -Bergamotene: 27.38% |
| | <i>alpha</i> -Copaene: 23.05% |
| | Oxygenated terpenoids: 9.00% |
| <i>C. zeylanicum</i> flowers | (E)-Cinnamyl acetate: 41.98% |
| | <i>trans-alpha</i> -Bergamotene: 7.97% |
| | Caryophyllene oxide: 7.20% |

The practice of metallic nanoparticles has been reported for the treatment of different disease like cancers, diabetes and leishmaniasis. Because, of the use of several hazardous capping and reducing chemicals in chemically produced nanoparticles, there are numerous difficulties. Consequently, the drug delivery is an attractive approach with usage of green synthesized nanoparticles. The ZnNPs have been used for some life-threatening disease treatment like cancer and diabetic (Alkaladi *et al.*, 2014; Delavari & Hashemabadi, 2014).

Silver ions and silver-based compounds are known to be exceedingly dangerous to microorganisms, including 16 major bacterial species. (Slawson, 1992 and Zhao *et al.*, 1998). Silver is a wonderful option for a range of medical applications. In order to produce antimicrobial effects, silver is frequently used in the nitrate form. However, when silver nanoparticles are used, the surface area available for the microbe to be exposed are greatly increases. Despite the fact that silver nano-particles uses in many anti-bacterial applications (Slawson *et al.*, 1992; Zhao & Stevens, 1998).

Further this study involves the toxicological studies of zinc nanoparticle on human macrophages to ensure their safer and suitable alternative therapeutic drug against leishmaniasis. In the current study, biologically synthesized zinc nanoparticles are assessed for the annihilation of *Leishmania tropica*. The most widely recognized phenomena elsewhere the anti-leishmanial adequacy of ZnNPs is their capacity to produce (ROS) reactive oxygen species (Nadhman et al., 2016). Numerous studies exposed that ZnNPs develop oxidative pressure which cause membrane damage because of their strong tendency to produce ROS in pathogens (Enad & Zghair, 2016). *Leishmania tropica* is very sensitive to these species.

1.14 Biosynthesis of nanoparticles from *Berberis lycium* Roots

Green NPs synthesis is originated from the nano-biotechnology, and nowadays, the major objective of the nanotechnology study is to develop the green nanoparticles (Haddad et al., 2013). Green nanoparticles have been developing as a new ways that are not harmful, friendly to environment, hygienic, less expensive, and virtually new methodology and also can be produced at room temperature and pressure (Samat & Nor, 2013; Yamini et al., 2018).

Green nanoparticle synthesis can be used as an alternative to biocompatible nanoparticle synthesis, which is the most recent acceptable strategy for associating material science and biotechnology. Thus, the synthesis of green NPs with controlled shape and size utilizing genetic modification strategies, cloning through molecular level, plants extracts, and other organic methods will be an overwhelming improvement in the nanobiotechnology (Narayanan & Sakthivel, 2010). Generally, for synthesise of nanoparticles, two methodologies are commonly used: bottom-up and top-down (Hussain et al., 2016; Schröfel et al., 2014). The top-down strategy often breaks down bulk materials into nanoparticles, whereas the bottom-up approach assembles molecules or atoms into NPs. The bottom-up approach is frequently used for green synthesis and chemical synthesis of NPs.(Narayanan & Sakthivel, 2010). Synthesis of Green NPs is an advanced strategy from the nanobiotechnology, Green nanomaterials are becoming the primary focus of nanotechnology research (Haddad et al., 2013).

A quick biological development of stable silver nanoparticles utilizing isolated aqueous leaf extract of *Berberis lycium* were investigated. The plant leaves were utilized for the cure of jaundice, in addition to tea auxiliary (Sood et al., 2012). Silver nanoparticles through utilizing plant resources, which tends to two central point i.e the requirement for the plant resources should be environment friendly and produce non harmful material, and for it to be less expensive and produced easily. Different concentration of silver nanoparticles has antibacterial effects which used against *Escherichia coli*, *Klebsiella pneumoniae*, *Pseudomonas aeruginosa*, and *Proteus* species (Mehmood et al., 2016).

1.15 Antimicrobial Activities

Mostly in developing countries the infectious disease are the chief reason of sickness and death among the wide-ranging population. Consequently, in current time different medical industries have been interested to develop latest antimicrobial medicines to control the constant appearance of resistant microbes to conventional antimicrobials.

Obviously, species of bacteria present and their genetic ability has to acquired ability to shows obstruction against presently antibacterial starins. Subsequently the successive reports on the separation of microbes that are known to be susceptible to medicines and became multi-resistant to different medicines available at marketplace (Nascimento et al., 2000; Sakagami & Kajimura, 2002). Therefore, normal procedures established by drug administrations to the marketplace with novel anti-microbial medicines integrate to change the structure at the molecular level of the current drugs so as to make them more proficient or improve the activity because of resistance mechanism of bacteria (Chartone-Souza, 1998).

The utilization of plants to cure sicknesses is as ancient processes. General examination on the utilization and adequacy of therapeutic plants fundamentally add to their pharmacological Characteristics, with the goal that they are oftentimes endorsed, regardless of whether their synthetic constituents are not constantly well known. Everywhere in the world, especially in south areas of America, the consumption of medicinal plants consumes supported crucial medical care (Maciel et al., 2002). Ranging from 250 to 500 thousand species of plant are assessed to found on the sphere,

and just somewhere in the range of 1 and 10% are exploited as food by humans and other living organism (Cowan, 1999).

Silver nanoparticles are of various shapes were produced by different methods. Silver nano plates with truncated triangular were detect to display the robust antibacterial activity due to their bigger surface area to bulk proportions and their crystallo-graphic surface structures (Ramya & Subapriya, 2012). Furthermore, Silver nanoparticles has also been integrated due to its antimicrobial activity into filters to purify drinking water and clean the pool water of swimming (WHO., 2002).

However, there are several speculations according to the accomplishment of silver nano-particles against microscopic organism to develop the effect on microbes. The capability of the silver nanoparticles is that to attached to the bacterial cell wall and then enter to the bacterial cell, therefore make organizational modification in the plasma membrane and make cell membrane permeable and cause death of cell. Due to attachment of silver NPs 'pits' formation occurred on the surface of cell and nanoparticles are accumulated at the surface of cell (Sondi & Salopek-Sondi, 2004). Another mechanism may be considered by which cell die due to development of free-radicals of silver nano-particles. The studies of electron spin resonance spectroscopy reported that when silver nanoparticles attached to the surface of bacteria to produced free radicals, and these free-radicals showed the capability to destroy the plasma membrane of bacterial cell and make it permeable which can finally lead the death of cell (Danilczuk et al., 2006; Kim et al., 2007).

It has additionally recommended that the influx of Ag ions from the NPs occurs (Feng et al., 2000) and these particles can subordinate with the thiol assemblies of various crucial enzymes and deactivate them (Matsumura et al., 2003). The cells of bacteria interact with Ag when receive the Ag particle, can damage cells by suppressing a few activities of the cell. At this stage, there is the ROS that are transported perhaps over the restraint of a respiratory chemical by silver particles and stabbing the cell itself. Silver is a soft acid, and there is a characteristic propensity of an acid to react to the base (Morones et al., 2005). The cells are encompassed of sulfur and phosphorus which are slight bases. The action of these nano-particles to the cell can prepare the response and hence lead to cell death. Other fact is that the DNA contains substantial amounts of sulphur and phosphorus; since nanoparticles can follow these sensitive bases and

damage the DNA, the cell would be immediately destroyed. (Hatchett & White, 1996). In addition to causing cell death in microorganisms, the interaction of AgNPs with the sulphur and phosphorus in DNA can cause problems with DNA duplication in microscopic organisms.

The effect of nanoparticle also has been investigated that it can regulate the signal transduction in bacteria. According to (Shrivastava, et al., (2007) the attachment of phosphorous to the protein substrate in bacteria effect transduction of bacteria. Dephosphorylation in tyrosine residues is observed only in gram-negative bacteria. The nanoparticles can modify the phospho-tyrosine profile of bacterial peptides. In addition, it has been observed that the peptide substrates on tyrosine residues dephosphorylated by nanoparticles, and inhibition of signal transduction occurred and therefore inhibition of growth occurred (Shrivastava et al., 2007).

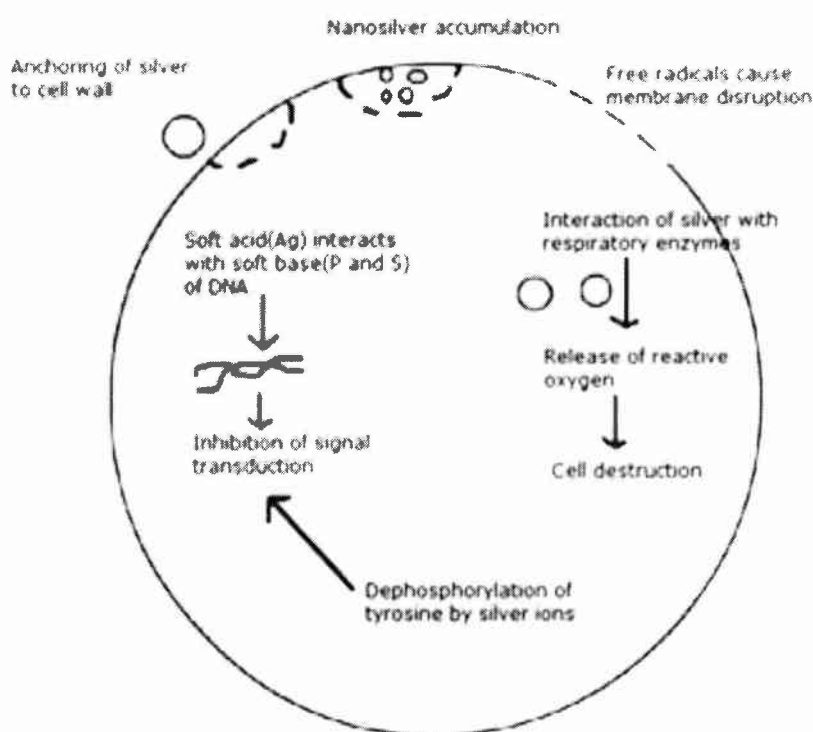


Figure 1.2: Nanoparticles Reaction Mechanisms on Bacterial Cell

The antifungal impact of silver NPs has got just minimal consideration and only a couple contemplates on this point has been published (Zeng et al., 2007). The analysis of nanoparticles is more specifically with their activity against clinical extract of ATTC strains of Trichophyton mentagrophytes and candida species (Kim et al., 2007).

ZnO nano-sized particles show various structures and shows significant antibacterial action over a different group of bacterial species explored by different groups of researchers (Buzea et al., 2007). Zinc oxide is presently being explored as an anti-bacterial in mutually micro-scale and nano-scale characterization. Zinc oxide shows substantial antimicrobial action when the molecules are compact to the size of nano-scale, at that point nano sized zinc oxide can absorb on the surface of bacteria where it enters inside the cell, and thusly NPs invade in bacteria and interfere the bacterial cell activities (Seil & Webster, 2012).

ZnONPs active with both Gram positive and Gram-negative microbes and furthermore, these NPs shows more extensive action against resistance spores of bacteria (Azam et al., 2012). They were likewise seen that fixing of zinc oxide nanoparticles through different metals, for example, gold, silver, chromium and so on enhanced the antimicrobial action of zinc oxide nanoparticles (Jiménez et al., 2015). Likewise, blockage impacts of zinc oxide nano-suspension are connected with their concentration and size. Higher the concentration of ZnNPs and smaller size of nanoparticles increases the antibacterial activity (Buzea et al., 2007; Padmavathy & Vijayaraghavan, 2008).

1.16 Antioxidant Activities

Oxidation is fundamental to many living beings for the creation of vitality to fuel natural procedures. It may be because of reactive oxygen species (ROS) that are formed in the process of digestion which may cause of numerous illnesses, for example, diabetes (Robertson & Harmon, 2006). Tumor formation (Valko et al., 2006) and cardio-vascular illnesses (Singh et al., 2005). On the other hand, to prevent the human body from the harm of ROS some natural compounds are used as an antioxidant (Issa et al., 2006; Kaliora et al., 2006). In plants, large number of phenolic compounds are present which act as an antioxidant. All the phenolic classes (basic phenolics, flavonoids, phenolic acids and anthocyanins) have the basic prerequisites of free radical scavengers and have use as food antioxidant (Sun et al., 2002). Antioxidant activity was evaluated for various *Berberis* species and shows significant activity in many tests. According to (Gauthami, et al., (2015) the green synthesized silver nanoparticles of Cinnamon showed better scavenging activity than crude extract of Cinnamon.

1.17 Leishmaniasis

Leishmaniasis is a stifling infection produced through protozoa of the *Leishmania* class, which are spread by the sand flies of phlebotomine. Condition of both on the harmfulness components of the parasite itself and on the resistant reaction set up by the host, a variety of illnesses called as leishmaniasis can appear (Braga et al., 2007). Leishmaniasis is viewed as a significant general medical condition (WHO, 2002), More than 20 infective causing agents parasites have been recognized subsequently, troubling more than 100 prevalent nations found mostly in humid, subtropical zones and southern Europe (Second WHO report on Neglected Tropical Diseases., 2013). The disease bears a broad spectrum of clinical syndromes and poses a serious complication with invariably increasing cases worldwide. It majorly affects the poorer regions of the world (Bhargava & Singh, 2012).

1.17.1 Classification of *Leishmania tropica*

| | |
|--------------|-------------------|
| ➤ Kindom | Proti |
| ➤ Subkingdom | Sarcomastigophora |
| ➤ Phylum | Protozoa |
| ➤ Subphylum | Mastigophor |
| ➤ Class | Zoomastigophora |
| ➤ Order | Kinetplastida |
| ➤ Genus | <i>Leishmania</i> |
| ➤ Specie | <i>Tropica</i> |

1.17.2 Epidemiology of *Leishmania tropica*

More than 12 million individuals at present experience the ill effects of leishmaniasis, and around 2 million individuals are affected yearly and developed a significant worldwide medical issue and a mistreated tropical illness (Croft et al., 2006).

Almost 350 million individuals living in the regions of vibrant transformation of *Leishmania*, through 12 million individuals all through Africa, Asia, Europe, and the Americas are legitimately infected by leishmaniasis. Over 90% of the cutaneous reports detected in various countries like, in Afghanistan, Saudi Arabia, Algeria, Brazil, Iran,

Iraq, Syria, and Sudan (Maria do Socorro et al., 2003). In Brazil, the examined report showed that, about 20.000 new cases of the infections appeared every year. An expansion in the occurrence of leishmaniasis can be related with metropolitan progress, destruction of forests, ecological variations and relocations of individuals to regions where the illness is prevalent (Ashford, 2000; De Carvalho et al., 2000; Patz et al., 2000).

The prevailing of this disease could be differed because it might be self-healing or incurable. Leishmaniasis can be classified on the bases of various infectious types.

- a) Cutaneous leishmaniasis
- b) Muoco-cutaneous leishmaniasis
- c) Instinctive leishmaniasis

Thus, about 0.5 and 1.5 million reports of visceral and cutaneous leishmaniasis are accounted correspondingly. In 1960 the first case of leishmaniasis was reported in northern region. Initially, it was kept to northern circle however now it is generally spreading throughout in all areas of the country (Oliveira et al., 2009). In all parts of the body, the cutaneous leishmaniasis targeted particularly the uncovered areas of the body. The primary cut may cause serious illness and may cause ulcer disease. Systemetic leishmaniasis infects inside organs of a body like, spleen and liver. uncommon in Pakistan however can end up being deadly. The various ulcers coming about because of different nibbles of sand fly are not an uncommon case in Pakistan. On other side, it is quickly spreading out making a frightening condition. Pakistan is now as a dangerous region with respect to this disease especially, Cutaneous and visceral leishmaniasis. Not withstanding of mucocutaneous leishmaniasis which is not reported very well (Bhutto et al., 2008).

1.17.3 Stages of leishmania

The two stages promastigotes and amastigotes developed from all species of Leishmania. The major properties of promastigotes are, transferrable, structure of motile flagella inside the grit which are removed into the host once they inject or enter into blood with meal (Dostálová & Volf, 2012).

Flagellum is not present in the amastigotes, live and grow in the macrophages of mammalian host, and ultimately transmit all through the host's reticuloendothelial framework (Vannier-Santos *et al.*, 2002). After infection the medical observation of an illness gets clear within several weeks to months, contingent upon the host immune response position and (sub) types of *Leishmania* (Vannier-Santos *et al.*, 2002).

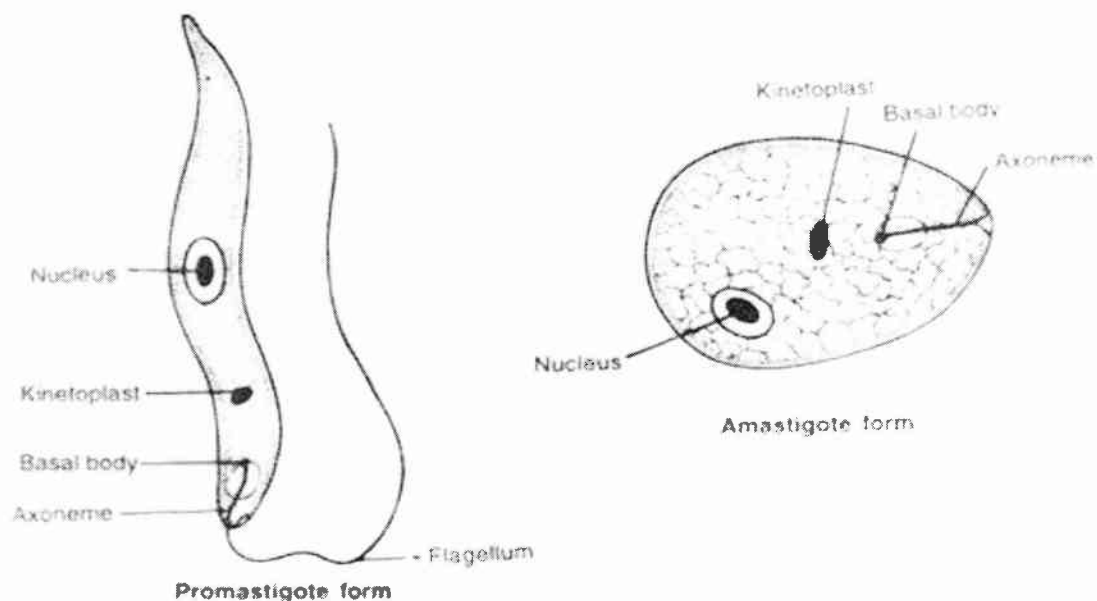


Figure 1.3: Morphological forms of *Leishmania tropica*

1.17.4 Life cycle of *Leishmania*

The leishmaniasis disease caused and spread through the bite of infected female phlebotomine sandflies. The infectious period (i.e., promastigotes) can be inserted through the sandflies from their antenna during meals of the blood. Macrophages and other type of mononuclear phagocytic cell phagocytized the infective cells which reach through puncture wound. Promastigotes change in the tissue of these cells which is the phase of the parasite (i.e., amastigotes), which duplicate by basic division and continue to affect other mono-nuclear engulfing cells. Parasite, host, and different components influence to confirmed whether the disease becomes indicative or whether cutaneous or visceral leishmaniasis. Sandflies become contaminated by eating diseased cells during blood meals. Amastigotes in sandflies develop into promastigotes in the gut. Leishmanial cells move from the hindbrain to the midbrain and move to the antenna (figure 1.6)

1.17.5 Life Cycle

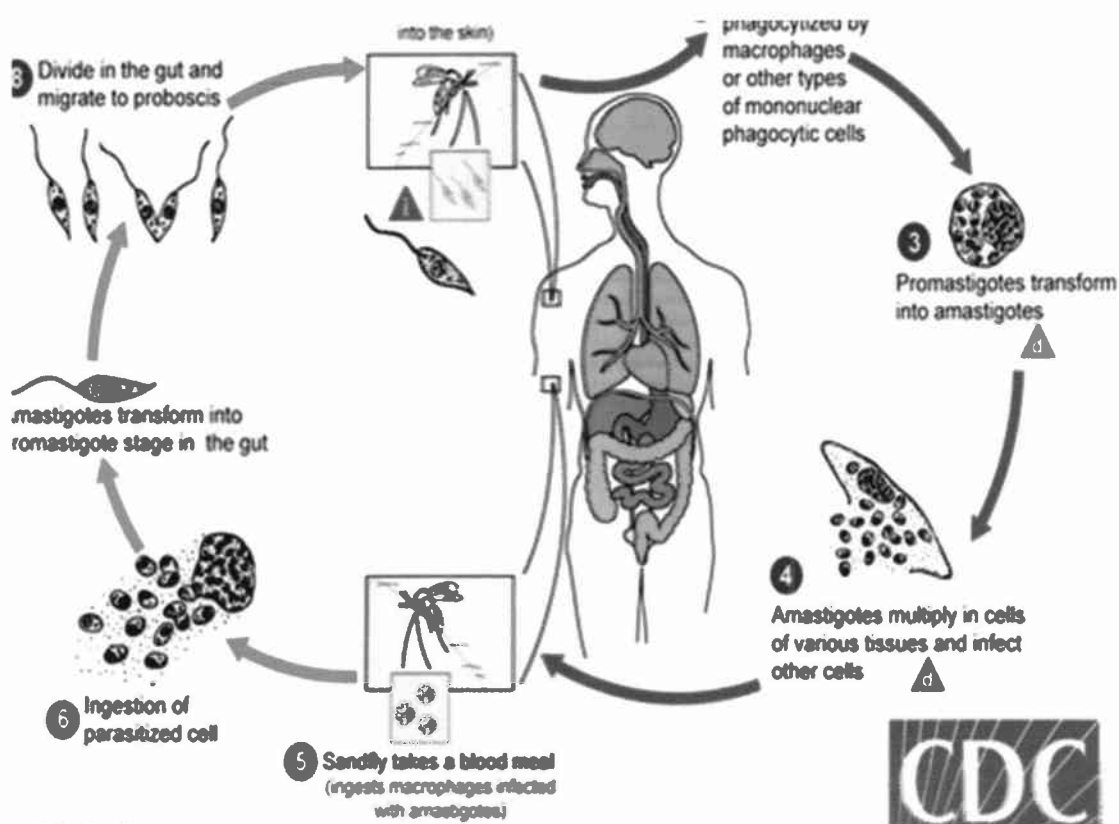


Figure 1.4: The life cycle of *Leishmania tropica*

1.17.6 Drugs for Leishmaniasis

Several drugs are available for the cure of leishmaniasis are noxious and drugs are becoming resistant to *Leishmania* species (Nadliman et al., 2016). The only available option for the control and treatment of leishmaniasis is antibiotic drugs but no effective vaccine has yet been synthesized against leishmaniasis to date (Yavar et al., 2013). Prof. Brahmchari from India, in 1929, developed the first effective drug for the treatment of leishmanial, for that, he was nominated for the Nobel Prize. He discovered this drug in 1912 (Sangshetti et al., 2015). Although it retains several side effects yet it initially saved many lives of effected poor people. Later on, discovery and development of pentavalent antimonials thus cut down these side effects quite greatly (Peter, 1981). The antimonial drugs were first introduced in 1945 and sustained as standard drugs against the disease at least about 6 decades (Sangshetti et al., 2015).

1.17.7 Limitations of drugs

Unfortunately, more than fifty years ago many drug were successfully developed but that was somewhat poisonous and inclined to cause resistance (Croft et al., 2006). Most of the frequently used drugs cause toxicity and do not completely eradicate the parasite from the bodies of infected individuals (Amato et al., 2008). The major reason of the failure of the treatment of leishmaniasis completely, is elevated chemo resistance of the parasite to available drugs (Natera et al., 2007). Since treatment is a thriving problem, novel medicines or alternative therapeutic options that might be able to replace or complement the currently available treatment, must be developed. Promising developments in chemotherapy have been made in recent years.

Continuous requirements for novel anti-parasitic drugs have drove attention of researchers towards exploring metallic nanoparticles for their advantage of being less toxic and having greater potential of anti-parasitic activity. Nanoparticles bear the capacity to infiltrate cell membrane and thus alter the genomic activities and metabolic of the cell and ultimately acts as drug to cure disease. But there is crucial need to understand the interfaces of metal nanoparticles with cellular particles.

1.18 Nanoparticles inducing toxicity

DNA damage can cause by nanomaterials by inducing ROS, oxidative stress, lipid peroxidation, protein modification, mitochondrial damage lading to cancer and cytotoxicity.

TH-27985

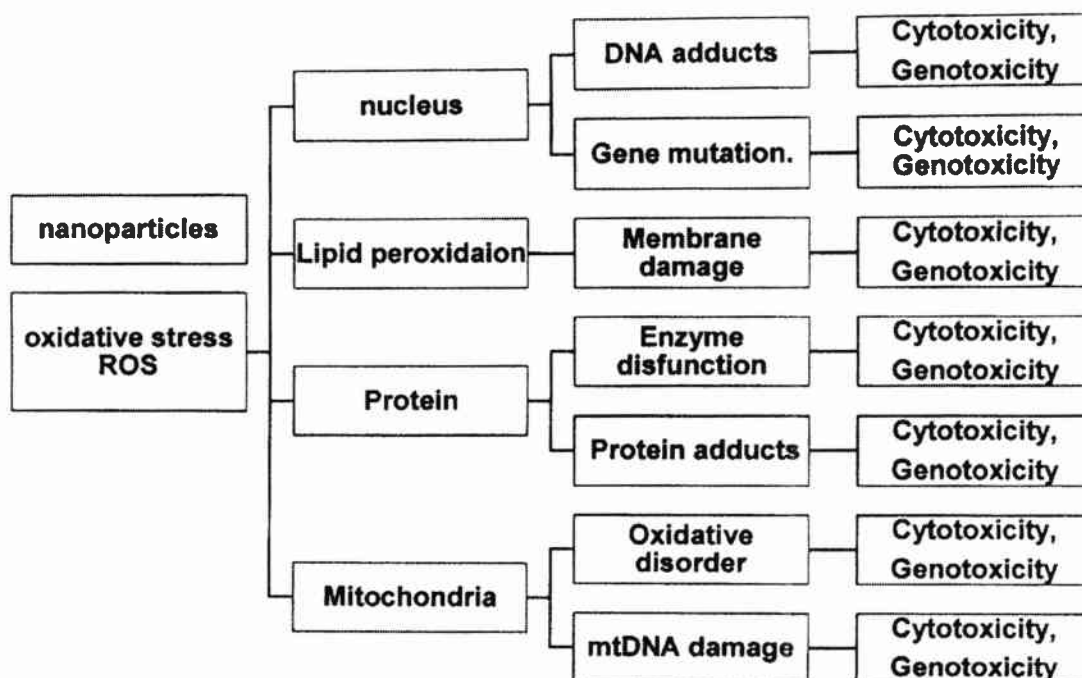


Figure 1.5: Nanoparticles inducing toxicity

On the other hand, toxicity of nanomaterials not only induce ROS but some other effects also induced. Karlsson *et al.*, 2008 reported an example by studying the side effects of different NPs (Fe_3O_4 , TiO_2 , CuZn , Fe_2O_3). The adverse effects caused by carbon nanoparticles on human lung cells was determined, like oxidative stress, DNA damaged and cytotoxicity. They concluded that NPs significantly increased intracellular ROS and also caused DNA damage, oxidative stress and cytotoxicity and NPs also caused DNA damage and cytotoxicity (Karlsson *et al.*, 2008).

1.19 Aim and Objectives

Aim

The aim of this study was the synthesis of metal nanoparticles by using selected medicinal plants and evaluation of their biological activities

Objectives

- i. Synthesis and characterization of Ag nanoparticles in the presence of *B. lycium* root extract, berberine, *Cinnamomum zeylanicum* bark extract and cinnamaldehyde
- ii. Synthesis and characterization of Zn nanoparticles in the presence of *B. lycium* root extract, berberine, *Cinnamomum zeylanicum* bark extract and cinnamaldehyde
- iii. Comparison of antibacterial, antifungal, antioxidant, antileishmanial and cytotoxic activities of both Ag and Zn nanoparticles

CHAPTER 2:
MATERIALS AND METHODS

MATERIALS AND METHODS

2.1 Collection of Plant Materials

Berberis lycium plant roots were collected from murree, Pakistan twice use tap water and twice use distilled water to clean and washed the roots. After drying the roots were crushed into fine powder. Berberine was purchased from USA which was in powder form.

Cinnamomum zeylanicum (cinnamon) bark was purchased from local market of Islamabad Pakistan. Cinnamaldehyde was purchased from USA which was in liquid form.

2.2 Green synthesis of Silver nanoparticles using *Berberis lycium* root extract and Berberine

Berberis lycium roots powder and berberine powder were weighed. 5gm of powder dissolved in 50 mL of distilled de-ionized water in a conical flask and used hot plate at 60°C for 30m and to get homogenous solution. Kept the flask on shaking bath under room temperature for 48hrs. After 48 plant extract were filtered through what man filter paper (90mm is the pore size of filter paper). This extract was used to reduce the Ag ions in to Ag nanoparticles, and incubated with the salt solution of silver nitrate. Six different molarities of salts solution were used for reaction, 15, 10, 7.5, 5, 2.5 and 1 mM. Plant extract were added to salt solution under 1:2 volume ratio and incubated for a time under varying pH. Visual observation of the colour change from pale yellow to dark brown was the sign of reduction of salt solution into silver ions but, the colour of the control were remain constant. At the end of the reaction the colloidal solution was subjected to centrifuge. Then centrifuged three times at 10,000 rpm for 10 minutes. Diversity in color of the experimental samples clearly indicates the formations silver nanoparticle (Bagheri et al., 2016). These nanoparticles were dried at room temperature.



Figure 2.1 : *B. lycium* root extract

2.3 Green synthesis of silver nanoparticles using *Cinnamomum zeylanicum* bark powder and cinnamaldehyde

Similarly, *C. zeylanicum* bark powder were weighed. 5gm of powder dissolved in 50ml of distilled de-ionized water in a conical flask on hot plate at 60°C and to get homogenous solution kept the flask on shaking bath under room temperature for 48hrs. After 48 hours mixture of extract and salt solution was placed for continues stirring with the magnetic stirrer. Plant extract were filtered through what man filter paper (90mm is the pore size of filter paper). This extract was used to reduce the Ag ion in to Ag nanoparticles, and incubated with the salt solution of silver nitrate. Six different molarities of salts solution were used for reaction, i.e 15, 10, 7.5, 5, 2.5 and 1 mM. Plant extract were added to salt solution under 1:2 volume ratio and incubated for a time under varying pH. Visual observation of the colour change from pale yellow to dark brown were the indication of reduction of salt solution into silver ions but the colour of the control were remain constant. At the end of the reaction the colloidal solution was subjected to centrifuge. Centrifuged three times at 10,000 rpm for 10 minutes. Diversity in colour of the experimental samples clearly indicated the formations silver nanoparticle (Bagheri et al., 2016). These nanoparticles were dried at room temperature

Cinnamaldehyde (5ml) taken and add to 50ml deionized water in a flask. Put magnetic stirrer in the flask. Six different molarities of salts solution were used for reaction, 15mM, 10mM, 7.5mM, 5mM, 2.5mM and 1 mM. Plant extract were added to salt solution under 1:2 volume ratio and incubated for a time under varying PH. Visual observation of the colour change from pale yellow to dark brown were the indication of reduction of salt solution into silver ions but, the colour of the control were remain constant. At the end of the reaction the colloidal solution was subjected to centrifuge.

Then centrifuged three times at 10,000 rpm for 10 minutes. Diversity in color of the experimental samples clearly indicates the formations silver nanoparticle (Bagheri et al., 2016). These nanoparticles were dried at room temperature.



Figure 2.2: *C. zeylanicum* bark extract

2.4 Green synthesis of Zinc Oxide nanoparticles of *Berberis lycium* roots and Berberine

B. lycium root extract was used to reduce the Ag ions in to Ag nanoparticles, and incubated with the salt solution of zinc sulphate. Six different molarities of salts solution were used for reaction, 15mM, 10mM, 7.5mM, 5mM, 2.5mM and 1 mM. Plant extract were added to salt solution under 1:2 volume ratio and incubated for a time under varying PH. Visual observation of the colour change from pale yellow to dark brown were the indication of reduction of salt solution into silver ions but the colour of the control were remain constant. At the end of the reaction the colloidal solution was subjected to centrifuge. Then centrifuged three times at 10,000 rpm for 10. Diversity in color of the experimental samples clearly indicate the formations zinc oxide nanoparticle (Bagheri et al., 2016). These nanoparticles were dried at room temperature.

2.5 Green synthesis of Zinc oxide nanoparticles using *Cinnamomum zeylanicum* and cinnamaldehyde.

The *C. zeylanicum* bark extract was used to reduce the zinc ions in to zinc nanoparticles, and incubated with the salt solution of zinc sulphate. Six different molarities of salts solution were used for reaction, 15, 10, 7.5, 5, 2.5 and 1 mM. Plant extract were added to 1mM salt solution under 1:2 volume ratio and incubated for time under varying PH. Visual observation of the colour change from pale yellow to dark

Chapter #. 2

brown were the indication of reduction of salt solution into zinc ions but, the colour of the control were remain constant. At the end of the reaction the colloidal solution was subjected to centrifuged. Then centrifuged three times at 10,000 rpm for 10 minutes. Diversity in color of the experimental samples clearly indicates the formations of zinc nanoparticle (Bagheri et al., 2016). These nanoparticles were dried at room temperature.

Cinnamaldehyde (5ml) taken and add to 50ml deionized water in a flask. Put magnetic stirrer in the flask. Six different molarities of salts solution were used for reaction, 1, 5, 10, 7.5, 5, 2.5 and 1mM. Plant extract were added to 1mM salt solution under 1:2 volume ratio and incubated for time under varying PH. Visual observation of the colour change from pale yellow to dark brown were the indication of reduction of salt solution into silver ions but, the colour of the constant were remain constant. At the end of the reaction the colloidal solution was subjected to centrifuge. Then centrifuged three times at 10,000 rpm for 10 minutes. Diversity in color of the experimental samples clearly indicates the formations of ZnO nanoparticle (Bagheri et al., 2016). These nanoparticles were dried at room temperature.

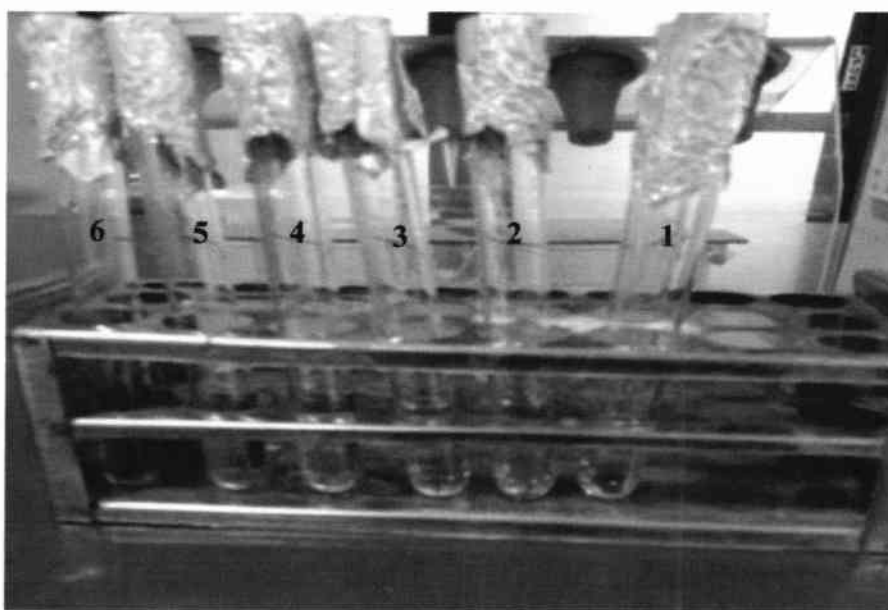


Figure 2.3: *C. zeylanicum* bark extract

2.6 Optimization of parameters

Optimizing the various parameters, the size and shape of nanoparticles were controlled and increased the nanoparticles synthesis.

2.6.1 Concentrations of plant extracts, silver nitrate solution

For the synthesis of nanoparticles from plant extract and compounds, different concentrations of the plant extract were used from the stock solution. Six different molarity of the silver salt solution (15, 10, 7.5, 5, 2.5 and 1 mM) were used in the reaction. Plant extract, compounds and the salt solution were used in 1:2 volume ratio and the reaction mixture were incubated at room temperature in the dark condition (Fig.2.4).

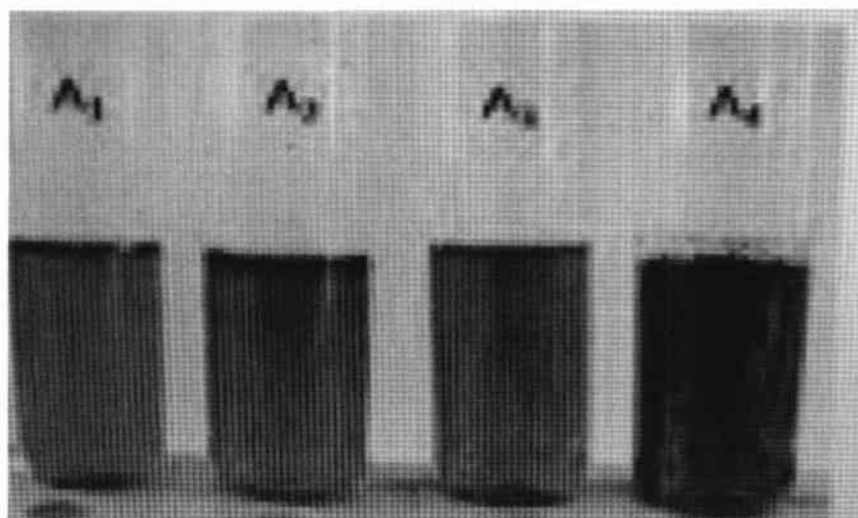


Figure 2.4: Photographs of AgNPs prepared in the presence of different conc. of plant extract, salt and water

2.6.2 Effect of pH

The optimum PH for the biological synthesis of AgNps and ZnNps was determined by following the method of (Mittal et al., 2012). The AgNps and ZnNps were synthesized at a variable PH rage from (2.0-9.0). The PH of the reaction mixture was adjusted by adding 0.1M hydrochloric acid and 0.1M sodium hydroxide solution.

2.6.3 Effect of Temperature

Test tubes containing the reaction mixture were kept in dark at different temperature ranges from (25°C to 60°C) keeping other parameter constant.

2.6.4 Effect of Time

Different reaction time were observed for nanoparticle synthesis (1hrs, 2hrs, 3hrs.....24hrs).

2.7 Characterization of the synthesized nanoparticles

Characterizations of NPs is important for understanding control synthesis of nanoparticles and their applications. Following methods are used for characterization of NPs by means of which we confirmed the formation of nanoparticles.

The optical property of NPs was determined by UV-visible spectrophotometer (TSO+, pg instruments) (Figure 2.5). UV-visible spectroscopy was used to analyze sample formation by showing the plasmon resonance. Fourier transform infrared spectroscopy (IRTracer-100, FTIR spectrophotometer, Germany) analysis of nanoparticles clearly indicate the functional group which is responsible for nanoparticle formation. The surface morphology of NPs was examined with SEM (JEOL JSM 6700F (JEOL, TOKYO, Japan). X-ray diffraction analysis was used to identify and determine the phase structure, crystallite size and relative crystallinity of the samples.

2.8 Antibacterial Activity

All of the research-related equipment, including Petri dishes, beakers, borers, micropipette tips, common pins, Eppendorf tubes, and medium, being sanitized using an autoclave (Daihan Scientific, Germany) at 121°C and 15 lbs/sq inch pressure for 15 minutes. To avoid contamination the entire process was carried out in a laminar hood.

2.8.1 Source and Maintenance of Microorganisms

2.8.1.1 Standard strains

Two non-pathogenic strains of bacteria, Gram-negative *Escherichia coli* (ATCC 8739), Gram positive *Staphylococcus aureus* (ATCC 6538), were standard strains obtained from Microbiology Research Lab, Quaid-i-Azam University, Islamabad, Pakistan.

2.8.1.2 Culture Media

Two separate media were produced in accordance with the manufacturer's instructions. Approximated 2.8g commercially available Nutrient Agar (Oxide, UK) media in 100ml of distilled water to fill a 250 ml autoclavable bottle. After being placed in an autoclave for 15 minutes at 121°C and 15 lbs to sterilized.

In a 1000 ml autoclavable bottle, 19g of Mueller-Hinton Agar (Oxide, UK) medium were dissolved in 500 ml of distilled water. With the aid of a thermo magnetic stirrer, media was dissolved. The media were kept in an autoclave for 15 minutes at 121°C with 15 lbs of weight to disinfect them.

2.8.2 Inoculum preparation

2.8.2.1 Nutrient broth

About 3.25g of the nutrient broth (Oxide, UK) medium were made in an autoclavable conical flask with 100 ml of distilled water. Using a thermo magnetic stirrer, the media was dissolved. In order to disinfect the media, place it in an autoclave weighing 15lbs set at 121°C for 15 minutes. The media was ready for the growth of bacteria. In the conical flask, the medium served as a stock for bacterial growth.

2.8.3 Inoculation of fresh bacterial culture

Take 20ml of prepared sterilized broth in a conical flask. Through sterile inoculation loops, bacteria were transferred from clean plates to the liquid nutrient broth in the conical flask. The conical flask was stored overnight in an incubator set at 37°C. The following day, sterilized Mueller-Hinton Agar were poured in 100mm-diameter Petri plates. Bacteria were transferred from conical flask by using sterilized cotton swab into Mueller-Hinton Agar-filled Petri plates. Overnight, the Petri plates were incubated in an incubator set to 37°C. This new culture was used for antibacterial activity.

2.8.4 Preparation of McFarland Standard (0.5%)

The 1% solution of each of sulphuric acid (H₂SO₄) and barium chlorid was prepared and mixed to form a turbid suspension. The resulting mixture were place in a foil covered tube. This was called McFarland standard and the turbidity of the McFarland standard tube and bacterial sample were visually compared against the black and white bars printed on the white page in the presence of good light. The turbidity of the log growth of the bacterial suspension were adjusted with the addition of broth or saline through sterilized tip to match the turbidity of the known McFarland standard. The standard McFarland turbidity is 0.5 which provide an optical density comparable to the optical density of bacterial suspension with a 1.5 x 10⁸ colony forming unit (CFU/ml).

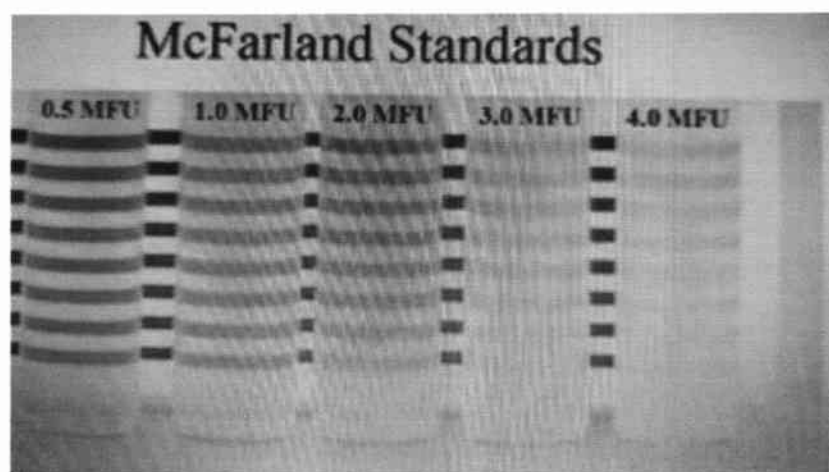


Figure 2.5: Photograph of McFarland Standard

2.8.5 Agar well diffusion assay

The agar well diffusion method by (Perez et al., 1990) was the technique employed for the *in vitro* antibacterial susceptibility test. In a laminar hood, 20ml of nutrient agar media was added into 100mm-diameter Petri plates, and they were allowed to cool for 15 minutes. When the media cooled down, it turns into jelly. Saline water were taken in a vial and add bacteria by using sterile loop. Adjusted the turbidity of the bacterial solution with the turbidity of McFarland standards. After adjusting the turbidity of the bacterial suspension take 20 μ l of bacterial suspension and added to each agar plate. In order to inoculate the Nutrient Agar medium surface with microorganisms, a sterile cotton swab was applied. Overnight, the Petri plates were incubated at 37°C in the incubator. After that, a sterile cork borer with a diameter of 5 mm was used to punch nine wells on the agar plate, eight of them along the edges of the plates and one in the centre. Nine peripheral wells were loaded aseptically with 20 μ l of the silver NPs and zinc NPs of *Berberis lycium* root extract, berberine, *Cinnamomum zeylanicum* bark extract and cinnamaldehyde. The wells were numbered from 1 to 10. The Eppendorf tube's having AgNPs and ZnNPs are thoroughly mixed through the mixer. Pure Nps in the first Eppendorf tube were used as stock solutions to make further dilutions. This stock solution of were sonicate with sonicator for 40 minutes. The concentration of NPs in the wells from 1st to 8th were done serial wise (100, 50, 25, 12.5, 6.25, 3.125 and 1.56 μ g/ml) in well no 8. Through a micropipette, water was administered to wells No. 9 as a negative control and pen-strep (0.05 percent) was administered to wells No. 10 as a positive control. Activity were done three times. After an hour in the refrigerator, the plates were removed (Esimone et al., 1998). The plates were remained for the next following day in an incubator set at 37°C. The Zone of Inhibition was assessed the following day by using a ruler to measure the wells' diameter in millimetres.

2.8.6 Spectrophotometric assay (Determination of MIC):

Each NPs exhibiting antibacterial action against test pathogens had its minimum inhibitory concentration (MIC) which was measured spectrophotometrically. To determine the MIC values, the broth micro-dilution method (Mehmood et al., 2012) was used. NPs were used with at 100 μ g/ml final concentration. Nps solutions (10 μ l) were added in the wells of first row of microtiter plate and in the remaining wells 180 μ l nutrient broth medium was added. Using a micropipette, two fold serial dilutions

were performed until each well had 10 μ l of a serially decreasing concentration of NPs solution. Following that, 10 μ l of inoculum were added to each well. Water served as the negative control while broth containing standard drug (pen-strep) served as the positive control. The microtiter plates underwent a 24h incubation period at 37°C. The experiment done in triplicate. Using an ELISA reader, the absorbance was measured at 620 nm.

2.9 Antifungal Activity

2.9.1 Fungal strains

Trichoderma herzianum) was used to check antifungal activity of biologically synthesized Ag and Zn nanoparticles.

2.9.2 Disc diffusion assay

With slight changes, the antifungal activity of biologically synthesized nanoparticles was assessed (Saha & Paul, 2012). The solution of potato dextrose agar (PDA) was made and autoclaved. 20ml of PDA solution was added to sterilize petri plates. Saline water were taken in a vial and add fungal solution from conical flask containing fungal culture. Adjusted the turbidity of the fungal solution with the turbidity of McFerland standard. After adjusting the turbidity of the fungal suspension take 20 μ l of fungal suspension and added to each potato dextrose agar plate. In order to inoculate the fungal strain on potato dextrose agar plate, a sterile cotton swab was used. Overnight, the Petri plates were incubated at 37°C. After that, a sterile cork borer with a diameter of 5mm was used to punch nine wells on the agar plate, eight of them at the edges of the plates and one in the middle. Nine peripheral wells were loaded aseptically with 20 μ l of the AgNps and ZnNps of *B. lycium* root extract, berberine, *C. zelynicum* bark extract and cinnamaldehyde. The wells were numbered from 1 to 10. The entire Ag and ZnNp mixture in the Eppendorf tube was mixed vigorously through the mixer. Nps in the 1st Eppendorf tube was used as stock solution for further dilutions. This stock solution of were sonicate with sonicator for 40 minutes. The concentration of Nps in the wells from 1st to 8th serial wise (100, 50, 25, 12.5, 6.25, 3.125 and 1.56 μ g/ml) in well no 8. In wells no. 9 water was used as a negative control, and amphotericin B (0.05 percent) was administered to wells no. 10 as a positive control. Activity were performed

in triplicates. After that the plates had been kept in an incubator overnight at 37°C (Esimone et al., 1998). The next day, the Zones of Inhibition were measured using a ruler in millimetres in diameter around the wells from the bottom of the plates.

2.9.3 Spectrophotometric assay (Determination of MIC)

Each Nps exhibiting antibacterial action against test pathogens had its minimum inhibitory concentration (MIC) measured spectrophotometrically. To determine the MIC values, the broth micro-dilution method (Chowdhary et al., 2018) was used. Nps were utilized with a 100µg/ml final concentration. Nps solutions (10µl) were added in the wells of first row of microtiter plate and in the remaining wells 180µl nutrient broth medium was added. Using a micropipette, two-fold serial dilutions were then performed until each well had a serially decreasing concentration of Nps solution. Thereafter 10µl inoculum was added to each well. Water was used as a negative control while broth containing standard drug (Amphotericin B 0.05%) used as a positive control. The microtiter plates kept for 24h at 37°C. Activity was performed in triplicates. Using an ELISA reader, the absorbance was measured at 520 nm.

2.10 Antioxidant Assay

The potential antioxidant properties of biocompatible AgNPs and ZnNps of *C. zeylanicum* bark extract, berberine, and *B. lycium* root extract were studied. DPPH (1, 1-diphenyl-2- 8 picrylhydrazyl) is a free radical reactive compound has been used to measure antioxidant activity. DPPH when react with the antioxidants the reaction proceeds with change in colour from deep violet colour to light yellow colour. The Nps were tested in free radical scavenging assay by the modified method of (Suresh et al., 2015). 2mg DPPH dissolve in 50ml of methanol and kept in dark for 30 minutes in a covered bottle because DPPH is a light sensitive. 2mg of ascorbic acid dissolve in 50ml methanol will be used as a positive control. All Nps dissolved in methanol with concentrations (100, 50, 25, 12.5, 6.5, 3, 1.5, 0.75µg/ml). 190ul of DPPH solution was added in microtiter plate and 10µl of NPs were added in each well. Methanol and DPPH used as a blank solution. Kept the microtiter plate in dark for 30 minutes to complete the reaction. After 30 minutes the absorbance was monitored at 518nm. The solution of ascorbic acid used as a positive control. Free radical scavenging activity was calculated by using the following formula.

$$\% \text{ Inhibition} = \frac{(A_B - A_E)}{A_B} * 100$$

Where A_B = Absorption of blank sample

A_E = Absorption of Nps

2.11 Antileishmanial activity

2.11.1 Anti-Promastigotes Assay

The antileishmanial activity of biologically synthesized nanoparticles was tested in-vitro against culture of *L. tropica* promastigotes. Media RPMI 1640 was prepared by the modified method of Nadhman (2016). Promastigotes from *L. tropica* were incubated at 24°C in media which contained 25mM HEPES buffer (4-(2-hydroxyethyl)-1-piper-azi-neethanesulfonic acid), sodium bicarbonate, supplemented with 10% heat inactivated FBS (Fetal bovine Serum) and 2% pen-strep antibiotic. The stock solution of the nanoparticles were prepared by suspending them in water and sonicate for 10 minutes for the the complete dispersion of aggregates.

Promastigotes form of *L. tropica* (1×10^6 cells/ml) harvested from logarithmic growth phase were seeded in each well in RPMI 1640 and 10%FBS. It is then allowed to proliferate for 48h in the presence of medium alone (control group) in water (negative control) and nanoparticles at different concentrations (100, 50, 25, 12, 6, 3 and 0.7 µg/ml). This micro-titer plate were incubated at 24 C° for 48h and the growth of the cells were checked in micro-plate reader by taking the OD of the cells. *In-vitro* reactions were carried out in triplicate and the antileishmanial activity were expressed as a ($IC_{50/72h}$).The concentration that inhibited parasite growth by 50%, (IC_{50}) as compared to untreated control. The reaction of antileishmanial activity were done in the month of October and November. When the external temperature was 24°C-27°C.This temperature is suitable for the growth of leishmania. IC_{50} values of all nanoparticles showing anti-leishmanial activity was determined by Graph pad prism.

2.11.2 Anti-amastigote Assay

Leishmania is dimorphic form of protozoan. Leishmania exist as long whipped promastigotes which forms in sand fly vector and when it is injected to another vertebrates it changes into immovable non -motile (round shaped amastigote) which are the cause of infection in both hosts. Amastigote grow outside the living cells that are known as axenic amastigotes. Bates (1993) developed rules for the cultivation of axenic amastigotes.

The algorithmic growth phase of axenic-amastigotes were also harvested and cultured in RPMI 1640 and 5.5pH was adjusted for their growth. At 33°C the cells were incubated for seven days in humufied CO₂ (5%). By changing the temperature and pH axenic amastigotes transformed into promastigotes. In each well of 96-well microtiter plate (10⁶ cells/ml) RPMI media containing culture of axenic-amastigotes were added. The different concentration of biologically synthesized nanoparticles (100, 50, 25, 12, 6, 3, 0.7µg/ml) along with water (negative control) and (Amphotericin B positive control) were added to each well and incubated at 25°C ± 1°C for 72 hours. Similar procedures were used for anti-promastigotes assay. All the experiment were performed in triplicate. Micro-plate reader were used for OD of the cells. IC₅₀ value of the biologically synthesized nanoparticles showing anti-amastigote activity were calculated by graph pad prism.

2.12 Hemolysis assay

Cytotoxic assay was performed to analyzed the cytotoxicity of biologically synthesized nanoparticles on fresh human blood cells. By destroying the external membrane of red blood cells, the hemoglobin was released. The quantity of destroyed cells were estimated by measuring the amount of hemoglobin in the sample. From healthy volunteers the fresh human blood was collected in vacutainer. By using phosphate buffer (PBS) washed the human blood cells three times and centrifuged at 3000 rpm for 2 minutes. After centrifugation the erythrocytes were separated from the blood. The blood cells suspension were serially incubated with biologically synthesized silver and zinc nanoparticles at 37°C for 3 hours. The reaction mixture were centrifuged at 6000 rpm after incubation for 10 minutes. Using UV-visible spectrophotometer, the released hemoglobin was monitored at 576nm. Experiment were performed in

triplicates. The red blood cells lysed with Triton X-100(0.1%) was used as a positive control and the cell suspensions (red blood) in PBS were used as negative control. Percentage hemolysis was calculated by using the formula.

$$\% \text{ Hemolysis} = (\text{OD of 576 in AgNps and ZnNps solution} - \text{OD at 576nm in PBS}) / (\text{OD at 576nm in 0.1\% Triton X-100} - \text{OD at 576nm in PBS}) \times 100$$

2.13 Statistical analysis

In the research, all the experiments were performed in triplicates and all the consequences are presented as mean \pm standard deviation (SD). To evaluate the significant differences linear regression analysis was performed. Calculated R²-values were significance slightly > 10. For statistical analysis graph pad prism were used.

**CHAPTER 3:
RESULTS**

RESULTS

3.1 Green synthesis of silver nanoparticles

Color change was observed from yellowish to dark brown when *B. lycium* root extract mixed with silver nitrate salt solution which was the initial indication of silver nanoparticles formation.

3.2 Optimization of nanoparticles

Optimizing the various parameters, the size and shape of nanoparticles were controlled and increased the nanoparticles synthesis.

3.2.1 Concentrations of plant extracts, silver nitrate solution

Different concentrations of the plant extract (0.25, 1.25, 2.5, 5 and 7.5 mg/ml) were used from the stock solution. Silver nitrate and zinc sulphate were utilized at concentration ranging from 0.25 to 15mM, the optimal value of silver nitrate salt solution concentration was 10mM and the optimal value of Zinc sulphate salt solution concentration was 15mM The yield of AgNPs and ZnNPs were increased as the concentration of AgNO₃ increased.

3.2.2 pH optimization

pH plays a key impact in the production of AgNPs and ZnNPs when applied in the range of 2–14. At different pH value Ag and Zn nanoparticles synthesis were optimized but neutral pH was optimal i-e pH-7. At this pH AgNPs showed sharp peak at UV-visible spectroscopy indicating the uniform size of AgNps formation (Iravani & Zolfaghari, 2013).

3.2.3 Temperature optimization

In terms of reaction temperature, the method of Ag and Zn nanoparticles biological synthesis has the advantage of producing stable nanoparticles at room temperature (25°C) (Nadagouda & Varma, 2008). It is possible to synthesized AgNPs at both temperature at low temperatures (below 25 degrees Celsius) and high temperatures (over 60 degrees Celsius) but the room temperature (25C°) was the

optimal temperature because at room temperature small and spherical AgNPs were synthesized and showed single plasmon resonance at UV-visible spectroscopy.

3.2.4 Time optimization

The size of the nanoparticle production was determined by the reaction time, or the length of time that the silver and zinc salt interacts with the plant extract. Ag and Zn NPs were synthesized at all reaction times but the yield were different at different reaction times. The yield of NPs rose as the salt concentration and reaction time were increased, with a shift in the surface plasmon band wavelength to a higher range, indicating the NPs agglomeration (Mashwani et al., 2015). AgNPs which were synthesized after 12hrs of reaction time in dark was the optimal time while other parameter constant which results better yield of AgNPs with a single and short wavelength peak at UV-visible spectroscopy. ZnNPs which were synthesized after 24hrs of reaction time was the optimal time while other parameter constant which results better yield of ZnNPs with a single and short wavelength peak at UV-visible spectroscopy.

3.3 Characterization of Nanoparticles

Various techniques were used for the characterization of silver and zinc nanoparticles which showed the production and confirmation of the nanoparticles.

3.3.1 UV-Vis Spectroscopy

3.3.1.1 Silver nanoparticles:

Silver (Ag) Nanoparticles optical property was determined by UV-Visible spectrophotometer (UV 6300 PC). The Plasmon resonance of UV-visible spectrophotometer is used to confirm the nanoparticles formation. Figure (3.1 and 3.2) shows the absorbance spectrum of biologically synthesized silver nanoparticles. Silver nanoparticles of *B. lycium* root extract Figure (3.1) showed sharp absorbance at (400 nm) and Berberine silver nanoparticles Figure (3.2) showed sharp absorbance at (432nm). The biologically synthesized Silver nanoparticles of *C. zeylanicum* bark extract Figure (3.3) showed sharp absorbance at (418 nm) and Cinnamaldehyde silver nanoparticles Figure (3.4) showed sharp absorbance at (422 nm).

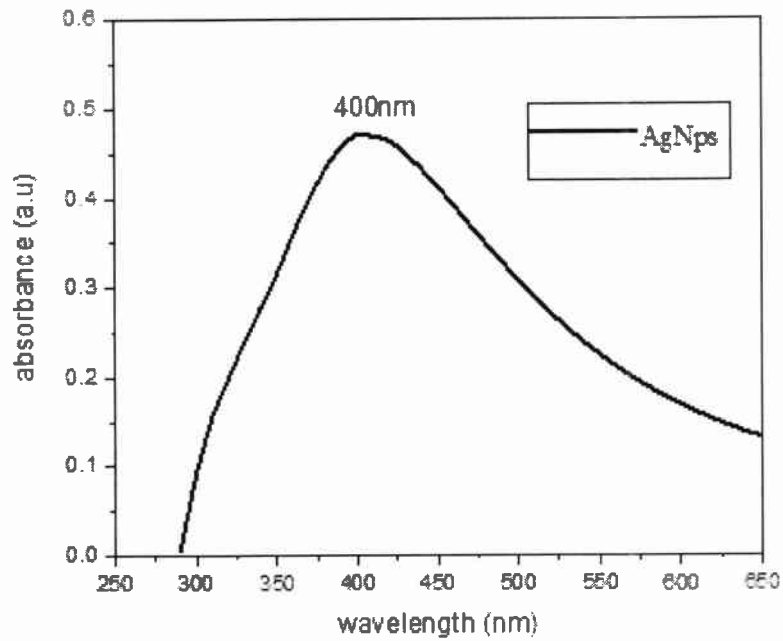


Figure No. 3.1: UV-vis Spectrum of AgNPs synthesized in the presence of *B. lycium* root extract

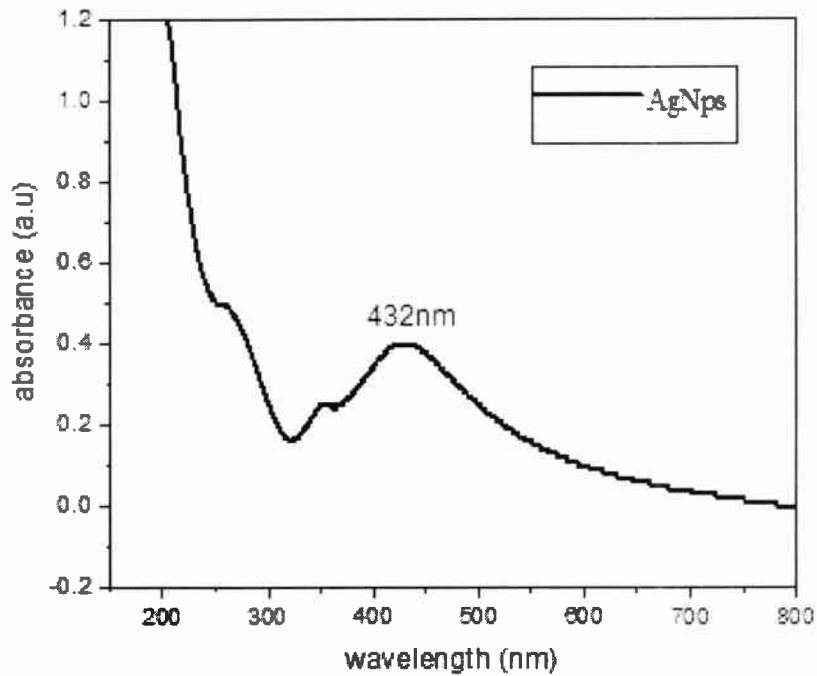


Figure No. 3.2: UV-Vis spectrum of AgNPs synthesized in the presence of berberine

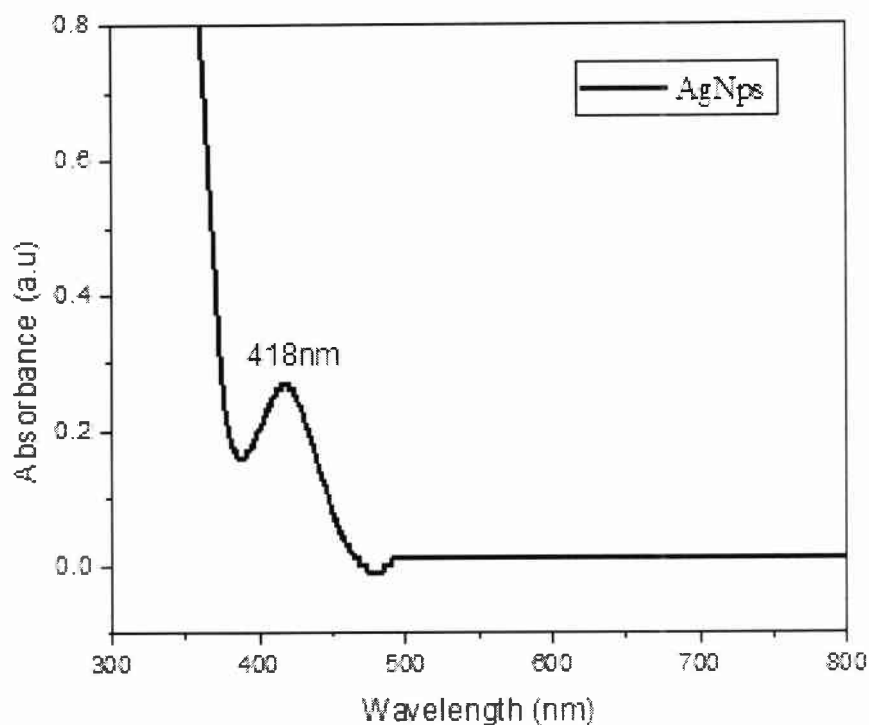


Figure No. 3.3: UV-Vis spectrum of AgNPs synthesized in the presence of *C. zeylanicum* bark extract

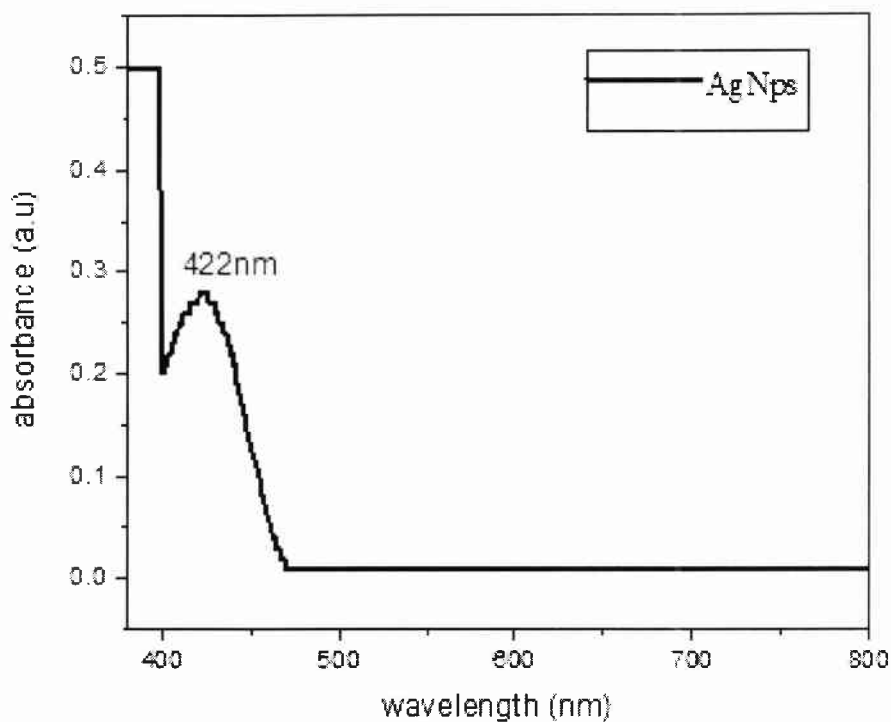


Figure No. 3.4: UV-Vis spectrum of AgNPs synthesized in the presence of Cinnamaldehyde

3.3.1.2. Zinc Nanoparticles:

Zinc (Zn) Nanoparticles optical property was determined by UV-Visible spectrophotometer (UV 6300 PC). The Plasmon resonance of UV-visible spectrophotometer is used to confirm the nanoparticles formation. Figure (3.5, 3.6, 3.7 and 3.8) showed the absorption spectrum of biologically synthesized Zinc Nanoparticles. Zinc nanoparticles of *B. lycium* root extract Figure (3.5) showed sharp absorbance at (340 nm) and Berberine Zinc Nanoparticles Figure (3.6) showed sharp absorbance at (339 nm). The absorption spectrum of biologically synthesized Zinc nanoparticles of *C. zeylanicum* Figure (3.7) showed sharp absorbance at (380 nm) and Cinnamaldehyde Zinc Nanoparticles Figure (3.8) showed sharp absorbance at (380 nm).

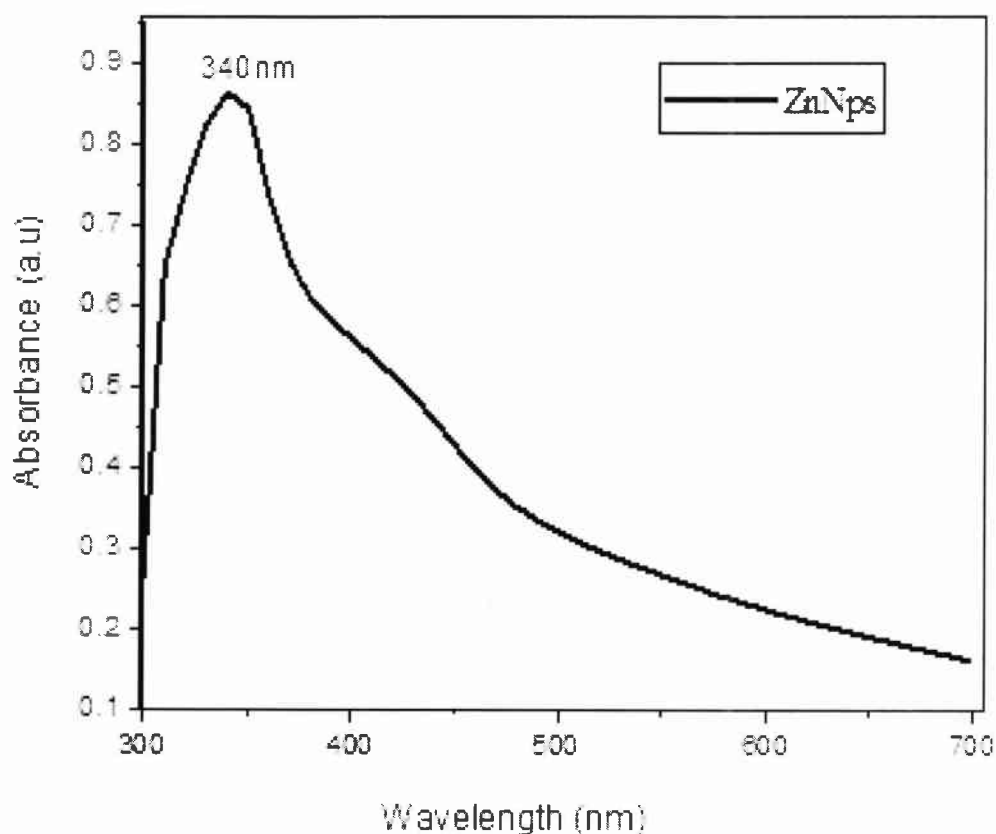


Figure No. 3.5: UV-Vis spectrum of ZnNPs synthesized in the presence of *B. lycium* root extract

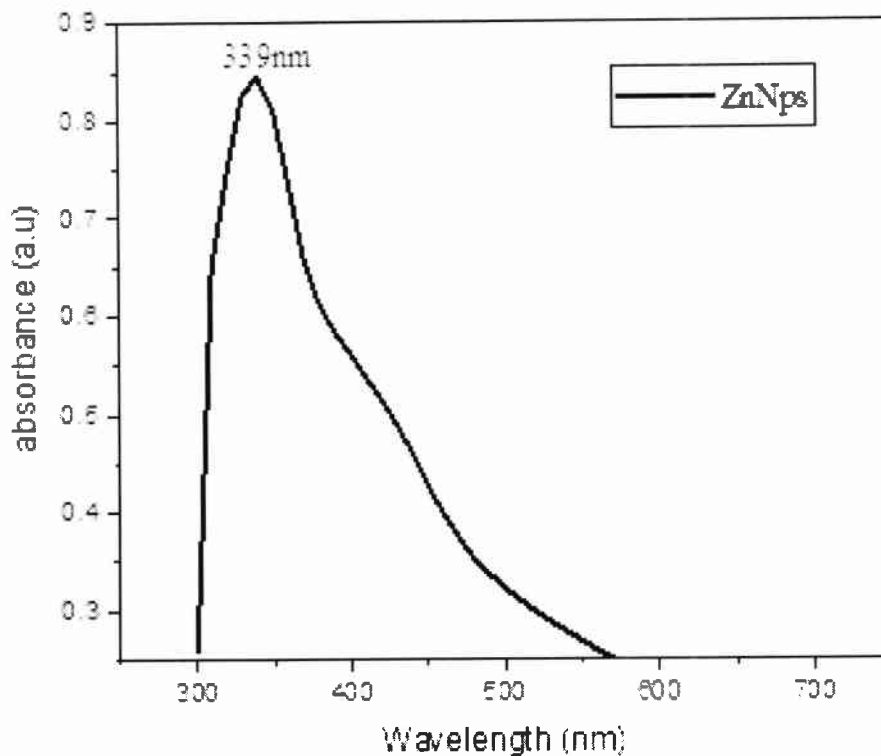


Figure No. 3.6: UV-Vis spectrum of ZnNPs synthesized in the presence of berberine

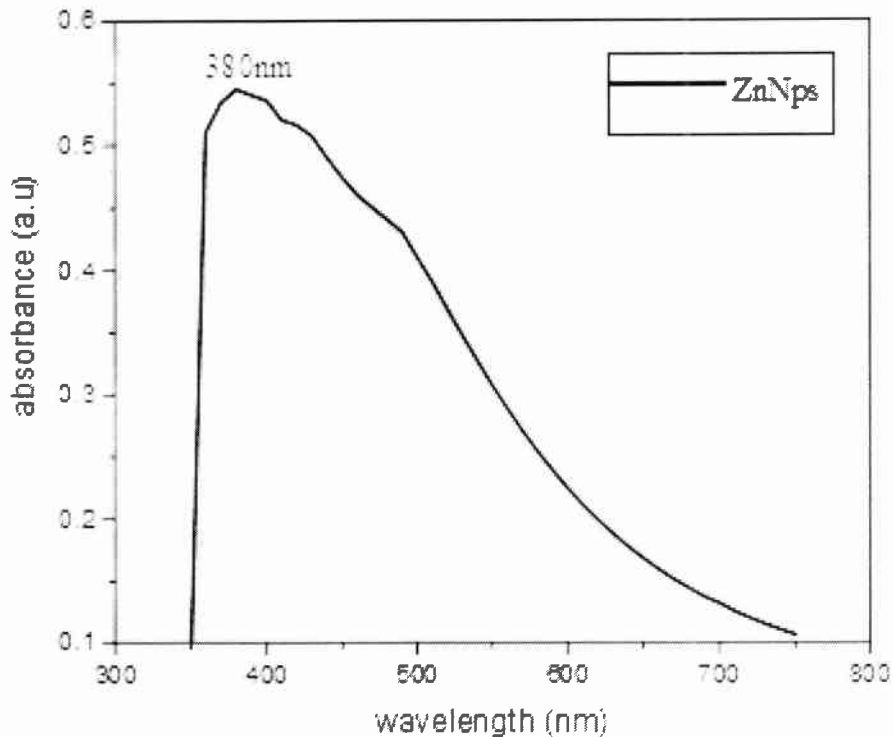


Figure No. 3.7: UV-Vis spectrum of ZnNPs synthesized in the presence of *C. zeylanicum* bark extract

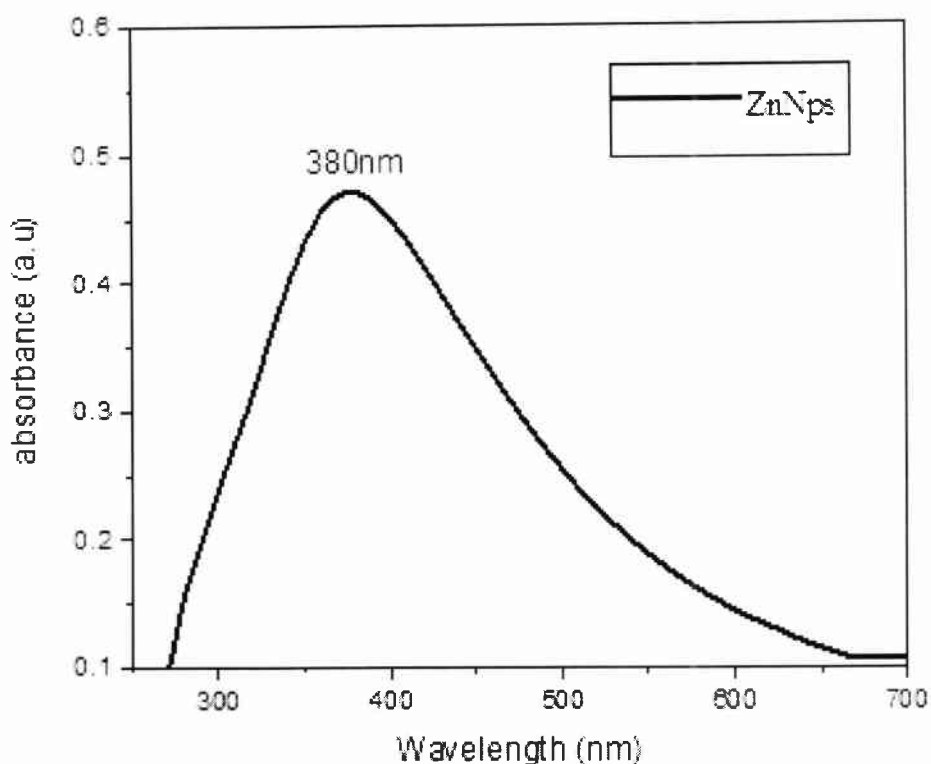


Figure No. 3.8: UV-Vis spectrum of ZnNPs synthesized in the presence of Cinnamaldehyde

3.3.2 FT-IR Spectrum

3.3.2.1 Silver Nanoparticles

The functional groups responsible for the reducing and capping agent of silver nanoparticles produced from plant extract of the roots of *B. lycium* were identified using FT-IR analysis of the silver nanoparticles. FT-IR was carried out at a resolution of 4 cm^{-1} Figure (3.9). The bands at 3549 , 2324 , 2193 , 1987 , 1848 , 1546 , 1497 , 1359 and 1051 cm^{-1} were observed in FT-IR spectrum. The spectrum at 3549 cm^{-1} were assigned for OH stretching of alcohol. 2324 cm^{-1} was specified for C-H stretching. 2193 cm^{-1} was assigned for $\text{C}\equiv\text{C}$ bond of alkynes. 1987 cm^{-1} for C=C asymmetric stretch. The peak at 1546 cm^{-1} was strong C-N stretching. 1497 cm^{-1} was assigned for C-C stretching or C-N of aromatic amine group or C=C of aromatic ring. The peak at 1359 cm^{-1} was strong C-N stretching of aromatic compounds. 1051 cm^{-1} was specified for C-O stretching.

FT-IR was used at resolution of 4cm^{-1} to identify the substance that served as the reducing and capping agent for silver nanoparticles made from the berberine compound. Figure (3.10) showed the bands at 2820.1, 2331, 2071, 1595, 1383.7, 1353.6, and 1051.9cm^{-1} . The 3423cm^{-1} was assigned for OH stretching of alcohol. The peak at 2331 and 2820.1cm^{-1} were assigned for C-H stretching. The peak at 2071cm^{-1} was assigned for $\text{C}\equiv\text{C}$. 1595cm^{-1} was assigned for $\text{C}=\text{C}$ and $\text{C}=\text{N}$ stretching. 1353-1383 cm^{-1} were specified for C-H stretching. 1051cm^{-1} was specified for C-O stretching.

FTIR measurement of green synthesized silver nanoparticles of *C. zeylanicum* bark extract. The possible biomolecules responsible for the reduction of Ag^+ ions and the capping of the bioreduced silver nanoparticles synthesized from the bark extract. The major peaks in the FTIR spectrum of silver nanoparticles Figure (3.10) were observed at 2996.92, 1775.19, 1380.8, 1245.0, 1048.2, 749.77cm^{-1} . The peak at 2996.92 were assigned for ($\text{C}-\text{H}$). The peak at 1775.9 in *C. zeylanicum* essential oil is related to the vibration stretching of the aldehyde carbonyl group ($\text{C}=\text{O}$) and the strong ($\text{C}=\text{O}$), indicating a high content of cinnamaldehyde and aldehydes. (Jeyaratnam et al., 2016). The peak was shifted from 1775.19 in AgNPs *C. zeylanicum* bark extract showed that formation of silver nanoparticles. The peak 1380 were showed C-H bending of alkane, 1245 was assigned for C-OH groups of phenolic compounds, peak 1048 were assigned for =CH of benzene ring. All of these peaks indicate that the high content of phenolic and aromatic chemicals, particularly cinnamaldehyde.

In order to determine the potential biomolecules responsible for the reduction of Ag^+ ions and capping of the bioreduced silver nanoparticles, FTIR measurement of the green produced Ag Nps of cinnamaldehyde was performed. The major peaks of AgNPs of cinnamaldehyde were observed at 3024.0, 1686.61, 1625.96, 1489.51, 1380.98, 770.51, 722.64, 681.94, 593.36cm^{-1} . 3024cm^{-1} ascribed to the aromatic C-H. 1686.61cm^{-1} corresponded to carbonyl group $\text{C}=\text{O}$. The 1625.96cm^{-1} was assigned for $\text{C}=\text{C}$ bond. 1489.51cm^{-1} were assigned for benzene derivatives. 1380.98-1489.51 were assigned for C-H bending. All of the peaks confirmed the purity of the NPs.

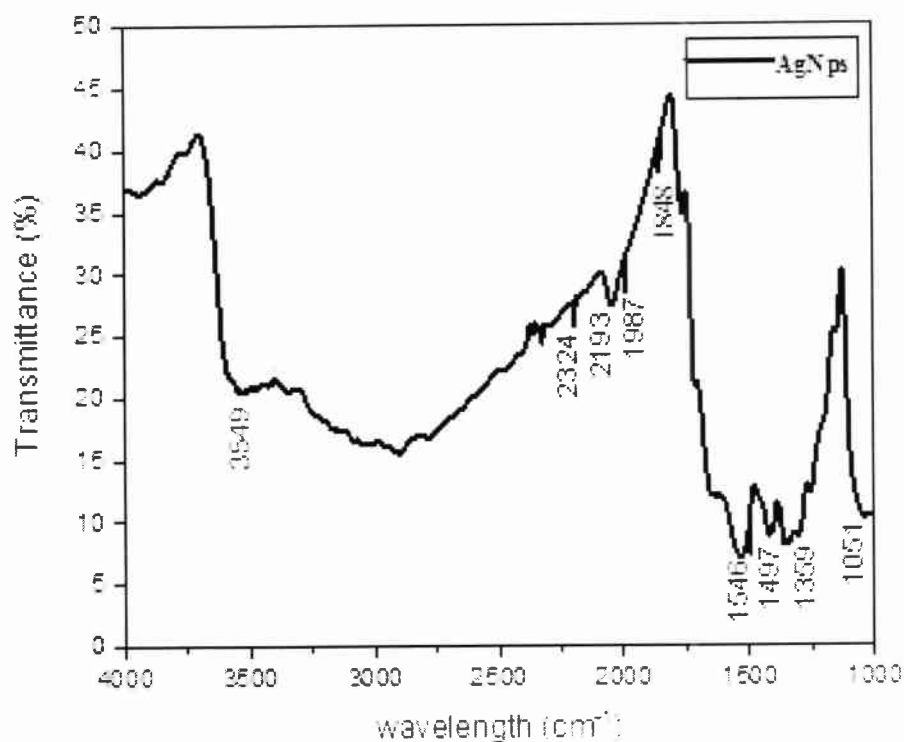


Figure No. 3.9: FTIR spectra of AgNPs synthesized in the presence of *B. lycium* root extract

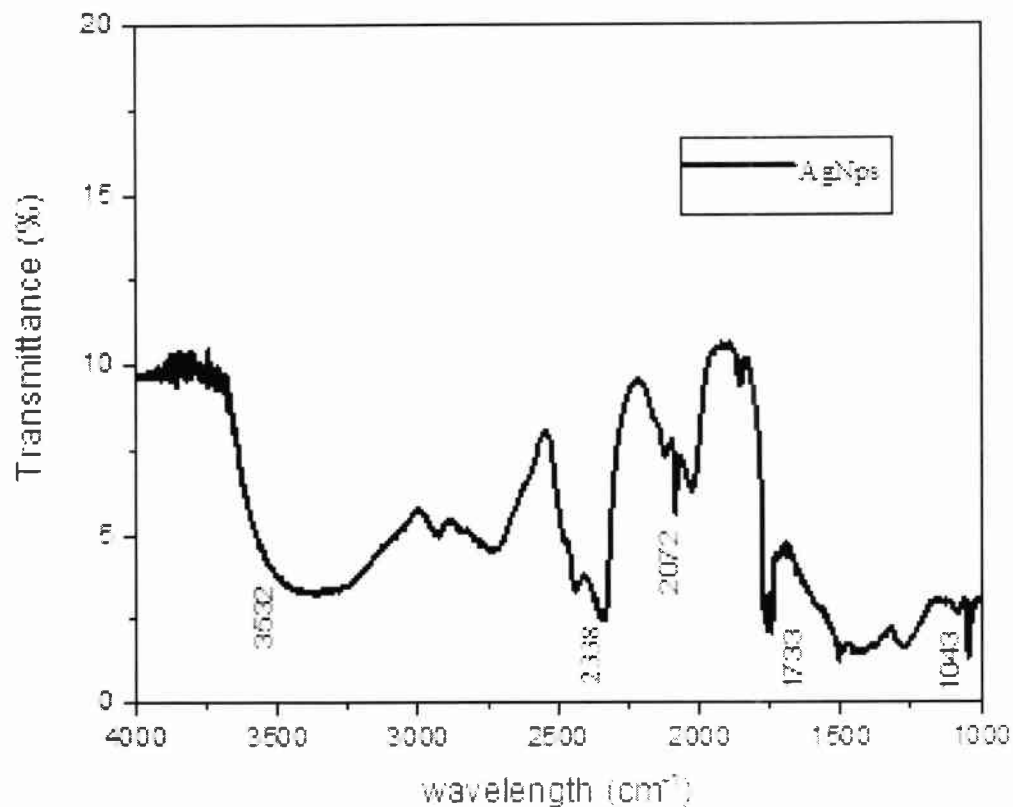


Figure No. 3.10: FTIR spectra of AgNPs synthesized in the presence of berberine

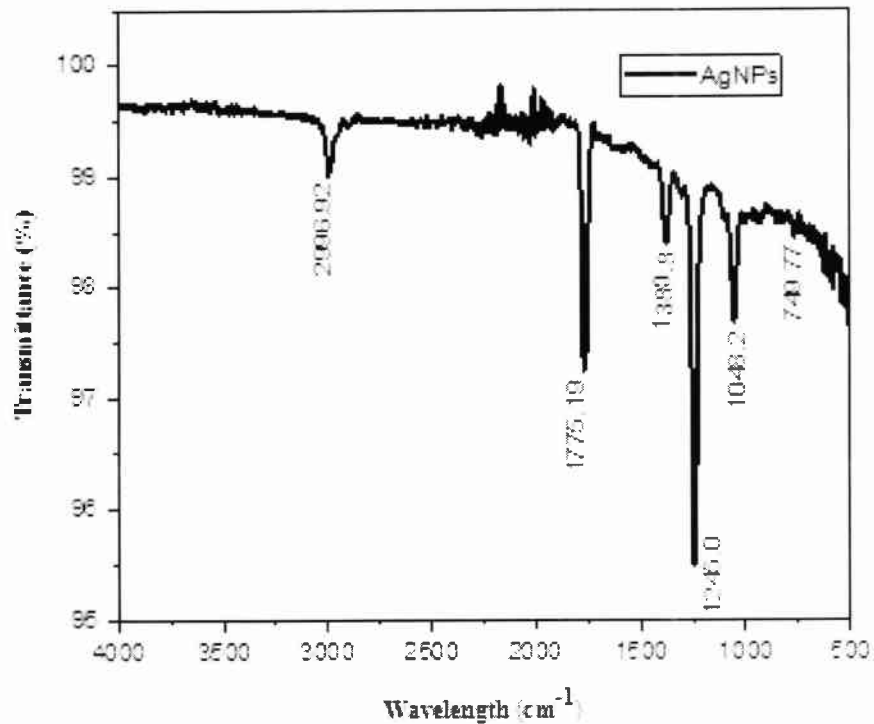


Figure No. 3.11: FTIR spectra of AgNPs synthesized in the presence of *C. zeylanicum* bark extract

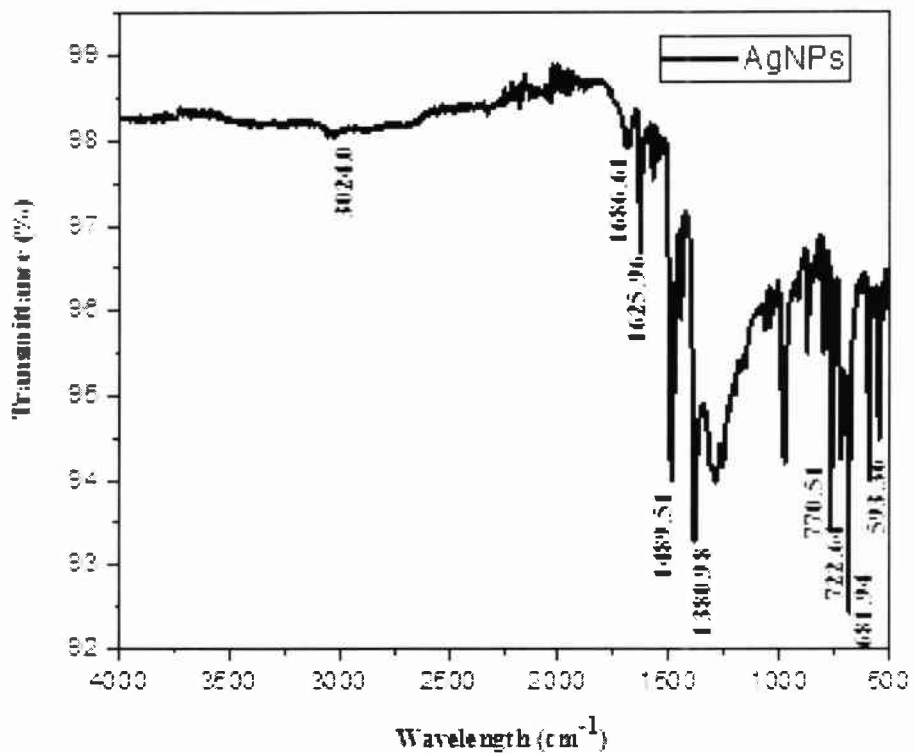


Figure No. 3.12: FTIR spectra of AgNPs synthesized in the presence of cinnamaldehyde

3.3.2.2 Zinc Nanoparticles

The characteristics bands showed several functional groups of FTIR spectra of Zinc Nps of *B. lycium* root extract. IR peaks were observed at 3406, 2158, 1625, 1487, 1125, 1011 and 612 cm^{-1} . The peak at 3406 cm^{-1} was medium NH stretching of primary amine. The peak at 2158 cm^{-1} was assigned for strong stretching of N=N=N. 1625 cm^{-1} was assigned for strong C=C stretching of α , β -unsaturated ketone. The peak at 1487 cm^{-1} was specified for medium C-H bending of aldehyde. The peaks at 1625 and 1011 cm^{-1} were specified for strong C-O stretching of aliphatic ether and the peak at 612 cm^{-1} was specified for strong C-Br stretching of halo compound. The findings suggested that the primary biomolecules in the plant extract that can decrease zinc ions and convert them to ZnONPs are polyhydroxyl phenolics and flavonoids. (Ahmad et al., 1998; Anzabi, 2018).

The FTIR spectra of berberine ZnNPs showed the characteristics peaks at 3423, 2345, 2077, 1619, 1510 and 1274 cm^{-1} . The peak at 3423 was assigned for strong O-H stretching of alcohol. The peak at 2077 was specified for strong N=C=S stretching of isothiocyanate. The peak at 1619 cm^{-1} was specified for strong C=C stretching of α , β -unsaturated ketone. The peak at 1510 was specified for N-O stretching of nitro compound and the peak at 1274 cm^{-1} was assigned for strong C-N stretching of aromatic amine. (Sahibzada et al., 2018)

The FTIR spectra of ZnNps of *C. zeylanicum* bark extract showed that the bands of functional group located at 2157, 2086, 1629, 1433, 1005 and 613 cm^{-1} . The peak present at 2157 cm^{-1} indicated for strong $\text{C}\equiv\text{N}$ stretching. The peak at 2086 cm^{-1} showed the presence of strong N=C=S stretching of isothiocyanate. The peak at 1629 cm^{-1} was assigned for medium C=C stretching of alkene. The peak at 1433 cm^{-1} was assigned for medium O-H bending of carboxylic acid. The peak at 1005 cm^{-1} was specified for C-F stretch of alkyl halide and the peak at 613 cm^{-1} was assigned for strong C-Br stretching of halo compound. (Sathishkumar et al., 2009).

Infrared Spectral analysis of the ZnNps of Cinnamaldehyde was carried out to identify the possible molecules responsible for capping the Zn nanoparticles formed. In Figure (3.16) showed the spectra of ZnNps of cinnamaldehyde. The following peaks were observed at 3059, 2883, 2360, 2033, 1958, 1882, 1752, 1631 and 1400 cm^{-1} . The peak

at 3059cm^{-1} was specified for medium C-H stretching of alkene. The peak at 2883cm^{-1} was assigned for medium C-H stretching of alkane. The peak at 2033cm^{-1} was assigned for weak C triple C stretching of alkyne. The peak at 1958cm^{-1} was specified for medium C=C=C stretching of allene. The peak at 1882cm^{-1} was specified for weak C-H bending of aromatic compounds. The peak at $1752\text{-}1631\text{cm}^{-1}$ was assigned for strong C=O stretching and the peak at 1400cm^{-1} was specified for strong CF stretching of fluoro compounds.(Ji et al., 2019).

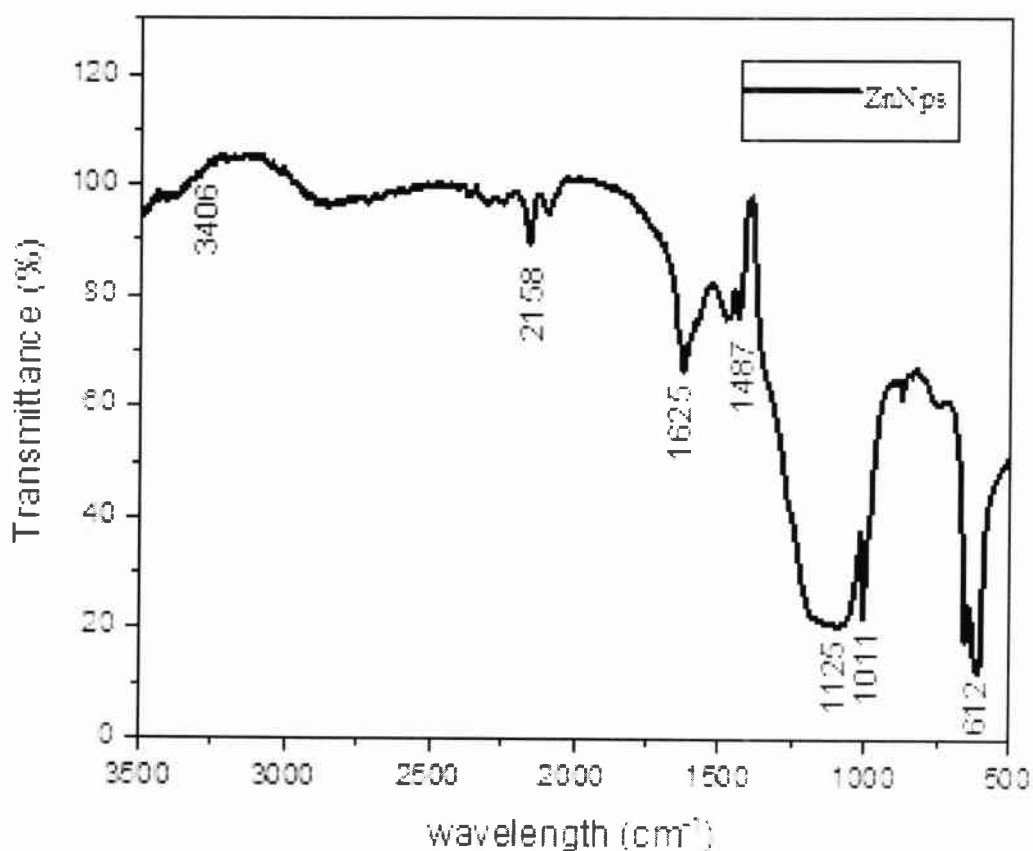


Figure No. 3.13: FTIR spectra of ZnNPs synthesized in the presence of *B. lycium* root extract

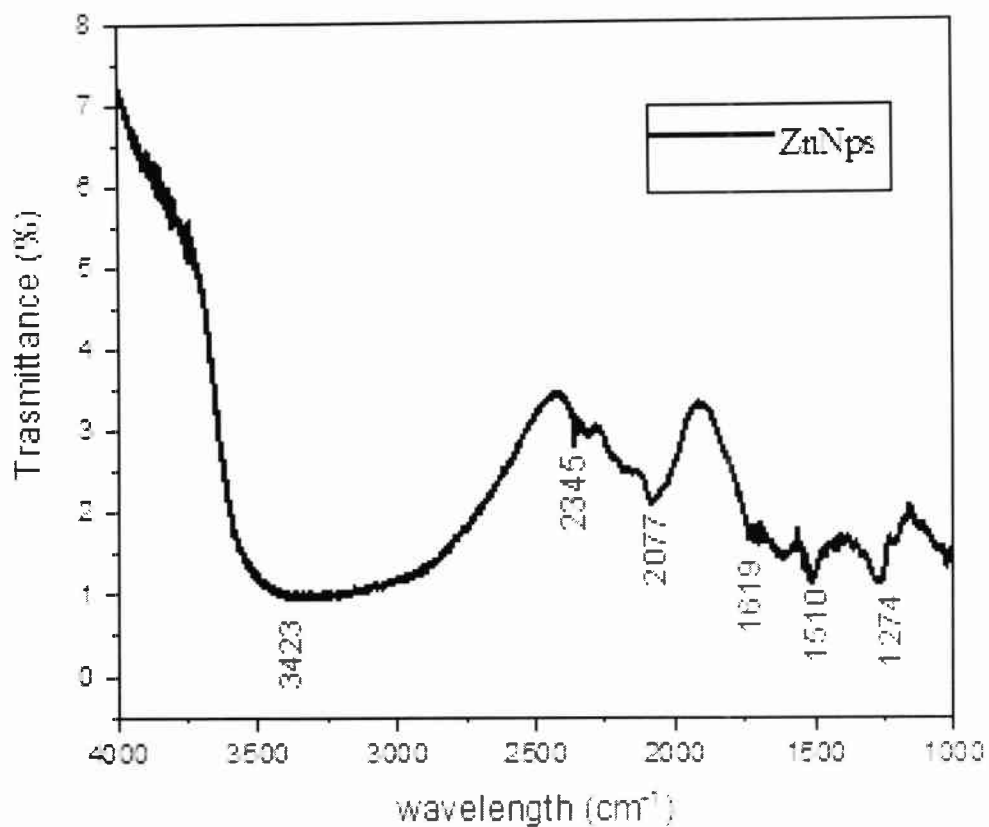


Figure No. 3.14: FTIR spectra of ZnNPs synthesized in the presence of berberine

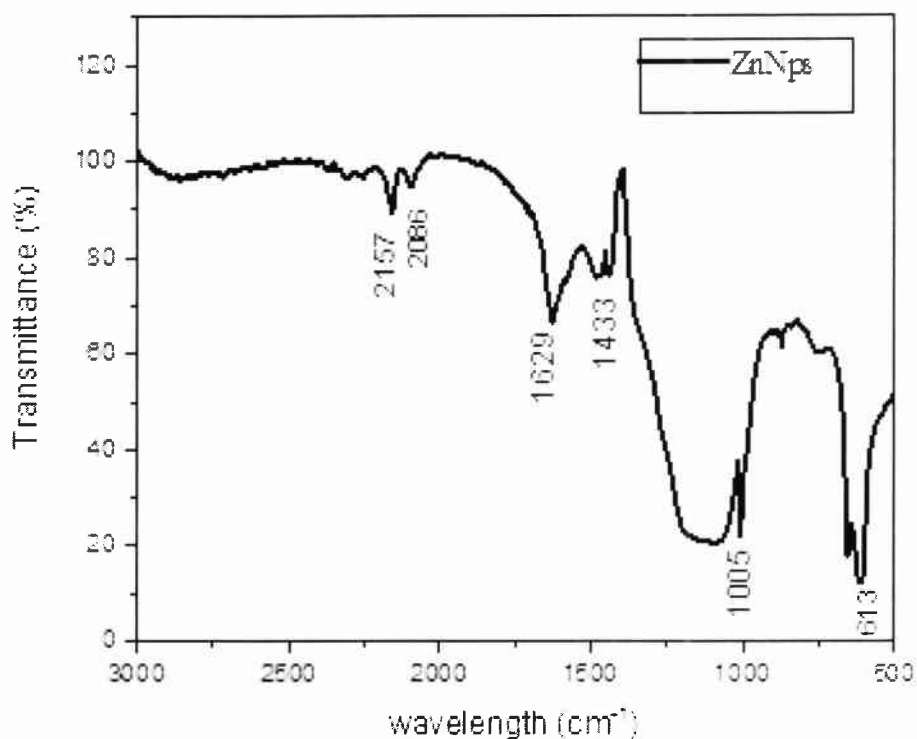


Figure No. 3.15: FTIR spectra of ZnNPs synthesized in the presence of *C. zeylanicum* bark extract

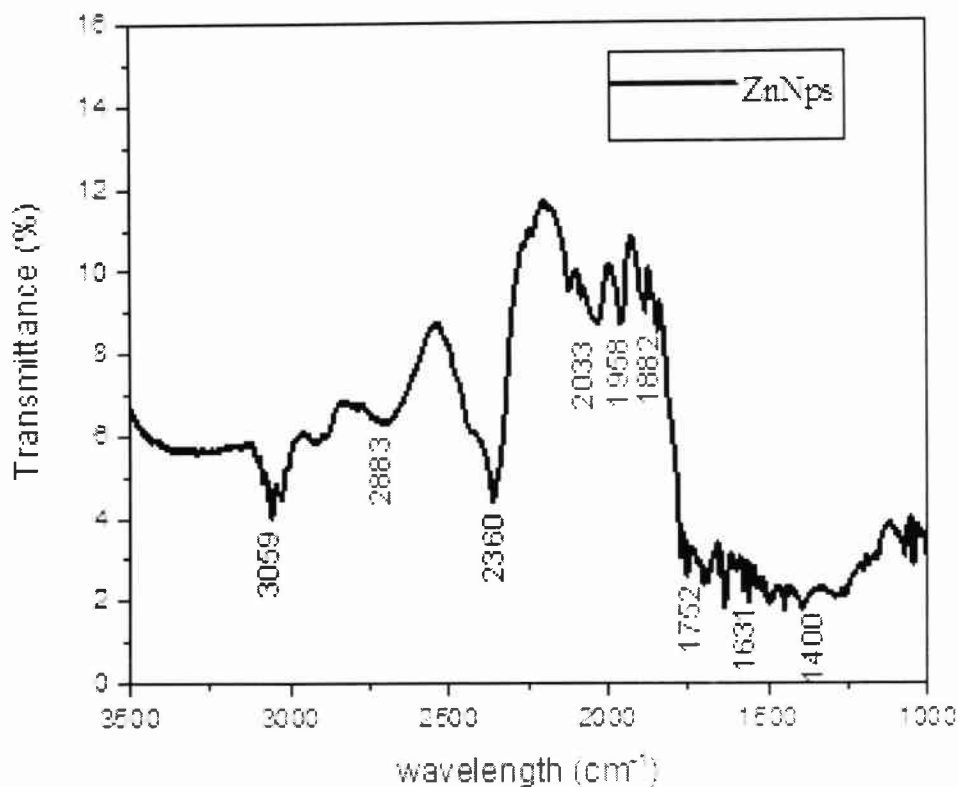


Figure No. 3.16: FTIR spectra of ZnNPs synthesized in the presence of cinnamaldehyde

3.3.3 XRD Analysis

3.3.3.1 Silver Nanoparticles

The crystalline nature of AgNps of *B. lycium* root extract and berberine was confirmed by XRD analysis. Fig.3.17 showed the XRD pattern of the *B. lycium* root extract and berberine nanoparticles from silver colloids. The diffraction peaks of both Nps were observed in the 2θ range of $30\text{--}70^\circ$ which was to be indexed to the (101) (102) (110) for *B. lycium* root extract and (111) (200) (220) for berberine Nps. Consequently, it was confirmed that the both the nanoparticles have crystalline cubic (CC) structure. In both cases, the results were in accordance with the international pattern of joint committee on powder diffraction data number is (JCPDS card no 00-003-0921). (Jung.*et al.*, 1926).

The Ag nanoparticles' high degree of crystallinity seen in the peaks' intensity. The broad diffraction peaks, however, suggested that the crystallites were smaller in size. (I.A. Wani, *et al.*, 2011). We analysed the XRD patterns and determined the full

width at half maximum (FWHM) data, including peak intensity, position, and width. The diffraction peaks have been indexed as crystalline cubic structure.

The average particle size of synthesized AgNPs of *B. lycium* root extract and Berberine were calculated from FWHM of the diffraction peaks using Debye-Scherrer equation (Bykkam *et al.*, 2015).

$$D = k\lambda / B\cos\Theta$$

In this equation, λ which is the radiation wavelength (1.5406 Å), D is the average size of the crystallites, K is the shape-dependent Scherrer's constant corresponding to the true shape of the crystallite (0.94 is used to correspond spherical crystallites with cubic symmetry), β is the full peak width (given in radians) caused by structural broadening due to crystallite size subtracted by instrumental broadening obtained by standard material (Si) in the same measurement Θ = diffraction angle. (Dubey *et al.*, 2010). The FWHM of the *B. lycium* root extract AgNPs of most isolated peaks at about 38° (101), 44° (102) and 64° (110) in 2Θ for *B. lycium* root extract AgNPs (structurally isomorphous with silver) were used for size evaluation. Average crystal size of 16nm was determined while, the FWHM of the berberine AgNPs most of isolated peaks at about 38°(111), 44°(200), and 64°(220) in 2Θ ((structurally isomorphous with silver) were used for size evaluation. For berberine the average crystal size was 47nm.

XRD study was performed to identify the crystalline structure of AgNPs of *C. zeylanicum* bark extract and Cinnamaldehyde. The intensity data were collected over a 2θ range of 30-70 °. Three intense diffraction peaks were observed at 38°.10 (111), 44°.60 (200), and 64°.67 (220) angles (2Θ degree) which correspond to 111, 200, and 220 Bragg's reflection, respectively (Figure 3.19 and 3.20). A definite line broadening of the XRD peaks indicates that the prepared material consists of particles in nanoscale range. Both AgNPs have crystal cubic structure (CC). In both Nps, the results were in accordance with the international pattern of joint committee on powder diffraction data is (JCPDS card no 00-004-0783).(Swanson, Tatge.,195356).

We identified the peaks' intensity, position, and width using this XRD patterns analysis, as well as their full width at half-maximum (FWHM) data. The diffraction peaks have been indexed as crystalline cubic structure.

Using the Debye-Scherrer equation, the average particle size of both AgNps was determined from the FWHM of the diffraction peaks (Bykkam *et al.*, 2015).

$$D = k\lambda/\beta\cos\Theta$$

Where D denotes the nanoparticle's size, λ denotes its wavelength, β denotes its full width at half maximum, and Θ denotes its diffraction angle. Calculations were assessed by determining the size of AgNPs based on several refraction peaks. The findings revealed that the average AgNp size of *C. zeylanicum* was 10.508 nm and that of cinnamonaldehyde was 19.634 nm.

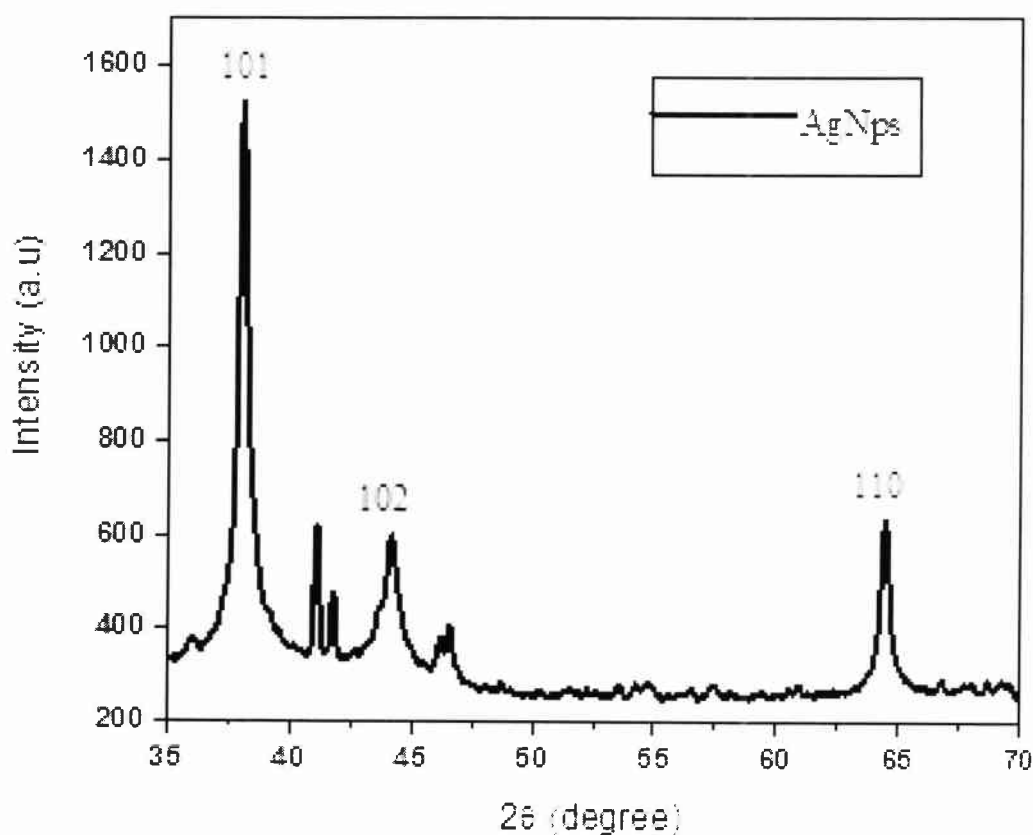


Figure No. 3.17: XRD spectra of AgNPs synthesized in the presence of *B. lycium* root extract

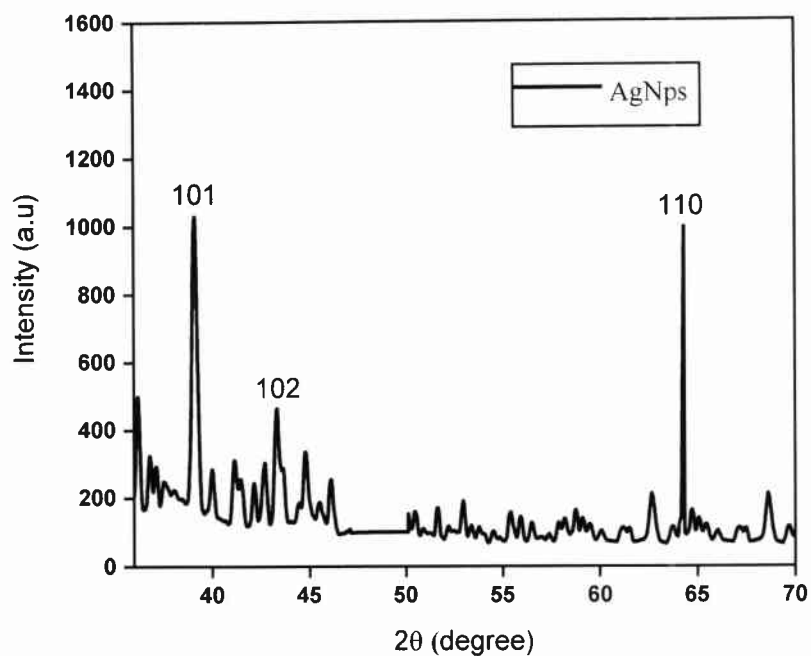


Figure No. 3.18: XRD spectra of AgNPs synthesized in the presence of berberine

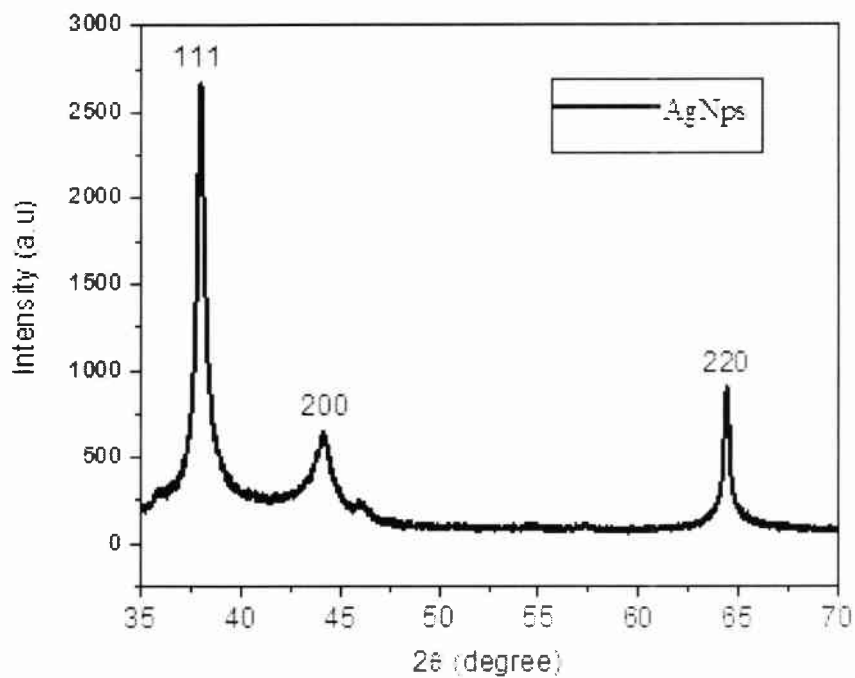


Figure No. 3.19: XRD spectra of AgNPs synthesized in the presence of *C. zeylanicum* bark extract

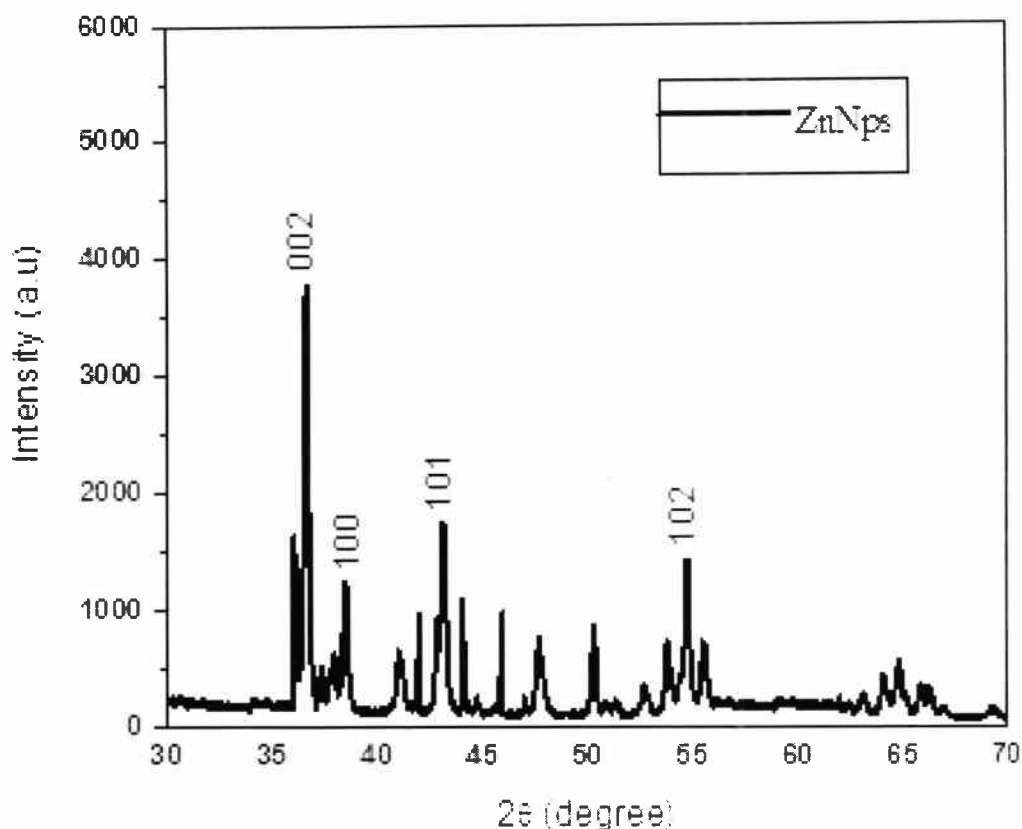


Figure No. 3.20: XRD spectra of AgNPs synthesized in the presence of cinnamaldehyde

3.3.3.2 Zinc nanoparticles

Figure (3.21, 3.22) showed the XRD patterns of ZnO nanoparticles synthesized using *B. lycium* root extract and berberine powder with different concentrations. All the peaks of both Nps were observed in the 2θ range of $30\text{--}70^\circ$ and the peaks were well indexed to the hexagonal wurtzite structure of ZnNps *B. lycium* root extract (JCPDS Card no. 00-004-0831) Swanson and Tatge.,1953 and the ZnNps of berberine (JCPDS Card no 00-001-1238) Hanawalt *et al.*,1938 . In both cases, In ZnNps the presence of 36° (002), 39° (100), 43° (101) and 54° (102) planes in XRD patterns indicated the formation of high purity of the ZnO nanoparticles. The ZnO diffraction peaks' strong intensity and narrow width suggested that the final product was highly crystalline in nature. Scherrer's formula was used to get the average crystallite size.

The average particle size of both ZnNps were calculated from FWHM of the diffraction peaks using Debye-Scherrer formula.(Suresh et al., 2015).

$$D = k\lambda/B\cos\Theta$$

Where D is the size of the nanoparticle, λ is the wavelength, β is the full width half maximum, and Θ is the diffraction angle. According to different refraction peaks, the size of AgNPs were calculated.

Average crystallite size of ZnNps of *B. lycium* root extract was estimated and it was found to be in the range of 16.876 nm and the average crystallite size of ZnNps of Berberine was found to be 38.786nm.

XRD patterns of *C. zeylanicum* bark extract and Cinnamaldehyde biologically mediated synthesis of Zn Nanoparticles showed the peaks which were assigned to diffraction angles of (002), (100), (101) and (102). The data for the intensity were gathered across a 2θ range of 30-70°. The XRD peaks' distinct line broadening revealed that the produced material contains particles in the nanoscale range. (Figure 3.23, 3.24). The XRD patterns determined the full width at half maximum (FWHM) data, including peak intensity, position, and width. The diffraction peaks located at 36.297°, 38.993°, 43.233° and 54.377° have been indexed as hexagonal wurtzite phase of ZnNps. In both Nps, the results were in accordance with the international pattern of joint committee on powder diffraction data (JCPDS card no 00-004-0831).(Swanson, Tatge.,1953) and further it also confirmed that Since Zn was the only distinctive peak present in the XRD pattrens, the produced nano powder was devoid of contaminants. Using the Debye-Scherrer formula, the diameter of the produced Zn nanoparticles was determined. (Khoshhesab ZM *et al.*, 2011)

$$D = k\lambda / \beta\cos\Theta$$

Where λ is the X-ray wavelength, Θ is the Bragg diffraction angle, and β is the full width at half-maximum (FWHM) of the diffraction peak corresponding to plane , 0.89 is Scherrer's constant . The average particle size of *C. zeylanicum* bark extract was found to be 10.508nm and the average particle size of Cinnamaldehyde was found to be 38.7366nm which is derived from the FWHM using Scherrer's formula.

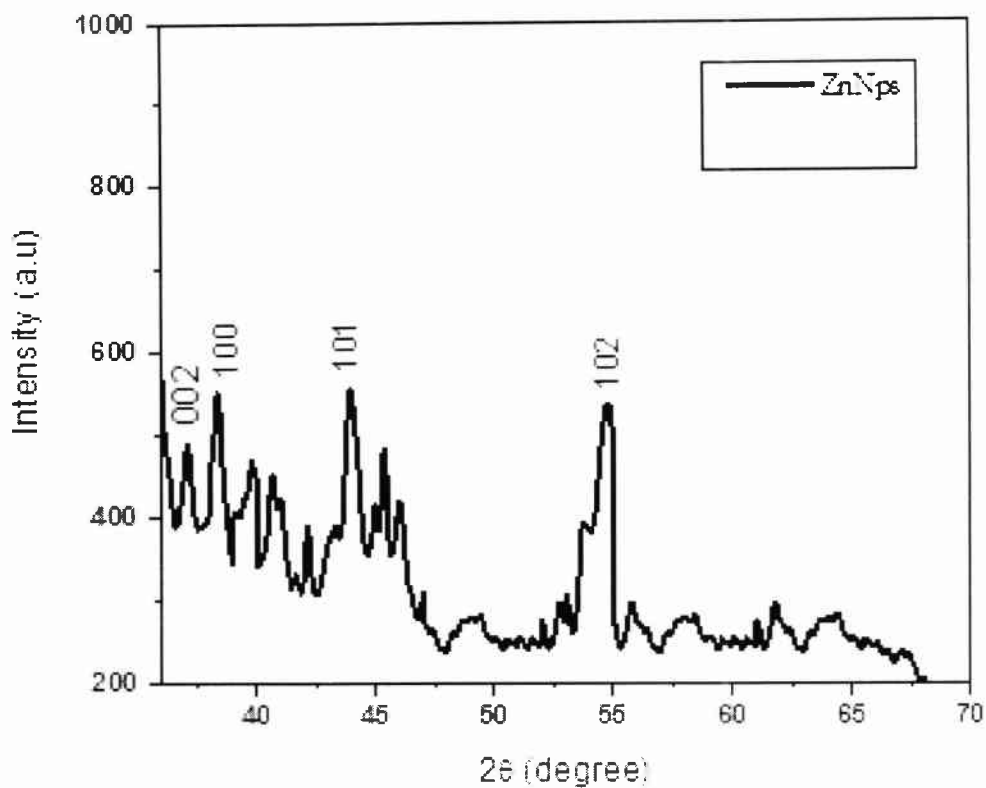


Figure No. 3.21: XRD spectra of ZnNPs synthesized in the presence of *B. lycium* root extract

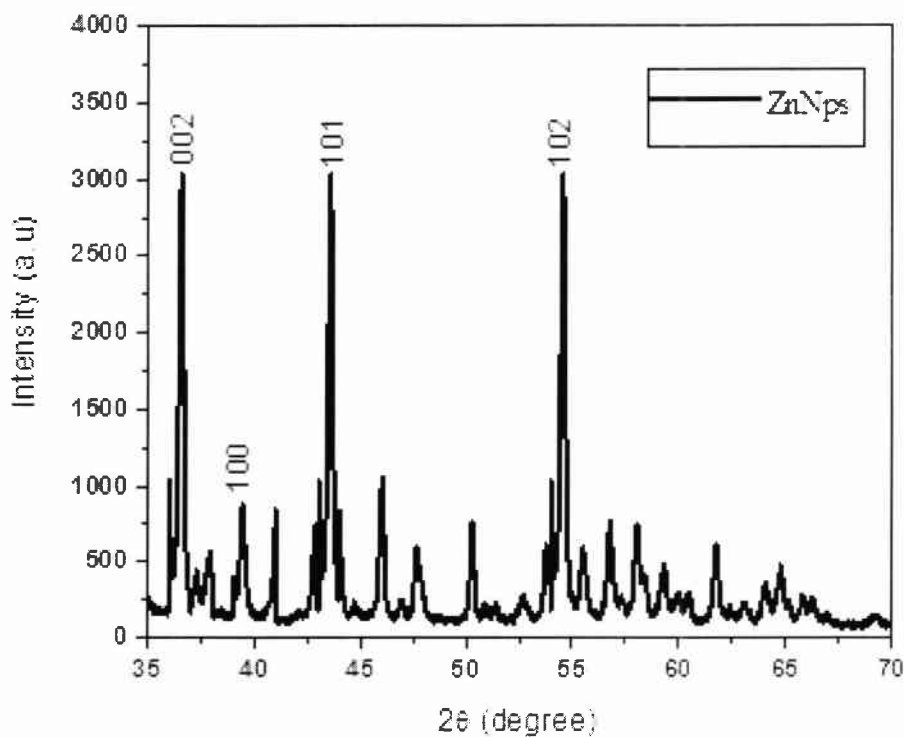


Figure No. 3.22: XRD spectra of ZnNPs synthesized in the presence of berberine

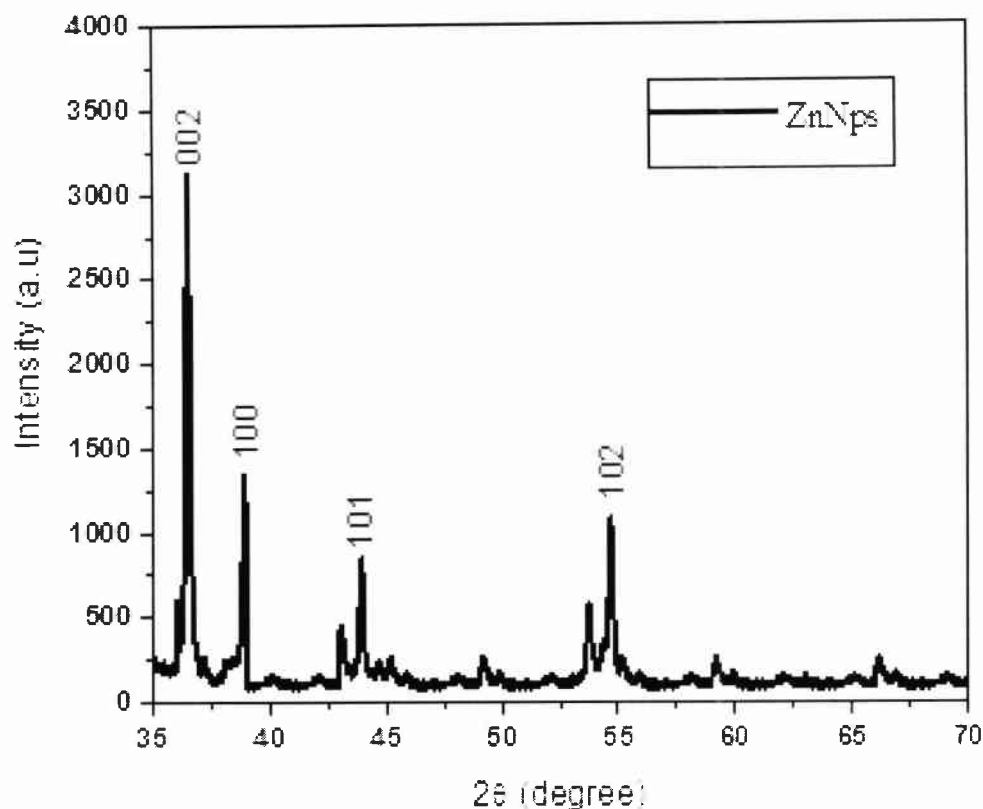


Figure No.3.23: XRD spectra of ZnNPs synthesized in the presence of *C. zeylanicum* bark extract

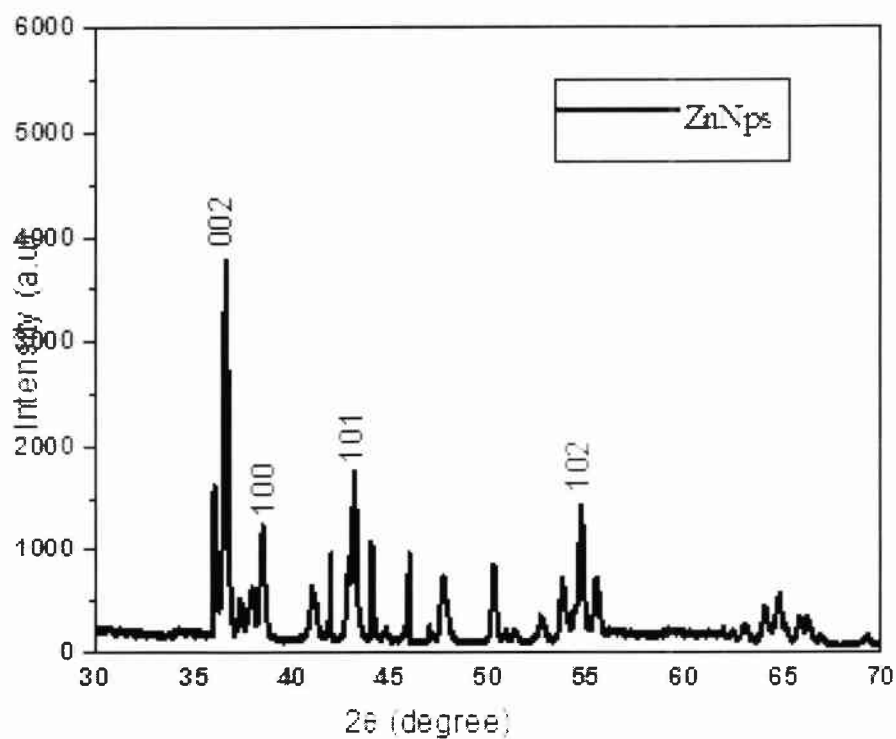


Figure No.3.24: XRD spectra of ZnNPs synthesized in the presence of cinnamaldehyde

3.3.4 Scanning electron microscopy (SEM)

Sample morphology were investigated using scanning electron microscope. Samples were prepared by sticking Ag nanoparticles to the carbon tape, and compressed air were used to blown away the excess powder from the carbon tape. The samples are sputter coated with a thin Au-Pd layer of about 3nm thickness in vacuum to avoid charging.

3.3.4.1 Silver nanoparticles

The Figures display SEM images of biologically created nanoparticles. The existence of metal nanoparticles was confirmed by the SEM investigation. The particles had a diameter of less than 100 nm and were spherical in form. SEM images of AgNPs of *B. lycium* (Figure 3.25) showed spherical shape. The average size of the AgNPs of *B. lycium* was found in the range of 47nm. The size ranges from 10-100nm was observed at magnification of X 40,000, X 50,000 and X44.1. Most particles were spherical in shape. SEM images were taken after 8 days after the completion of all reaction and synthesis process, The particles did not agglomerate.

SEM images of AgNPs of Berberine (Figure 3.26) was observed and found that the particles are in nano-size. The diameter of NPs were below 100nm and the average size of NPs was found in the range of 65-66nm. The particles were observed at magnification of X20, 000, X40, 000 and X80, 000. The SEM images showed that the AgNps of Berberine are mostly spherical in shape.

SEM images of AgNPs of *C. zeylanicum* bark extract (Figure 3.27) was observed and it was confirmed that the diameter of NPs were below from 100nm at magnification of X 40,000, X 80,000 and X 80,000. Particles were observed spherical in shape. The average size of AgNPs of *C. zeylanicum* bark extract were in the range of 53-66nm.

SEM micrograph of prepared AgNPs of Cinnamaldehyde (Figure 3.28) were observed. The average size of NPs were in the range of 70-80nm. The NPs were observed at magnification of X20,000, X40,000 and X 40,000. Mostly, NPs were

spherical in shape and some are oval in shape. All AgNPs were crystalline in nature which is already confirmed by XRD analysis.

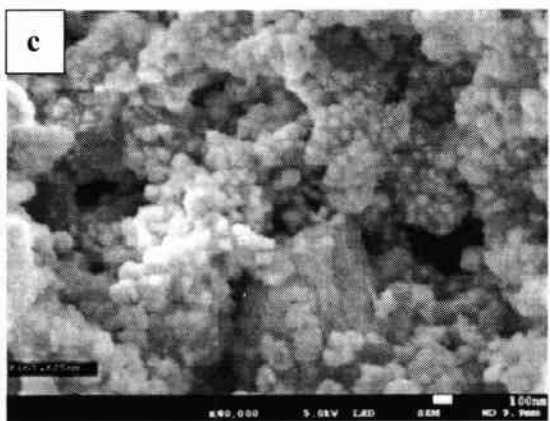
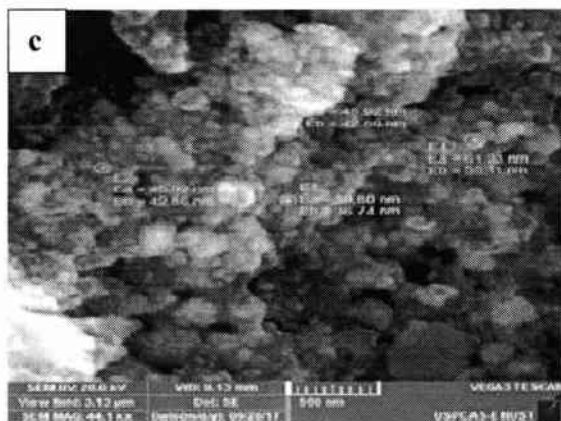
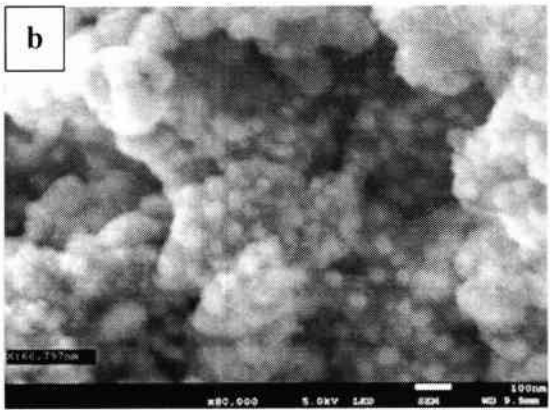
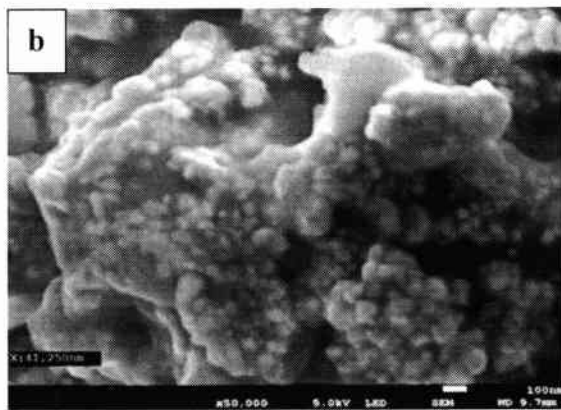
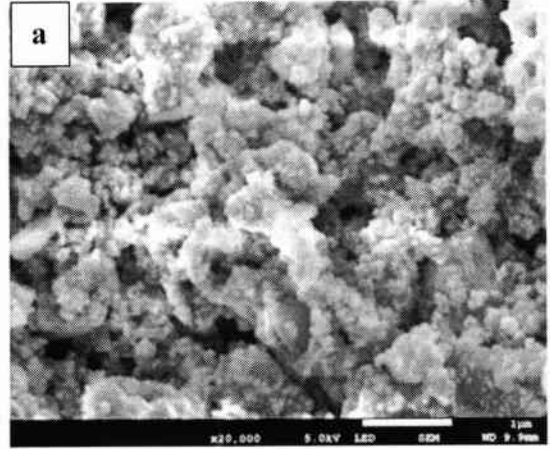
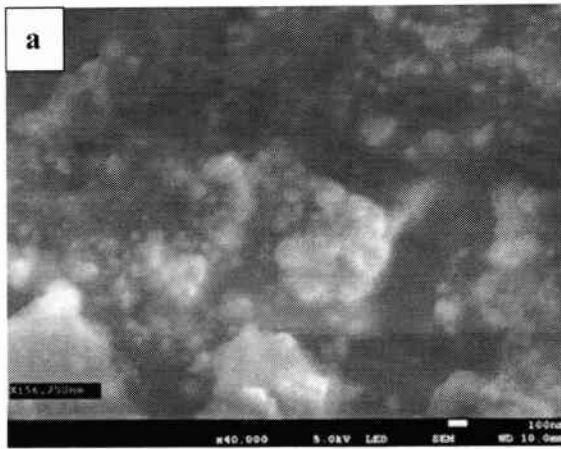


Figure No. 3. 25: Field emission scanning electron micrographs of AgNPs synthesized in the presence of *B. lycium* root extract (a) 100nm (b) 100nm 500nm

Figure No. 3. 26: Field emission scanning electron micrographs of Ag NPs synthesized in the presence of Berberine (a) 100nm (b) 100nm (c) 500nm

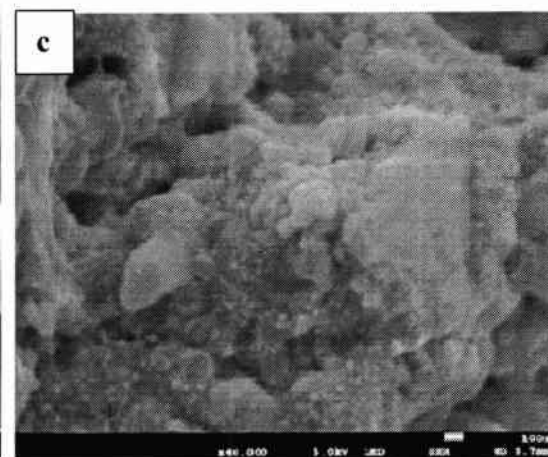
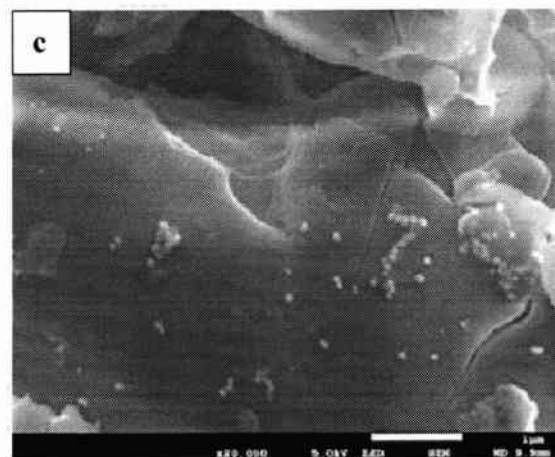
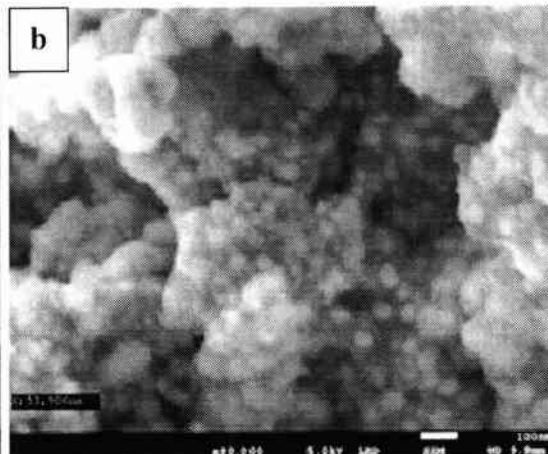
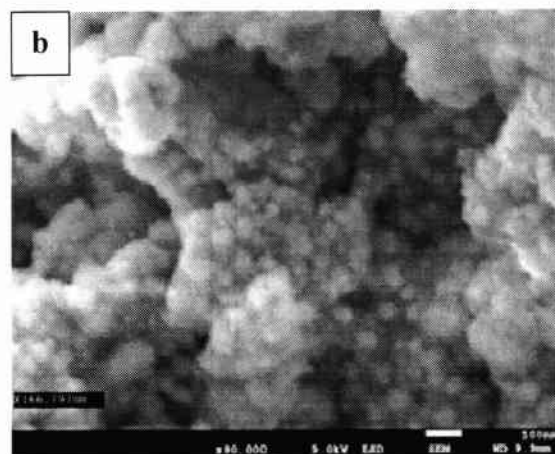
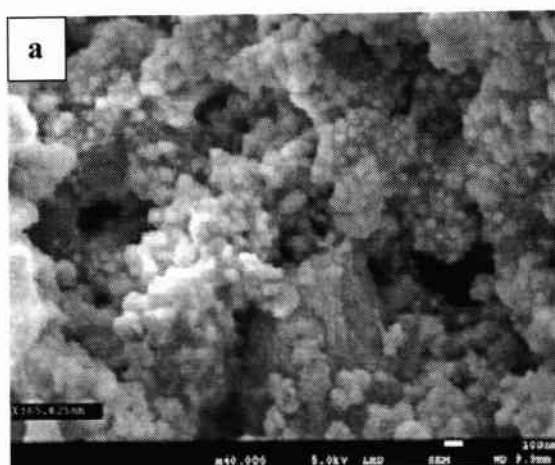


Figure No. 3.27: Field emission scanning electron micrographs of Ag NPs synthesized in the presence of *C. zeylanicum* bark extract (a) 100nm (b) 100nm (c) 100nm

Figure No. 3.28: Field emission scanning electron micrographs of AgNPs synthesized in the presence of Cinnamaldehyde (a) 100nm (b) 1µm (c) 100nm

3.3.4.2 Zinc Nanoparticles

The SEM images of ZnNPs of *B. lycium* root extract showed the hexagonal and spherical morphology and crystalline in nature which is already confirmed by XRD. The size were lies in the range of 36-66nm (Bala saha *et al.*, 2015). SEM images of ZnNPs with a low magnification (Figure 3.29) showed that the sample was composed of microstructure. The SEM images were observed at magnification of X 20,000, X44.6 and X40,000. The SEM images with high magnification revealed that the ZnNPs microstructure has hexagonal and spherical shape. However, aggregation is also seen, most likely as a result of the high surface energy of ZnNPs that often happens during synthesis in an aqueous media as well as perhaps as a result of densification outcomes that there was narrow space between particles. (Selvarajan and V. Mohanasrinivasan., 2013, H. A. Salam *et al.*, 2014)

From the micrographs (Figure 3.30), it was observed that ZnNPs of Berberine also showed hexagonal and spherical morphology and was crystalline in nature, previously confirmed by XRD. The SEM images were observed at magnification of X20,000, X40,000 and X20,000. The ZnNPs ranged in size from 31 to 60 nm on average. Due to the increased surface area of NPs were because of the particle size reduction, the NPs' solubility, dissolving rate, and bioavailability of NPs were improved. (Sahibzada *et al.*, 2018).

The SEM micrographs of ZnNPs of *C. zeylanicum* showed that ZnO nanoparticle dispersion was clearly seen. The powders produced ranged in particle size from 63 to 99 nm with slight variations, and they were homogenous and agglomerated. SEM images were observed at magnification of X 20,000 X40,000 and X40,000. The images (Figure 3.31) shows spherical and hexagonal shapes with some elongated discs of nanoparticles, which are in accord with the XRD. Oxidized metal anions are distributed uniformly throughout the three-dimensional polymeric network structure, the consequences of densification and the close spacing between particles may cause agglomeration. (S.W. Yun *et al.*, 1998) (J.H. Ryu., 2002). The XRD and SEM measurements of nanoparticle size showed just a minor change. There is a variations in the derived values of the particle size of the generated ZnONPs nanoparticle in XRD analysis and in SEM analysis because, XRD calculations measure the wide crystalline region that diffracts X-rays coherently rather than the visible grain boundaries as in

SEM measurements So, the XRD method has a more stringent criteria which shows the smaller sizes of nanoparticles. (S. Bandyopadhyay *et al.*, 2002).

From (Figure 3.32) it was evident that the morphology of zinc nanoparticles of Cinnamaldehyde was spherical and hexagonal in shaped and well distributed with aggregation observed which was very similar to earlier studies of XRD. The SEM images were examined at magnification of X20,000, X40,000 X20,000. The average size of Zn Nps were observed in the range of 36-82nm. However, aggregation is also noted, likely as a result of densification, which results in a small gap between particles, as well as the high surface energy of ZnONPs that often happend when synthesis is carried out in an aqueous media. (Selvarajan & Mohanasrinivasan, 2013).

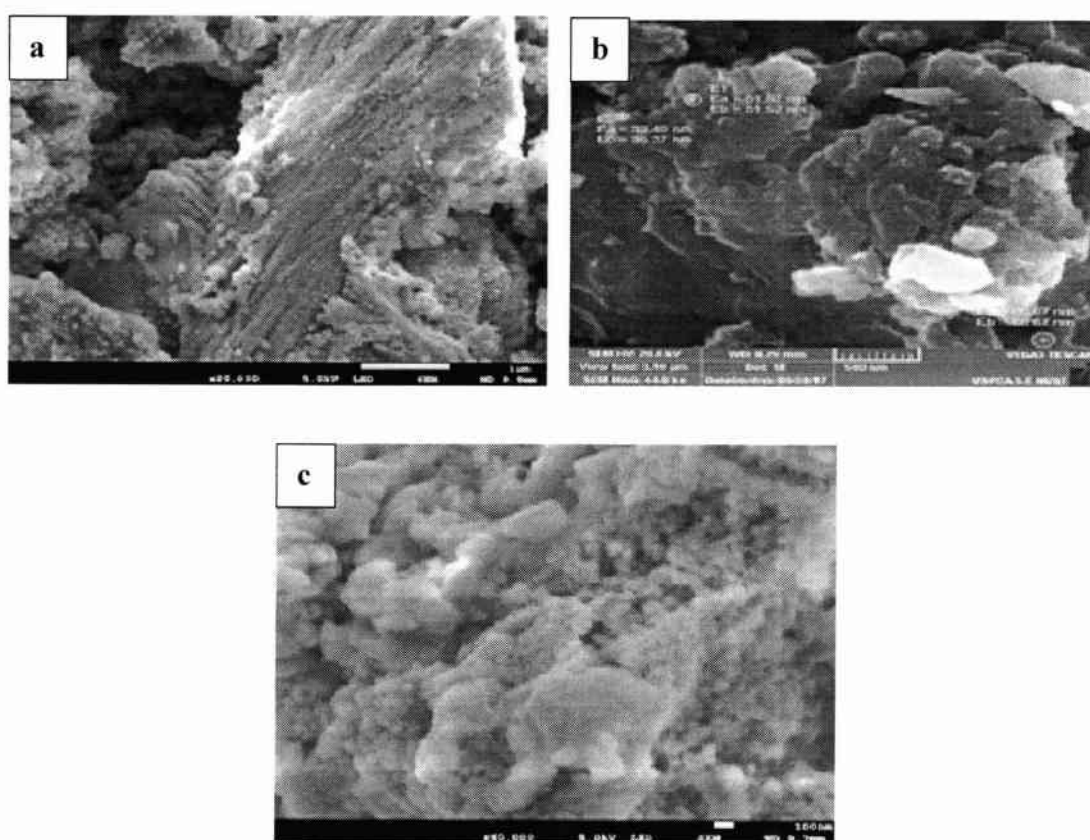


Figure No. 3.29: Field emission scanning electron micrographs of ZnNPs synthesized in the presence of *B. lycium* root extract (a) 1µm (b) 500nm (c) 100nm

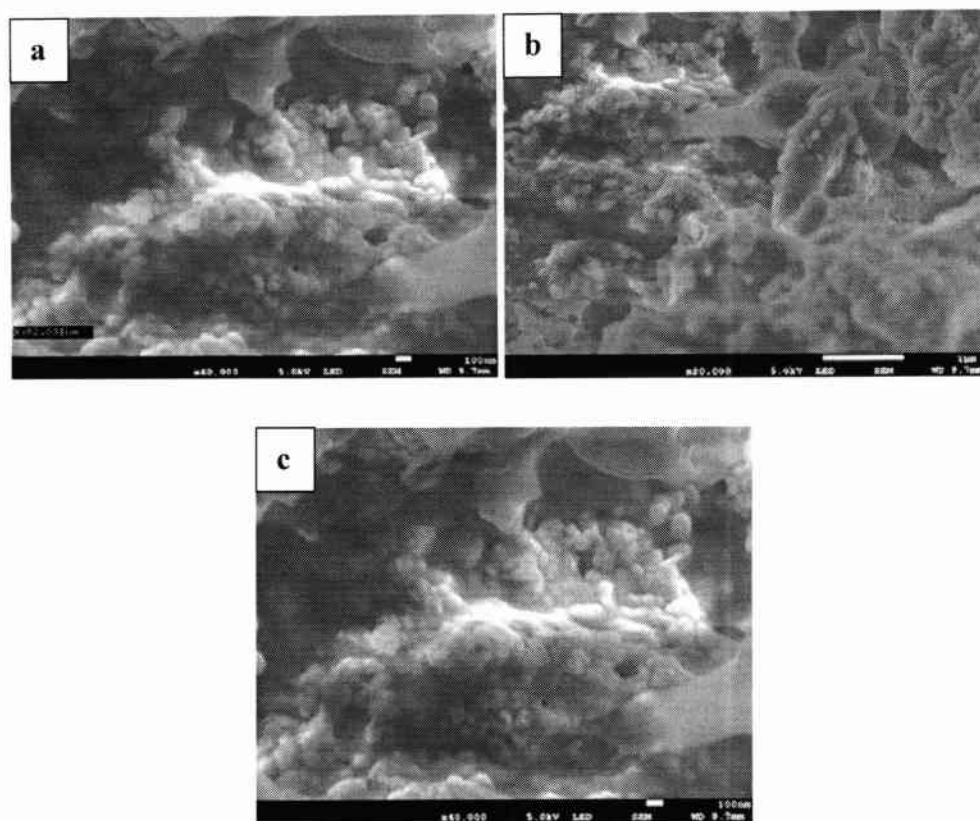


Figure No. 3.30: Field emission scanning electron micrographs of ZnNPs synthesized in the presence of Berberine (a) 100 nm (b) 1 μ m (c) 100nm

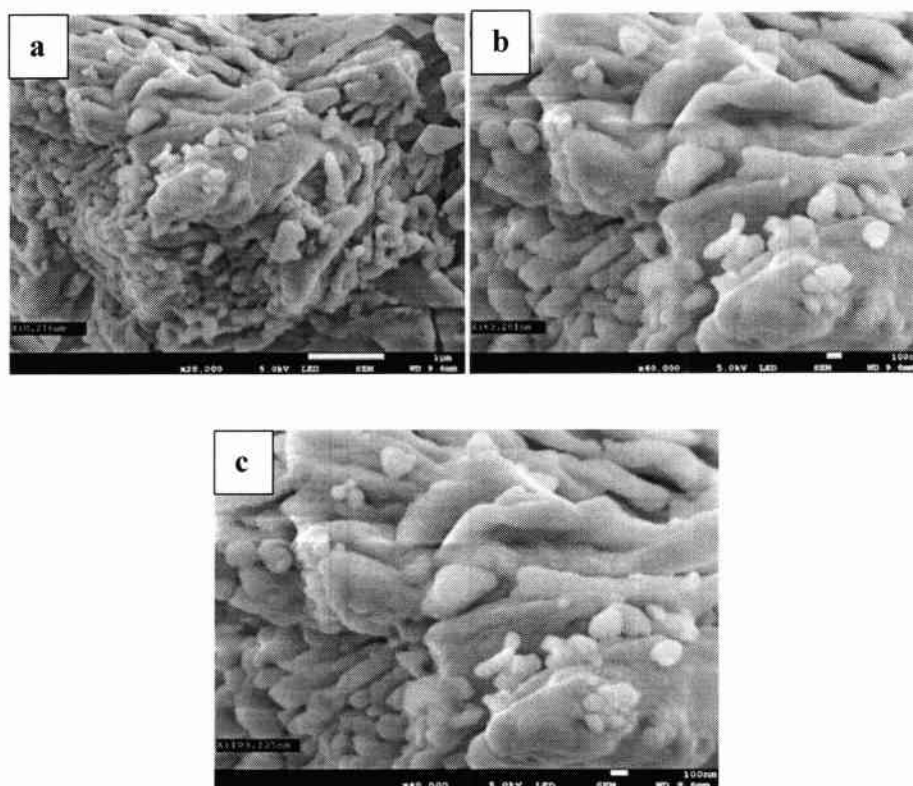


Figure No. 3.31: Field emission scanning electron micrographs of ZnNPs synthesized in the presence of *C. zeylanicum* (a) 100 nm (b) 1 μ m (c) 100nm

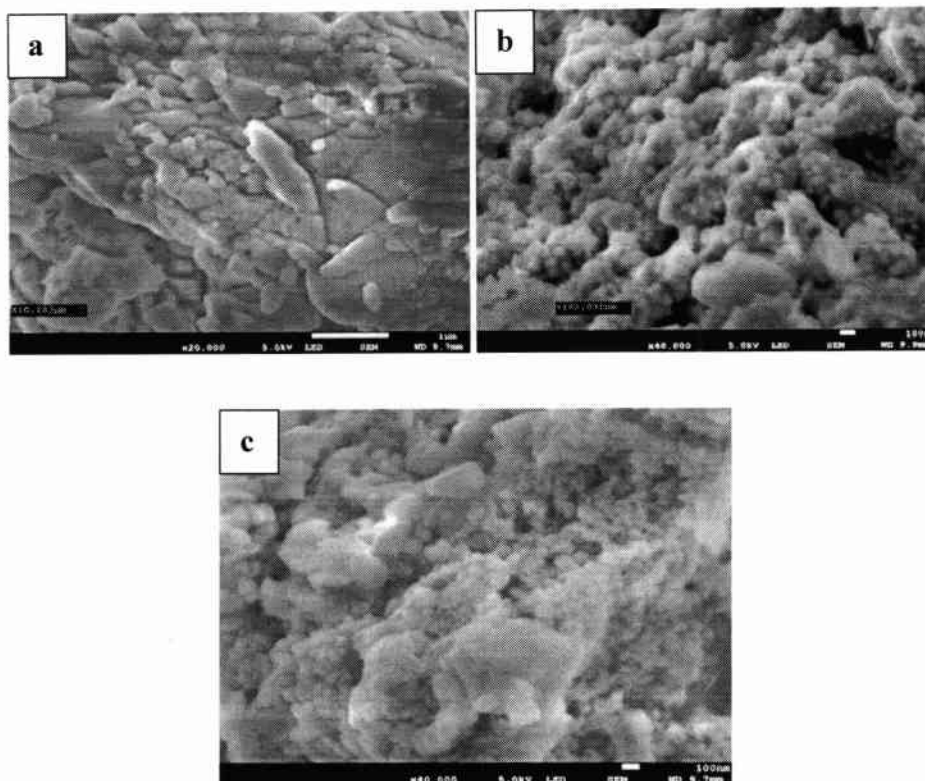


Figure No. 3.32: Field emission scanning electron micrographs of ZnNPs synthesized in the presence of Cinnamaldehyde (a) 100 nm (b) 1 μ m (c) 100nm

3.4 Antibacterial Activity

3.4.1 Antibacterial assay of biologically synthesized Silver and Zinc Nanoparticles a giant *E. coli* strain (ATCC: 8739)

The antibacterial activity results revealed that the biologically synthesized silver nanoparticles were very active against Gram-negative bacterial strain (*E. coli* and Gram-positive bacterial strain (*S. aureus*). Table 3.1 showed that the zones of inhibition of nanoparticles (100, 50, 25, 12.5, 6.25, 3, 1.5, 0.75 μ g/ml), negative control (H_2O) and positive control (pen-strep). Silver nanoparticles of *B. lycium* root extract showed highest activity against *E. coli* (14.66 \pm 0.57mm) at 100 μ g/ml. The lowest antibacterial activity reported against *E. coli* was (9 \pm 1mm) 12.5 μ g/ml concentration. The zone of inhibition of negative control (0 \pm 0mm) and positive control (22 \pm 0mm). The AgNps of *B. lycium* root extract at concentration (6.25, 3, 1.5 and 0.75 μ g/ml) did not show any activity. Minimum inhibitory concentration (MIC) of AgNps *B. lycium* root extract was 1.5 μ g/ml and IC50 value 2.463.

The biologically synthesized AgNPs of berberine showed highest activity against *E. coli* (13.66±0.57mm) at 100µg/ml. The lowest antibacterial activity of AgNPs berberine was reported against *E. coli* was (6±0mm). At concentration of (3, 1.5 and 0.75µg/ml) AgNPs of berberine did not show any activity. The Minimum inhibitory concentration (MIC) of AgNps berberine was 2.5µg/ml and IC50 value 2.599.

Silver nanoparticles of *C. zeylanicum* bark extract showed highest activity against *E. coli* (17.66±0.57mm) at 100µg/ml. The lowest antibacterial activity was reported against *E. coli* was (3.3±2.8mm) at conc. Of 3µg/ml. The zone of inhibition of negative control (0±0mm) and positive control (22±0mm). The AgNPs of *C. zeylanicum* bark extract at concentration (1.5 and 0.75µg/ml) did not show any activity. Minimum inhibitory concentration (MIC) of *C. zeylanicum* bark extract was 6.25 µg/ml and IC50 value 5.1576.

The biologically synthesized AgNPs of Cinnamaldehyde showed highest activity against *E. coli* (17.33±0.57mm) at 100µg/ml. The lowest antibacterial activity of AgNPs Cinnamaldehyde was reported against *E. coli* (6.33±0.57mm) at 3µg/ml concentration. At concentration of (1.5 and 0.75µg/ml) AgNPs of Cinnamaldehyde did not show any activity. The Minimum inhibitory concentration (MIC) of AgNPs cinnamaldehyde was 6.25 µg/ml and IC50 value 5.161.

Zinc nanoparticles of *B. lycium* root extract showed highest activity against *E. coli* (13.66mm) at 100µg/ml. The lowest antibacterial activity reported against *E. coli* was (6 ±0mm) 6.25 µg/ml concentration. The zone of inhibition of negative control (0±0mm) and positive control (23±0mm). The ZnNPs of *B. lycium* root extract at concentration (3, 1.5 and 0.75µg/ml) did not show any activity. Minimum inhibitory concentration (MIC) of ZnNPs *B. lycium* root extract was 6.25µg/ml and IC50 value 5.073.

The biologically synthesized ZnNPs of berberine showed highest activity against *E. coli* (17.33±0.57mm) at 100µg/ml. The lowest antibacterial activity of ZnNPs berberine was reported against *E. coli* (5.3±0.75mm). At concentration of (3, 1.5 and 0.75µg/ml) ZnNPs of berberine did not show any activity. The Minimum

inhibitory concentration (MIC) of ZnNPs berberine was 6.25µg/ml with IC50 value 6.257.

Zinc nanoparticles of *C. zeylanicum* bark extract showed highest activity against *E. coli* (18.6± 1.15mm) at 100µg/ml. The lowest antibacterial activity was reported against *E. coli* (6.3±0.57mm) at conc. Of 6.25µg/ml. The zone of inhibition of negative control (0±0mm) and positive control (23±0mm). The ZnNPs of *C. zeylanicum* bark extract at concentration (3, 1.5 and 0.75µg/ml) did not show any activity. Minimum inhibitory concentration (MIC) of *C. zeylanicum* bark extract was 12.5 µg/ml and IC50 value 13.95.

The biologically synthesized ZnNPs of Cinnamaldehyde showed highest activity against *E. coli* was (19.33±0.57mm) at 100µg/ml. The lowest antibacterial activity of AgNPs Cinnamaldehyde was reported against *E. coli* was (6±0.0mm) at 6.25ug/ml concentration. At concentration of (3, 1.5 and 0.75µg/ml) AgNPs of Cinnamaldehyde did not show any activity. The Minimum inhibitory concentration (MIC) of AgNPs cinnamaldehyde was 9.5 µg/ml and IC50 value 12.11.

Table No. 3.1: Evaluation of antibacterial activities of different concentration of AgNPs synthesized in the presence of *B. lycium* root extract and berberine (n=3, results are expressed mean \pm SE)

| <i>Escherichia coli</i> (ATCC: 8739) | | | |
|---|-------|---------------------|---|
| NPs | Wells | Conc. (μ g/ml) | Zone of inhibition(mm) Mean \pm SD |
| AgNPs of <i>B. lycium</i> root extract | 1 | 100 | 14.66 \pm 0.57 |
| | 2 | 50 | 13.33 \pm 0.57 |
| | 3 | 25 | 11.33 \pm 0.57 |
| | 4 | 12.5 | 9 \pm 1 |
| | 5 | 6.25 | 0 \pm 0.0 |
| | 6 | 3 | 0 \pm 0.0 |
| | 7 | 1.5 | 0 \pm 0.0 |
| | 8 | 0.75 | 0 \pm 0.0 |
| Negative Control | 9 | -- | 0 \pm 0.0 |
| Positive Control | 10 | -- | 22 \pm 0.0 |
| AgNPs Berberine | 1 | 100 | 13.66 \pm 0.57 |
| | 2 | 50 | 11.66 \pm 0.57 |
| | 3 | 25 | 9 \pm 0.0 |
| | 4 | 12.5 | 8 \pm 0.0 |
| | 5 | 6.25 | 6 \pm 0.0 |
| | 6 | 3 | 0 \pm 0.0 |
| | 7 | 1.5 | 0 \pm 0.0 |
| | 8 | 0.75 | 0 \pm 0.0 |
| Negative Control | 9 | -- | 0 \pm 0.0 |
| Positive Control | 10 | -- | 22 \pm 0.0 |

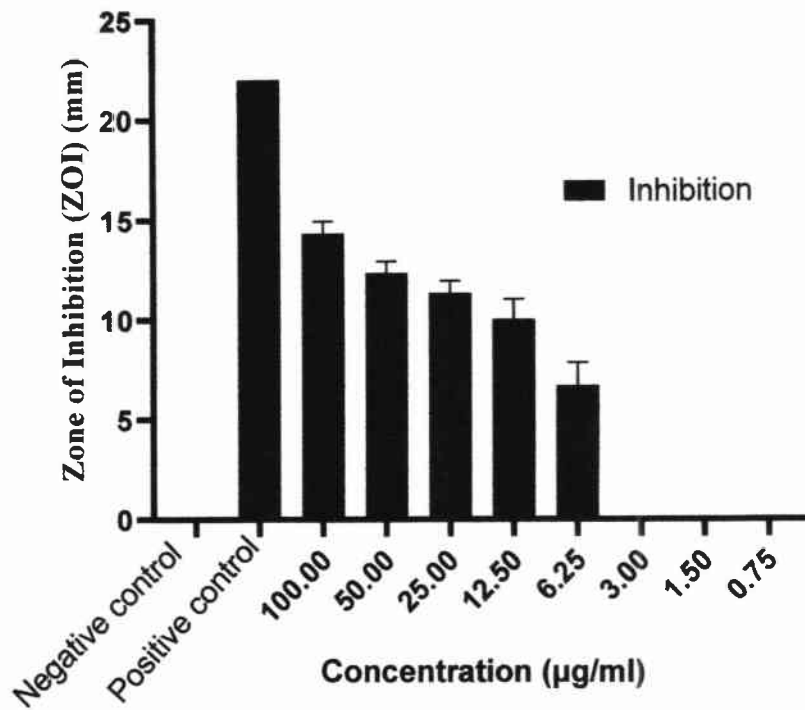


Figure No. 3.33: Evaluation of antibacterial activity of AgNPs synthesized in the presence of *B. lycium* root extract via agar well diffusion method against *E. coli* ATCC # 8739 (Gram negative bacterial strain)

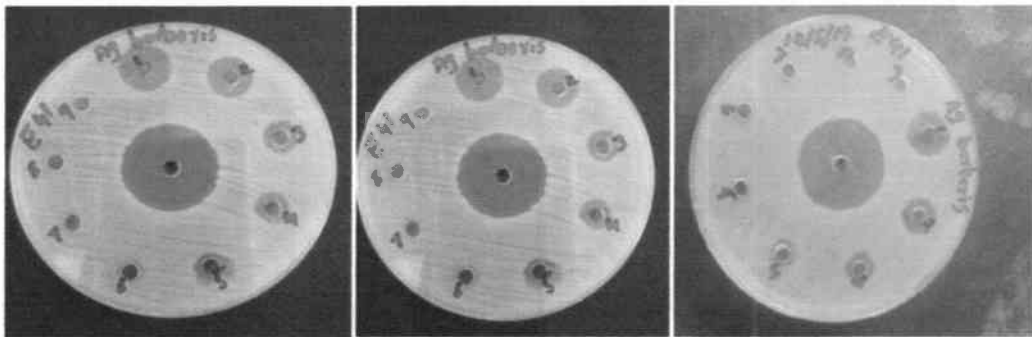


Figure No. 3.34: Photographs of Zone of inhibition of AgNPs synthesized in the presence of *B. lycium* root extract against *E. coli* ATCC # 8739 (Gram negative bacterial strain)

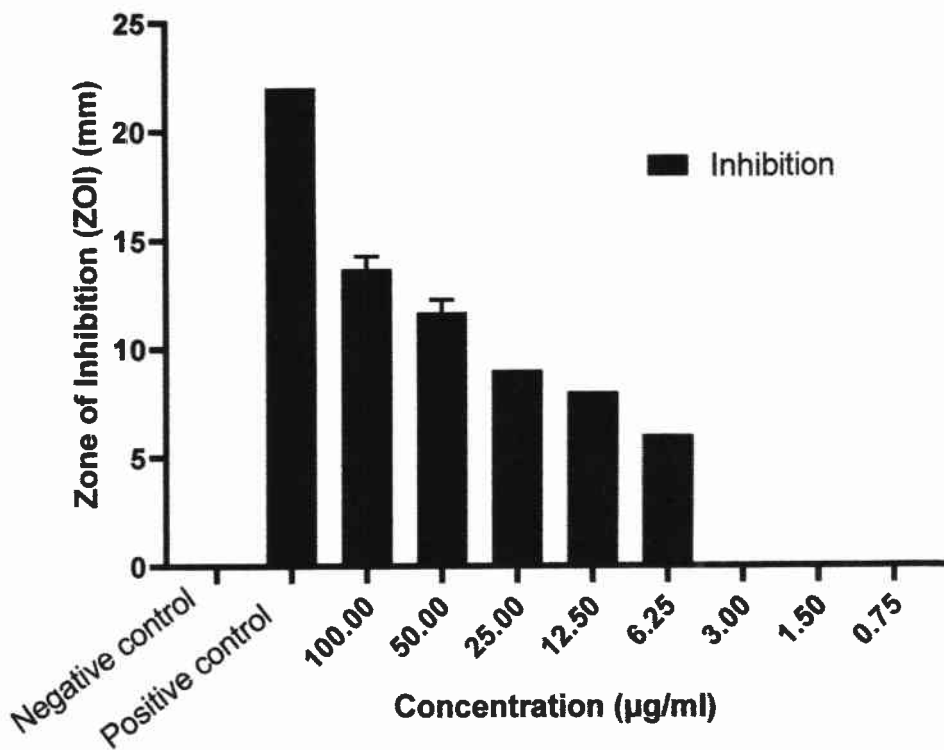


Figure No. 3.35: Evaluation of antibacterial activity of AgNPs synthesized in the presence of berberine via agar well diffusion method against *E. coli* ATCC # 8739 (Gram negative bacterial strain)

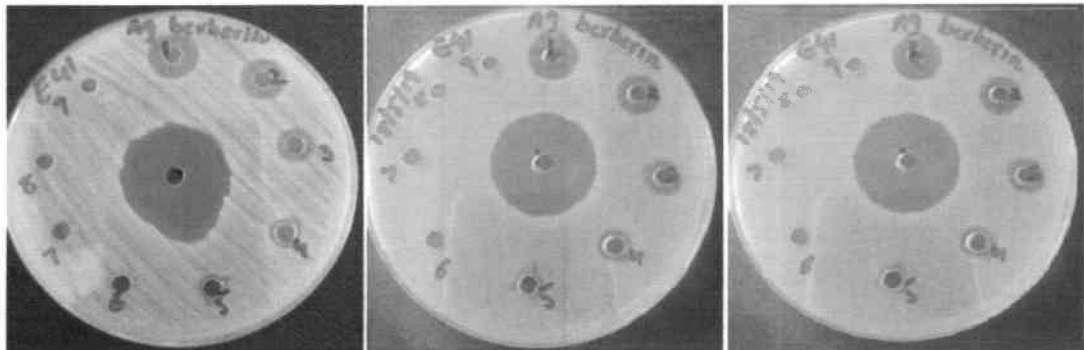


Figure No. 3.36: Photographs of Zone of inhibition of AgNPs synthesized in the presence of berberine against *E. coli* ATCC # 8739 (Gram negative bacterial strain)

Table No. 3.2: Evaluation of antibacterial activities of different concentration of AgNPs synthesized in the presence of *C. zeylanicum* bark Extract and Cinnamaldehyde (n=3, results are expressed mean \pm SE)

| <i>Escherichia coli</i> (ATCC: 8739) | | | |
|---|------|----------------------------|--------------------------------------|
| NPs | Well | Conc. ($\mu\text{g/ml}$) | Zone of Inhibition(mm) Mean \pm SD |
| AgNPs of <i>C. zeylanicum</i> bark Extract | 1 | 100 | 17.66 \pm 0.57 |
| | 2 | 50 | 16.66 \pm 0.57 |
| | 3 | 25 | 14 \pm 1 |
| | 4 | 12.5 | 11 \pm 1 |
| | 5 | 6.25 | 8.33 \pm 0.57 |
| | 6 | 3 | 3.3 \pm 2.8 |
| | 7 | 1.5 | 0 \pm 0.0 |
| | 8 | 0.75 | 0 \pm 0.0 |
| Negative Control | 9 | -- | 0 \pm 0.0 |
| Positive Control | 10 | -- | 22 \pm 0.0 |
| AgNPs Cinnamaldehyde | 1 | 100 | 17.33 \pm 0.57 |
| | 2 | 50 | 15.33 \pm 0.57 |
| | 3 | 25 | 13.33 \pm 0.57 |
| | 4 | 12.5 | 11.33 \pm 0.57 |
| | 5 | 6.25 | 8.33 \pm 0.57 |
| | 6 | 3 | 6.33 \pm 0.57 |
| | 7 | 1.5 | 0 \pm 0.0 |
| | 8 | 0.75 | 0 \pm 0.0 |
| Negative Control | 9 | -- | 0 \pm 0.0 |
| Positive Control | 10 | -- | 22 \pm 0.0 |

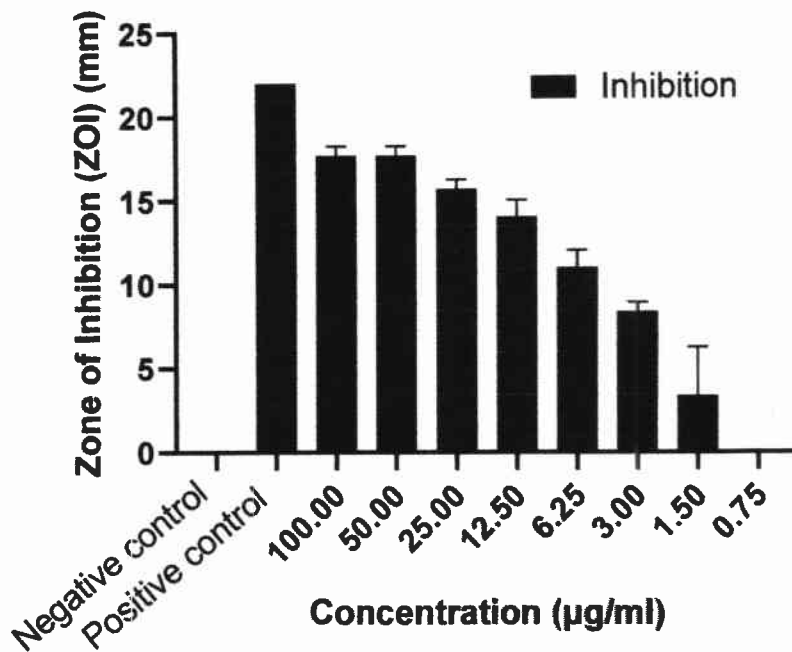


Figure No. 3.37: Evaluation of antibacterial activity of AgNPs synthesized in the presence of *C. zeylanicum* bark extract via agar well diffusion method against *E. coli* ATCC # 8739 (Gram negative bacterial strain)

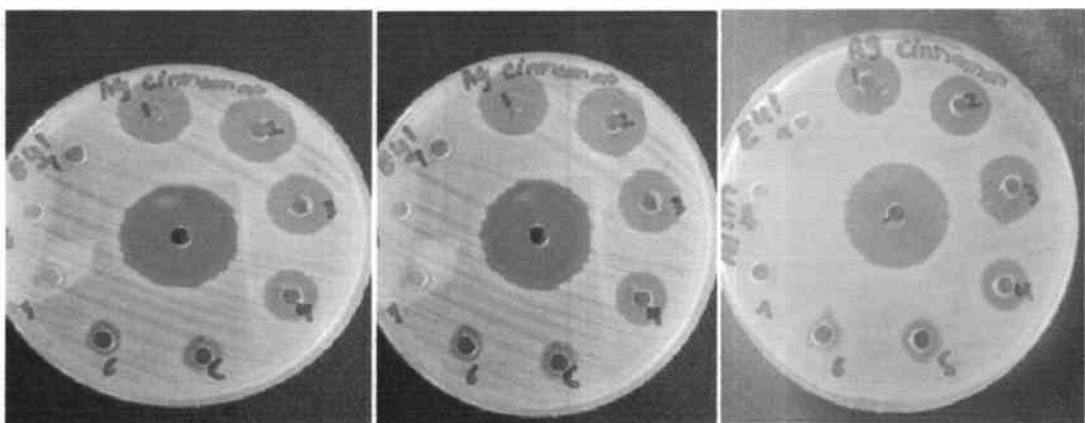


Figure No. 3.38: Photographs of Zone of inhibition of AgNPs synthesized in the presence of *C. zeylanicum* bark extract against *E. coli* ATCC # 8739 (Gram negative bacterial strain)

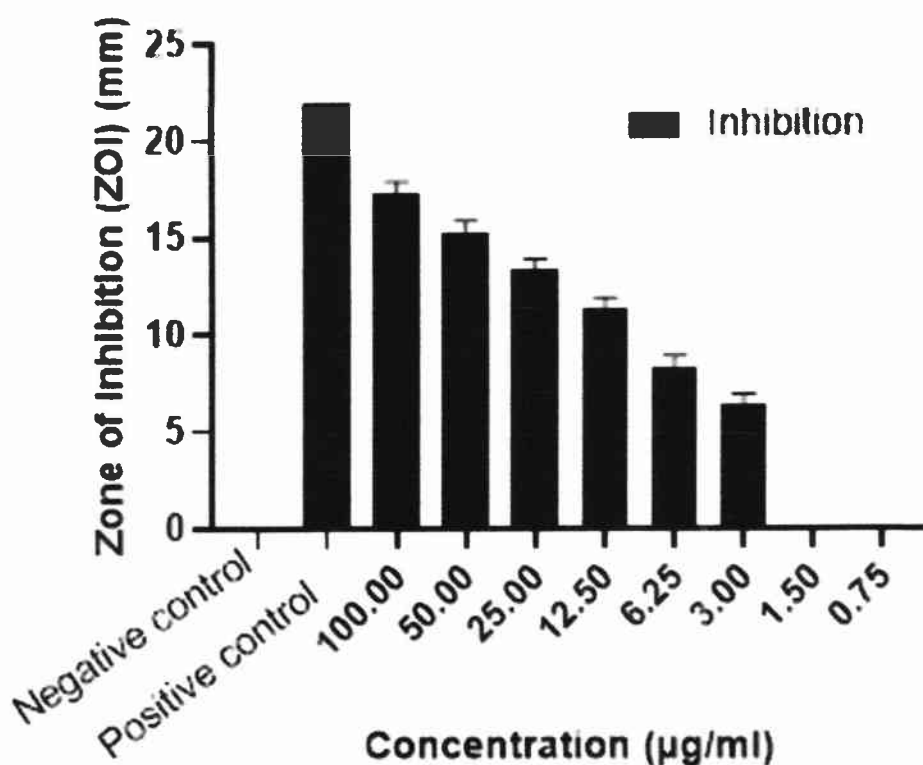


Figure No. 3.39: Evaluation of antibacterial activity of AgNPs synthesized in the presence of cinnamaldehyde via agar well diffusion method against *E. coli* ATCC # 8739 (Gram negative bacterial strain)

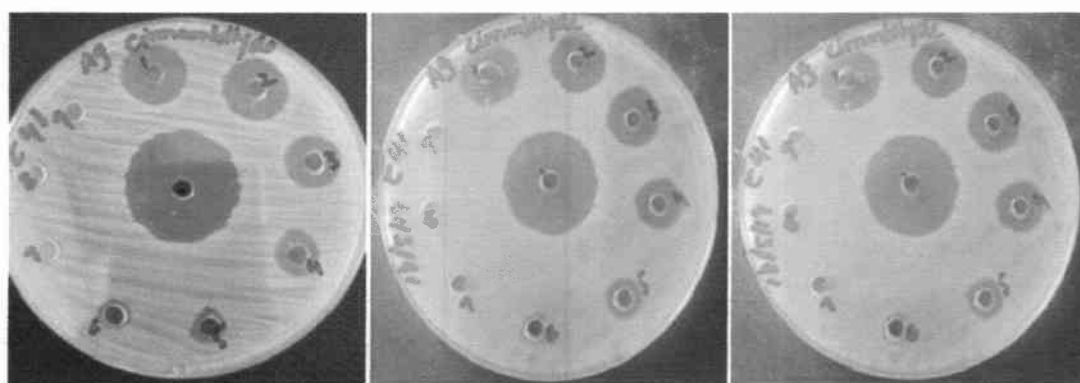


Figure No. 3.40: Photographs of Zone of inhibition of AgNPs synthesized in the presence of Cinnamaldehyde against *E. coli* ATCC # 8739 (Gram negative bacterial strain)

Table No. 3.3: Evaluation of antibacterial activities of different concentration of ZnNPs synthesized in the presence of *B. lycium* root extract and berberine (n=3, results are expressed mean \pm SE)

| <i>Escherichia coli</i> (ATCC : 8739) | | | |
|---|-------|----------------------------|---|
| NPs | Wells | Conc. ($\mu\text{g/ml}$) | Zone of inhibition(mm) Mean \pm SD |
| ZnNPs of <i>B. lycium</i> root extract | 1 | 100 | 13.66 \pm 1.15 |
| | 2 | 50 | 10 \pm 0.0 |
| | 3 | 25 | 7 \pm 1 |
| | 4 | 12.5 | 6 \pm 0.0 |
| | 5 | 6.25 | 6 \pm 0.0 |
| | 6 | 3 | 0 \pm 0.0 |
| | 7 | 1.5 | 0 \pm 0.0 |
| | 8 | 0.75 | 0 \pm 0.0 |
| Negative Control | 9 | -- | 0 \pm 0.0 |
| Positive Control | 10 | -- | 23 \pm 0.0 |
| ZnNPs Berberine | 1 | 100 | 17.33 \pm 0.57 |
| | 2 | 50 | 11.66 \pm 1.15 |
| | 3 | 25 | 8.66 \pm 1.15 |
| | 4 | 12.5 | 6.66 \pm 1.15 |
| | 5 | 6.25 | 5.33 \pm 0.57 |
| | 6 | 3 | 0 \pm 0.0 |
| | 7 | 1.5 | 0 \pm 0.0 |
| | 8 | 0.75 | 0 \pm 0.0 |
| Negative Control | 9 | -- | 0 \pm 0.0 |
| Positive Control | 10 | -- | 23 \pm 0.0 |

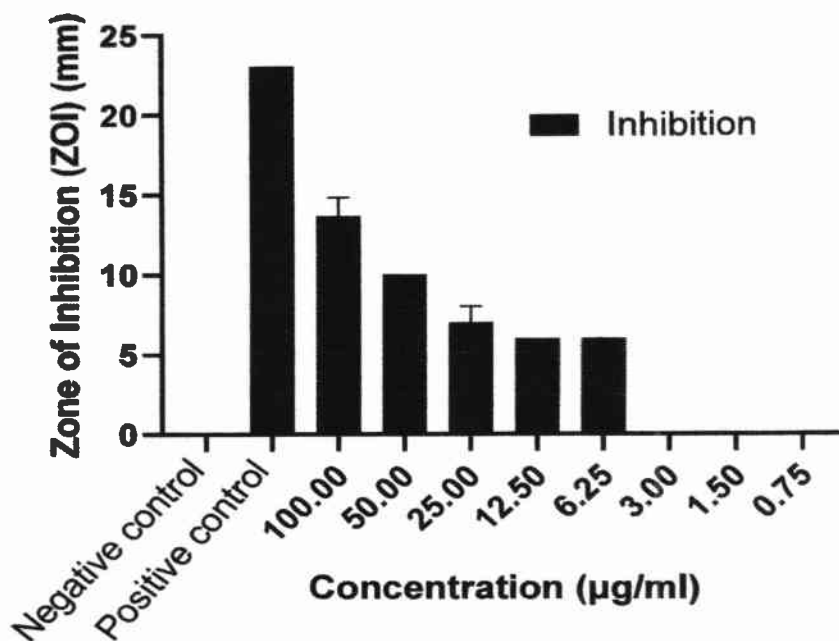


Figure No. 3.41: Evaluation of antibacterial activity of ZnNPs synthesized in the presence of *B. lycium* root extract via agar well diffusion method against *E. coli* ATCC # 8739 (Gram negative bacterial strain)

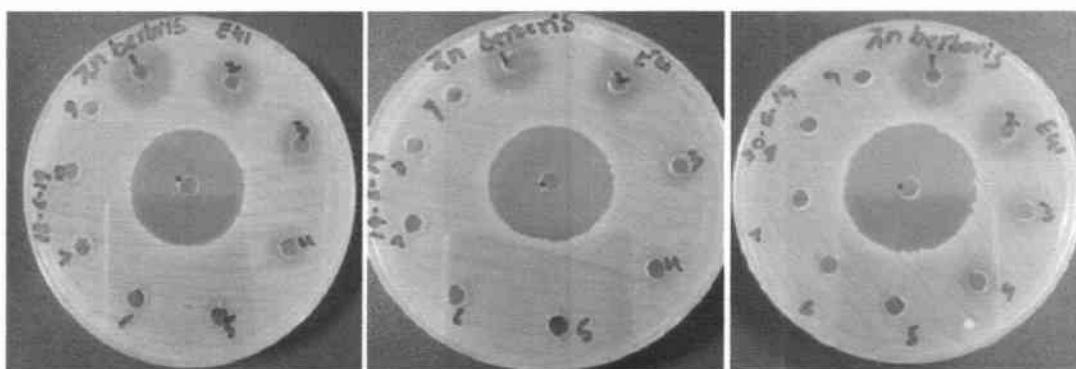


Figure No. 3.42: Photographs of Zone of inhibition of ZnNPs synthesized in the presence of *B. lycium* root extract against *E. coli* ATCC # 8739 (Gram negative bacterial strain)

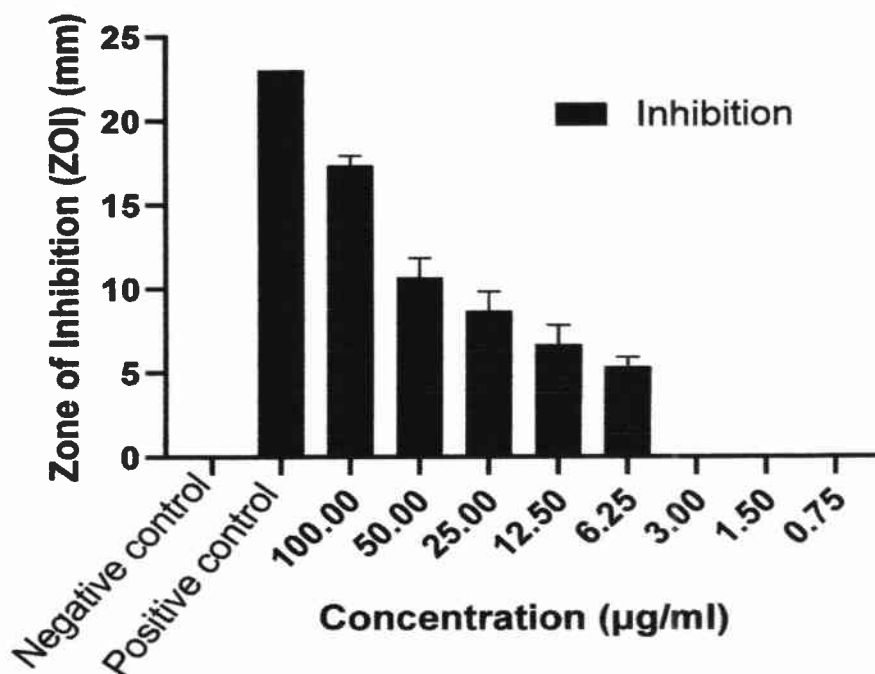


Figure No. 3.43: Evaluation of antibacterial activity of ZnNPs synthesized in the presence of berberine via agar well diffusion method against *E. coli* ATCC # 8739 (Gram negative bacterial strain)

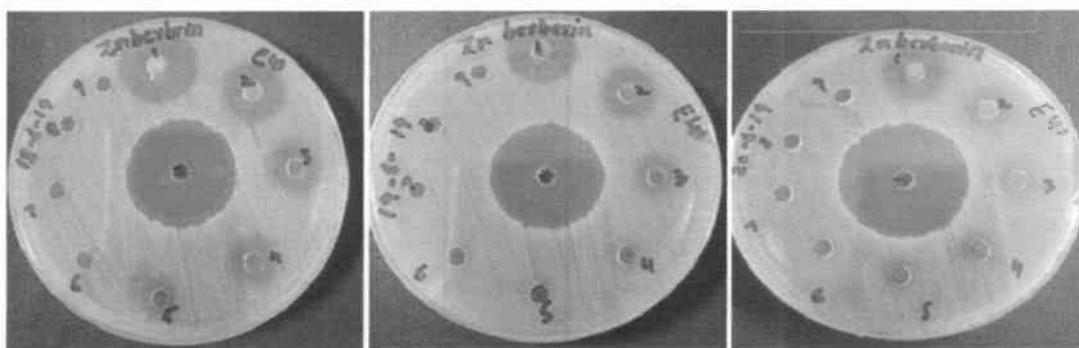


Figure No. 3.44: Photographs of Zone of inhibition of ZnNPs synthesized in the presence of berberine against *E. coli* ATCC # 8739 (Gram negative bacterial strain)

Table No. 3.4: Evaluation of antibacterial activities of different concentration of ZnNPs synthesized in the presence of *C. zeylanicum* bark Extract and Cinnamaldehyde (n=3, results are expressed mean \pm SE)

| <i>Escherichia coli</i> (ATCC: 8739) | | | |
|--|-------|----------------------------|---|
| NPs | Wells | Conc. ($\mu\text{g/ml}$) | Zone of inhibition(mm) Mean \pm SD |
| ZnNPs of <i>C. zeylanicum</i> extract | 1 | 100 | 18.6 \pm 1.15 |
| | 2 | 50 | 16.33 \pm 0.57 |
| | 3 | 25 | 10.66 \pm 1.15 |
| | 4 | 12.5 | 8.6 \pm 1.15 |
| | 5 | 6.25 | 6.3 \pm 0.57 |
| | 6 | 3 | 0 \pm 0.0 |
| | 7 | 1.5 | 0 \pm 0.0 |
| | 8 | 0.75 | 0 \pm 0.0 |
| Negative Control | 9 | -- | 0 \pm 0.0 |
| Positive Control | 10 | -- | 23 \pm 0.0 |
| ZnNPs Cinnamaldehyde | 1 | 100 | 19.33 \pm 0.57 |
| | 2 | 50 | 16.33 \pm 0.57 |
| | 3 | 25 | 9 \pm 0.0 |
| | 4 | 12.5 | 10 \pm 0.57 |
| | 5 | 6.25 | 6 \pm 0.0 |
| | 6 | 3 | 0 \pm 0.0 |
| | 7 | 1.5 | 0 \pm 0.0 |
| | 8 | 0.75 | 0 \pm 0.0 |
| Negative Control | 9 | -- | 0 \pm 0.0 |
| Positive Control | 10 | -- | 23 \pm 0.0 |

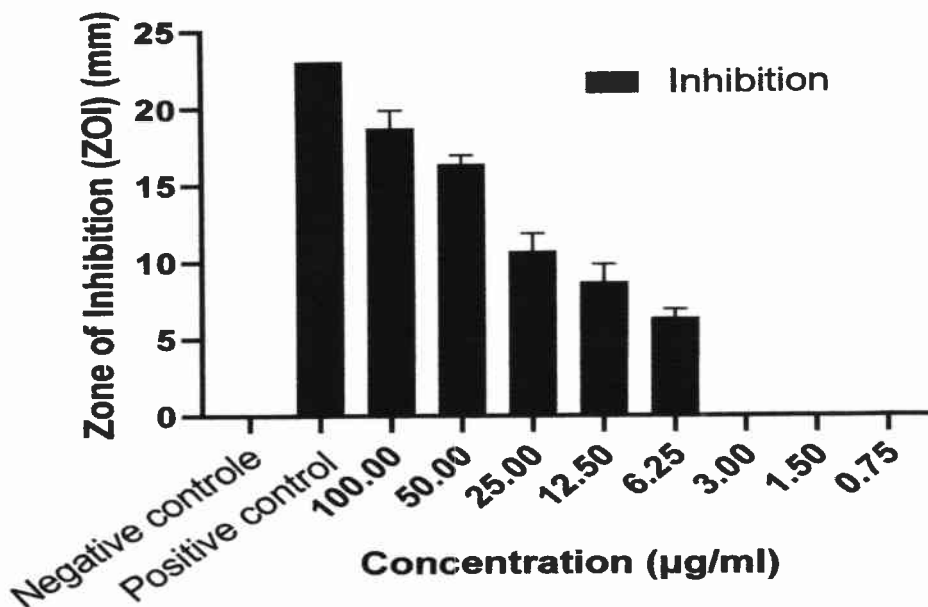


Figure No. 3.45: Evaluation of antibacterial activity of ZnNPs synthesized in the presence of *C. zeylanicum* bark extract via agar well diffusion method against *E. coli* ATCC # 8739 (Gram negative bacterial strain)

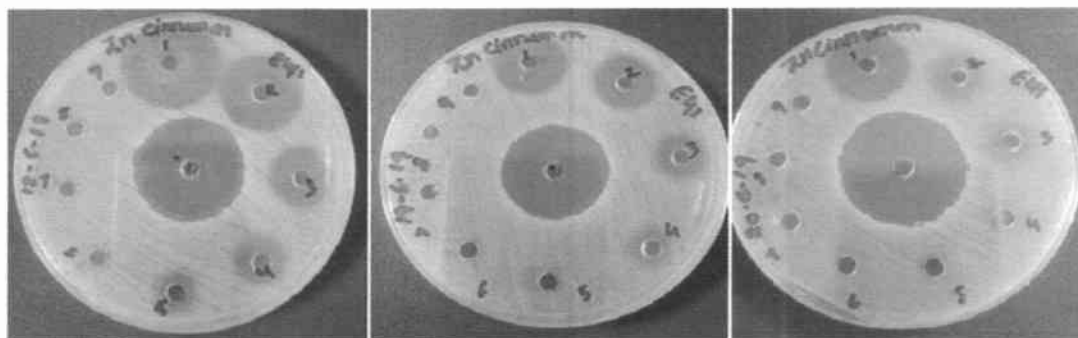


Figure No. 3.46: Photographs of Zone of inhibition of ZnNPs synthesized in the presence of *C. zeylanicum* bark extract against *E. coli* ATCC # 8739 (Gram negative bacterial strain)

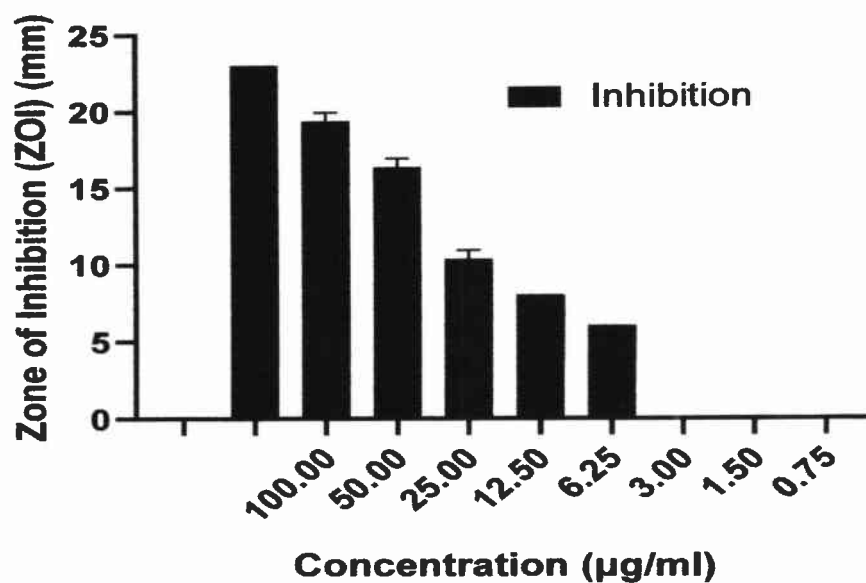


Figure No. 3.47: Evaluation of antibacterial activity of ZnNPs synthesized in the presence of cinnamaldehyde via agar well diffusion method against *E. coli* ATCC # 8739 (Gram negative bacterial strain)

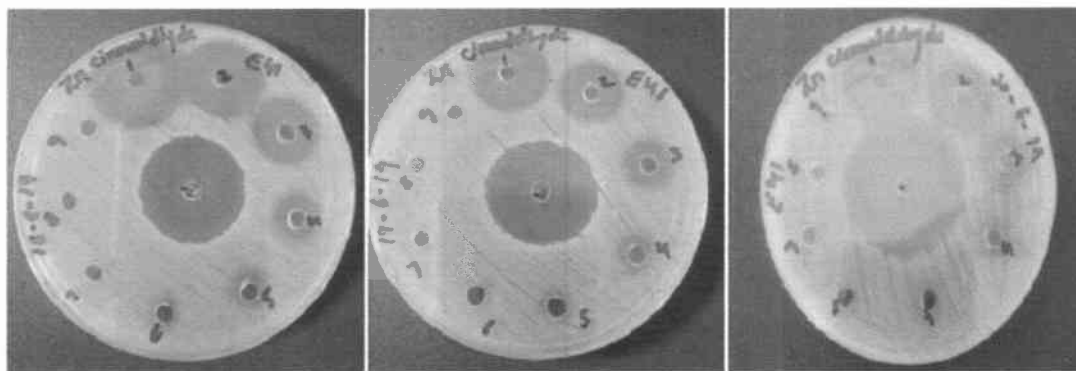


Figure No. 3.48: Photographs of Zone of inhibition of ZnNPs synthesized in the presence of cinnamaldehyde against *E. coli* ATCC # 8739 (Gram negative bacterial strain)

3.4.2 Antibacterial assay of biologically synthesized Silver and Zinc Nanoparticles against *S. aureus* strain (ATCC: 6538)

The antibacterial activity results showed that the biologically synthesized AgNPs were active against Gram-positive bacteria (*S. aureus*). Table 3.5 showed that the nanoparticles showed zones of inhibition of at concentrations (100, 50, 25, 12.5, 6.25, 3, 1.5, 0.75 µg/ml, negative control (H₂O) and positive control (pen-strep). Silver nanoparticles of *B. lycium* root extract showed highest activity against *S. aureus* was (16.33±0.57mm) at 100 µg/ml. The lowest antibacterial activity reported against *S. aureus* was (8.66 ±0.57mm) 6.25 µg/ml concentration. The zone of inhibition of negative control (0±0mm) and positive control (23±0mm). The AgNPs of *B. lycium* root extract at concentration of (3, 1.5 and 0.75 µg/ml) did not show any activity. Minimum inhibitory concentration (MIC) of AgNPs *B. lycium* root extract was 1.5 µg/ml and IC₅₀ value 2.514.

The biologically synthesized AgNPs of berberine showed highest activity against *S. aureus* (13.66±0.57mm) at 100 µg/ml. The lowest antibacterial activity of AgNPs berberine was reported against *S. aureus* (7±1mm). At concentration of (3, 1.5 and 0.75 µg/ml). AgNPs of berberine did not show any activity. The Minimum inhibitory concentration (MIC) of AgNPs berberine was 1.5 µg/ml and IC₅₀ value 2.922.

Silver nanoparticles of *C. zeylanicum* bark extract showed highest activity against *S. aureus* (19.66±0.57mm) at 100 µg/ml. The lowest antibacterial activity was reported against *S. aureus* (12.66±0.57mm) at conc. Of 3 µg/ml. The zone of inhibition of negative control (0±0mm) and positive control (23±0mm). The AgNPs of *C. zeylanicum* bark extract at concentration (1.5 and 0.75 µg/ml) did not show any activity. Minimum inhibitory concentration (MIC) of *C. zeylanicum* bark extract was 2.5 µg/ml and IC₅₀ value 3.735.

The biologically synthesized AgNPs of Cinnamaldehyde showed highest activity against *S. aureus* (17.33±0.57mm) at 100 µg/ml. The lowest antibacterial activity of AgNPs Cinnamaldehyde was reported against *S. aureus* (6.33±0.57mm) at 3 µg/ml concentration. At concentration of (1.5 and 0.75 µg/ml) AgNPs of

Cinnamaldehyde did not show any activity. The Minimum inhibitory concentration (MIC) of AgNPs cinnamaldehyde was 1.5µg/ml and IC50 value 1.729.

Zinc nanoparticles of *B. lycium* root extract showed highest activity against *S. aureus* (14.33mm) at 100µg/ml. The lowest antibacterial activity reported against *S. aureus* was (0 ±0mm) 6.25 µg/ml concentration. The zone of inhibition of negative control (0±0mm) and positive control (23±0mm). The ZnNps of *B. lycium* root extract at concentration (3, 1.5 and 0.75µg/ml) did not show any activity. Minimum inhibitory concentration (MIC) of ZnNPs *B. lycium* root extract was 6.5µg/ml and IC50 value 2.463.

The biologically synthesized ZnNPs of berberine showed highest activity against *S. aureus* (17.33±0.57mm) at 100µg/ml. The lowest antibacterial activity of ZnNPs berberine was reported against *S. aureus* (5.66±0.75mm). At concentration of (3, 1.5 and 0.75µg/ml) ZnNPs of berberine did not show any activity. The Minimum inhibitory concentration (MIC) of ZnNPs berberine was 2.5µg/ml and IC50 value 3.735.

Zinc nanoparticles of *C. zeylanicum* bark extract showed highest activity against *S. aureus* (15.66± 0.57mm) at 100µg/ml. The lowest antibacterial activity was reported against *S. aureus* (1.66±2.88mm) at conc. Of 12.5µg/ml. The zone of inhibition of negative control (0±0mm) and positive control (23±0mm). The ZnNPs of *C. zeylanicum* bark extract at concentration (6.25, 3, 1.5 and 0.75µg/ml) did not show any activity. Minimum inhibitory concentration (MIC) of *C. zeylanicum* bark extract was 6.25 µg/ml and IC50 value 5.073.

The biologically synthesized ZnNPs of Cinnamaldehyde showed highest activity against *S. aureus* (20.66±0.57mm) at 100µg/ml. The lowest antibacterial activity of AgNPs Cinnamaldehyde was reported against *S. aureus* (5.33±0.57mm) at 6.25ug/ml concentration. At concentration of (3, 1.5 and 0.75µg/ml) AgNPs of Cinnamaldehyde did not show any activity. The Minimum inhibitory concentration (MIC) of AgNPs cinnamaldehyde was 6.25 µg/ml and IC50 value 5.161.

Table No. 3.5: Evaluation of antibacterial activities of different concentration of AgNPs synthesized in the presence of *B. lycium* root extract and berberine (n=3, results are expressed mean \pm SE)

| <i>Staphylococcus aureus</i> (ATCC: 6538) | | | |
|---|-------|---------------------|---|
| NPs | Wells | Conc. (μ g/ml) | Zone of inhibition(mm) Mean \pm SD |
| AgNPs of <i>B. lycium</i> root extract | 1 | 100 | 16.33 \pm 0.57 |
| | 2 | 50 | 14.66 \pm 0.57 |
| | 3 | 25 | 13.33 \pm 0.57 |
| | 4 | 12.5 | 10.66 \pm 0.57 |
| | 5 | 6.25 | 8.66 \pm 0.57 |
| | 6 | 3 | 0 \pm 0.0 |
| | 7 | 1.5 | 0 \pm 0.0 |
| | 8 | 0.75 | 0 \pm 0.0 |
| Negative Control | 9 | -- | 0 \pm 0.0 |
| Positive Control | 10 | -- | 23 \pm 0.0 |
| AgNPs Berberine | 1 | 100 | 13.66 \pm 0.57 |
| | 2 | 50 | 12 \pm 1 |
| | 3 | 25 | 11 \pm 1.73 |
| | 4 | 12.5 | 9 \pm 1 |
| | 5 | 6.25 | 7 \pm 1 |
| | 6 | 3 | 0 \pm 0.0 |
| | 7 | 1.5 | 0 \pm 0.0 |
| | 8 | 0.75 | 0 \pm 0.0 |
| Negative Control | 9 | -- | 0 \pm 0.0 |
| Positive Control | 10 | -- | 23 \pm 0.0 |

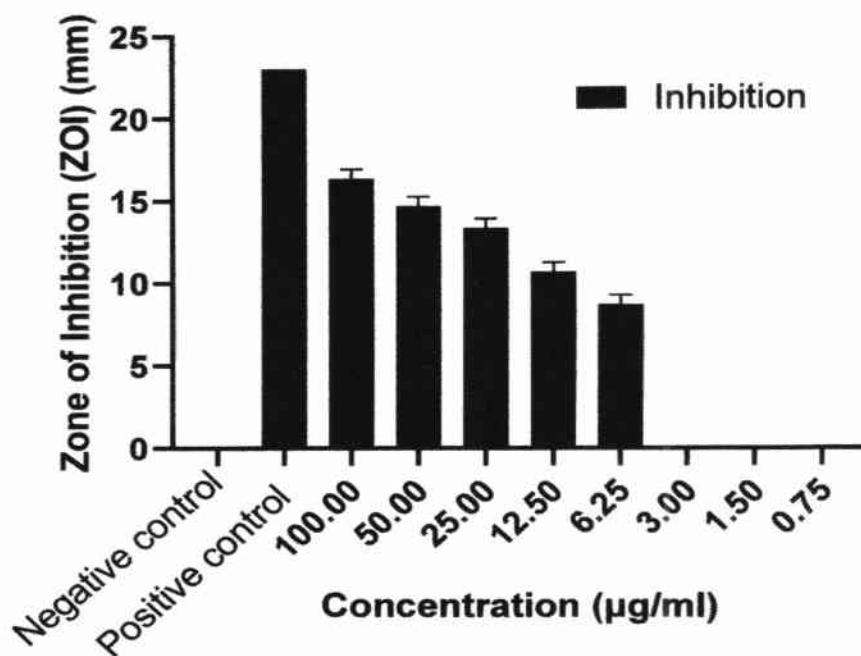


Figure No. 3.49: Evaluation of antibacterial activity of AgNPs synthesized in the presence of *B. lycium* root extract via agar well diffusion method against *S. aureus* ATCC: 6538 (Gram positive bacterial strain)

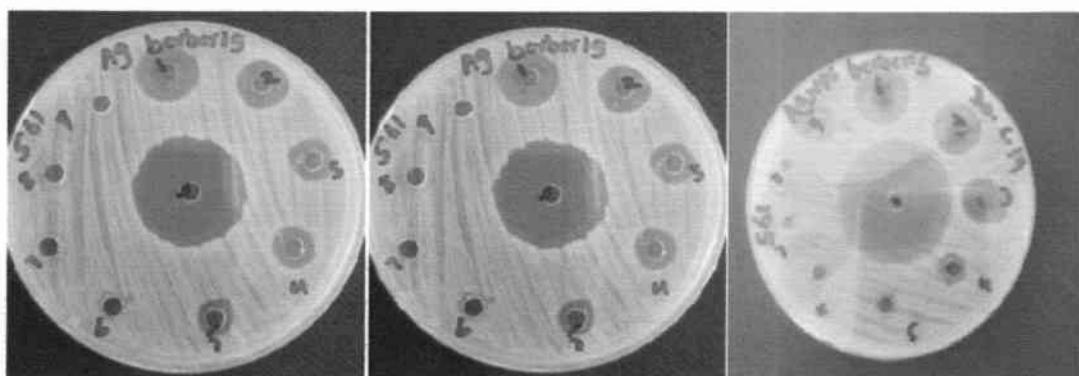


Figure No. 3.50: Photographs of Zone of inhibition of AgNPs synthesized in the presence of *B. lycium* root extract against *S. aureus* ATCC: 6538 (Gram positive bacterial strain)

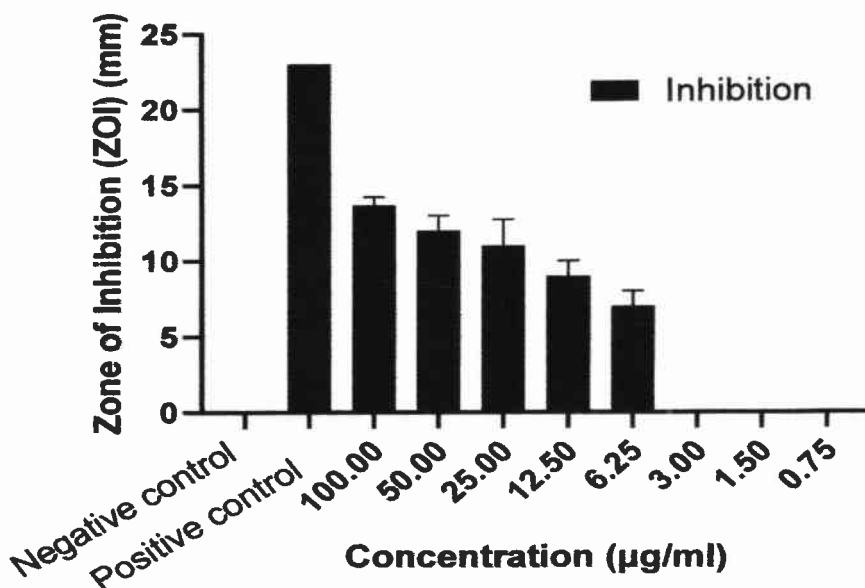


Figure No. 3.51: Evaluation of antibacterial activity of AgNPs synthesized in the presence of berberine via agar well diffusion method against *S. aureus* ATCC: 6538 (Gram positive bacterial strain)

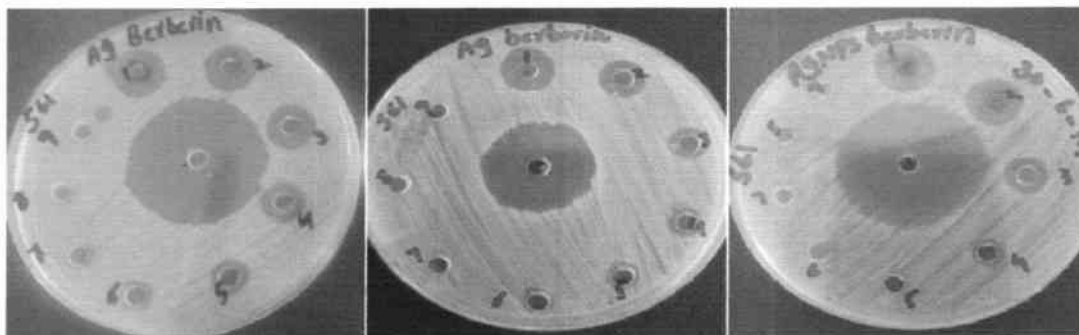


Figure No. 3.52: Photographs of Zone of inhibition of AgNPs synthesized in the presence of berberine against *S. aureus* ATCC: 6538 (Gram positive bacterial strain)

Table No. 3.6: Evaluation of antibacterial activities of different concentration of synthesized in the presence of AgNPs of *C. zeylanicum* bark Extract and Cinnamaldehyde (n=3, results are expressed mean \pm SE)

| <i>Staphylococcus aureus</i> (ATCC: 6538) | | | |
|--|-------|---------------------|---|
| NPs | Wells | Conc. (μ g/ml) | Zone of inhibition(mm) Mean \pm SD |
| AgNPs of <i>C. zeylanicum</i> extract | 1 | 100 | 19.66 \pm 0.57 |
| | 2 | 50 | 18 \pm 0.0 |
| | 3 | 25 | 16.66 \pm 0.57 |
| | 4 | 12.5 | 16 \pm 1 |
| | 5 | 6.25 | 13.66 \pm 0.57 |
| | 6 | 3 | 12.66 \pm 0.57 |
| | 7 | 1.5 | 5 \pm 0.0 |
| | 8 | 0.75 | 0 \pm 0.0 |
| Negative Control | 9 | -- | 0 \pm 0.0 |
| Positive Control | 10 | -- | 23 \pm 0.0 |
| AgNPs Cinnamaldehyde | 1 | 100 | 17.66 \pm 0.57 |
| | 2 | 50 | 15.66 \pm 0.57 |
| | 3 | 25 | 14.66 \pm 0.57 |
| | 4 | 12.5 | 11.66 \pm 0.57 |
| | 5 | 6.25 | 8.66 \pm 0.57 |
| | 6 | 3 | 6.33 \pm 0.57 |
| | 7 | 1.5 | 0 \pm 0.0 |
| | 8 | 0.75 | 0 \pm 0.0 |
| Negative Control | 9 | -- | 0 \pm 0.0 |
| Positive Control | 10 | -- | 23 \pm 0.0 |

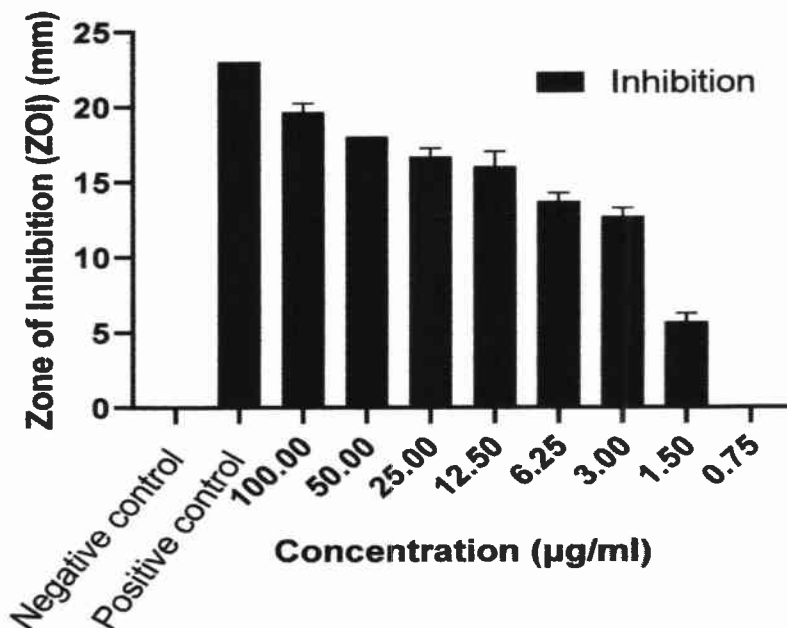


Figure No. 3.53: Evaluation of antibacterial activity of AgNPs synthesized in the presence of *C. zeylanicum* bark extract via agar well diffusion method against *S. aureus* ATCC: 6538 (Gram positive bacterial strain)

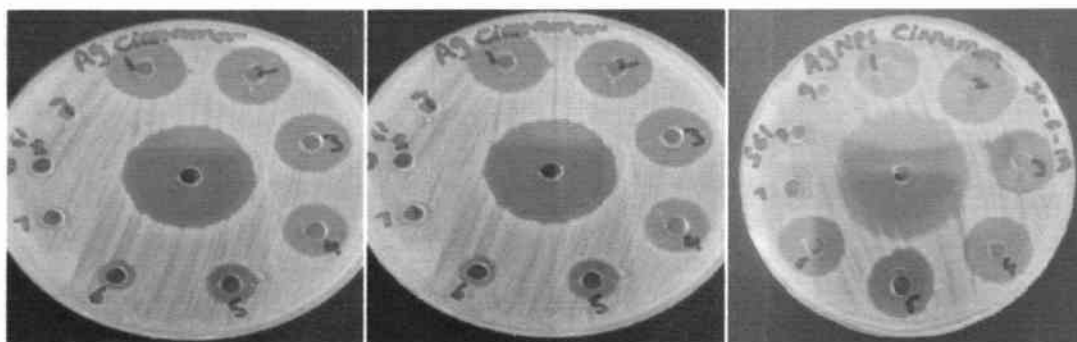


Figure No. 3.54: Photographs of Zone of inhibition of AgNPs synthesized in the presence of *C. zeylanicum* bark extract against *S. aureus* ATCC: 6538 (Gram positive bacterial strain)

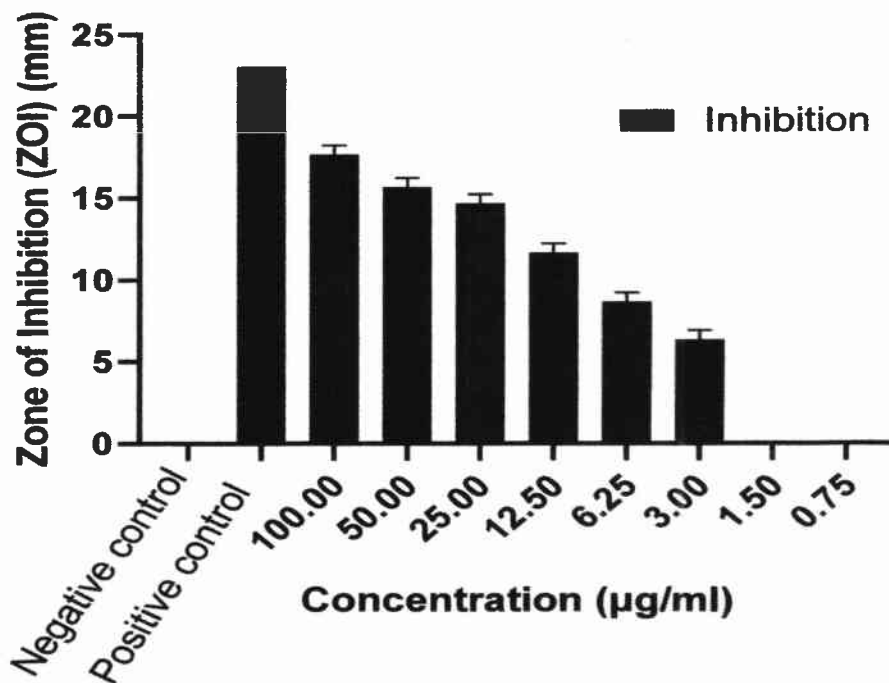


Figure No. 3.55: Evaluation of antibacterial activity of AgNPs synthesized in the presence of cinnamaldehyde via agar well diffusion method against *S. aureus* ATCC: 6538 (Gram positive bacterial strain)

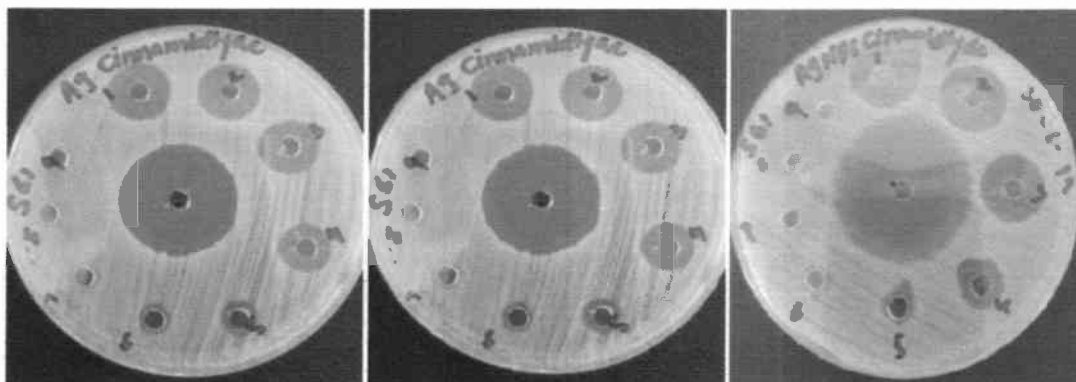


Figure No. 3.56: Photographs of Zone of inhibition of AgNPs synthesized in the presence of cinnamaldehyde against *S. aureus* ATCC: 6538 (Gram positive bacterial strain)

Table No. 3.7: Evaluation of antibacterial activities of different concentration of ZnNPs synthesized in the presence of *B. lycium* root extract and berberine (n=3, results are expressed mean \pm SE).

| <i>Staphylococcus aureus</i> (ATCC: 6538) | | | |
|---|-------|----------------------------|--|
| NPs | Wells | Conc. ($\mu\text{g/ml}$) | Zone of inhibition (mm) Mean \pm SD |
| ZnNPs of <i>B. lycium</i> extract | 1 | 100 | 14.33 \pm 1.15 |
| | 2 | 50 | 13 \pm 1 |
| | 3 | 25 | 10 \pm 1 |
| | 4 | 12.5 | 5.66 \pm 0.57 |
| | 5 | 6.25 | 0 \pm 0.0 |
| | 6 | 3 | 0 \pm 0.0 |
| | 7 | 1.5 | 0 \pm 0.0 |
| | 8 | 0.75 | 0 \pm 0.0 |
| Negative Control | 9 | -- | 0 \pm 0.0 |
| Positive Control | 10 | -- | 23 \pm 0.0 |
| ZnNPs Berberine | 1 | 100 | 17.66 \pm 0.57 |
| | 2 | 50 | 16.33 \pm 0.577 |
| | 3 | 25 | 10 \pm 0.57 |
| | 4 | 12.5 | 7.3 \pm 0.57 |
| | 5 | 6.25 | 5.66 \pm 0.57 |
| | 6 | 3 | 0 \pm 0.0 |
| | 7 | 1.5 | 0 \pm 0.0 |
| | 8 | 0.75 | 0 \pm 0.0 |
| Negative Control | 9 | -- | 0 \pm 0.0 |
| Positive Control | 10 | -- | 23 \pm 0.0 |

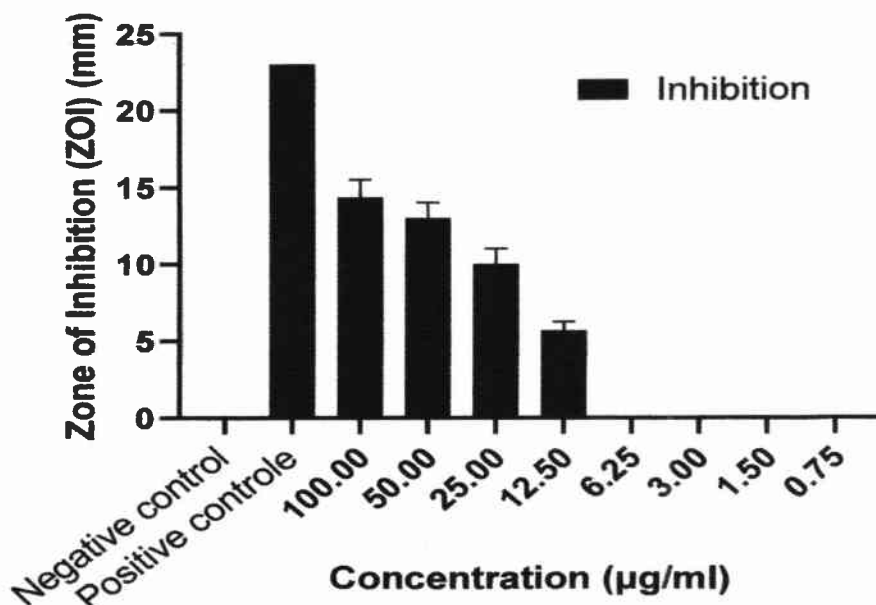


Figure No. 3.57: Evaluation of antibacterial activity of ZnNPs synthesized in the presence of *B. lycium* root extract via agar well diffusion method against *S. aureus* ATCC: 6538 (Gram positive bacterial strain)



Figure No. 3.58: Photographs of Zone of inhibition of ZnNPs synthesized in the presence of *B. lycium* root extract against *S. aureus* ATCC: 6538 (Gram positive bacterial strain)

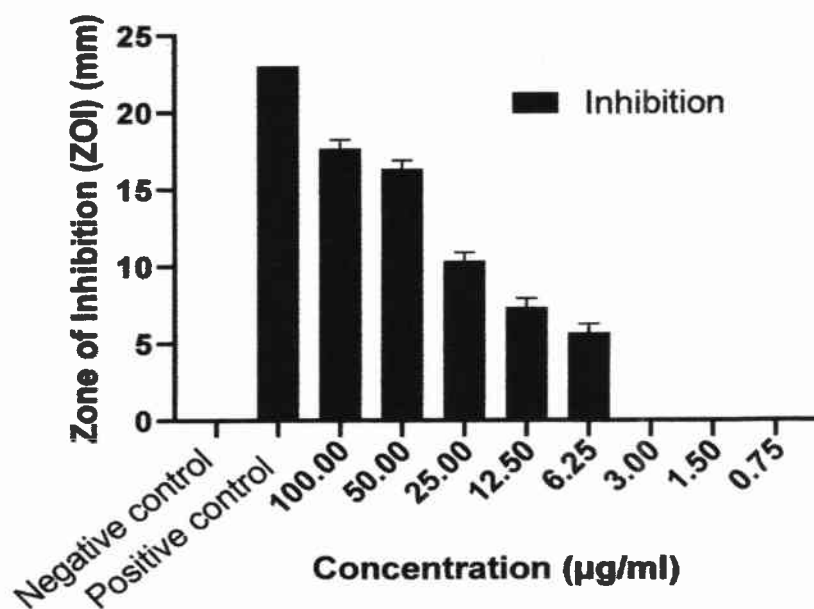


Figure No. 3.59: Evaluation of antibacterial activity of ZnNPs synthesized in the presence of berberine via agar well diffusion method against *S. aureus* ATCC: 6538 (Gram positive bacterial strain)

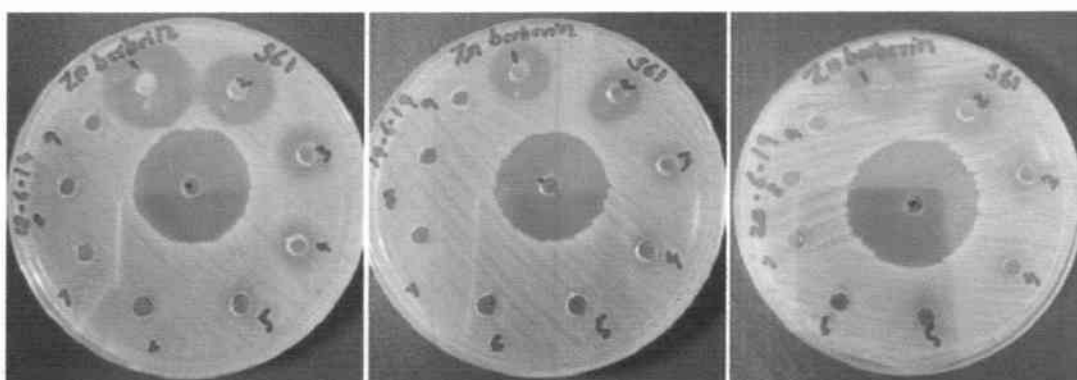


Figure No. 3.60: Photographs of Zone of inhibition of ZnNPs synthesized in the presence of berberine against *S. aureus* ATCC: 6538 (Gram positive bacterial strain)

Table No. 3.8: Evaluation of antibacterial activities of different concentration of ZnNPs synthesized in the presence of *C. zeylanicum* bark Extract and Cinnamaldehyde (n=3, results are expressed mean \pm SE)

| <i>Staphylococcus aureus</i> (ATCC: 6538) | | | |
|--|-------|----------------------------|---|
| NPs | Wells | Conc. ($\mu\text{g/ml}$) | Zone of inhibition(mm) Mean \pm SD |
| ZnNPs of <i>C. zeylanicum</i> extract | 1 | 100 | 15.66 \pm 0.57 |
| | 2 | 50 | 12.33 \pm 0.57 |
| | 3 | 25 | 11 \pm 1 |
| | 4 | 12.5 | 1.66 \pm 0.288 |
| | 5 | 6.25 | 0 \pm 0.0 |
| | 6 | 3 | 0 \pm 0.0 |
| | 7 | 1.5 | 0 \pm 0.0 |
| | 8 | 0.75 | 0 \pm 0.0 |
| Negative Control | 9 | -- | 0 \pm 0.0 |
| Positive Control | 10 | -- | 23 \pm 0.0 |
| ZnNPs Cinnamaldehyde | 1 | 100 | 20.66 \pm 0.57 |
| | 2 | 50 | 18.66 \pm 0.577 |
| | 3 | 25 | 16.33 \pm 0.57 |
| | 4 | 12.5 | 10 \pm 0.57 |
| | 5 | 6.25 | 5.33 \pm 0.57 |
| | 6 | 3 | 0 \pm 0.0 |
| | 7 | 1.5 | 0 \pm 0.0 |
| | 8 | 0.75 | 0 \pm 0.0 |
| Negative Control | 9 | -- | 0 \pm 0.0 |
| Positive Control | 10 | -- | 23 \pm 0.0 |

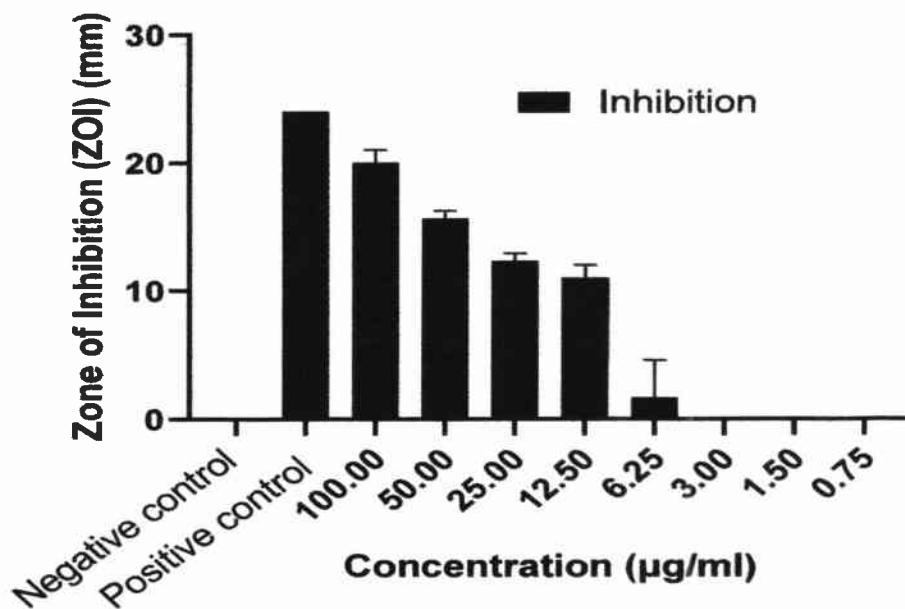


Figure No. 3.61: Evaluation of antibacterial activity of ZnNPs synthesized in the presence of *C. zeylanicum* bark extract via agar well diffusion method against *S. aureus* ATCC: 6538 (Gram positive bacterial strain)



Figure No. 3.62: Photographs of Zone of inhibition of ZnNPs synthesized in the presence of *C. zeylanicum* bark extract against *S. aureus* ATCC: 6538 (Gram positive bacterial strain)

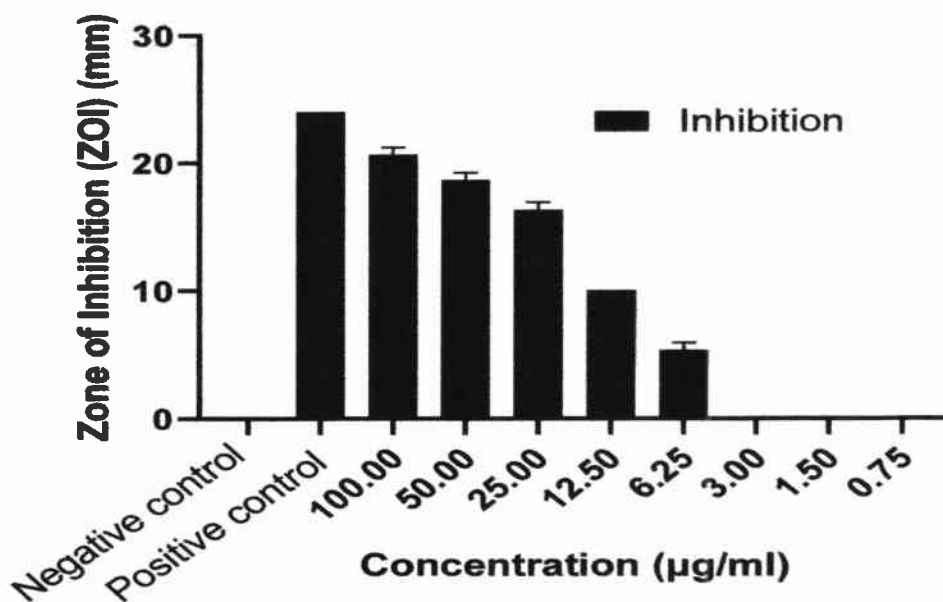


Figure No. 3.63: Evaluation of antibacterial activity of ZnNPs synthesized in the presence of cinnamaldehyde via agar well diffusion method against *S. aureus* ATCC: 6538 (Gram positive bacterial strain)

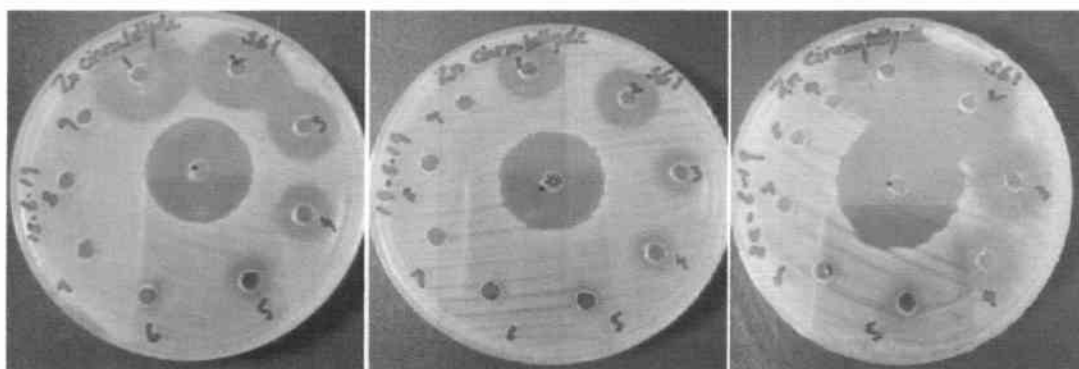


Figure No. 3.64: Photographs of Zone of inhibition of ZnNPs synthesized in the presence of cinnamaldehyde against *S. aureus* ATCC: 6538 (Gram positive bacterial strain)

Table No. 3.9: MIC and IC50 of AgNPs and ZnNPs against *E. coli*

| MIC and IC50 of <i>E. coli</i> strain (ATCC # 8739) | | |
|--|--|---|
| AgNPs | MIC ($\mu\text{g/ml}$) | IC50 ($\mu\text{g/ml}$) |
| AgNPs <i>B. lycium</i> root extract | 1.5 | 2.463 |
| AgNPs Berberine | 2.5 | 2.599 |
| AgNPs <i>C. zeylanicum</i> | 6.25 | 5.161 |
| AgNPs cinnamaldehyde | 6.25 | 5.156 |
| ZnNPs | MIC ($\mu\text{g/ml}$) | IC50 ($\mu\text{g/ml}$) |
| ZnNPs <i>B. lycium</i> root extract | 6.25 | 5.073 |
| ZnNPs Berberine | 6.25 | 6.257 |
| ZnNPs <i>C. zeylanicum</i> | 12.5 | 13.95 |
| ZnNPs Cinnamaldehyde | 9.5 | 12.11 |

Table No. 3.10: MIC and IC50 of AgNPs and ZnNPs against *S. aureus*

| MIC and IC50 of <i>S. aureus</i> (ATCC: 6538) | | |
|--|--|---|
| AgNPs | MIC ($\mu\text{g/ml}$) | IC50 ($\mu\text{g/ml}$) |
| AgNPs <i>B. lycium</i> root extract | 1.5 | 2.514 |
| AgNPs Berberine | 1.5 | 2.922 |
| AgNPs <i>C. zeylanicum</i> | 2.5 | 3.735 |
| AgNPs cinnamaldehyde | 1.5 | 1.729 |
| ZnNPs | MIC ($\mu\text{g/ml}$) | IC50 ($\mu\text{g/ml}$) |
| ZnNPs <i>B. lycium</i> root extract | 2.5 | 2.463 |
| ZnNPs Berberine | 2.5 | 3.735 |
| ZnNPs <i>C. zeylanicum</i> | 6.25 | 5.073 |
| ZnNPs Cinnamaldehyde | 6.25 | 5.161 |

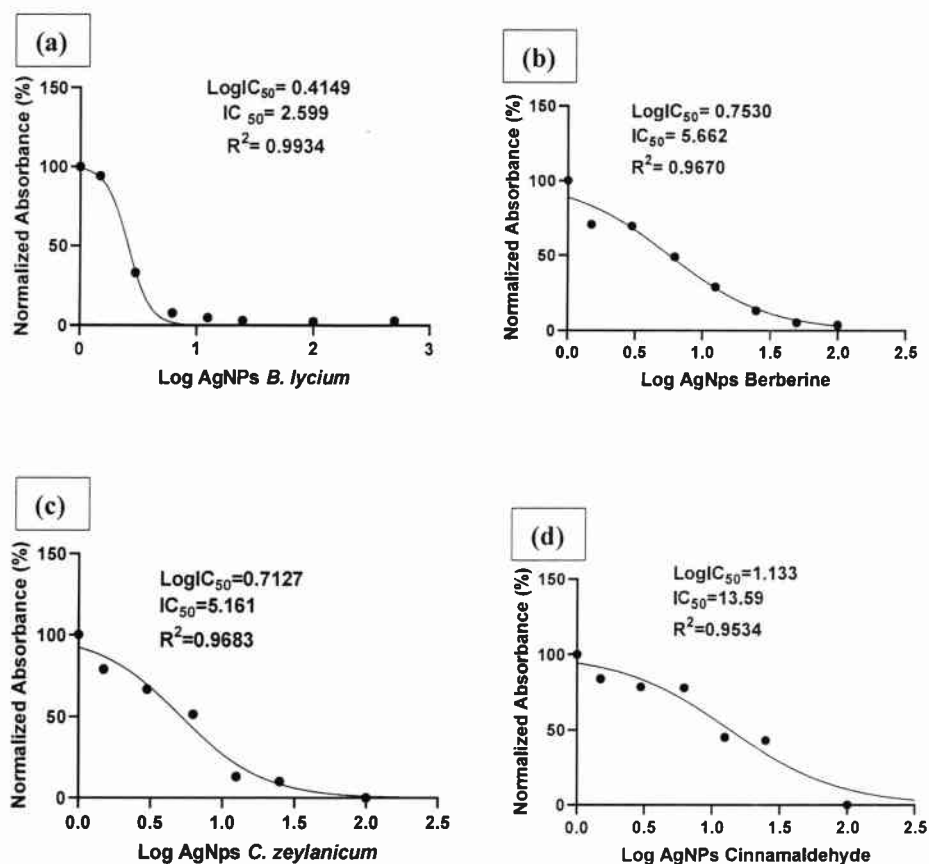


Figure No. 3.65: Comparison of IC_{50} value of AgNPs synthesized in the presence of (a) *B. lycium* root extract (b) Berberine (c) Cinnamaldehyde (d) *C. zeylanicum* bark extract against *E. coli* (ATCC # 8739)

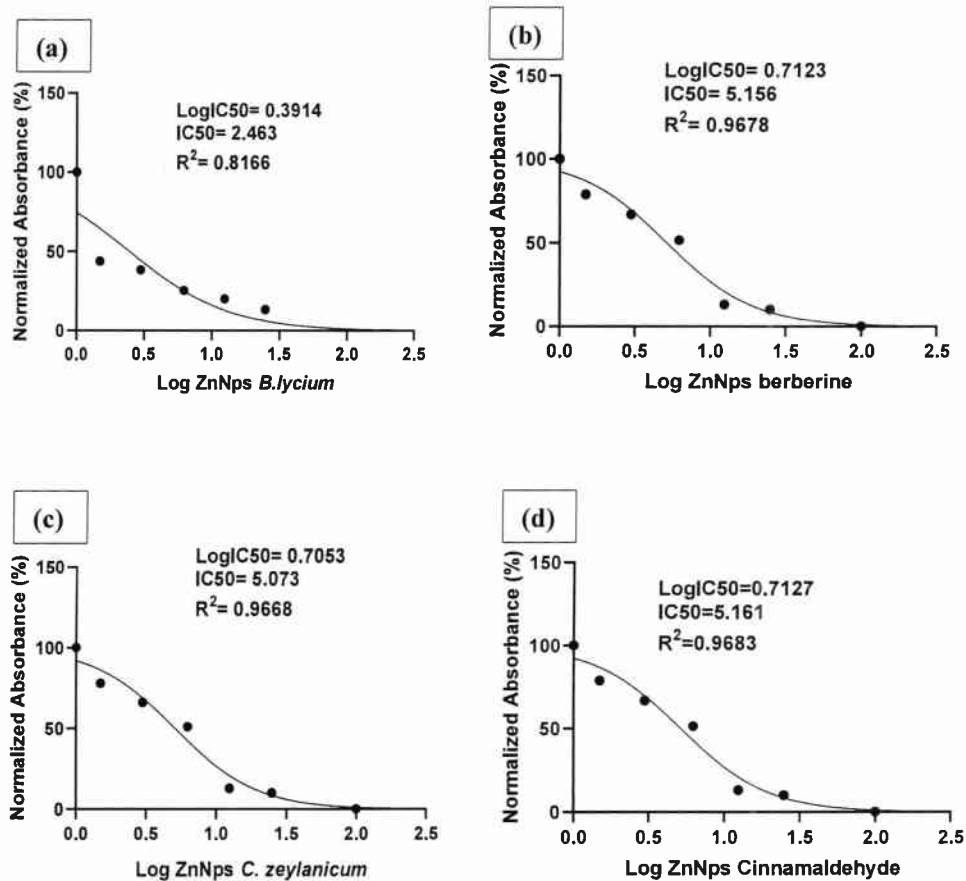


Figure No. 3.66: Comparison of IC₅₀ value of ZnNPs synthesized in the presence of (a) *B. lycium* root extract (b) Berberine (c) Cinnamaldehyde (d) *C. zeylanicum* bark extract against *E. coli* (ATCC # 8739)

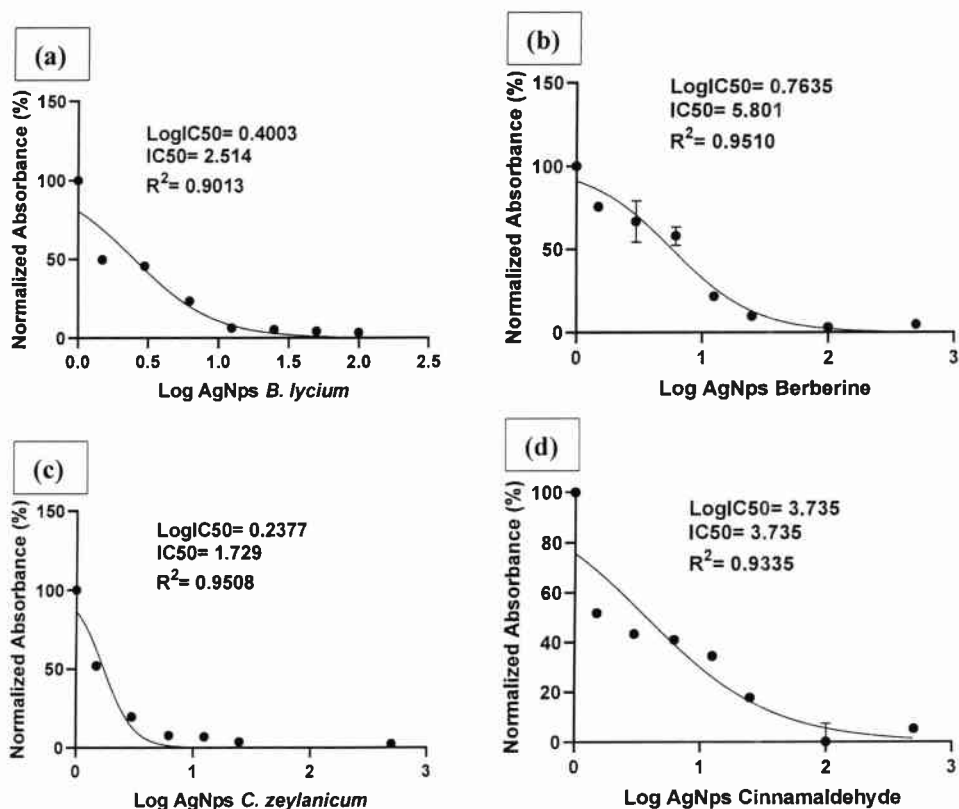


Figure No. 3.67: Comparison of IC₅₀ value of AgNPs synthesized in the presence of (a) *B. lycium* root extract (b) Berberine (c) Cinnamaldehyde (d) *C. zeylanicum* bark extract against *S. aureus* (ATCC: 6538)

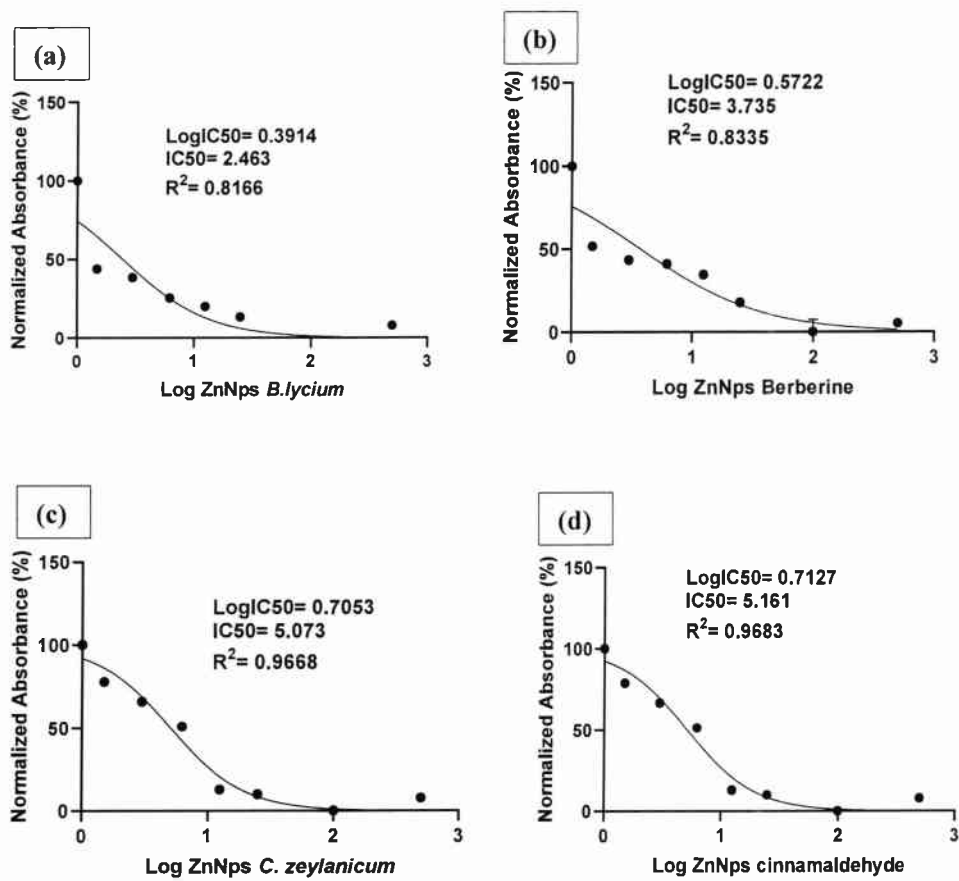


Figure No. 3.68: Comparison of IC₅₀ value of ZnNPs synthesized in the presence of (a) *B. lycium* root extract (b) Berberine (c) Cinnamaldehyde (d) *C. zeylanicum* bark extract against *S. aureus* (ATCC: 6538)

3.5 Antifungal Activity

3.5.1 Antifungal assay of biologically synthesized Silver Nanoparticles against *Trichoderma herzianum*.

The Antifungal activity results revealed that the biologically synthesized silver nanoparticles were very active against fungal strain (*Trichoderma herzianum*). Table 3.10 showed the zones of inhibition of nanoparticles at different concentrations (100, 50, 25, 12.5, 6.25, 3, 1.5, 0.75 μg/ml, negative control (H₂O) and positive control (Amphotericin B). Silver nanoparticles of *B. lycium* root extract showed highest activity (11.66±1.53mm) at 100 μg/ml. The lowest antifungal activity reported against *Trichoderma herzianum* was (9 ±1.73mm) at 3 μg/ml concentration. The zone of inhibition of negative control (0±0mm) and positive control (14.66±0.57mm). The

Chapter #. 3

AgNPs of *B. lycium* root extract at concentration (1.5 and 0.75 μ g/ml) did not show any activity. Minimum inhibitory concentration (MIC) of AgNps *B. lycium* root extract was 1 μ g/ml and IC50 value was 1.444.

The biologically synthesized AgNPs of berberine showed highest activity against *Trichoderma herzianum* (10.66 \pm 0.57mm) at 100 μ g/ml. The lowest antifungal activity of AgNPs berberine was reported at 0.75 μ g/ml (7.33 \pm 0.57mm). The Minimum inhibitory concentration (MIC) of AgNPs berberine was 1.5 μ g/ml and IC50 value was 2.342.

Silver nanoparticles of *C. zeylanicum* bark extract showed highest activity against *Trichoderma herzianum* (11.33 \pm 1.52mm) at 100 μ g/ml. The lowest antibacterial activity was reported against (7 \pm 1mm) at conc. Of 3 μ g/ml. The zone of inhibition of negative control (0 \pm 0mm) and positive control (14.33 \pm 0.57mm). The AgNPs of *C. zeylanicum* bark extract at concentration (1.5 and 0.75 μ g/ml) did not show any activity. Minimum inhibitory concentration (MIC) of *C. zeylanicum* bark extract was 3 μ g/ml and IC50 value 2.488.

The biologically synthesized AgNPs of Cinnamaldehyde showed highest activity against *Trichoderma herzianum* (13.33 \pm 1mm) at 100 μ g/ml. The lowest antifungal activity of AgNPs Cinnamaldehyde was reported (6.33 \pm 0.57mm) at 3 μ g/ml concentration. At concentration of (1.5 and 0.75 μ g/ml) AgNPs of Cinnamaldehyde did not show any activity. The Minimum inhibitory concentration (MIC) of AgNPs cinnamaldehyde was 1 μ g/ml and IC50 value was 1.

Table No. 3.11: Evaluation of antifungal activities of different concentration of AgNPs synthesized in the presence of *B. lycium* root extract and berberine (n=3, results are expressed mean \pm SE)

| <i>Trichoderma herzianum</i> | | | |
|---|-------|---------------------|---|
| bNps | Wells | Conc. (μ g/ml) | Zone of inhibition(mm) Mean \pm SD |
| AgNPs of <i>B. lycium</i> root extract | 1 | 100 | 11.66 \pm 1.53 |
| | 2 | 50 | 10.66 \pm 1.53 |
| | 3 | 25 | 10.33 \pm 1.2 |
| | 4 | 12.5 | 10 \pm 1 |
| | 5 | 6.25 | 9.33 \pm 1.154 |
| | 6 | 3 | 9 \pm 1.73 |
| | 7 | 1.5 | 7.66 \pm 1.52 |
| | 8 | 0.75 | 6.66 \pm 1.52 |
| Negative Control | 9 | -- | 0 \pm 0.0 |
| Positive Control | 10 | -- | 14.66 \pm 0.57 |
| AgNPs Berberine | 1 | 100 | 10.66 \pm 0.57 |
| | 2 | 50 | 11 \pm 0.0 |
| | 3 | 25 | 11 \pm 0.0 |
| | 4 | 12.5 | 10 \pm 0.0 |
| | 5 | 6.25 | 9.66 \pm 0.57 |
| | 6 | 3 | 8.66 \pm 0.57 |
| | 7 | 1.5 | 8.33 \pm 0.57 |
| | 8 | 0.75 | 7.33 \pm 0.57 |
| Negative Control | 9 | -- | 0 \pm 0.0 |
| Positive Control | 10 | -- | 15 \pm 0.0 |

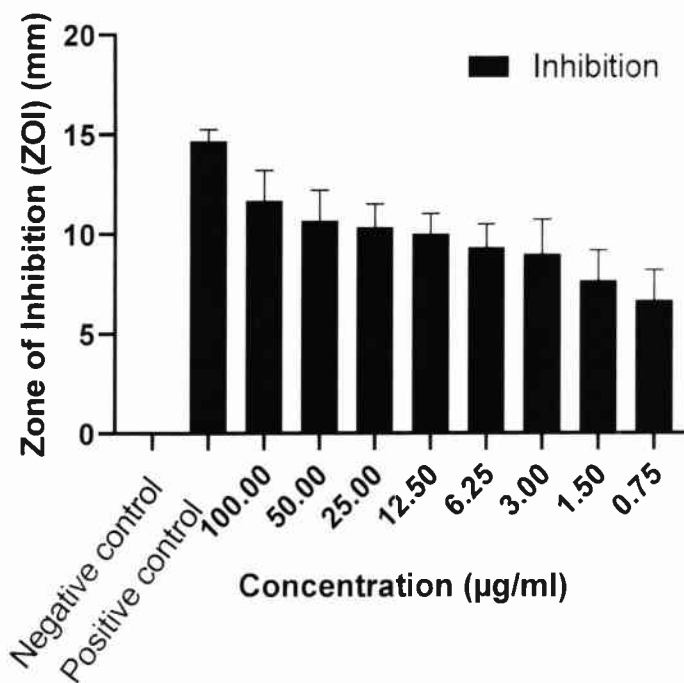


Figure No. 3.69: Evaluation of antifungal activity of AgNPs synthesized in the presence of *B. lycium* root extract via agar well diffusion method against *Trichoderma herzianum* (Fungal strain)

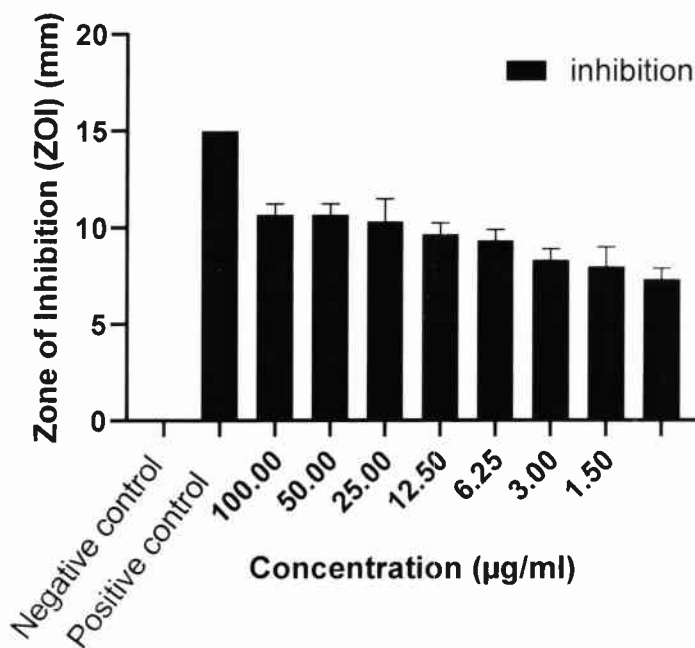


Figure No. 3.70: Evaluation of antifungal activity of AgNPs synthesized in the presence of berberine via agar well diffusion method against *Trichoderma herzianum* (Fungal strain)

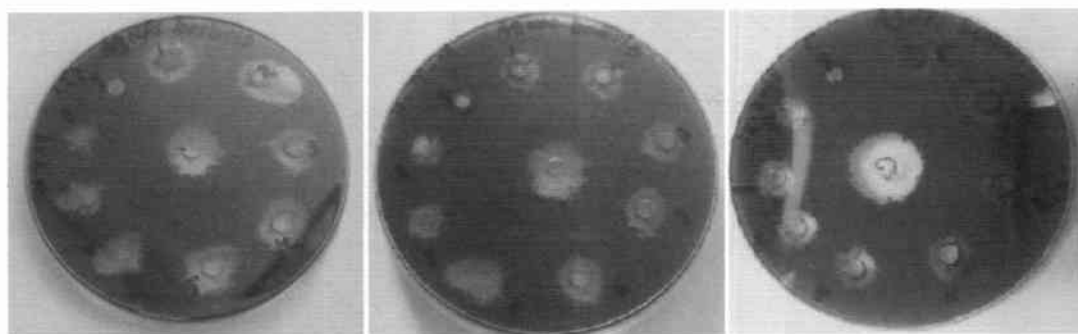


Figure No. 3.71: Photographs of Zone of inhibition of AgNPs synthesized in the presence of *B. lycium* root extract against *Trichoderma herzianum* (Fungal strain)

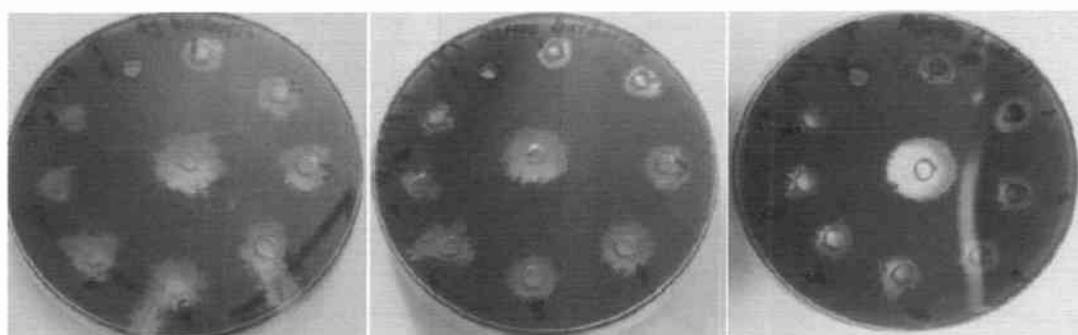


Figure No. 3.72: Photographs of Zone of inhibition of AgNPs synthesized in the presence of berberine against *Trichoderma herzianum* (Fungal strain)

Table No. 3.12: Evaluation of antifungal activity of different concentration of synthesized in the presence of AgNPs of *C. zeylanicum* bark Extract and Cinnamaldehyde (n=3, results are expressed mean \pm SE)

| <i>Trichoderma herzianum</i> | | | |
|--|-------|----------------------------|---|
| bNPs | Wells | Conc. ($\mu\text{g/ml}$) | Zone of inhibition(mm) Mean \pm SD |
| AgNPs of <i>C. zeylanicum</i> extract | 1 | 100 | 11.33 \pm 1.52 |
| | 2 | 50 | 10.33 \pm 1.52 |
| | 3 | 25 | 10 \pm 2 |
| | 4 | 12.5 | 9.66 \pm 2.08 |
| | 5 | 6.25 | 7.33 \pm 0.57 |
| | 6 | 3 | 7 \pm 1 |
| | 7 | 1.5 | 0 \pm 0.0 |
| | 8 | 0.75 | 0 \pm 0.0 |
| Negative Control | 9 | -- | 0 \pm 0.0 |
| Positive Control | 10 | -- | 14.33 \pm 0.57 |
| AgNPs Cinnamaldehyde | 1 | 100 | 13 \pm 1 |
| | 2 | 50 | 12.33 \pm 0.57 |
| | 3 | 25 | 11.66 \pm 0.57 |
| | 4 | 12.5 | 11.66 \pm 0.57 |
| | 5 | 6.25 | 10.66 \pm 0.57 |
| | 6 | 3 | 6.33 \pm 0.57 |
| | 7 | 1.5 | 0 \pm 0.0 |
| | 8 | 0.75 | 0 \pm 0.0 |
| Negative Control | 9 | -- | 0 \pm 0.0 |
| Positive Control | 10 | -- | 14.66 \pm 0.57 |

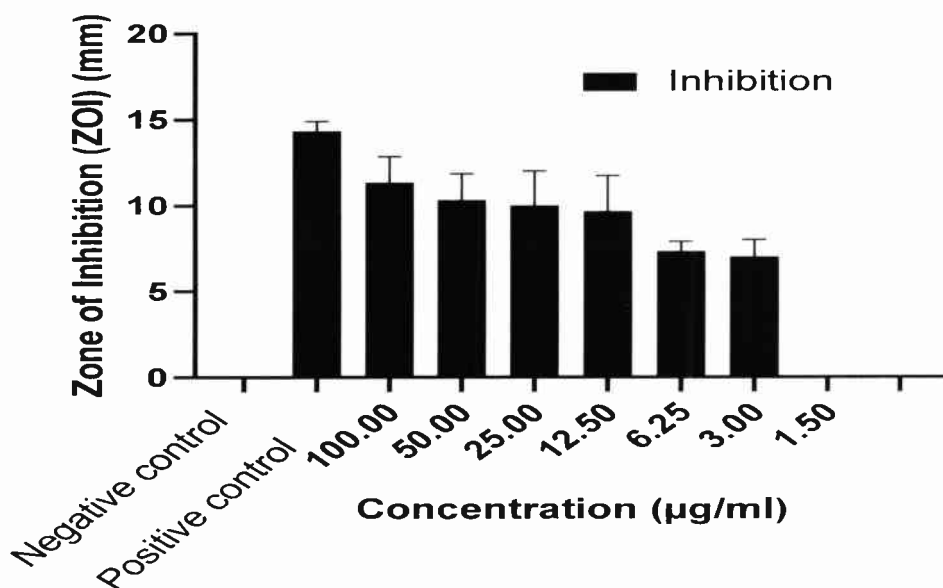


Figure No. 3.73: Evaluation of antifungal activity of AgNPs synthesized in the presence of *C. zeylanicum* bark extract via agar well diffusion method against *Trichoderma herzianum* (Fungal strain)

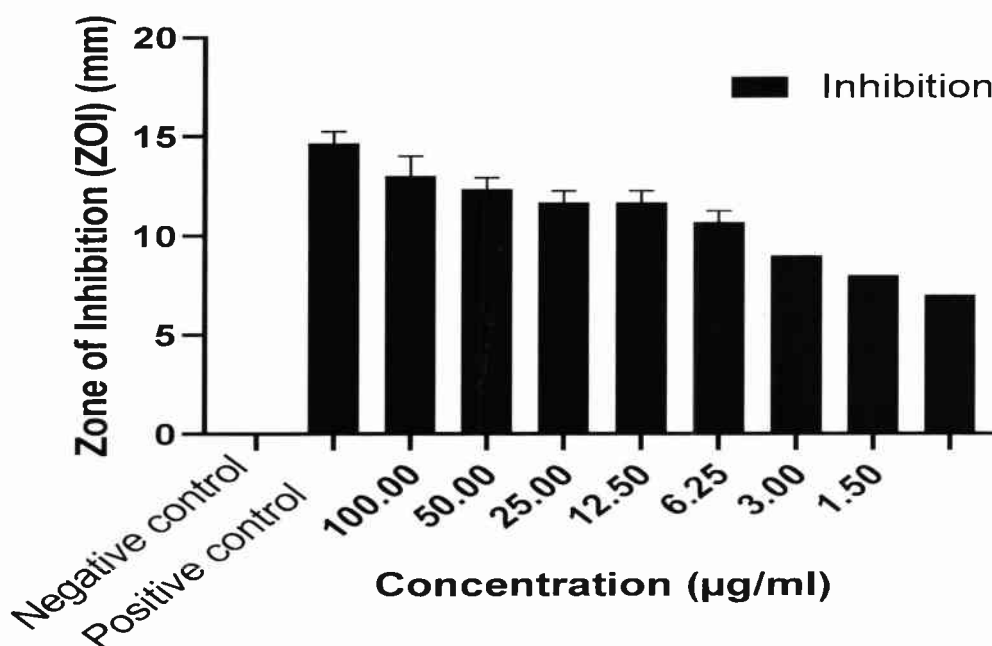


Figure No. 3.74: Evaluation of antifungal activity of AgNPs synthesized in the presence of Cinnamaldehyde via agar well diffusion method against *Trichoderma herzianum* (Fungal strain)

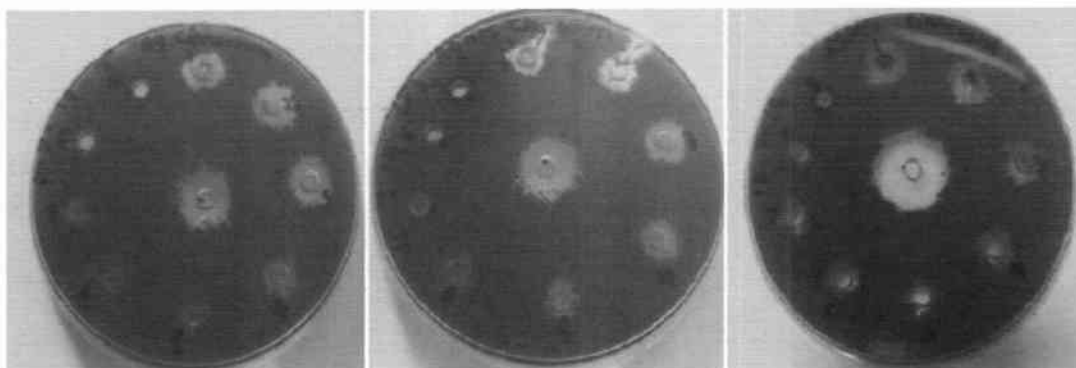


Figure No. 3.75: Photographs of Zone of inhibition of AgNPs synthesized in the presence of *C. zeylanicum* bark extract against *Trichoderma herzianum* (Fungal strain)

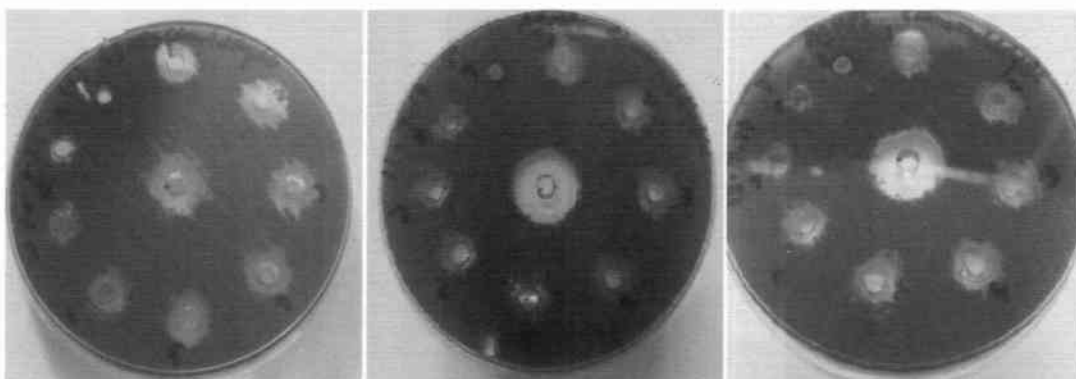


Figure No. 3.76: Photographs of Zone of inhibition of AgNPs synthesized in the presence of cinnamaldehyde against *Trichoderma herzianum* (Fungal strain)

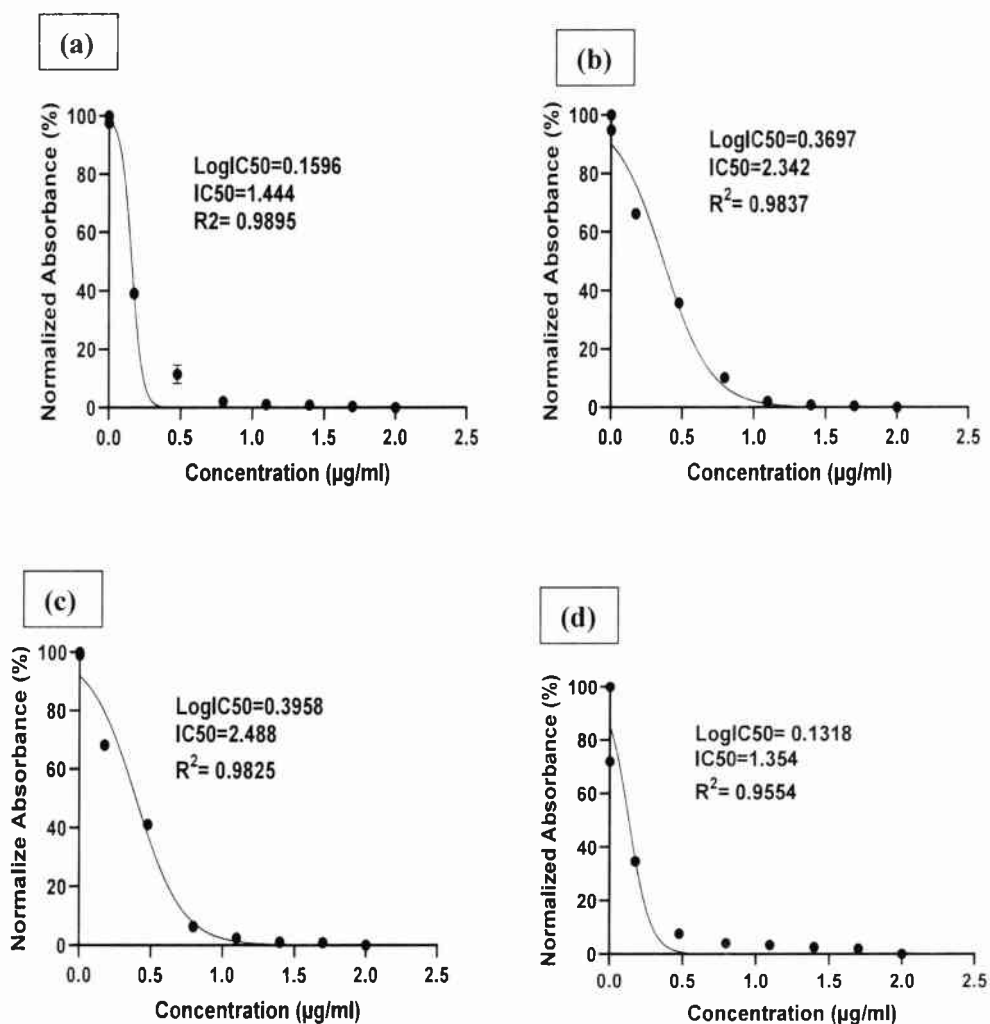


Figure No. 3.77: Comparison of IC_{50} value of AgNPs synthesized in the presence of (a) *B. lycium* root extract (b) Berberine (c) Cinnamaldehyde (d) *C. zeylanicum* bark extract against *Trichoderma herzianum*

Table No. 3.13: Comparison of MIC and IC50 value of AgNPs synthesized in the presence of extract and compounds against *Trichoderma herzianum*

| MIC and IC50 of Antifungal activity | | |
|-------------------------------------|--------------------------|--------------------------|
| AgNPs | MIC ($\mu\text{g/ml}$) | IC50($\mu\text{g/ml}$) |
| AgNPs <i>B. lycium</i> root extract | 1 | 1.444 |
| AgNPs Berberine | 1.5 | 2.342 |
| AgNPs <i>C. zeylanicum</i> | 3 | 2.488 |
| AgNPs cinnamaldehyde | 1 | 1.354 |

3.6 Antioxidant activity

3.6.1 DPPH free radical scavenging activity (Spectrophotometric method):

DPPH assay used to evaluate free radical scavenging activity of biologically synthesized Nanoparticles (Sim et al., 2010). A free radical with a nitrogen centered called DPPH is stable at ambient temperature. It is employed to assess NPs' capacity to scavenge free radicals. In its free radical state, DPPH emits a purple colour. When receiving a proton from the plant's bioactives, particularly phenolics, during the reaction, the purple colour turns yellow.(Sultana et al., 2007). This change in colour is quantified as a decrease in absorbance, which shows the plant extract's ability to scaveng free radicals (function as an antioxidant). (Daud et al., 2011).

The % inhibition of the tested NPs' ability to scavenge DPPH radicals at various concentrations. At various concentrations, significant differences in the antioxidant profile were observed. The effect of different concentrations of NPs on DPPH radical scavenging activities (% inhibition) is given in Table (3.13).

3.6.2 Silver Nanoparticle

In case of AgNps of *B. lycium* root extract and AgNPs of berberine The maximum DPPH radical scavenging activity (%inhibition) of AgNPs *B. lycium* root extract was shown (63%) at 100ug/ml as compared to AgNPs of berberine which showed maximum DPPH radical scavenging activity (%inhibition) was (30%) at 100ug/ml.

In case of AgNPs of *C. zeylanicum* bark extract and AgNPs Cinnamaldehyde, maximum DPPH radical scavenging activity was shown by AgNPs Cinnamaldehyde which was 63% at 100ug/ml as compared to AgNPs of *C. zeylanicum* bark extract which shows maximum DPPH radical scavenging activity (%inhibition) which was 60% at 100ug/ml, respectively. With decreasing the concentrations of AgNPs the DPPH radical scavenging activity (%inhibition) also decreased.

Table No. 3.14: Effect of different concentrations of AgNPs synthesized in the presence of *B. lycium* root extract on %Inhibition of DPPH

| S. No | Concentration µg/ml | %Inhibition | S. No | Concentration µg/ml | %Inhibition |
|-------|------------------------|-------------|-------|------------------------|-------------|
| 1 | 100 | 61 | 6 | 3 | 37 |
| 2 | 50 | 54 | 7 | 1.5 | 33 |
| 3 | 25 | 46 | 8 | 0.7 | 24 |
| 4 | 12.5 | 44 | 9 | Ascorbic acid | 80 |
| 5 | 6.25 | 40 | 10 | IC50 | 50.47 |

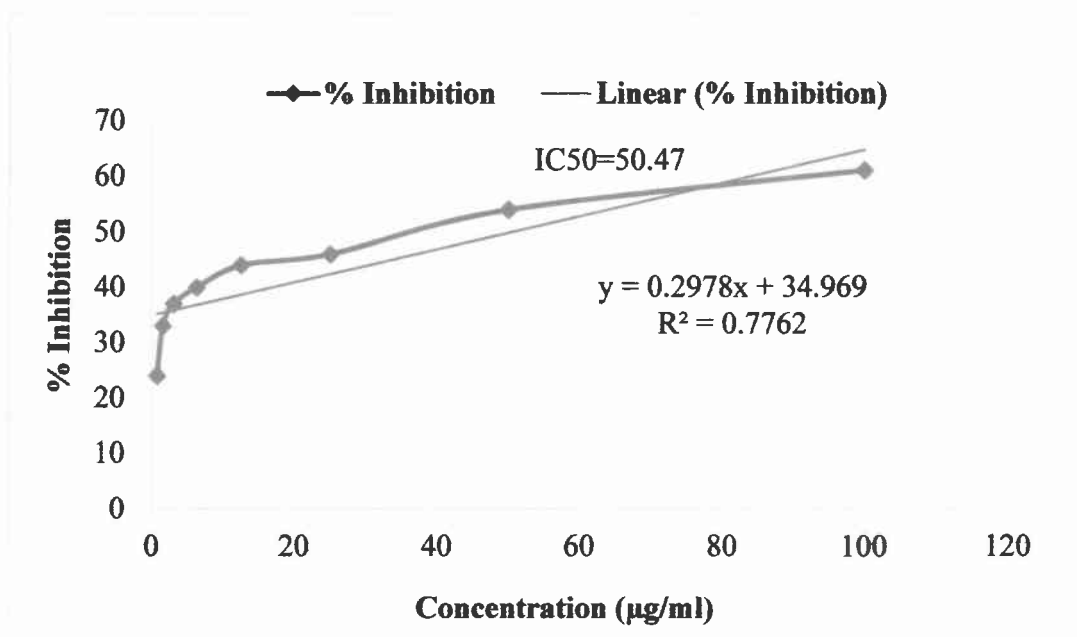


Figure No. 3.78: DPPH scavenging activity of AgNPs synthesized in the presence of *B. lycium* root extract

Table No. 3.15: Effect of different concentration of AgNPs synthesized in the presence of berberine on %Inhibition of DPPH

| S. No | Concentration $\mu\text{g/ml}$ | %Inhibition | S. No | Concentration $\mu\text{g/ml}$ | %Inhibition |
|-------|-----------------------------------|-------------|-------|-----------------------------------|-------------|
| 1 | 100 | 30 | 6 | 3 | 5 |
| 2 | 50 | 25 | 7 | 1.5 | 3.5 |
| 3 | 25 | 20 | 8 | 0.7 | 1 |
| 4 | 12.5 | 15 | 9 | Ascorbic acid | 80 |
| 5 | 6.25 | 10 | 10 | IC50 | 45.23 |

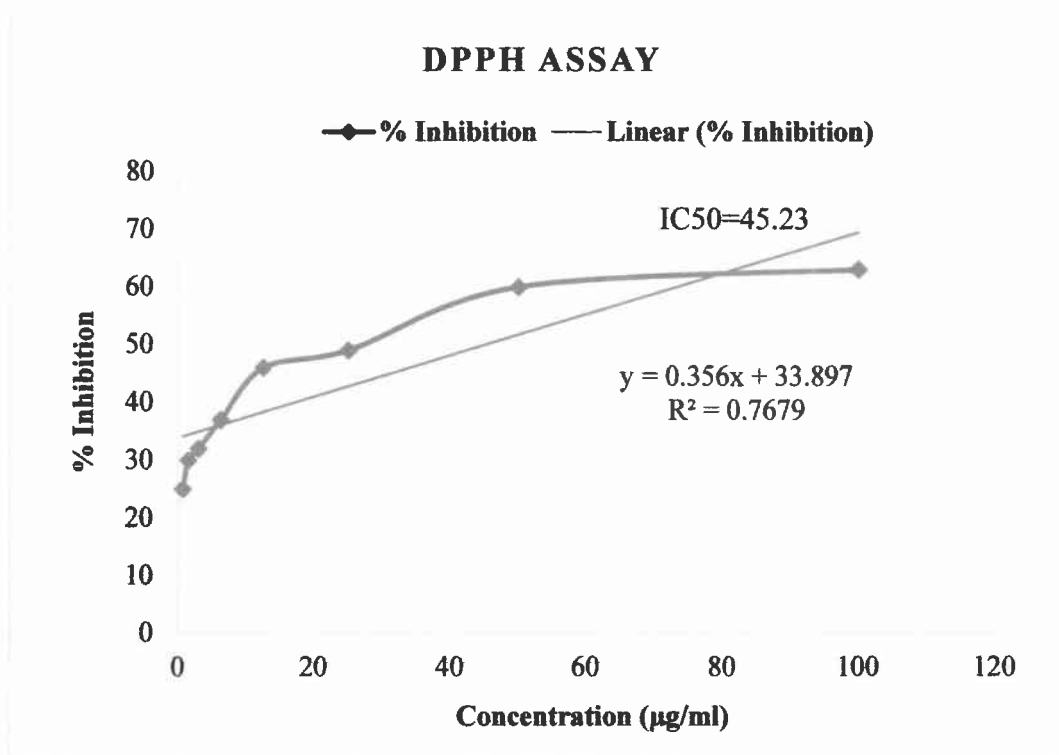


Figure No. 3.79: DPPH scavenging activity of AgNPs synthesized in the presence of berberine

Table No. 3.16: Effect of different concentration of AgNPs synthesized in the presence of *C. zeylanicum* bark extract on %Inhibition of DPPH

| S. No | Concentration (µg/ml) | %Inhibition | S. No | Concentration (µg/ml) | %Inhibition |
|-------|-----------------------|-------------|-------|-----------------------|-------------|
| 1 | 100 | 60 | 6 | 3 | 49 |
| 2 | 50 | 58 | 7 | 1.5 | 47 |
| 3 | 25 | 57 | 8 | 0.7 | 44 |
| 4 | 12.5 | 55 | 9 | Ascorbic acid | 80 |
| 5 | 6.25 | 53 | 10 | IC50 | 54 |

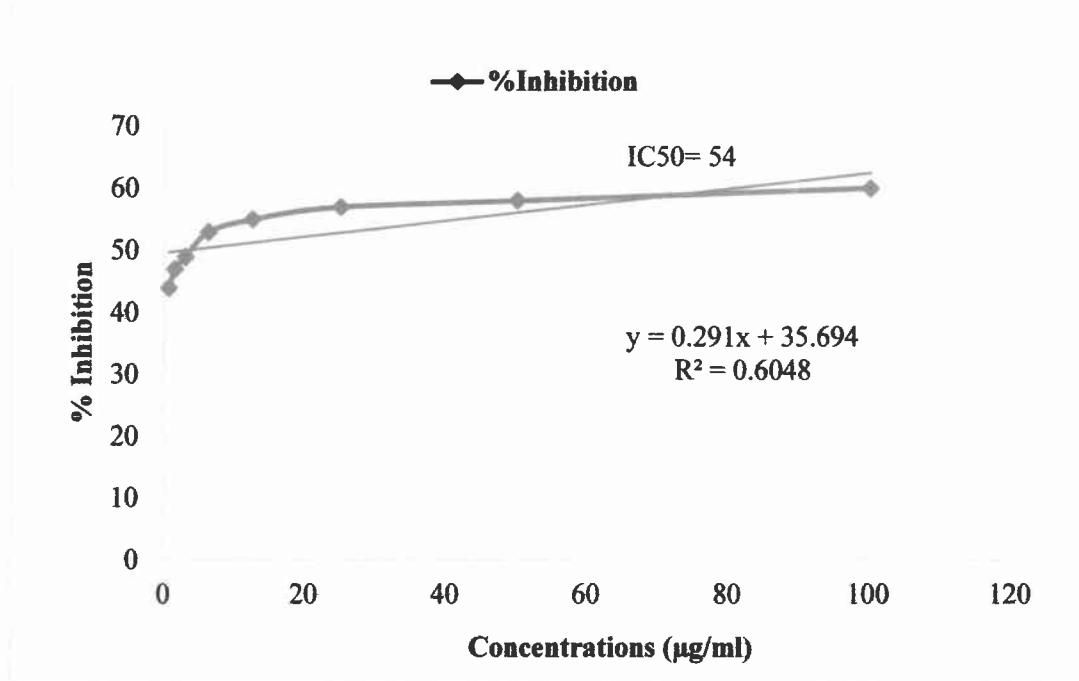


Figure No. 3.80: DPPH scavenging activity of AgNPs synthesized in the presence of *C. zeylanicum* bark extract

Table No. 3.17: Effect of different concentration of AgNPs synthesized in the presence of cinnamaldehyde on %Inhibition of DPPH

| S. No | Concentration (µg/ml) | %Inhibition | S. No | Concentration (µg/ml) | %Inhibition |
|-------|-----------------------|-------------|-------|-----------------------|-------------|
| 1 | 100 | 63 | 6 | 3 | 38 |
| 2 | 50 | 61 | 7 | 1.5 | 36 |
| 3 | 25 | 53 | 8 | 0.7 | 33 |
| 4 | 12.5 | 48 | 9 | Ascorbic acid | 80 |
| 5 | 6.25 | 40 | 10 | IC50 | 56.21 |

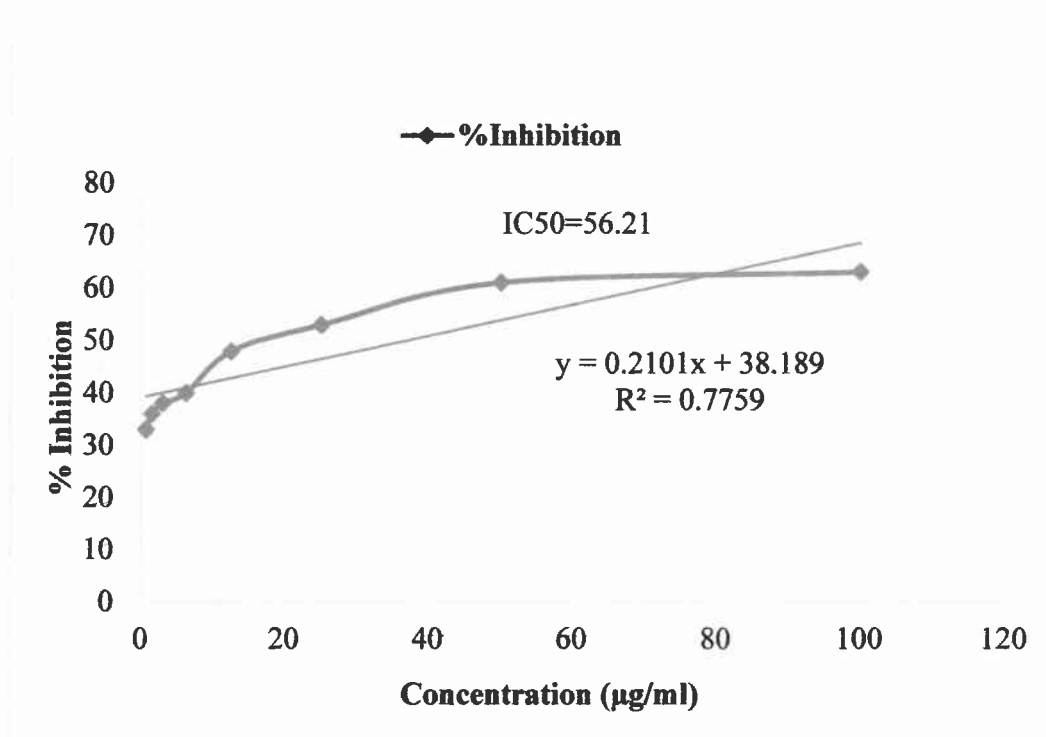


Figure No. 3.81: DPPH scavenging activity of AgNPs synthesized in the presence of cinnamaldehyde

3.6.3 Zinc Nanoparticles

DPPH radical scavenging activity (% inhibition) of the tested biologically synthesized ZnNPs at different concentrations. Considerable variations in antioxidant profile were recorded at different concentrations. The effect of different concentrations of ZnNPs on DPPH radical scavenging activities (% inhibition) were given in (Figure 3.82). In case of ZnNPs of *B. lycium* root extract and ZnNPs of berberine The maximum DPPH radical scavenging activity (%inhibition) of ZnNPs *B. lycium* root extract was shown (69%) at 100µg/ml as compared to ZnNPs of berberine which shown maximum DPPH radical scavenging activity (%inhibition) was (58%) at 100µg/ml.

In case of ZnNps of *C. zeylanicum* bark extract and ZnNPs Cinnamaldehyde, maximum DPPH radical scavenging activity was shown by ZnNPs of *C. zeylanicum* bark extract which was 61% at 100µg/ml as compared to ZnNPs Cinnamaldehyde which shows maximum DPPH radical scavenging activity (%inhibition) which was 58% at 100µg/ml, respectively. With decreasing the concentrations of ZnNPs the DPPH radical scavenging activity (%inhibition) also decreased.

Table No. 3.18: Effect of different concentration of ZnNPs synthesized in the presence of *B. lycium* root extract on %Inhibition of DPPH

| S. No | Concentration (µg/ml) | %Inhibition | S. No | Concentration (µg/ml) | %Inhibition |
|-------|-----------------------|-------------|-------|-----------------------|-------------|
| 1 | 100 | 69 | 6 | 3 | 37 |
| 2 | 50 | 54 | 7 | 1.5 | 30 |
| 3 | 25 | 49 | 8 | 0.7 | 24 |
| 4 | 12.5 | 46 | 9 | Ascorbic acid | 80 |
| 5 | 6.25 | 44 | 10 | IC50 | 40.91 |

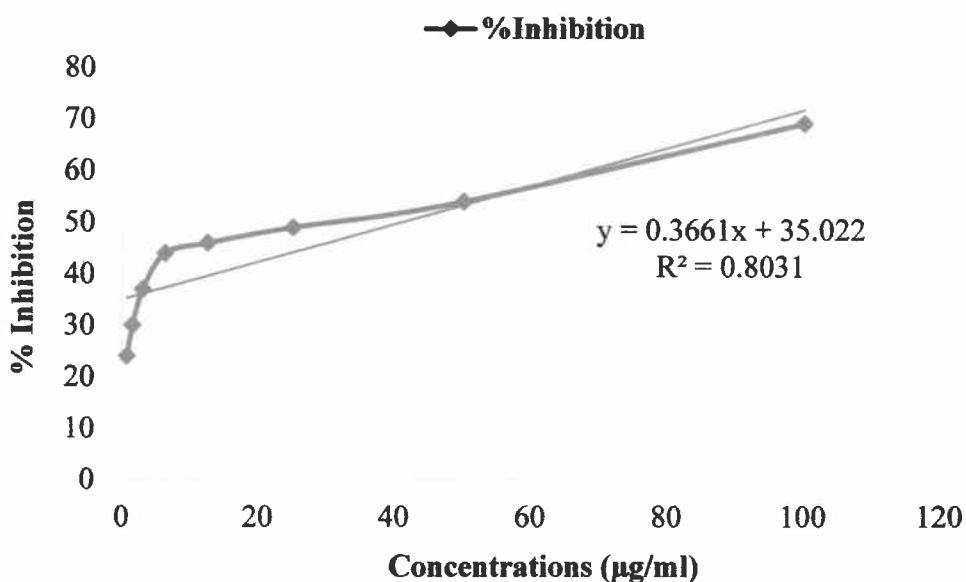


Figure No. 3.82: DPPH scavenging activity of ZnNPs synthesized in the presence of *B. lycium* root extract

Table No. 3.19: Effect of different concentration of ZnNPs synthesized in the presence of berberine on %Inhibition of DPPH

| S. No | Concentration (µg/ml) | %Inhibition | S. No | Concentration (µg/ml) | %Inhibition |
|-------|-----------------------|-------------|-------|-----------------------|-------------|
| 1 | 100 | 31 | 6 | 3 | 6 |
| 2 | 50 | 21 | 7 | 1.5 | 3.5 |
| 3 | 25 | 16 | 8 | 0.7 | 1 |
| 4 | 12.5 | 10 | 9 | Ascorbic acid | 80 |
| 5 | 6.25 | 8 | 10 | IC50 | 44 |

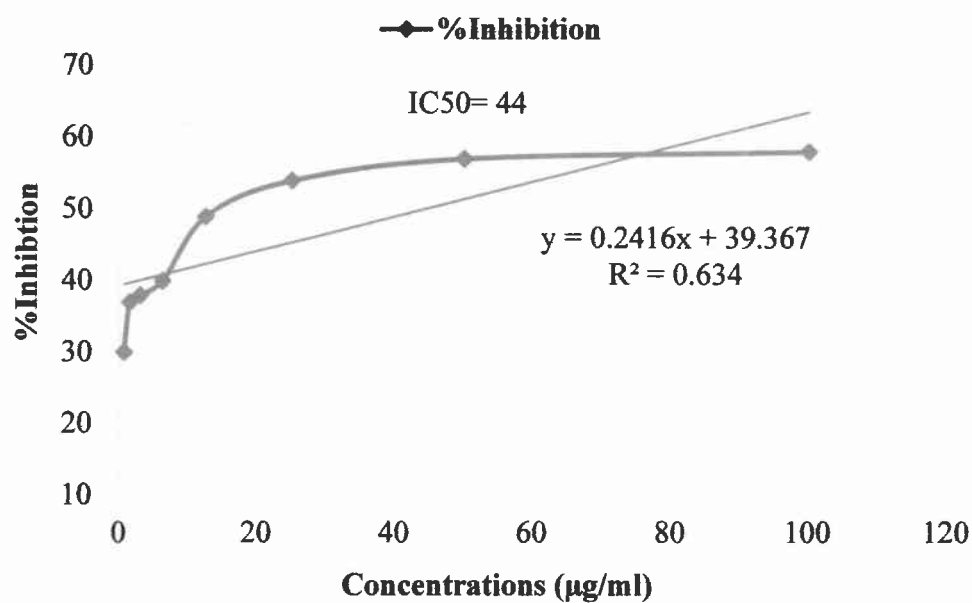


Figure No. 3.83: DPPH scavenging activity of ZnNPs synthesized in the presence of berberine

Table No. 3.20: Effect of different concentration of ZnNPs synthesized in the presence of *C. zeylanicum* bark extract on %Inhibition of DPPH

| S. No | Concentration (µg/ml) | %Inhibition | S. No | Concentration (µg/ml) | %Inhibition |
|-------|-----------------------|-------------|-------|-----------------------|-------------|
| 1 | 100 | 61 | 6 | 3 | 37 |
| 2 | 50 | 57 | 7 | 1.5 | 32 |
| 3 | 25 | 53 | 8 | 0.7 | 33 |
| 4 | 12.5 | 49 | 9 | Ascorbic acid | 80 |
| 5 | 6.25 | 46 | 10 | IC50 | 40.5 |

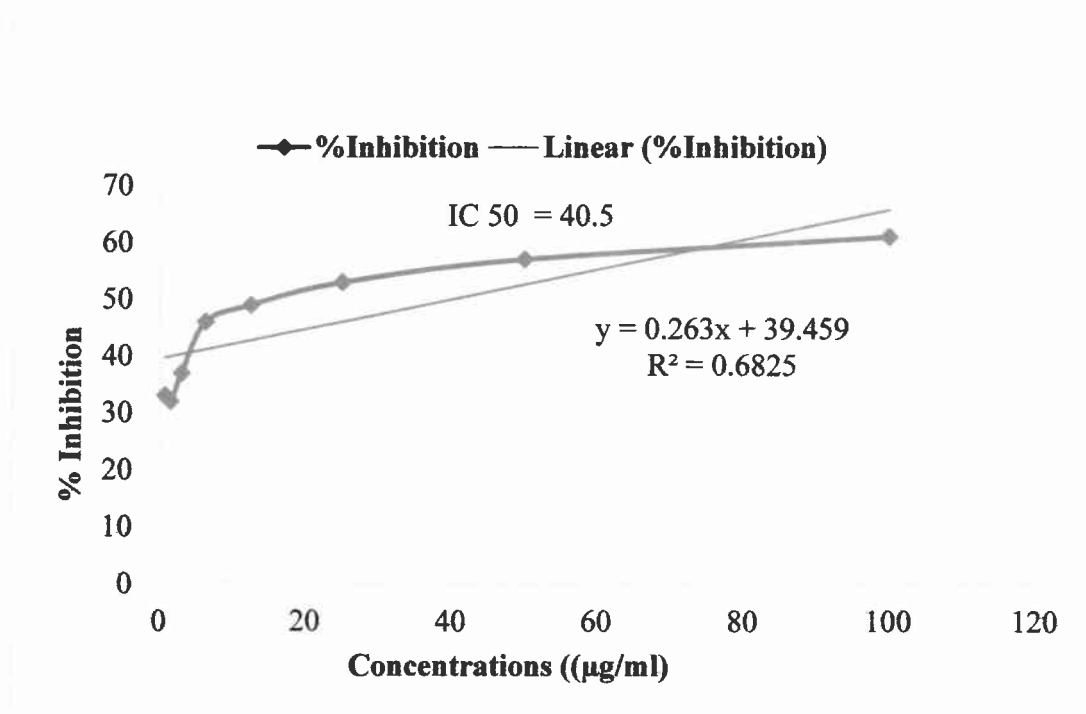
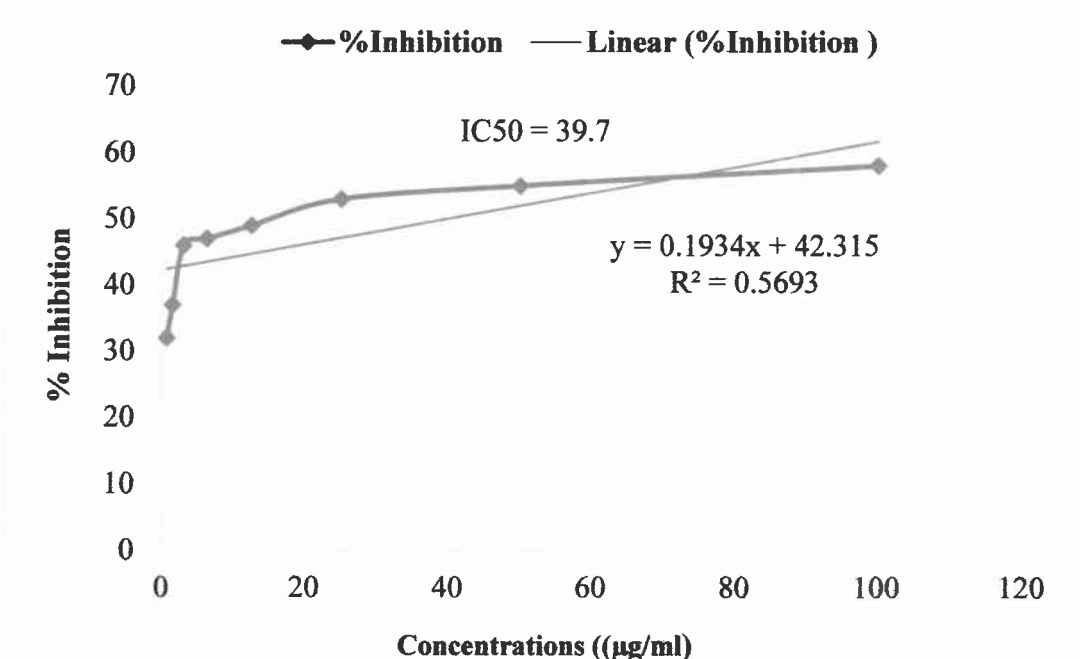


Figure No. 3.84: DPPH scavenging activity of ZnNPs synthesized in the presence of *C. zeylanicum*

Table No. 3.21: Effect of different concentration of ZnNPs synthesized in the presence of Cinnamaldehyde on %Inhibition of DPPH

| S. No | Concentration (µg/ml) | %Inhibition | S. No | Concentration (µg/ml) | %Inhibition |
|-------|-----------------------|-------------|-------|-----------------------|-------------|
| 1 | 100 | 58 | 6 | 3 | 46 |
| 2 | 50 | 55 | 7 | 1.5 | 37 |
| 3 | 25 | 53 | 8 | 0.7 | 32 |
| 4 | 12.5 | 49 | 9 | Ascorbic acid | 80 |
| 5 | 6.25 | 47 | 10 | IC50 | 39.7 |

**Figure No. 3.85: DPPH scavenging activity of ZnNPs synthesized in the presence of cinnamaldehyde**

3.7 Antileishmanial Activity of AgNPs against *Leishmania tropica*

3.7.1 Anti-promastigote Assay of AgNPs:

Antileishmanial efficacy of biologically synthesized AgNPs were analyzed on the strain of *leishmania tropica* (KWH23). The effect of AgNPs on metabolic activity of promastigote against eight different concentrations (100µg/ml, 50µg/ml, 25µg/ml,

12.5µg/ml, 6.25µg/ml, 3µg/ml, 1.5µg/ml, 0.75µg/ml) was determined. The viability of promastigotes cells were checked in both control and test groups at 72hours of incubation. After 72hours of incubation the metabolic activity of promastigotes decreased with increasing the concentration of AgNPs. In experimental group when leishmanial cells were treated with high concentration (100µg/ml) of AgNPs of *B. lycium* root extract and AgNPs of Berberine The amount of viable cells were very low at higher concentration. It was clearly shown that 100% leishmanial cells killing. The IC₅₀ value of AgNPs of *B. lycium* root extract was 1.011µg/ml and the IC₅₀ value of AgNPs of Berberine was 1.134µg/ml. Same effect was observed during all the evaluated Incubation time period which is shown in the graphs.

The effects of AgNPs of *C. zeylanicum* bark extract and AgNPs of Cinnamaldehyde on the metabolic activity of *Leishmania tropica* were also studied. The effects of different concentration of AgNPs (100µg/ml, 50µg/ml, 25µg/ml, 12.5µg/ml, 6.25µg/ml, 3µg/ml, 1.5µg/ml, 0.75µg/ml) on *leishmania tropica* shows that the metabolic activity of leishmanial cells consistently decreased by increasing the concentration of AgNPs. It was noticed, that the metabolic activity of *Leishmania tropica* promastigotes at each concentration of AgNPs were negatively affected in comparison to control group. The IC₅₀ value of AgNPs of *C. zeylanicum* was 2.664µg/ml and the IC₅₀ value of AgNPs of Cinnamaldehyde was 2.011µg/ml. In result, AgNPs Showed the maximum suppressive effect on higher concentration 100µg/ml in comparison to the control group, at the same concentration the metabolic activity value of promastigotes decreased.

The results indicated, that with the increase of concentration of AgNPs the cell viability of *leishmania tropica* decreased. The highest concentration of AgNPs was 100µg/ml shown maximum effects on metabolic activity of promastigotes and it was visualized clearly in the (Figures 3.86). According to the figures, these results demonstrated better effects of AgNPs on the viable cells of promastigotes on all the concentration except 1.5µg/ml and 0.75µg/ml. So, it was concluded that the biologically synthesized AgNPs at low concentrations expressively killing the leishmanial cells and these nanoparticles are considered as the suitable candidates for the leishmania treatment.

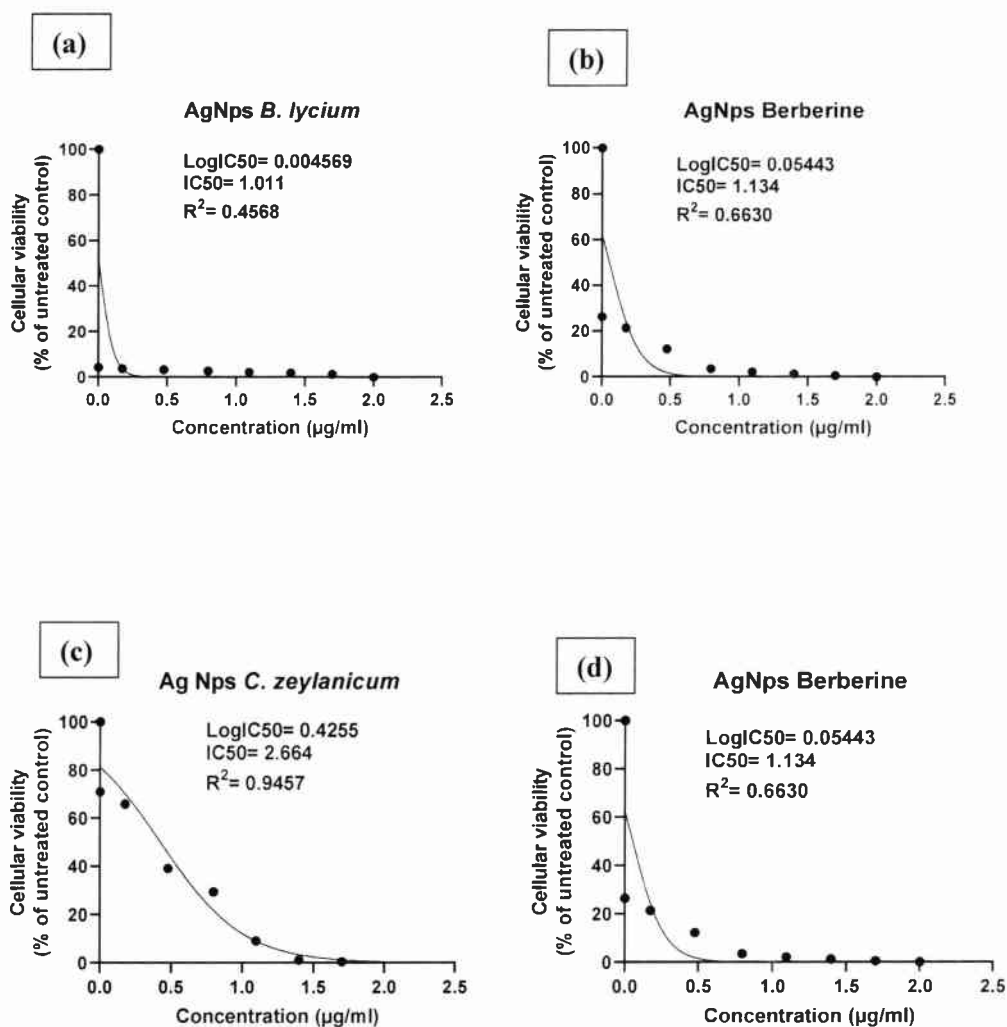


Figure No. 3.86: Inhibitory concentration (IC₅₀) of promastigotes of *L. tropica* at different concentration of AgNPs synthesized in the presence of (a) *B. lycium* root extract (b) Berberine (c) *C. zeylanicum* bark extract (d) Cinnamaldehyde

3.7.2 Anti-promastigote Assay of ZnNPs

Antileishmanial efficacy of biologically synthesized ZnNPs were analyzed on the strain of *leishmania tropica*. The metabolic activity of promastigotes decreased with increasing the concentration of ZnNPs. In experimental group when leishmanial cells were treated with high concentration (100µg/ml) of ZnNPs of *B. lycium* root extract and ZnNPs of Berberine. The amount of viable cells were very low at higher concentration. It was clearly shown that 100% leishmanial cells were killed. The IC₅₀ value of ZnNPs of *B. lycium* was 4.171µg/ml and the IC₅₀ value of ZnNPs of Berberine was 3.793µg/ml. Same effect was observed during all the evaluated Incubation time period which is shown in the (Figures 3.87).

The effects of ZnNPs of *C. zeylanicum* and ZnNPs of Cinnamaldehyde on the metabolic activity of *Leishmania tropica* were also studied. The effects of different concentration (100µg/ml, 50µg/ml, 25µg/ml, 12.5µg/ml, 6.25µg/ml, 3µg/ml, 1.5µg/ml, 0.75µg/ml) of ZnNPs on *leishmania tropica* shows that the metabolic activity of leishmanial cells consistently decreased by increasing the concentration of ZnNPs.

It was noticed, that the metabolic activity of *Leishmania tropica* promastigotes at each concentration of ZnNPs were negatively affected in comparison to control group. The IC₅₀ value of ZnNPs of *C. zeylanicum* was 2.664µg/ml and the IC₅₀ value of ZnNPs of Cinnamaldehyde was 2.011µg/ml.

In result, ZnNPs Shows the maximum suppressive effect on higher concentration 100µg/ml in comparison to the control group, at the same concentration the metabolic activity value of promastigotes decreased.

The results indicated, that with the increase of concentration of ZnNPs the cell viability of *leishmania tropica* decreased. The highest concentration of ZnNPs was 100µg/ml shown maximum effects on metabolic activity of promastigotes and it was visualized clearly in the (figures 3.87). According to the figures, these results demonstrated better effects of ZnNPs on the viable cells of promastigotes on all the concentration but on higher concentration the metabolic activity of promastigotes decreased. So, it was concluded that the biologically synthesized ZnNPs at low concentrations expressively killing the leishmanial cells and these nanoparticles are considered as the suitable drug for the *leishmania* treatment.

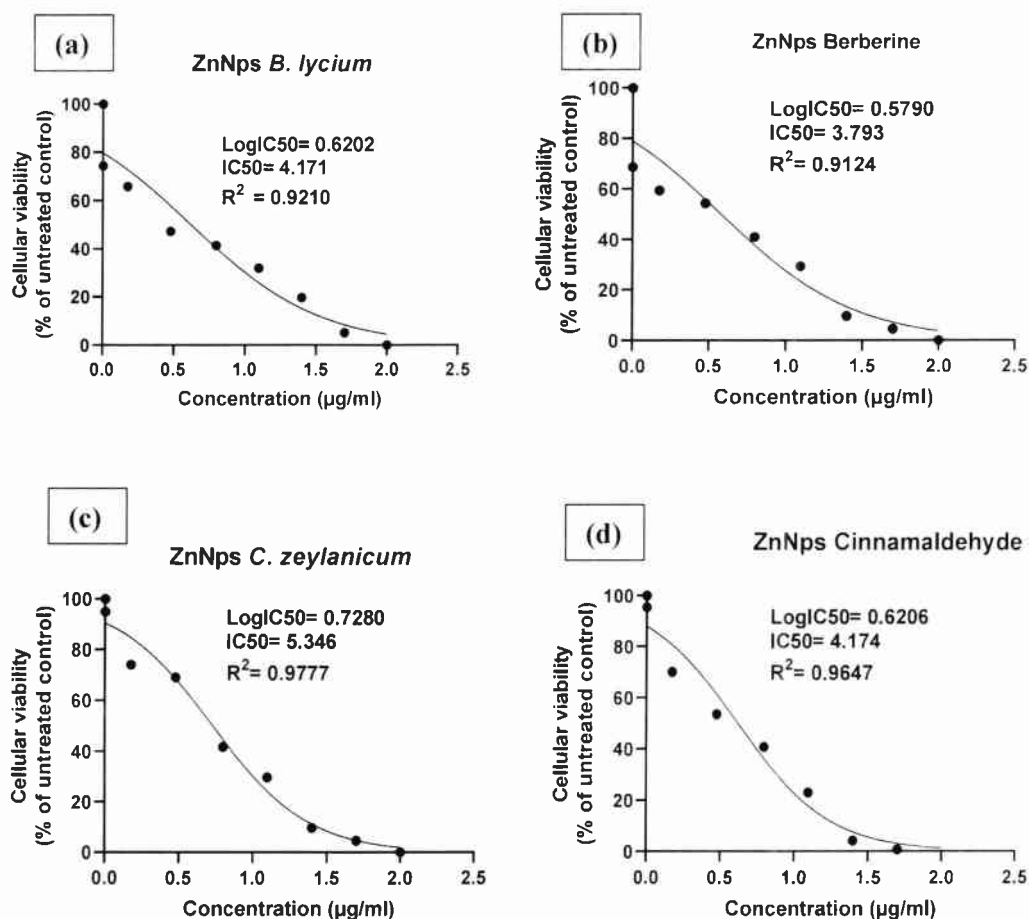


Figure No. 3.87: Inhibitory concentration (IC₅₀) of promastigotes of *L. tropica* at different concentration of ZnNPs synthesized in the presence of (a) *B. lycium* root extract (b) Berberine (c) *C. zeylanicum* bark extract (c) Cinnamaldehyde

3.7.3 Anti-amastigote Assay of AgNPs:

Leishmania is a dimorphic organism. It exists as a long whipped promastigotes which is a vector in a sand fly and change to non-motile form when enter into another vertebrates (round shape). This round shape leishmania leads to infection in both hosts. In vitro culturing of amastigotes provide alive culture which is free of contamination and can be used for drug estimation. Amastigotes grow outside the living cell that are recognized as axenic amastigotes. (Bates, 1993) developed rules for the cultivation of axenic amastigotes.

The alogrithemic growth phase of axenic amastigotes were also harvested and cultured in RPMI 1640 and 5.5PH was adjusted for their growth. At 33° the cells were incubated for seven days in humufied CO₂ (5%). By changing the temperature and PH

axenic amastigotes transformed into promastigotes. In each well of 96-well microtiter plate (106 cells/ml) RPMI media containing culture of axenic-amastigotes were added. The different concentration of biologically synthesized nanoparticles (100µg/ml, 50µg/ml, 25µg/ml, 12.5µg/ml, 6.25µg/ml, 3µg/ml, 1.5µg/ml, 0.75µg/ml) along with water (negative control) and (TA positive control) were added to each well and incubated at 25°C ± 1°C for 72 hours.

Similar procedure were used for anti-promastigotes assay. All the experiment were performed in triplicate. Micro-plate reader were used for OD of the cells. IC50 value of the biologically synthesized nanoparticles showing anti-amastigote activity were calculated by graph pad prism.

In experimental group when leishmanial cells were treated with high concentration (100µg/ml) of AgNPs of *B. lycium* root extract and AgNPs of Berberine. The amount of viable cells were very low at higher concentration. It was clearly shown that 100% leishmanial cells killing. The IC50 value of AgNPs of *B. lycium* was 1.011µg/ml and the IC50 value of AgNPs of Berberine was 1.134µg/ml. Same effect was observed during all the evaluated Incubation time period which is shown in the graphs.

The effects of AgNPs of *C. zeylanicum* bark extract and AgNPs of Cinnamaldehyde on the metabolic activity of *Leishmania tropica* were also studied. The effects of different concentration (100µg/ml, 50µg/ml, 25µg/ml, 12.5µg/ml, 6.25µg/ml, 3µg/ml, 1.5µg/ml, 0.75µg/ml) of AgNPs of *C. zeylanicum* bark extract and AgNPs cinnamaldehyde on *leishmania tropica* shows that the metabolic activity of leishmanial cells consistently decreased by increasing the concentration of AgNPs (Figure 3.88).

It was noticed, that the metabolic activity of *Leishmania tropica* amastigotes at each concentration of AgNPs were negatively affected in comparison to control group. The IC50 value of AgNPs of *C. zeylanicum* was 1.123µg/ml and the IC50 value of AgNPs of Cinnamaldehyde was 1.207µg/ml.

In result, AgNPs Shows the maximum suppressive effect on higher concentration 100µg/ml in comparison to the control group, at the same concentration the metabolic activity value of promastigotes decreased.

The results indicated, that with the increase of concentration of AgNPs the cell viability of *leishmania tropica* decreased. The highest concentration of AgNPs was 100µg/ml shown maximum effects on metabolic activity of promastigotes and it was visualized clearly in the (Figure 3.89).

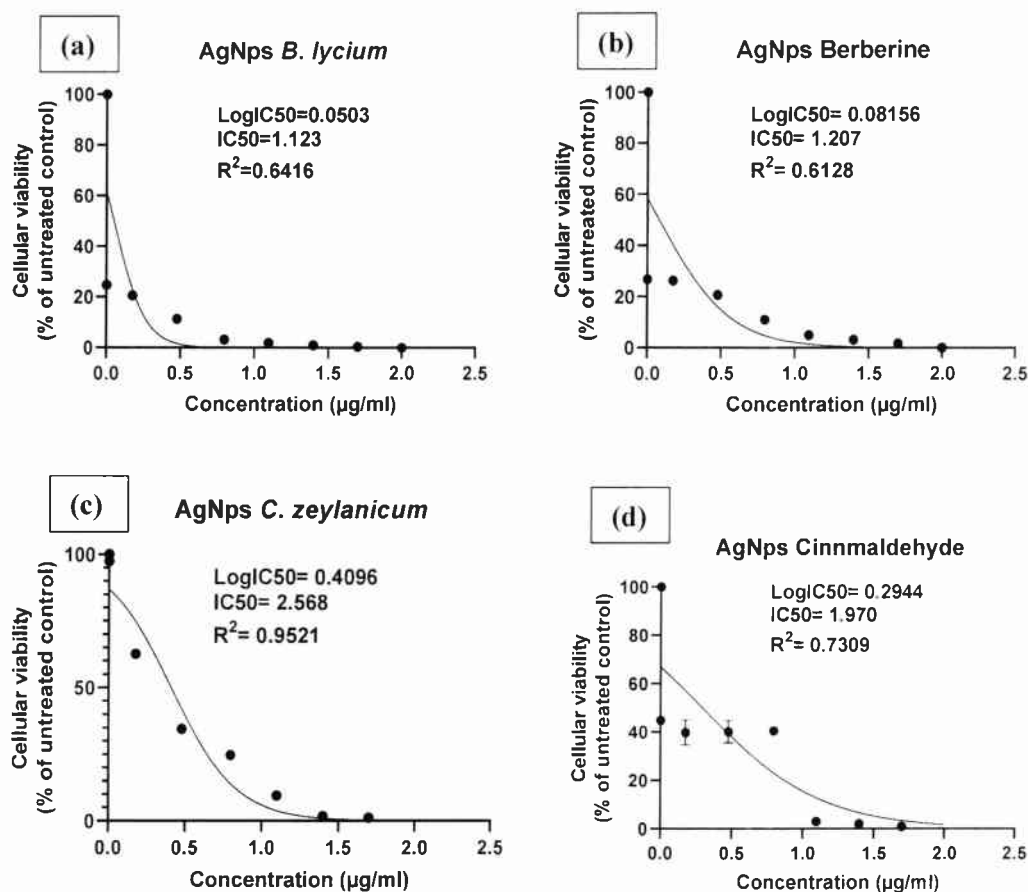


Figure No. 3.88: Inhibitory concentration (IC₅₀) of Anti-amastigotes of *L. tropica* at different concentration of AgNPs synthesized in the presence of (a) *B. lycium* root extract (b) Berberine (c) *C. zeylanicum* bark extract (d) Cinnamaldehyde

3.7.4 Anti-amastigote Assay of ZnNPs:

Antileishmanial efficacy of biologically synthesized ZnNPs were analyzed on the strain of *leishmania tropica*. The metabolic activity of amastigotes decreased with increasing the concentration of ZnNPs. In experimental group when leishmanial cells were treated with high concentration (100µg/ml) of ZnNPs of *B. lycium* and ZnNPs of Berberine. The amount of viable cells were very low at higher concentration. It was clearly shown that 100% leishmanial cells killing. The IC₅₀ value of ZnNPs of *B.*

lycium root extract was 3.925µg/ml and the IC50 value of ZnNPs of Berberine was 4.569µg/ml. Same effect was observed during all the evaluated Incubation time period which is shown in the graphs.

The effects of ZnNPs of *C. zeylanicum* bark extract and ZnNPs of Cinnamaldehyde on the metabolic activity of *Leishmania tropica* were also studied.

It was noticed, that the metabolic activity of *Leishmania tropica* amastigotes at each concentration of ZnNPs were negatively affected in comparison to control group. The IC50 value of ZnNPs of *C. zeylanicum* bark extract was 2.919µg/ml and the IC50 value of ZnNPs of Cinnamaldehyde was 2.062µg/ml.

In result, ZnNPs Shows the maximum suppressive effect on higher concentration 100ug/ml in comparison to the control group, at the same concentration the metabolic activity value of amastigotes decreased.

The results indicated, that with the increase of concentration of ZnNPs the cell viability of *leishmania tropica* decreased. The highest concentration of ZnNPs was 100µg/ml shown maximum effects on metabolic activity of amastigotes and it was visualized clearly in the (Figures. 3.89). According to the figures, these results demonstrated better effects of ZnNPs on the viable cells of amastigotes on all the concentration but on higher concentration the metabolic activity of amastigotes decreased. So, it was concluded that the biologically synthesized ZnNPs at low concentrations expressively killing the leishmanial cells and these nanoparticles are considered as the suitable candidates for the *leishmania* treatment.

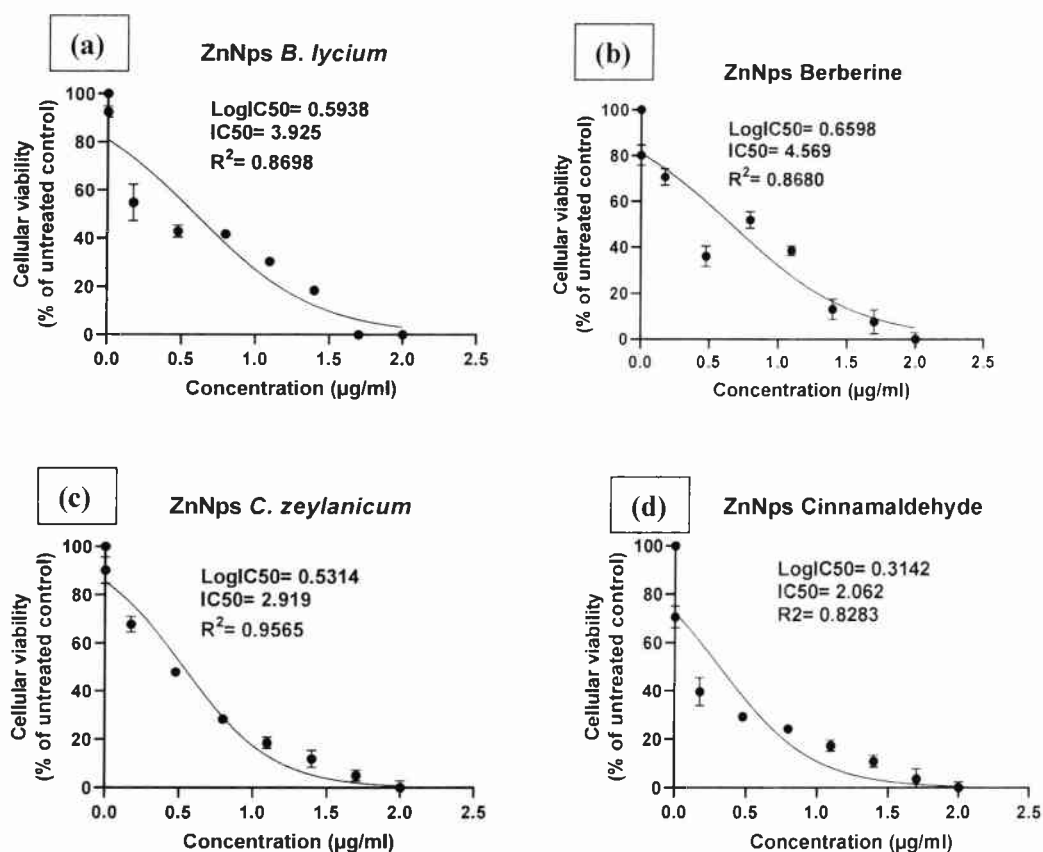


Figure No. 3.89: Inhibitory concentration (IC_{50}) of Anti-amastigotes of *L. tropica* at different concentration of ZnNPs synthesized in the presence of (a) *B. lycium* root extract (b) Berberine (c) *C. zeylanicum* bark extract (d) ZnNPs Cinnamaldehyde

3.8 Cytotoxic Activity

3.8.1 Assessment of cytotoxic effect of AgNPs in normal cell (Hemolytic assay)

Hemolytic activity was performed on fresh human blood cells. It was important to develop less toxic and more effective nanoparticles to cure the pathogenic diseases. In Hemolytic assay the external membrane of red blood cell was destroyed to release the hemoglobin. The quantity of destroy cells was estimated by measuring the amount of hemoglobin in the sample. It was necessary to evaluate the biocompatibility of these NPs on normal human cells to ensure their non-toxic usage. In this study, the biologically synthesized NPs were used at different concentrations and evaluated for their cytotoxicity against human macrophages.

It was clear from the results that all the NPs were non-biocompatible on 200ug/ml. AgNPs of *B. lycium* root extract showed highest hemolytic activity (hemolysis > 80%) on concentration 200ug/ml while AgNPs of berberine shows similar hemolytic activity (hemolysis >80%) at concentration 200ug/ml. The AgNPs of *B. lycium* root extract at 12.5ug/ml concentration showed (hemolysis >30%) and AgNPs of berberine at 12.5ug/ml showed similar hemolytic activity (>30%). The released hemoglobin was monitored at 576nm using 96-well micro-plate reader. Experiment were performed in triplicate. The suspension of red blood cells in PBS without NPs was taken as a negative control. The red blood cells lysed with Triton-X (0.1%) was taken as a positive control.

The hemolytic activity of AgNPs of *C. zeylanicum* showed hemolytic activity (< 80%) at 200ug/ml concentration and (<30%) at concentration 12.5ug/ml while AgNPs of Cinnamaldehyde at 200ug/ml concentration showed (<80%) hemolytic activity and at concentration 12.5ug/ml the hemolytic activity was (>30%). The results indicated that the AgNPs are non-biocompatible at higher concentration and biocompatible at lower concentration when compared with 0.5% Triton X-100 (as positive control).

Silver and Zinc Nanoparticles could be considered as good modality for the treatment of fatal diseases. The present investigation suggested that at limited dosage, the *B. lycium* root extract and *Berberine* and *C. zeylanicum* bark extract and *Cinnamaldehyde* mediated AgNPs and ZnNPs can be used as an effective antimicrobial agent with minimum toxicity.

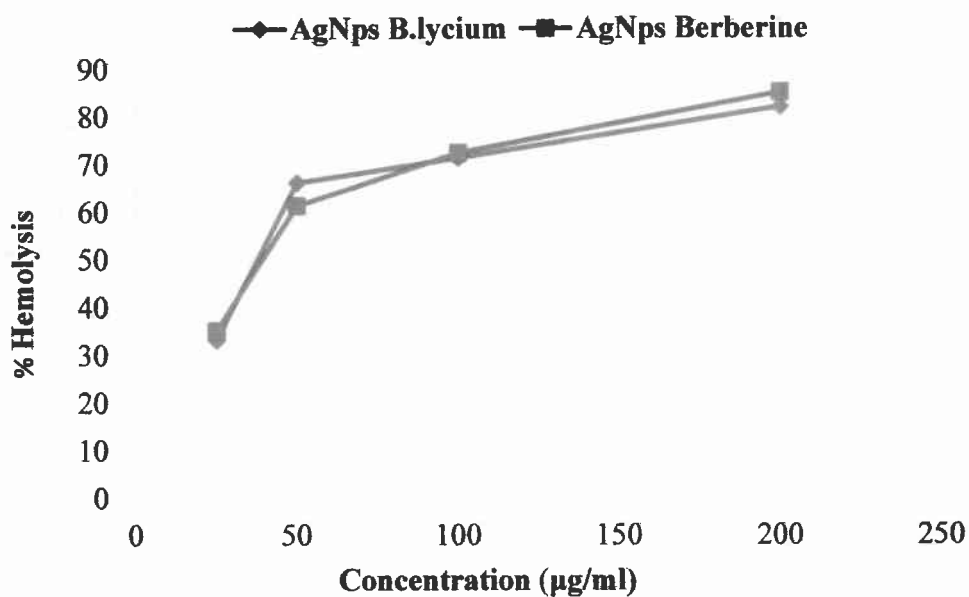


Figure No 3.90: Hemolysis of AgNPs synthesized in the presence of *B. lycium* root extract and berberine on normal human blood cell

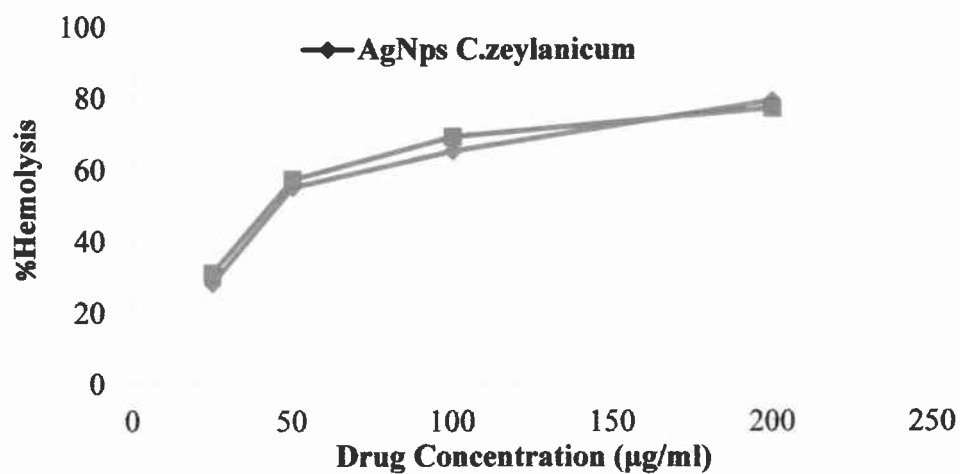


Figure No 3.91: Hemolysis of AgNPs synthesized in the presence of *C. zeylanicum* root extract and Cinnamaldehyde on normal human blood cell

3.8.2 Assessment of cytotoxic effect of ZnNPs in normal cell (Hemolytic assay)

Hemolytic activity was performed on fresh human blood cells. It is important to develop less toxic and more effective agent to cure the pathogenic diseases. In Hemolytic assay the external membrane of red blood cell was destroyed to release the hemoglobin. The quantity of destroy cells was estimated by measuring the amount of hemoglobin in the sample. It was necessary to evaluate the biocompatibility of these Nps on normal human cells to ensure their non-toxic usage. In this study, the biologically synthesized Nps were used at different concentrations and evaluated for their cytotoxicity against human macrophages.

It was cleared from the results that all the ZnNPs are non-biocompatible on 200ug/ml. ZnONPs of *B. lycium* root extract showed highest hemolytic activity (hemolysis 90%) at concentration 200ug/ml while ZnNPs of berberine shows similar hemolytic activity (hemolysis 90%) at concentration 200ug/ml. The ZnNPs of *B. lycium* root extract at 12.5ug/ml concentration showed (hemolysis >10%) and AgNPs of berberine at 12.5ug/ml showed similar hemolytic activity (>10%). The released hemoglobin was monitored at 576nm using 96-well micro-plate reader. Experiment were performed in triplicate. The suspension of red blood cells in PBS without NPs was taken as a negative control. The red blood cells lysed with Triton-X (0.1%) was taken as a positive control.

The hemolytic activity of ZnNPs of *C. zeylanicum* showed (80%) hemolysis at 200ug/ml concentration and (<10%) at concentration 12.5ug/ml while AgNPs of Cinnamaldehyde at 200ug/ml concentration showed (<80%) hemolytic activity and at concentration 12.5ug/ml the hemolytic activity was (<10%). The results indicated that the ZnNPs were non-biocompatible at 200, 100 and 50ug/ml and at 12.5ug/ml concentration the ZnNPs are nontoxic, biologically active and biocompatible when compared with 0.5% Triton X-100 (as positive control).

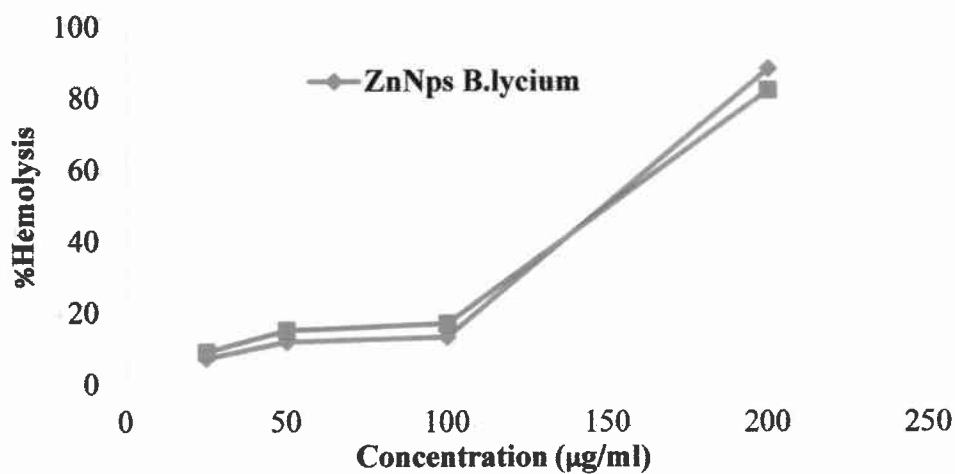


Figure No 3.92: Hemolysis of ZnNPs synthesized in the presence of *B. lycium* root extract and berberine on normal human blood cell

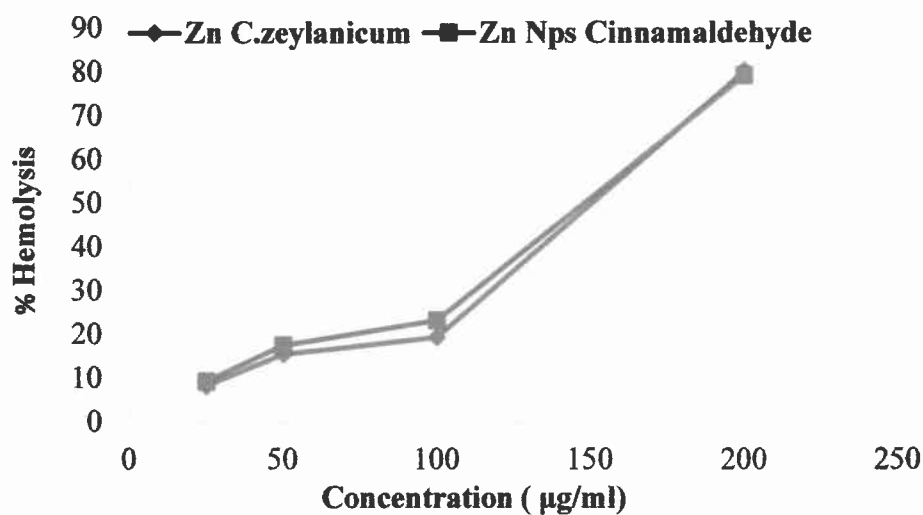
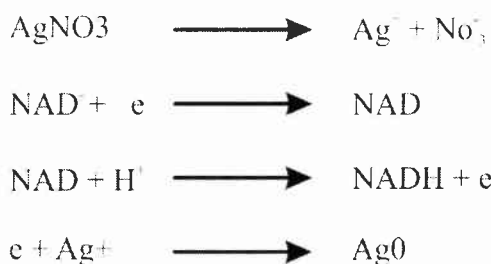


Figure No 3.93: Hemolysis of ZnNPs synthesized in the presence of *C. zeylanicum* root extract and Cinnamaldehyde on normal human blood cell

**CHAPTER 4:
DISCUSSION**

DISCUSSION

In the synthesis of AgNPs, color change is the important factor. As a result of surface plasmon vibrations AgNPs appear brown in the aqueous medium. Other studies have reported that color change from yellowish brown to dark brown is the indication of colloidal AgNPs (Banerjee et al., 2014; Vigneshwaran et al., 2006). For the analysis of NPs, UV-vis spectroscopy is a very helpful approach. UV-Vis spectroscopy was used primarily to characterise the NPs. AgNO₃ in the aqueous solution is converted to Ag⁺ ions by the compounds in the plant extract. The reduction of Ag ions to AgNPs, as indicated by the activation of plasmon vibrations of AgNPs in the solution and verified by UV-Vis spectra. AgNPs' biosynthetic mechanism is not fully understood. However Ahmad et al., (2016) have suggested that Nicotinamide adenine dinucleotide (NAD), is electrons carrier and carrying electrons from one reaction to another. It accept electron from other molecules and itself reduced (oxidizing agent). This oxidizing reaction forms NADH, which can donate electrons further. The main function of NAD is to transfer electrons in the reactions.



NAD deoxidized constantly and regenerate electrons which is called redox reactions. These redox reactions might be responsible for the formation of Ag⁰ from Ag⁺.

Many studies have reported that the surface plasmon resonance for the colloidal silver ranging from 320-390nm (Huang et al., 2009) while others reported 420-450nm (Banerjee et al., 2014) 400-500nm (Mehmood et al., 2014). It is suggested that the molecules present in the plant extract is act as a capping agent for AgNPs which could affect the SPR of the AgNps. According to Otunola et al. (2017) from the UV-absorption of plant extract AgNPs it was implies that the bioactive compounds such as proteins stabilized and prevented the transition of electrons from the surface of AgNPs.

The SPR obtained of the colloidal silver system shows that only AgNPs are present in the dispersion.

To identify the functional groups in silver nanoparticles made from plants which are responsible for reducing and capping of AgNPs. FTIR analysis of the particles was performed. The FTIR spectrum of pure substances is so distinct that it resembles and seems to be a molecule fingerprint (Sasidharan et al., 2011). It was observed from the study that the stretching vibrations responsible for compounds such as phenol, flavonoids, terpenoids and proteins and confirmed that these molecules are responsible for the capping, stabilizing and capping of silver nanoparticles (Mehmood et al., 2016). Several studied of AgNPs from plant extract have been reported *Urtica dioica* (Jyoti et al., 2016), *Lippia nodiflora* (Liu et al., 2007), *Azadirachta indica* (Ahmed et al., 2016), and *Pedalium murex* (Khanna & Nair, 2009).

The ZnNPs results showed that polyhydroxyl phenolics and flavonoids are the primary biomolecules that can reduce zinc ions and convert them to ZnONPs in the plant extract.(Ahmad et al., 1998; Anzabi, 2018).. We identified peak intensity, orientation, and full width at half-maximum (FWHM) data from the analysis of XRD patterns. The peaks of the diffraction have been determined as cubic crystal structure. The Ag nanoparticles' high degree of crystallinity is reflected in the intensity of the peaks. However, the diffraction peaks are broad which indicate that small crystallite size (Wani et al., 2011). The XRD patterns of ZnNPs indicated the formation of high purity of the ZnO nanoparticles. The ZnONPs diffraction peaks' have strong intensity and smaller width suggested that the final product was extremely crystalline in nature. Scherrer's formula was used to estimate the size of the average crystallite. The formation of metal particles in nanosize was confirmed by the SEM examination of AgNPs. The particles had a diameter of less than 100 nm and were spherical in appearance. SEM images the ZnNPs microstructure has hexagonal and spherical shape. However, aggregation is also noticed, likely as a result of densification, which results in a small gap between particles, as well as the high surface energy of ZnONPs that often happens when synthesis is carried out in an aqueous media. (Salam et al., 2014; Selvarajan & Mohanasrinivasan, 2013).

According to the results of the antibacterial activity tests, biologically produced AgNPs and ZnNPs nanoparticles were effective against both Gram positive including (*E. coli*) and Gram negative bacterial strains (*S. aureus*). It was previously known that the alkaloid Berberine found in *Berberis* bark has significant antibacterial activity. It is evident that increasing the concentration of *C. zeylanicum* bark extract silver nanoparticles also increases their inhibitory activity. The high surface area to volume ratio of AgNPs was the reason of their increased antibacterial activity. AgNPs' greater activity compared to aqueous extract and was concluded that AgNPs have greater activity because of composite of biomolecules with silver NPs. Silver ions significantly reduce bacterial growth. (Liau et al., 1997). Previous investigations also showed that het strong antibacterial properties of AgNPs produced from plant extract. (Reddy & Gandhi, 2012).

Silver nanoparticles modify the permeability of the cell membrane when they adhere to the bacterial cell wall and penetrate in the bacteria, which causes cell death. On the cell's surface, pits are formed and there is an accumulation of nanoparticles in those pits. (Sondi & Salopek-Sondi, 2004). Another cause of cell death is that silver nanoparticles' responsible for the generation of free radicals. Spectroscopy of electron spin resonance reveals that, when silver nanoparticles and bacteria come into contact, free radicals are produced. These free radicals cause the cell membrane to become permeable and chang the cell membrane structure. Ultimately, these modifications to the cell membrane result in cell death. (Danil'chuk et al., 2006; Kim et al., 2007). As antibacterial agents, silver nanoparticles are now frequently employed in coatings, textiles, and wood flooring. High antibacterial activity was demonstrated by these biogenically produced silver nanoparticles, which may be utilized in these products.

AgNPs have the capacity to firmly attach to molecules containing sulphur and phosphorus (Zhang et al., 2009) and because to this characteristic, they can weaken sulfur-containing proteins, which in turn can harm the bacterial cell membrane.. AgNPs can enter bacteria and harm DNA with phosphorus and sulfur-containing enzymes. AgNPs are also known to accumulate significantly within mitochondria, and it has been shown that this oxidative stress damages mitochondrial function.(Asharani et al., 2009; AshaRani et al., 2009; Xia et al., 2006). Adenosine triphosphate (ATP) synthesis is well

known to stop when mitochondrial enzymes are affected. Therefore, it is believed that AgNPs have the capacity to block ATP synthesis which is the cause of their antibacterial actions. (Feng et al., 2000; Song et al., 2006).

The particular mechanism by which ZnONPs exert their antibacterial effects is currently unclear and not fully developed. (Jalal et al., 2010). The primary factors influencing ZnONPs' antibacterial effect include their size, shape, surface chemistry, and unique physicochemical features. (Brayner et al., 2006; Jones et al., 2008). In the current study, we suggested a potential mechanism for how biosynthesized ZnONPs work as an antibiotic. ZnONPs entered the bacteria's cell due to their small size and electrostatic interactions with the cell membrane. Once inside the bacterial cell, ZnONPs begin to interact with the cell's organelles, depleting the cell's internal resources and interfering with DNA replication by releasing reactive oxygen species (ROS).. The excessive production of zinc ions (Zn^{2+}) and ROS, particularly hydroxyl radicals (HO), singlet oxygen (O_2), and hydrogen peroxide (H_2O_2), led to cell membrane rupture and disorder. As a result, bacterial cells with damaged cell membranes which followed by cytoplasmic leakage were leads to the cell death. Due to their high reactivity and oxidising ability, the ROS are toxic to bacteria. (Zhang et al., 2009). Yamamoto (2001) identified the production of ROS as the primary mechanism behind the antibacterial action of ZnONPs.

Results of the antifungal activity tests showed that biologically produced silver nanoparticles were particularly effective against a strain of fungus (*Trichoderma herzianum*) but the ZnONPs were not active against (*Trichoderma herzianum*) and didn't show any zone of inhibition by using higher concentration as well. Similar to the antifungal activity in the MIC values of Amphotericin B, which was utilised as a positive control, Ag-NPs showed similar antifungal action against the fungal strains examined.. These findings showed that AgNPs have outstanding potential as an antifungal agent for treating infectious fungal infections. Nasrollahi (2018) reported same results against fungal strains *albicans* and *Saccharomyces cerevisiae*.

According to (Dorau et al., 2012), the inactivation of sulfhydryl groups in the fungal cell wall and the breakdown of membrane-bound lipids and enzymes, which results the cell lysis, were the cause of antifungal properties of silver NPs. By using the agar well diffusion method, colloidal silver nanoparticle suspension was used

to study the antifungal activities against fungal strains of the *Aspergillus* species. It was found that a clear zone of inhibition formed around the cavities where the suspension of silver nanoparticles was added. (Roy et al., 2013).

Percentage inhibition of the tested NPs' ability to scavenge DPPH radicals at various concentrations were observed. Considerable variations in antioxidant profile were recorded at different concentrations. Different flavonoids extracted from cinnamon exhibit antioxidant and free radical scavenging activities. (Rao & Gan, 2014). *C. zeylanicum*'s extract is a powerful antioxidant and free radical scavenger, and it has anti-inflammatory, anti-fungal, anti-viral, anti-bacterial and anti-hyperglycemic properties. (Jakhetia et al., 2010; Kumaravel & Srinivasan, 2017). By using the DPPH Method, the antioxidant activity of cinnamon extract and the cinnamon AgNPs was examined. The percentage of inhibition was 11.34 ± 0.56 % by Cinnamon extract and 22.41 ± 0.25 % by silver nanoparticles synthesized from cinnamon. Consequently, 2 times more antioxidant activity was observed by the silver nanoparticle than by cinnamon extract. Thus, it is determined that the synthetic silver nanoparticles have more antioxidant potential than cinnamon extract. Antileishmanial efficacy of biologically synthesized AgNPs and ZnNPs were analyzed on the strain of *leishmania tropica* KWH23 and found very active. The results indicated that with the increase of concentration of ZnNps and AgNPs the cell viability of *leishmania tropica* decreased. Leishmania is known to be extremely sensitive to these oxygen species. Medicines that cause ROS will therefore be excellent antileishmanial agents. Macrophages (host cells for *Leishmania*) produce high concentration of these ROS to disinfect microbial agents (Lodge & Descoteaux, 2006).

Leishmania, however, avoids the oxidative damage brought on by ROS by suppressing the enzymes responsible for producing ROS. (Mehta & Shaha, 2006). A significant reservoir of silver and gold ions would be created by using Ag and Au nanoparticles as leishmanicidal agents, acting as a non-enzymatic source of ROS that will kill the parasite that has infiltrated the body. The formation of free radicals from silver ions has been verified by electron spin resonance spectroscopy, and these radicals harm microbial organisms in a various ways. (Kim et al., 2007).

Hemolytic activity was performed on fresh human blood cells. It was important to develop less toxic and more effective agent to cure the pathogenic diseases. Cytotoxicity is an important assay which must be dealt before. Silver and Zinc Nanoparticles can be considered as good modality for the treatment of fatal diseases. The present investigation suggested that at limited dosage of AgNPs and ZnONPs can be used as an effective antimicrobial agent with minimum toxicity.

CHAPTER 5:
CONCLUSION AND FUTURE ASPECTS

CONCLUSION

Green synthesis is a substitute process for using harmful chemicals to create environmentally acceptable metallic nanoparticles. Citric acid, cyclic peptides, gellic acid, tenines and retinoic acid are some of the significant functional groups found in plant extracts that not only work as a bio-reduction but also operate as capping and stabilising agents. The reduction of Ag ions into AgNPs and Zn ions into ZnNPs was obtained by naturally occurring biomaterials, which is present in plants. Synthesis of AgNPs and ZnNPs (green synthesis) has been an important and innovative technology especially in the medical field and in the control of pathogenic microorganisms.

- The current study first to demonstrate the comparative analysis of green synthesized Silver and Zinc nanoparticles of *B. lycium* root extract and Berberine and *C. zeylanicum* bark extract and Cinnamaldehyde.
- The biological activities of green synthesized AgNPs of *B. lycium* root extract was > AgNPs of berberine and AgNPs of Cinnamaldehyde > AgNPs of *C. zeylanicum* bark extract.
- The biological activities of ZnNPs have similar results.
- AgNPs *B. lycium* root extract biological activities was greater than AgNPs of Berberine which means that in *B. lycium* root extract some other compounds are present which have some synergistic effects to enhance the biological activity of green synthesized AgNPs and ZnNPs of *B. lycium* root extract.
- The biological activities of AgNPs and ZnNPs of Cinnamaldehyde were greater than AgNPs and ZnNPs of *C. zeylanicum* bark extract which means that in *C. zeylanicum* bark extract some other compounds are present other than Cinnamaldehyde which decreases their effects against microorganisms.
- ZnNPs didn't showed any activity against *Trichoderma herzianium* even, at higher concentrations.

FUTURE ASPECTS

Consequently, this method of creating silver and zinc nanoparticles is one of the best way to handle therapeutically the antibiotic-resistant microbes in preventing infection. This finding will benefit other scientists studying the biological applications of metallic nanoparticles synthesized through green synthesis.

**CHAPTER 6:
REFERENCES**

REFERENCES

- Ahmad, I., Mehmood, Z., & Mohammad, F. (1998). Screening of some Indian medicinal plants for their antimicrobial properties. *Journal of ethnopharmacology*, 62(2), 183-193.
- Ahmad, N., Sharma, S., Alam, M. K., Singh, V., Shamsi, S., Mehta, B., & Fatma, A. (2010). Rapid synthesis of silver nanoparticles using dried medicinal plant of basil. *Colloids and Surfaces B: Biointerfaces*, 81(1), 81-86.
- Ahmed, S., Saifullah, Ahmad, M., Swami, B. L., & Ikram, S. (2016). Green synthesis of silver nanoparticles using *Azadirachta indica* aqueous leaf extract. *Journal of radiation research and applied sciences*, 9(1), 1-7.
- Ali, H., Uddin, S., & Jalal, S. (2015). Chemistry and biological activities of *Berberis lycium* Royle. *Journal of Biologically Active Products from Nature*, 5(5), 295-312.
- Ali, M., & Sharma, S. (1996). Heterocyclic constituents from *Berberis lycium* roots. *Indian Journal of Heterocyclic Chemistry*, 6(2), 127-130.
- Alivisatos, A. P. (1996). Semiconductor clusters, nanocrystals, and quantum dots. *Science*, 271(5251), 933-937.
- Alkaladi, A., Abdelazim, A. M., & Afifi, M. (2014). Antidiabetic activity of zinc oxide and silver nanoparticles on streptozotocin-induced diabetic rats. *International journal of molecular sciences*, 15(2), 2015-2023.
- Al-Snafi, A. E. (2013). Pharmacological effects of *Allium* species grown in Iraq. An overview. *International Journal of Pharmaceutical and health care Research*, 1(4), 132-147.
- Al-Snafi, A. E. (2015). The pharmacological and therapeutic importance of *Agrimonia eupatoria*-A review. *Asian Journal of Pharmaceutical Science and Technology*, 5(2), 112-117.

- Amato, V. S., Tuon, F. F., Bacha, H. A., Neto, V. A., & Nicodemo, A. C. (2008). Mucosal leishmaniasis: current scenario and prospects for treatment. *Acta tropica*, 105(1), 1-9.
- Andola, H., Rawal, R., Rawat, M., Bhatt, I., & Purohit, V. (2010). Analysis of berberine content using HPTLC fingerprinting of root and bark of three Himalayan Berberis species. *Asian Journal of Biotechnology*, 2(4), 239-245.
- Aneja, K. R., Joshi, R., & Sharma, C. (2009). Antimicrobial activity of Dalchini (Cinnamomum zeylanicum bark) extracts on some dental caries pathogens. *J Pharm Res*, 2(9), 1387-1390.
- Anzabi, Y. (2018). Biosynthesis of ZnO nanoparticles using barberry (Berberis vulgaris) extract and assessment of their physico-chemical properties and antibacterial activities. *Green Processing and Synthesis*, 7(2), 114-121.
- Asharani, P., Hande, M. P., & Valiyaveetil, S. (2009). Anti-proliferative activity of silver nanoparticles. *BMC cell biology*, 10(1), 1-14.
- AshaRani, P., Low Kah Mun, G., Hande, M. P., & Valiyaveetil, S. (2009). Cytotoxicity and genotoxicity of silver nanoparticles in human cells. *ACS nano*, 3(2), 279-290.
- Ashford, R. W. (2000). The leishmaniases as emerging and reemerging zoonoses. *International journal for parasitology*, 30(12-13), 1269-1281.
- Ashokkumar, S., Ravi, S., Kathiravan, V., & Velmurugan, S. (2014). RETRACTED: Synthesis, characterization and catalytic activity of silver nanoparticles using Tribulus terrestris leaf extract. In: Elsevier.
- Asif, A., Kakub, G., Mehmood, S., Khunum, R., & Gulfranz, M. (2007). Wound healing activity of root extracts of Berberis lyceum Royle in rats. *Phytotherapy Research: An International Journal Devoted to Pharmacological and Toxicological Evaluation of Natural Product Derivatives*, 21(6), 589-591.

- Azam, A., Ahmed, A. S., Oves, M., Khan, M. S., Habib, S. S., & Memic, A. (2012). Antimicrobial activity of metal oxide nanoparticles against Gram-positive and Gram-negative bacteria: a comparative study. *International Journal of Nanomedicine*, 7, 6003.
- Bagheri, A., Arandiyani, H., Boyer, C., & Lim, M. (2016). Lanthanide-doped upconversion nanoparticles: emerging intelligent light-activated drug delivery systems. *Advanced Science*, 3(7), 1500437.
- Balandrin, M. F., Kinghorn, A. D., & Farnsworth, N. R. (1993). Plant-derived natural products in drug discovery and development: an overview. In *ACS Symposium Series*. American Chemical Society.
- Bali, R., Razak, N., Lumb, A., & Harris, A. (2006). The synthesis of metallic nanoparticles inside live plants. 2006 International Conference on Nanoscience and Nanotechnology,
- Bandara, T., Uluwaduge, I., & Jansz, E. (2012). Bioactivity of cinnamon with special emphasis on diabetes mellitus: a review. *International journal of food sciences and nutrition*, 63(3), 380-386.
- Banerjee, P., Satapathy, M., Mukhopahayay, A., & Das, P. (2014). Leaf extract mediated green synthesis of silver nanoparticles from widely available Indian plants: synthesis, characterization, antimicrobial property and toxicity analysis. *Bioresources and Bioprocessing*, 1(1), 1-10.
- Bar, H., Bhui, D. K., Sahoo, G. P., Sarkar, P., De, S. P., & Misra, A. (2009). Green synthesis of silver nanoparticles using latex of *Jatropha curcas*. *Colloids and surfaces A: Physicochemical and engineering aspects*, 339(1-3), 134-139.
- Basavaraja, S., Balaji, S., Lagashetty, A., Rajasab, A., & Venkataraman, A. (2008). Extracellular biosynthesis of silver nanoparticles using the fungus *Fusarium semitectum*. *Materials Research Bulletin*, 43(5), 1164-1170.
- Bates, P. (1993). Axenic culture of *Leishmania amastigotes*. *Parasitology Today*, 9(4), 143-146.

- Bhardwaj, D., & Kaushik, N. (2012). Phytochemical and pharmacological studies in genus *Berberis*. *Phytochemistry reviews*, 11(4), 523-542.
- Bhargava, P., & Singh, R. (2012). Developments in diagnosis and antileishmanial drugs. *Interdisciplinary perspectives on infectious diseases*, 2012, 1-14.
- Bhutto, A. M., Soomro, F. R., & Katakura, K. (2008). Leishmaniasis in Sindh, Pakistan: outbreak and review of the literature. *Journal of Pakistan Association of Dermatologists*, 18(4), 212-219.
- Braga, F. G., Bouzada, M. L. M., Fabri, R. L., Matos, M. d. O., Moreira, F. O., Scio, E., & Coimbra, E. S. (2007). Antileishmanial and antifungal activity of plants used in traditional medicine in Brazil. *Journal of ethnopharmacology*, 111(2), 396-402.
- Brayner, R., Ferrari-Iliou, R., Brivois, N., Djediat, S., Benedetti, M. F., & Fiévet, F. (2006). Toxicological impact studies based on *Escherichia coli* bacteria in ultrafine ZnO nanoparticles colloidal medium. *Nano letters*, 6(4), 866-870.
- Bruchez Jr, M., Moronne, M., Gin, P., Weiss, S., & Alivisatos, A. P. (1998). Semiconductor nanocrystals as fluorescent biological labels. *Science*, 281(5385), 2013-2016.
- Buzea, C., Pacheco, I. I., & Robbie, K. (2007). Nanomaterials and nanoparticles: sources and toxicity. *Biointerphases*, 2(4), MR17-MR71.
- Cao, G., & Liu, D. (2008). Template-based synthesis of nanorod, nanowire, and nanotube arrays. *Advances in colloid and interface science*, 136(1-2), 45-64.
- Chaloupka, K., Malam, Y., & Seifalian, A. M. (2010). Nanosilver as a new generation of nanoparticle in biomedical applications. *Trends in biotechnology*, 28(11), 580-588.
- Chan, W. C., & Nie, S. (1998). Quantum dot bioconjugates for ultrasensitive nonisotopic detection. *Science*, 281(5385), 2016-2018.

- Chang, S.-T., Chen, P.-F., & Chang, S.-C. (2001). Antibacterial activity of leaf essential oils and their constituents from *Cinnamomum osmophloeum*. *Journal of ethnopharmacology*, 77(1), 123-127.
- Chao, L. K., Hua, K.-F., Hsu, H.-Y., Cheng, S.-S., Liu, J.-Y., & Chang, S.-T. (2005). Study on the antiinflammatory activity of essential oil from leaves of *Cinnamomum osmophloeum*. *Journal of agricultural and food chemistry*, 53(18), 7274-7278.
- Chartone-Souza, E. (1998). Bactérias ultra-resistentes: uma guerra quase perdida. *Cienc Hoje*, 23(138), 27-35.
- Chauhan, N. (1990). *Medicinal and aromatic plants of Himachal Pradesh, National work-shop on Cold Desert Area, India*.
- Chen, L., Chen, Z., Shang, X., Liu, C., Xu, S., & Fu, Q. (2006). Effect of annealing temperature on density of ZnO quantum dots. *Solid state communications*, 137(10), 561-565.
- Cheng, S.-S., Liu, J.-Y., Huang, C.-G., Hsui, Y.-R., Chen, W.-J., & Chang, S.-T. (2009). Insecticidal activities of leaf essential oils from *Cinnamomum osmophloeum* against three mosquito species. *Bioresource technology*, 100(1), 457-464.
- Cheng, S.-S., Liu, J.-Y., Tsai, K.-H., Chen, W.-J., & Chang, S.-T. (2004). Chemical composition and mosquito larvicidal activity of essential oils from leaves of different *Cinnamomum osmophloeum* provenances. *Journal of agricultural and food chemistry*, 52(14), 4395-4400.
- Chiang, H., & Hanssen, C. (1977). The Alkaloids. *J. Org. Chem*, 42, 3190-3192.
- Chopra, R. N., & Chopra, I. C. (1994). *Indigenous drugs of India*. Academic publishers.
- Chowdhary, A., Prakash, A., Sharma, C., Kordalewska, M., Kumar, A., Sarma, S., . . . Upadhyay, S. (2018). A multicentre study of antifungal susceptibility patterns among 350 *Candida auris* isolates (2009–17) in India: role of the ERG11 and

- FKS1 genes in azole and echinocandin resistance. *Journal of Antimicrobial Chemotherapy*, 73(4), 891-899.
- Cioffi, N., Torsi, L., Ditaranto, N., Tantillo, G., Ghibelli, L., Sabbatini, L., . . . Traversa, E. (2005). Copper nanoparticle/polymer composites with antifungal and bacteriostatic properties. *Chemistry of Materials*, 17(21), 5255-5262.
- Coe, S., Woo, W.-K., Bawendi, M., & Bulović, V. (2002). Electroluminescence from single monolayers of nanocrystals in molecular organic devices. *Nature*, 420(6917), 800-803.
- Cowan, M. M. (1999). Plant products as antimicrobial agents. *Clinical microbiology reviews*, 12(4), 564-582.
- Croft, S. L., Seifert, K., & Yardley, V. (2006). Current scenario of drug development for leishmaniasis. *The Indian journal of medical research*, 123(3), 399-410.
- Danil'chuk, L., Okunev, A., & Tkal, V. (2006). X-ray Diffraction Topography of Defects in Crystals on the Basis of the Borrmann Effect. *Yaroslav-the-Wise Novgorod State University: Veliky Novgorod*.
- Danilczuk, M., Lund, A., Sadlo, J., Yamada, H., & Michalik, J. (2006). Conduction electron spin resonance of small silver particles. *Spectrochimica Acta Part A: Molecular and Biomolecular Spectroscopy*, 63(1), 189-191.
- Daud, J. M., Hassan, H. H. M., Hashim, R., & Taher, M. (2011). Phytochemicals screening and antioxidant activities of Malaysian *Donax grandis* extracts. *European Journal of Scientific Research*, 61(4), 572-577.
- De Carvalho, P. B., Arribas, M. d. G., & Ferreira, E. I. (2000). Leishmaniasis. What do we know about its chemotherapy? *Revista Brasileira de Ciências Farmacêuticas*, 36(1), 69-96.
- Delavari, V., & Hashemabadi, S. H. (2014). CFD simulation of heat transfer enhancement of Al₂O₃/water and Al₂O₃/ethylene glycol nanofluids in a car radiator. *Applied thermal engineering*, 73(1), 380-390.

- Dostálová, A., & Volf, P. (2012). Leishmania development in sand flies: parasite-vector interactions overview. *Parasites & vectors*, 5(1), 1-12.
- Dubey, S. P., Lahtinen, M., & Sillanpää, M. (2010). Tansy fruit mediated greener synthesis of silver and gold nanoparticles. *Process Biochemistry*, 45(7), 1065-1071.
- Elad, Y., Yunis, H., & Katan, T. (1992). Multiple fungicide resistance to benzimidazoles, dicarboximides and diethofencarb in field isolates of *Botrytis cinerea* in Israel. *Plant Pathology*, 41(1), 41-46.
- Elechiguerra, J. L., Burt, J. L., Morones, J. R., Camacho-Bragado, A., Gao, X., Lara, H. H., & Yacaman, M. J. (2005). Interaction of silver nanoparticles with HIV-1. *Journal of nanobiotechnology*, 3(1), 1-10.
- El-Rafie, M., El-Naggar, M., Ramadan, M., Fouda, M. M., Al-Deyab, S. S., & Hebeish, A. (2011). Environmental synthesis of silver nanoparticles using hydroxypropyl starch and their characterization. *Carbohydrate Polymers*, 86(2), 630-635.
- Enad, A. T., & Zghair, K. H. (2016). Cytotoxic Effect of ZnO Nanoparticles on the Viability of *Leishmania donovani* Promastigotes in vitro. *Iraqi Journal of Science*, 2811-2817.
- Esimone, C., Adikwu, M., & Okonta, J. (1998). Preliminary antimicrobial screening of the ethanolic extract from the lichen *Usnea subfloridans* (L). *J. Pharm. Res. Dev*, 3(2), 99-101.
- Fedlheim, D. L., & Foss, C. A. (2001). *Metal nanoparticles: synthesis, characterization, and applications*. CRC press.
- Feng, Q. L., Wu, J., Chen, G. Q., Cui, F., Kim, T., & Kim, J. (2000). A mechanistic study of the antibacterial effect of silver ions on *Escherichia coli* and *Staphylococcus aureus*. *Journal of biomedical materials research*, 52(4), 662-668.

- Forough, M., & Farhadi, K. (2010). Biological and green synthesis of silver nanoparticles. *Turkish journal of engineering and environmental sciences*, 34(4), 281-287.
- Gade, A., Ingle, A., Whiteley, C., & Rai, M. (2010). Mycogenic metal nanoparticles: progress and applications. *Biotechnology letters*, 32(5), 593-600.
- Gardea-Torresdey, J. L., Gomez, E., Peralta-Videa, J. R., Parsons, J. G., Troiani, H., & Jose-Yacaman, M. (2003). Alfalfa sprouts: a natural source for the synthesis of silver nanoparticles. *Langmuir*, 19(4), 1357-1361.
- Gardea-Torresdey, J. L., Parsons, J., Gomez, E., Peralta-Videa, J., Troiani, H., Santiago, P., & Yacaman, M. J. (2002). Formation and growth of Au nanoparticles inside live alfalfa plants. *Nano letters*, 2(4), 397-401.
- Gauthami, M., Srinivasan, N., M Goud, N., Boopalan, K., & Thirumurugan, K. (2015). Synthesis of silver nanoparticles using *Cinnamomum zeylanicum* bark extract and its antioxidant activity. *Nanoscience & Nanotechnology-Asia*, 5(1), 2-7.
- Goodsell, D. S. (2004). *Bionanotechnology: lessons from nature*. John Wiley & Sons.
- Gulbranson, S. H., Hud, J. A., & Hansen, R. C. (2000). Argyria following the use of dietary supplements containing colloidal silver protein. *CUTIS-NEW YORK*, 66(5), 373-378.
- Gulfraz, M., Mehmood, S., Ahmad, A., Fatima, N., Praveen, Z., & Williamson, E. (2008). Comparison of the antidiabetic activity of *Berberis lyceum* root extract and berberine in alloxan-induced diabetic rats. *Phytotherapy Research*, 22(9), 1208-1212.
- Gurunathan, S., Lee, K.-J., Kalishwaralal, K., Sheikpranbabu, S., Vaidyanathan, R., & Eom, S. H. (2009). Antiangiogenic properties of silver nanoparticles. *Biomaterials*, 30(31), 6341-6350.
- Haddad, R., Kasneci, A., Sebag, I. A., & Chalifour, L. E. (2013). Cardiac structure/function, protein expression, and DNA methylation are changed in

- adult female mice exposed to diethylstilbestrol in utero. *Canadian Journal of Physiology and Pharmacology*, 91(9), 741-749.
- Hamidulla, S., Shah, A., Parveen, S., Khattak, S., & Khattak, K. (2003). Physicochemical composition of wild medicinal plant *Berberis lyceum*. *Pak. J. Appl. Sci*, 6, 370-375.
- Hanley, C., Layne, J., Punnoose, A., Reddy, K., Coombs, I., Coombs, A., . . . Wingett, D. (2008). Preferential killing of cancer cells and activated human T cells using ZnO nanoparticles. *Nanotechnology*, 19(29), 295103.
- Hasan, A., Khan, M., & Ahmad, M. (2007). Authenticity of folk medicinal plants of Pakistan. *Taxonomic Chemical methods*, 1, 1-5.
- Hassan, H. F. H., Mansour, A. M., Abo-Youssef, A. M. H., Elsadek, B. E., & Messiha, B. A. S. (2017). Zinc oxide nanoparticles as a novel anticancer approach; in vitro and in vivo evidence. *Clinical and Experimental Pharmacology and Physiology*, 44(2), 235-243.
- Hatchett, D. W., & White, H. S. (1996). Electrochemistry of sulfur adlayers on the low-index faces of silver. *The Journal of Physical Chemistry*, 100(23), 9854-9859.
- He, L., Liu, Y., Mustapha, A., & Lin, M. (2011). Antifungal activity of zinc oxide nanoparticles against *Botrytis cinerea* and *Penicillium expansum*. *Microbiological research*, 166(3), 207-215.
- Hooker, J. D. (1882). *Impatiens sultanii*. *The Botanical Magazine (Curtis)*, 108(t), 6643.
- Huang, He, C., Zeng, Y., Xia, X., Yu, X., Yi, P., & Chen, Z. (2009). A novel label-free multi-throughput optical biosensor based on localized surface plasmon resonance. *Biosensors and Bioelectronics*, 24(7), 2255-2259.
- Huang, J., Li, Q., Sun, D., Lu, Y., Su, Y., Yang, X., He, N. (2007). Biosynthesis of silver and gold nanoparticles by novel sundried *Cinnamomum camphora* leaf. *Nanotechnology*, 18(10), 105104.

- Huang, T.-C., Fu, H.-Y., Ho, C.-T., Tan, D., Huang, Y.-T., & Pan, M.-H. (2007). Induction of apoptosis by cinnamaldehyde from indigenous cinnamon *Cinnamomum osmophloeum* Kaneh through reactive oxygen species production, glutathione depletion, and caspase activation in human leukemia K562 cells. *Food chemistry*, *103*(2), 434-443.
- Hussain, S., Khan, F., Cao, W., Wu, L., & Geng, M. (2016). Seed priming alters the production and detoxification of reactive oxygen intermediates in rice seedlings grown under sub-optimal temperature and nutrient supply. *Frontiers in plant science*, *7*, 439.
- Imanshahidi, M., & Hosseinzadeh, H. (2008). Pharmacological and therapeutic effects of *Berberis vulgaris* and its active constituent, berberine. *Phytotherapy research*, *22*(8), 999-1012.
- Iravani, S., & Zolfaghari, B. (2013). Green synthesis of silver nanoparticles using *Pinus eldarica* bark extract. *BioMed research international*, *2013*.
- Issa, O. M., Bissonnais, Y. L., Planchon, O., Favis-Mortlock, D., Silvera, N., & Wainwright, J. (2006). Soil detachment and transport on field-and laboratory-scale interrill areas: erosion processes and the size-selectivity of eroded sediment. *Earth Surface Processes and Landforms*, *31*(8), 929-939.
- Jakhetia, V., Patel, R., Khatri, P., Pahuja, N., Garg, S., Pandey, A., & Sharma, S. (2010). Cinnamon: a pharmacological review. *Journal of advanced scientific research*, *1*(2), 19-23.
- Jalal, R., Goharshadi, E. K., Abareshi, M., Moosavi, M., Yousefi, A., & Nancarrow, P. (2010). ZnO nanofluids: green synthesis, characterization, and antibacterial activity. *Materials Chemistry and Physics*, *121*(1-2), 198-201.
- Jamwal, V., Gupta, S., & Bhagat, M. (2016). Analysis of phytochemical and biological potential of *Berberis lycium* roots. *Arch. Pharm. Biol. Sci*, *4*, 117-123.

- Jeambey, Z., Johns, T., Talhouk, S., & Batal, M. (2009). Perceived health and medicinal properties of six species of wild edible plants in north-east Lebanon. *Public health nutrition*, 12(10), 1902-1911.
- Jeyaratnam, N., Nour, A. H., Kanthasamy, R., Nour, A. H., Yuvaraj, A., & Akindoyo, J. O. (2016). Essential oil from *Cinnamomum cassia* bark through hydrodistillation and advanced microwave assisted hydrodistillation. *Industrial Crops and Products*, 92, 57-66.
- Jha, A. K., Prasad, K., & Prasad, K. (2009). A green low-cost biosynthesis of Sb₂O₃ nanoparticles. *Biochemical engineering journal*, 43(3), 303-306.
- Ji, M., Sun, X., Guo, X., Zhu, W., Wu, J., Chen, L., . . . Zhang, Q. (2019). Green synthesis, characterization and in vitro release of cinnamaldehyde/sodium alginate/chitosan nanoparticles. *Food hydrocolloids*, 90, 515-522.
- Jiménez, S., Domingo, A., Brazeiro, A., Defeo, O., & Phillips, R. A. (2015). Marine debris ingestion by albatrosses in the southwest Atlantic Ocean. *Marine pollution bulletin*, 96(1-2), 149-154.
- Jones, N., Ray, B., Ranjit, K. T., & Manna, A. C. (2008). Antibacterial activity of ZnO nanoparticle suspensions on a broad spectrum of microorganisms. *FEMS microbiology letters*, 279(1), 71-76.
- Jones, S. M., Ravani, P., Hemmelgarn, B. R., Muruve, D., & MacRae, J. M. (2011). Morphometric and biological characterization of biofilm in tunneled hemodialysis catheters. *American journal of kidney diseases*, 57(3), 449-455.
- Jyoti, K., Baunthiyal, M., & Singh, A. (2016). Characterization of silver nanoparticles synthesized using *Urtica dioica* Linn. leaves and their synergistic effects with antibiotics. *Journal of radiation research and applied sciences*, 9(3), 217-227.
- Kaliora, A., Dedoussis, G., & Schmidt, H. (2006). Dietary antioxidants in preventing atherogenesis. *Atherosclerosis*, 187(1), 1-17.

- Kamat, P. V. (2002). Photophysical, photochemical and photocatalytic aspects of metal nanoparticles. In: ACS Publications.
- Karlsson, H. L., Cronholm, P., Gustafsson, J., & Moller, L. (2008). Copper oxide nanoparticles are highly toxic: a comparison between metal oxide nanoparticles and carbon nanotubes. *Chemical research in toxicology*, 21(9), 1726-1732.
- Kaviya, S., Santhanalakshmi, J., Viswanathan, B., Muthumary, J., & Srinivasan, K. (2011). Biosynthesis of silver nanoparticles using Citrus sinensis peel extract and its antibacterial activity. *Spectrochimica Acta Part A: Molecular and Biomolecular Spectroscopy*, 79(3), 594-598.
- Khan, I., Qayum, A., & Qureshi, Z. (1969). Study of the hypotensive action of berbamine, an alkaloid isolated from Berberis lycium. *Life sciences*, 8(17), 993-1001.
- Khan, M., Giessrigl, B., Vonach, C., Madlener, S., Prinz, S., Herbaceck, I., . . . Mikulits, W. (2010). Berberine and a Berberis lycium extract inactivate Cdc25A and induce α -tubulin acetylation that correlate with HL-60 cell cycle inhibition and apoptosis. *Mutation Research/Fundamental and Molecular Mechanisms of Mutagenesis*, 683(1-2), 123-130.
- Khanna, P. K., & Nair, C. (2009). Synthesis of silver nanoparticles using cod liver oil (fish oil): green approach to nanotechnology. *International Journal of Green Nanotechnology: Physics and Chemistry*, 1(1), P3-P9.
- Kim, J. S., Kuk, E., Yu, K. N., Kim, J.-H., Park, S. J., Lee, H. J., . . . Hwang, C.-Y. (2007). Antimicrobial effects of silver nanoparticles. *Nanomedicine: Nanotechnology, Biology and Medicine*, 3(1), 95-101.
- Kim, S. H., Hyun, S. H., & Choung, S. Y. (2006). Anti-diabetic effect of cinnamon extract on blood glucose in db/db mice. *Journal of ethnopharmacology*, 104(1-2), 119-123.

- Klabunde, K. J., Stark, J., Koper, O., Mohs, C., Park, D. G., Decker, S., . . . Zhang, D. (1996). Nanocrystals as stoichiometric reagents with unique surface chemistry. *The Journal of Physical Chemistry*, *100*(30), 12142-12153.
- Klevenz, H. (2004). Nanobiotechnology: from molecules to systems. *Engineering in life sciences*, *4*(3), 211-218.
- Kokura, S., Handa, O., Takagi, T., Ishikawa, T., Naito, Y., & Yoshikawa, T. (2010). Silver nanoparticles as a safe preservative for use in cosmetics. *Nanomedicine: Nanotechnology, Biology and Medicine*, *6*(4), 570-574.
- Krane, B. D., & Shamma, M. (1982). The isoquinolone alkaloids. *Journal of Natural Products*, *45*(4), 377-384.
- Krumov, N., Perner-Nochta, I., Oder, S., Gotcheva, V., Angelov, A., & Posten, C. (2009). Production of inorganic nanoparticles by microorganisms. *Chemical Engineering & Technology: Industrial Chemistry-Plant Equipment-Process Engineering-Biotechnology*, *32*(7), 1026-1035.
- Kumar, A., Vemula, P. K., Ajayan, P. M., & John, G. (2008). Silver-nanoparticle-embedded antimicrobial paints based on vegetable oil. *Nature materials*, *7*(3), 236-241.
- Kumar, B., Kumari, S., Cumbal, L., & Debut, A. (2015). Lantana camara berry for the synthesis of silver nanoparticles. *Asian Pacific Journal of Tropical Biomedicine*, *5*(3), 192-195.
- Kumar, B., Smita, K., Cumbal, L., Debut, A., Camacho, J., Hernández-Gallegos, E., . . . Rosero, G. (2015). Potosynthesis and biological activity of silver nanoparticles using *Passiflora tripartita* fruit extracts. *Advanced Materials Letters*, *6*(2), 127-132.
- Kumar, Tonda, S., Kumar, B., Shanker, V., & Sreedhar, B. (2014). Cost-effective and eco-friendly synthesis of novel and stable N-doped ZnO/gC 3 N 4 core-shell nanoplates with excellent visible-light responsive photocatalysis. *Nanoscale*, *6*(9), 4830-4842.

- Kumaravel, S., & Srinivasan, K. (2017). Antioxidant and Antimicrobial Activity of Silver Nanoparticles Synthesized Using *Cinnamomum Zeylanicum*. *Indo American Journal of Pharmaceutical Sciences*, 4(1), 8-12.
- Le Ouay, B., & Stellacci, F. (2015). Antibacterial activity of silver nanoparticles: a surface science insight. *Nano today*, 10(3), 339-354.
- Leung, A. Y., & Foster, S. (1996). *Encyclopedia of common natural ingredients used in food, drugs, and cosmetics*. John Wiley & Sons, Inc.
- Li, Huang, Y. F., Ding, Y., Yang, Z. L., Li, S. B., Zhou, X. S., Wu, D. Y. (2010). Shell-isolated nanoparticle-enhanced Raman spectroscopy. *Nature*, 464(7287), 392-395.
- Li, S., Shen, Y., Xie, A., Yu, X., Qiu, L., Zhang, L., & Zhang, Q. (2007). Green synthesis of silver nanoparticles using *Capsicum annuum* L. extract. *Green Chemistry*, 9(8), 852-858.
- Li, X., Xu, H., Chen, Z.-S., & Chen, G. (2011). Biosynthesis of nanoparticles by microorganisms and their applications. *Journal of Nanomaterials*, 2011, 1-16.
- Liau, S., Read, D., Pugh, W., Furr, J., & Russell, A. (1997). Interaction of silver nitrate with readily identifiable groups: relationship to the antibacterial action of silver ions. *Letters in applied microbiology*, 25(4), 279-283.
- Lin, H.-F., Liao, S.-C., & Hung, S.-W. (2005). The dc thermal plasma synthesis of ZnO nanoparticles for visible-light photocatalyst. *Journal of photochemistry and photobiology A: Chemistry*, 174(1), 82-87.
- Liu, X., Atwater, M., Wang, J., & Huo, Q. (2007). Extinction coefficient of gold nanoparticles with different sizes and different capping ligands. *Colloids and Surfaces B: Biointerfaces*, 58(1), 3-7.
- Lodge, R., & Descoteaux, A. (2006). Phagocytosis of *Leishmania donovani* amastigotes is Rac1 dependent and occurs in the absence of NADPH oxidase activation. *European journal of immunology*, 36(10), 2735-2744.

- Lopes, M. d. F. S., Ribeiro, T., Abrantes, M., Marques, J. J. F., Tenreiro, R., & Crespo, M. T. B. (2005). Antimicrobial resistance profiles of dairy and clinical isolates and type strains of enterococci. *International journal of food microbiology*, *103*(2), 191-198.
- Maciel, M. A. M., Pinto, A. C., Veiga Jr, V. F., Grynberg, N. F., & Echevarria, A. (2002). Medicinal plants: the need for multidisciplinary scientific studies. *Química Nova*, *25*, 429-438.
- Maria do Socorro, S. R., Mendonça-Filho, R. R., Bizzo, H. R., de Almeida Rodrigues, I., Soares, R. M. A., Souto-Pradón, T., Lopes, A. H. C. (2003). Antileishmanial activity of a linalool-rich essential oil from *Croton cajucara*. *Antimicrobial agents and chemotherapy*, *47*(6), 1895.
- Masaki, T., & Kim, S. (2003). Synthesis of nano-sized ZnO powders prepared by precursor process. *Journal of Ceramic Processing & Research*, *4*(3), 135-139.
- Mashwani, Z.-u.-R., Khan, T., Khan, M. A., & Nadhman, A. (2015). Synthesis in plants and plant extracts of silver nanoparticles with potent antimicrobial properties: current status and future prospects. *Applied microbiology and biotechnology*, *99*(23), 9923-9934.
- Matsumura, Y., Yoshikata, K., Kunisaki, S.-i., & Tsuchido, T. (2003). Mode of bactericidal action of silver zeolite and its comparison with that of silver nitrate. *Applied and environmental microbiology*, *69*(7), 4278-4281.
- Matsunaga, K., Klein, T. W., Friedman, H., & Yamamoto, Y. (2001). Involvement of nicotinic acetylcholine receptors in suppression of antimicrobial activity and cytokine responses of alveolar macrophages to *Legionella pneumophila* infection by nicotine. *The Journal of Immunology*, *167*(11), 6518-6524.
- Mehmood, A., Murtaza, G., Bhatti, T. M., & Kausar, R. (2014). Enviro-friendly synthesis of silver nanoparticles using *Berberis lycium* leaf extract and their antibacterial efficacy. *Acta Metallurgica Sinica (English Letters)*, *27*(1), 75-80.

- Mehmood, A., Murtaza, G., Bhatti, T. M., Kausar, R., & Ahmed, M. J. (2016). Biosynthesis, characterization and antimicrobial action of silver nanoparticles from root bark extract of *Berberis lycium* Royle. *Pakistan Journal of Pharmaceutical Sciences*, 29(1), 131-137.
- Mehta, A., & Shaha, C. (2006). Mechanism of metalloid-induced death in *Leishmania* spp.: role of iron, reactive oxygen species, Ca²⁺, and glutathione. *Free Radical Biology and Medicine*, 40(10), 1857-1868.
- Miana, G. (1973). Tertiary dihydroprotoberberine alkaloids of *Berberis lycium*. *Phytochemistry*.
- Mittal, A. K., Kaler, A., & Banerjee, U. C. (2012). Free Radical Scavenging and Antioxidant Activity of Silver Nanoparticles Synthesized from Flower Extract of *Rhododendron dauricum*. *Nano Biomedicine & Engineering*, 4(3), 118-124.
- Miyata, H., Kono, J., Ushijima, S., Igawa, G., Miyasato, K., Fukui, K., Yanagida, T. (2001). Comparative study on clinical presentation of patients addicted to nicotine, alcohol, stimulants, organic solvents, or sedatives. *Nihon shinkei seishin yakurigaku zasshi= Japanese journal of psychopharmacology*, 21(5), 165-167.
- Mokhtari, N., Daneshpajouh, S., Seyedbagheri, S., Atashdehghan, R., Abdi, K., Sarkar, S., Shahverdi, A. R. (2009). Biological synthesis of very small silver nanoparticles by culture supernatant of *Klebsiella pneumoniae*: The effects of visible-light irradiation and the liquid mixing process. *Materials Research Bulletin*, 44(6), 1415-1421.
- Morones, J. R., Elechiguerra, J. L., Camacho, A., Holt, K., Kouri, J. B., Ramírez, J. T., & Yacaman, M. J. (2005). The bactericidal effect of silver nanoparticles. *Nanotechnology*, 16(10), 2346.
- Mubarak, A. D., Thajuddin, N., Jeganathan, K., & Gunasekaran, M. (2011). Plant extract mediated synthesis of silver and gold nanoparticles and its antibacterial activity against clinically isolated pathogens. *Colloids and Surfaces B: Biointerfaces*, 85(2), 360-365.

- Nadagouda, M. N., & Varma, R. S. (2008). Green synthesis of silver and palladium nanoparticles at room temperature using coffee and tea extract. *Green Chemistry*, *10*(8), 859-862.
- Nadhman, A., Khan, M. I., Nazir, S., Khan, M., Shahnaz, G., Raza, A., . Yasinzai, M. (2016). Annihilation of Leishmania by daylight responsive ZnO nanoparticles: a temporal relationship of reactive oxygen species-induced lipid and protein oxidation. *International Journal of Nanomedicine*, *11*, 2451.
- Nadworny, P. L., Wang, J., Tredget, E. E., & Burrell, R. E. (2008). Anti-inflammatory activity of nanocrystalline silver in a porcine contact dermatitis model. *Nanomedicine: Nanotechnology, Biology and Medicine*, *4*(3), 241-251.
- Narayanan, K. B., & Sakthivel, N. (2010). Phytosynthesis of gold nanoparticles using leaf extract of *Coleus amboinicus* Lour. *Materials characterization*, *61*(11), 1232-1238.
- Nascimento, G. G., Locatelli, J., Freitas, P. C., & Silva, G. L. (2000). Antibacterial activity of plant extracts and phytochemicals on antibiotic-resistant bacteria. *Brazilian journal of microbiology*, *31*, 247-256.
- Nasrollahi, P., Khajeh, K., Tamjid, E., Taleb, M., Soleimani, M., & Nie, G. (2018). Sustained release of sodium deoxycholate from PLGA–PEG–PLGA thermosensitive polymer. *Artificial Cells, Nanomedicine, and Biotechnology*, *46*(sup2), 1170-1177.
- Natera, J., Otero, L., Sereno, L., Fungo, F., Wang, N.-S., Tsai, Y.-M., . Wong, K.-T. (2007). A novel electrochromic polymer synthesized through electropolymerization of a new donor– acceptor bipolar system. *Macromolecules*, *40*(13), 4456-4463.
- Nayak, R. R., Pradhan, N., Behera, D., Pradhan, K. M., Mishra, S., Sukla, L. B., & Mishra, B. K. (2011). Green synthesis of silver nanoparticle by *Penicillium purpurogenum* NPMF: the process and optimization. *Journal of Nanoparticle Research*, *13*(8), 3129-3137.

- Nazari, H., Mohammadi, A., Safaryeh, M., & Khaleghian, A. (2013). Effect of Cinnamon zeylanicum essence and distillate on the clotting time. *Journal of Medicinal Plants Research*, 7(19), 1339-1343.
- Oliveira, F., Vazquez, L., De Campos, N., & De Franca, F. (2009). Production of rhamnolipids by a *Pseudomonas alcaligenes* strain. *Process Biochemistry*, 44(4), 383-389.
- Otunola, G. A., Afolayan, A. J., Ajayi, E. O., & Odeyemi, S. W. (2017). Characterization, antibacterial and antioxidant properties of silver nanoparticles synthesized from aqueous extracts of *Allium sativum*, *Zingiber officinale*, and *Capsicum frutescens*. *Pharmacognosy magazine*, 13(Suppl 2), S201.
- Padmavathy, N., & Vijayaraghavan, R. (2008). Enhanced bioactivity of ZnO nanoparticles—an antimicrobial study. *Science and technology of advanced materials*, 1-8.
- Parashar, V., Parashar, R., Sharma, B., & Pandey, A. C. (2009). Parthenium leaf extract mediated synthesis of silver nanoparticles: a novel approach towards weed utilization. *Digest Journal of Nanomaterials & Biostructures (DJNB)*, 4(1).
- Park, Kim, S.-H., Kim, H.-J., & Choi, S.-H. (2006). A new composition of nanosized silica-silver for control of various plant diseases. *The plant pathology journal*, 22(3), 295-302.
- Park, Y., Noh, H. J., Han, L., Kim, H.-S., Kim, Y.-J., Choi, J. S., . . . Cho, S. (2012). *Artemisia capillaris* extracts as a green factory for the synthesis of silver nanoparticles with antibacterial activities. *Journal of nanoscience and nanotechnology*, 12(9), 7087-7095.
- Patz, J. A., Graczyk, T. K., Geller, N., & Vittor, A. Y. (2000). Effects of environmental change on emerging parasitic diseases. *International journal for parasitology*, 30(12-13), 1395-1405.

- Perez, R., Ineichen, P., Seals, R., Michalsky, J., & Stewart, R. (1990). Modeling daylight availability and irradiance components from direct and global irradiance. *Solar energy*, 44(5), 271-289.
- Peter, W. (1981). The treatment of kala-azar: new approach to an old problem. *Ind J Med Res*, 73, 1-18.
- Philip, D. (2009). Biosynthesis of Au, Ag and Au–Ag nanoparticles using edible mushroom extract. *Spectrochimica Acta Part A: Molecular and Biomolecular Spectroscopy*, 73(2), 374-381.
- Prabhu, S., & Poulouse, E. K. (2012). Silver nanoparticles: mechanism of antimicrobial action, synthesis, medical applications, and toxicity effects. *International nano letters*, 2(1), 32.
- Prathna, T., Chandrasekaran, N., Raichur, A. M., & Mukherjee, A. (2011). Kinetic evolution studies of silver nanoparticles in a bio-based green synthesis process. *Colloids and Surfaces A: Physicochemical and Engineering Aspects*, 377(1-3), 212-216.
- Ramya, M., & Subapriya, M. S. (2012). Green synthesis of silver nanoparticles. *Int J Pharm Med Biol Sci*, 1(1), 54-61.
- Rao, P. V., & Gan, S. H. (2014). Cinnamon: a multifaceted medicinal plant. *Evidence-Based Complementary and Alternative Medicine*, 2014.
- Raveendran, P., Fu, J., & Wallen, S. L. (2003). Completely “green” synthesis and stabilization of metal nanoparticles. *Journal of the American Chemical Society*, 125(46), 13940-13941.
- Reddy, G., & Gandhi, N. (2012). Environmental friendly biosynthesis, characterization and antibacterial activity of silver nanoparticles by using Senna Saimea plant leaf aqueous extract. *Int J Iins Pharm Life Sci*, 2(1), 186-193.

- Robertson, R. P., & Harmon, J. S. (2006). Diabetes, glucose toxicity, and oxidative stress: a case of double jeopardy for the pancreatic islet β cell. *Free Radical Biology and Medicine*, 41(2), 177-184.
- Roy, S., Mukherjee, T., Chakraborty, S., & Das, T. K. (2013). Biosynthesis, characterisation & antifungal activity of silver nanoparticles synthesized by the fungus *Aspergillus foetidus* MTCC8876. *Digest Journal of Nanomaterials and Biostructures*, 8(1), 197-205.
- Saha, D., & Paul, S. (2012). Antifungal activity of ethanol extract of *Pouzolzia Zeylanica* (L.) Benn. *International Journal of Pharmacy Teaching and Practices*, 3(2), 272-274.
- Sahibzada, M. U. K., Sadiq, A., Faidah, H. S., Khurram, M., Amin, M. U., Haseeb, A., & Kakar, M. (2018). Berberine nanoparticles with enhanced in vitro bioavailability: characterization and antimicrobial activity. *Drug design, development and therapy*, 12, 303.
- Sakagami, Y., & Kajimura, K. (2002). Bactericidal activities of disinfectants against vancomycin-resistant enterococci. *Journal of Hospital Infection*, 50(2), 140-144.
- Salam, H. A., Sivaraj, R., & Venckatesh, R. (2014). Green synthesis and characterization of zinc oxide nanoparticles from *Ocimum basilicum* L. var. *purpurascens* Benth.-Lamiaceae leaf extract. *Materials Letters*, 131, 16-18.
- Samat, N. A., & Nor, R. M. (2013). Sol-gel synthesis of zinc oxide nanoparticles using *Citrus aurantifolia* extracts. *Ceramics International*, 39, S545-S548.
- Sangal, A. (2011). Role of cinnamon as beneficial antidiabetic food adjunct: A review. *Advances in Applied Science Research*, 2(4), 440-450.
- Sangshetti, J. N., Khan, F. A. K., Kulkarni, A. A., Arote, R., & Patil, R. H. (2015). Antileishmanial drug discovery: Comprehensive review of the last 10 years. *Rsc Advances*, 5(41), 32376-32415.

- Sasidharan, S., Chen, Y., Saravanan, D., Sundram, K., & Latha, L. Y. (2011). Extraction, isolation and characterization of bioactive compounds from plants' extracts. *African journal of traditional, complementary and alternative medicines*, 8(1-10).
- Sasikala, D., Govindaraju, K., Tamilselvan, S., & Singaravelu, G. (2012). Soybean protein: a natural source for the production of green silver nanoparticles. *Biotechnology and Bioprocess Engineering*, 17(6), 1176-1181.
- Sathishkumar, M., Sneha, K., Won, S., Cho, C.-W., Kim, S., & Yun, Y.-S. (2009). Cinnamon zeylanicum bark extract and powder mediated green synthesis of nano-crystalline silver particles and its bactericidal activity. *Colloids and Surfaces B: Biointerfaces*, 73(2), 332-338.
- Schröfel, A., Kratošová, G., Šafařík, I., Šafaříková, M., Raška, I., & Šor, L. M. (2014). Applications of biosynthesized metallic nanoparticles—a review. *Acta biomaterialia*, 10(10), 4023-4042.
- Schwarz, A. E. (2009). Green dreams of reason. Green nanotechnology between visions of excess and control. *Nanoethics*, 3(2), 109-118.
- Seil, J. T., & Webster, T. J. (2012). Antimicrobial applications of nanotechnology: methods and literature. *International Journal of Nanomedicine*, 7, 2767.
- Selvarajan, E., & Mohanasrinivasan, V. (2013). Biosynthesis and characterization of ZnO nanoparticles using *Lactobacillus plantarum* VITES07. *Materials Letters*, 112, 180-182.
- Senanayake, U. M., Lee, T. H., & Wills, R. B. (1978). Volatile constituents of cinnamon (*Cinnamomum zeylanicum*) oils. *Journal of agricultural and food chemistry*, 26(4), 822-824.
- Shah, G. M., & Khan, M. A. (2006). Common medicinal folk recipes of siran valley, Mansehra, Pakistan. *Ethnobotanical leaflets*, 2006(1), 5.

- Shahverdi, A. R., Minaeian, S., Shahverdi, H. R., Jamalifar, H., & Nohi, A.-A. (2007). Rapid synthesis of silver nanoparticles using culture supernatants of Enterobacteria: a novel biological approach. *Process Biochemistry*, 42(5), 919-923.
- Shan, B., Cai, Y. Z., Sun, M., & Corke, H. (2005). Antioxidant capacity of 26 spice extracts and characterization of their phenolic constituents. *Journal of agricultural and food chemistry*, 53(20), 7749-7759.
- Sharma, R. K., Agrawal, M., & Marshall, F. M. (2009). Heavy metals in vegetables collected from production and market sites of a tropical urban area of India. *Food and chemical toxicology*, 47(3), 583-591.
- Shen, C., Wang, S., Yang, H., Long, K., & Wang, F. (2006). The adsorption stability & inhibition by allyl-thiourea of bulk nanocrystalline ingot iron in dilute HCl solution. *Applied Surface Science*, 253(4), 2118-2122.
- Shinwari, Z. K., Malik, S., Karim, A. M., Faisal, R., & Qaiser, M. (2015). Biological activities of commonly used medicinal plants from Ghazi Brotha, Attock district. *Pak J Bot*, 47(1), 113-120.
- Shrivastava, S., Bera, T., Roy, A., Singh, G., Ramachandrarao, P., & Dash, D. (2007). Characterization of enhanced antibacterial effects of novel silver nanoparticles. *Nanotechnology*, 18(22), 225103.
- Sim, K., Sri Nurestri, A., & Norhanom, A. (2010). Phenolic content and antioxidant activity of crude and fractionated extracts of *Pereskia bleo* (Kunth) DC.(Cactaceae). *African Journal of Pharmacy and Pharmacology*, 4(5), 193-201.
- Singh, G., Maurya, S., DeLampasona, M., & Catalan, C. A. (2007). A comparison of chemical, antioxidant and antimicrobial studies of cinnamon leaf and bark volatile oils, oleoresins and their constituents. *Food and chemical toxicology*, 45(9), 1650-1661.

- Singh, U., Devaraj, S., & Jialal, I. (2005). Vitamin E, oxidative stress, and inflammation. *Annual review of nutrition*, 25, 151.
- Slawson, R. M., Trevors, J. T., & Lee, H. (1992). Silver accumulation and resistance in *Pseudomonas stutzeri*. *Archives of microbiology*, 158(6), 398-404.
- Sondi, I., & Salopek-Sondi, B. (2004). Silver nanoparticles as antimicrobial agent: a case study on *E. coli* as a model for Gram-negative bacteria. *Journal of colloid and interface science*, 275(1), 177-182.
- Song, H., Ko, K., Oh, L., & Lee, B. (2006). Fabrication of silver nanoparticles and their antimicrobial mechanisms. *Eur Cells Mater*, 11(Suppl 1), 58.
- Song, J. Y., Jang, H.-K., & Kim, B. S. (2009). Biological synthesis of gold nanoparticles using *Magnolia kobus* and *Diopyros kaki* leaf extracts. *Process Biochemistry*, 44(10), 1133-1138.
- Sood, R., Swarup, D., Bhatia, S., Kulkarni, D., Dey, S., Saini, M., & Dubey, S. (2012). Antiviral activity of crude extracts of *Eugenia jambolana* Lam. against highly pathogenic avian influenza (H5N1) virus. *Indian J Exp Biol*, 50(3), 179-186.
- Stoimenov, P. K., Klinger, R. L., Marchin, G. L., & Klabunde, K. J. (2002). Metal oxide nanoparticles as bactericidal agents. *Langmuir*, 18(17), 6679-6686.
- Subash, B., Krishnakumar, B., Pandiyan, V., Swaminathan, M., & Shanthi, M. (2013). Synthesis and characterization of novel WO₃ loaded Ag-ZnO and its photocatalytic activity. *Materials Research Bulletin*, 48(1), 63-69.
- Subash, B., Krishnakumar, B., Swaminathan, M., & Shanthi, M. (2013). Highly efficient, solar active, and reusable photocatalyst: Zr-loaded Ag-ZnO for reactive red 120 dye degradation with synergistic effect and dye-sensitized mechanism. *Langmuir*, 29(3), 939-949.
- Subash, B., Krishnakumar, B., Velmurugan, R., Swaminathan, M., & Shanthi, M. (2012). Synthesis of Ce co-doped Ag-ZnO photocatalyst with excellent

performance for NBB dye degradation under natural sunlight illumination. *Catalysis Science & Technology*, 2(11), 2319-2326.

- Sultana, B., Anwar, F., & Przybylski, R. (2007). Antioxidant activity of phenolic components present in barks of *Azadirachta indica*, *Terminalia arjuna*, *Acacia nilotica*, and *Eugenia jambolana* Lam. trees. *Food chemistry*, 104(3), 1106-1114.
- Sun, J., Chu, Y.-F., Wu, X., & Liu, R. H. (2002). Antioxidant and antiproliferative activities of common fruits. *Journal of agricultural and food chemistry*, 50(25), 7449-7454.
- Suresh, D., Nethravathi, P., Rajanaika, H., Nagabhushana, H., & Sharma, S. (2015). Green synthesis of multifunctional zinc oxide (ZnO) nanoparticles using *Cassia fistula* plant extract and their photodegradative, antioxidant and antibacterial activities. *Materials Science in Semiconductor Processing*, 31, 446-454.
- Tang, H., Murphy, C. J., Zhang, B., Shen, Y., Van Kirk, E. A., Murdoch, W. J., & Radosz, M. (2010). Curcumin polymers as anticancer conjugates. *Biomaterials*, 31(27), 7139-7149.
- Thomé, A., Reddy, K. R., Reginatto, C., & Cecchin, I. (2015). Review of nanotechnology for soil and groundwater remediation: Brazilian perspectives. *Water, Air, & Soil Pollution*, 226(4), 1-20.
- Tian, Z.-Q., & Ren, B. (2004). Adsorption and reaction at electrochemical interfaces as probed by surface-enhanced Raman spectroscopy. *Annu. Rev. Phys. Chem.*, 55, 197-229.
- Vafaei, M., & Ghamsari, M. S. (2007). Preparation and characterization of ZnO nanoparticles by a novel sol-gel route. *Materials Letters*, 61(14-15), 3265-3268.
- Valko, M., Rhodes, C., Moncol, J., Izakovic, M., & Mazur, M. (2006). Free radicals, metals and antioxidants in oxidative stress-induced cancer. *Chemico-biological interactions*, 160(1), 1-40.

- Vannier-Santos, M., Martiny, A., & Souza, W. d. (2002). Cell biology of *Leishmania* spp. invading and evading. *Current pharmaceutical design*, 8(4), 297-318.
- Velmurugan, P., Cho, M., Lee, S.-M., Park, J.-H., Bae, S., & Oh, B.-T. (2014). Antimicrobial fabrication of cotton fabric and leather using green-synthesized nanosilver. *Carbohydrate Polymers*, 106, 319-325.
- Verspohl, E. J., Bauer, K., & Neddermann, E. (2005). Antidiabetic effect of *Cinnamomum cassia* and *Cinnamomum zeylanicum* in vivo and in vitro. *Phytotherapy Research: An International Journal Devoted to Pharmacological and Toxicological Evaluation of Natural Product Derivatives*, 19(3), 203-206.
- Vigneshwaran, N., Kumar, S., Kathe, A., Varadarajan, P., & Prasad, V. (2006). Functional finishing of cotton fabrics using zinc oxide–soluble starch nanocomposites. *Nanotechnology*, 17(20), 5087-5095.
- Vijayaraghavan, K., Nalini, S. K., Prakash, N. U., & Madhankumar, D. (2012). Biomimetic synthesis of silver nanoparticles by aqueous extract of *Syzygium aromaticum*. *Materials Letters*, 75, 33-35.
- Waghmare, S., Deshmukh, A., Kulkarni, S., & Oswaldo, L. (2011). Biosynthesis and characterization of manganese and zinc nanoparticles. *Universal Journal of Environmental Research & Technology*, 1(1).
- Wang, S.-Y., Chen, P.-F., & Chang, S.-T. (2005). Antifungal activities of essential oils and their constituents from indigenous cinnamon (*Cinnamomum osmophloeum*) leaves against wood decay fungi. *Bioresource technology*, 96(7), 813-818.
- Wani, I. A., Ganguly, A., Ahmed, J., & Ahmad, T. (2011). Silver nanoparticles: ultrasonic wave assisted synthesis, optical characterization and surface area studies. *Materials Letters*, 65(3), 520-522.
- Waxman, E., & Bahcall, J. (1998). High energy neutrinos from astrophysical sources: An upper bound. *Physical Review D*, 59(2), 023002.

- Wei, D., & Qian, W. (2008). Facile synthesis of Ag and Au nanoparticles utilizing chitosan as a mediator agent. *Colloids and Surfaces B: Biointerfaces*, 62(1), 136-142.
- Wiley, B. J., Im, S. H., Li, Z.-Y., McLellan, J., Siekkinen, A., & Xia, Y. (2006). Maneuvering the surface plasmon resonance of silver nanostructures through shape-controlled synthesis. In (Vol. 110, pp. 15666-15675): ACS Publications.
- Wilkinson, J., Ucer, K. B., & Williams, R. (2004). Picosecond excitonic luminescence in ZnO and other wide-gap semiconductors. *Radiation Measurements*, 38(4-6), 501-505.
- Wondrak, G., Villeneuve, N. F., Lamore, S. D., Bause, A. S., Jiang, T., & Zhang, D. D. (2010). The cinnamon-derived dietary factor cinnamic aldehyde activates the Nrf2-dependent antioxidant response in human epithelial colon cells. *Molecules*, 15(5), 3338-3355.
- Wu, H., Qiu, D., Cai, Y., Xu, X., & Chen, N. (2002). Optical studies of ZnO quantum dots grown on Si (0 0 1). *Journal of crystal growth*, 245(1-2), 50-55.
- Xia, T., Kovoichich, M., Brant, J., Hotze, M., Sempf, J., Oberley, T., Nel, A. E. (2006). Comparison of the abilities of ambient and manufactured nanoparticles to induce cellular toxicity according to an oxidative stress paradigm. *Nano letters*, 6(8), 1794-1807.
- Yamamoto, O. (2001). Influence of particle size on the antibacterial activity of zinc oxide. *International Journal of Inorganic Materials*, 3(7), 643-646.
- Yamini, G., Shakeri, A., Zohuriaan-Mehr, M. J., & Kabiri, K. (2018). Cyclocarbonated lignosulfonate as a bio-resourced reactive reinforcing agent for epoxy biocomposite: from natural waste to value-added bio-additive. *Journal of CO2 Utilization*, 24, 50-58.
- Yavar, R., Hadi, K., Reza, A. M., Mohebbali, M., Hasan, B., Ali, O. M., Manuchehr, G. (2013). First detection of *Leishmania infantum* DNA in wild caught

Phlebotomus papatasi in endemic focus of cutaneous leishmaniasis, South of Iran. *Asian Pacific Journal of Tropical Biomedicine*, 3(10), 825-829.

Yeh, H.-F., Luo, C.-Y., Lin, C.-Y., Cheng, S.-S., Hsu, Y.-R., & Chang, S.-T. (2013). Methods for thermal stability enhancement of leaf essential oils and their main constituents from indigenous cinnamon (*Cinnamomum osmophloeum*). *Journal of agricultural and food chemistry*, 61(26), 6293-6298.

Zargar, M., Hamid, A. A., Bakar, F. A., Shamsudin, M. N., Shameli, K., Jahanshiri, F., & Farahani, F. (2011). Green synthesis and antibacterial effect of silver nanoparticles using *Vitex negundo* L. *Molecules*, 16(8), 6667-6676.

Zeng, F., Hou, C., Wu, S., Liu, X., Tong, Z., & Yu, S. (2007). Silver nanoparticles directly formed on natural macroporous matrix and their anti-microbial activities. *Nanotechnology*, 18(5), 055605.

Zhang, H., Chen, Q.-Y., Xiang, M.-L., Ma, C.-Y., Huang, Q., & Yang, S.-Y. (2009). In silico prediction of mitochondrial toxicity by using GA-CG-SVM approach. *Toxicology in Vitro*, 23(1), 134-140.

Zhao, G., & Stevens, S. E. (1998). Multiple parameters for the comprehensive evaluation of the susceptibility of *Escherichia coli* to the silver ion. *Biometals*, 11(1), 27-32.